THESIS APPROVAL

GRADUATE SCHOOL, KASETSART UNIVERSITY

Doctor of Philosophy (Chemistry)

DEGREE

Chemistry	Chemistry
FIELD	**DEPARTMENT**

TITLE: Aluminum Complexes Supported by Bis(pyrrolidene) Schiff-base and Salan Ligands for the Ring-Opening Polymerization of Lactides and ε-Caprolactone

NAME: Mr. Sittichoke Tabthong

THIS THESIS HAS BEEN ACCEPTED BY

THESIS ADVISOR

(Miss Pimpa Hormnirun, Ph.D.)

THESIS CO-ADVISOR

(Mr. Tanin Nanok, Ph.D.)

THESIS CO-ADVISOR

(Assistant Professor Pitak Chuawong, Ph.D.)

DEPARTMENT HEAD

(Associate Professor Waraporn Parasuk, Ph.D.)

APPROVED BY THE GRADUATE SCHOOL ON _____

DEAN

(Associate Professor Gunjana Theeragool, D.Agr.)

Copyright by Kasetsart University All rights reserved

THESIS

ALUMINUM COMPLEXES SUPPORTED BY BIS(PYRROLIDENE) SCHIFF-BASE AND SALAN LIGANDS FOR THE RING-OPENING POLYMERIZATION OF LACTIDES AND ε-CAPROLACTONE

SITTICHOKE TABTHONG

A Thesis Submitted in Partial Fulfillment of
the Requirements for the Degree of
Doctor of Philosophy (Chemistry)
Graduate School, Kasetsart University
2015

Copyright by Kasetsart University All rights reserved

Sittichoke Tabthong 2015: Aluminum Complexes Supported by Bis(pyrrolidene) Schiff-base and Salan Ligands for the Ring-Opening Polymerization of Lactides and ε-Caprolactone. Doctor of Philosophy (Chemistry), Major Field: Chemistry, Department of Chemistry. Thesis Advisor: Miss Pimpa Hormnirum, Ph.D. 183 pages.

This thesis consists of two parts. In the first part, a series of aluminum complexes bearing bis(pyrrolidene) Schiff-base ligands (**L^1AlMe-L^7AlMe**) were successfully synthesized and characterized by NMR spectroscopy and elemental analysis. In the presence of benzyl alcohol, complexes **L^1AlMe-L^7AlMe** were found to catalyze the ring-opening polymerization (ROP) of *L*-LA and *rac*-LA with a well-controlled fashion. The ROP of *L*-LA was typically faster than that of *rac*-LA. Kinetic studies revealed the first order dependence on monomer. The flexibility of the ligand framework has a significant influence on the polymerization rate. The rates of polymerization decrease in the order **L^4AlMe** > **L^2AlMe** > **L^3AlMe** > **L^5AlMe** > **L^7AlMe** > **L^1AlMe** > **L^6AlMe**. Among these complexes, **L^3AlMe** had the highest stereoselectivity (P_m = 0.80).

In the second part, a series of aluminum complexes bearing bis(phenoxy-amine) or Salan ligands (**L^{1A}AlMe-L^{3C}AlMe**) were synthesized and were characterized by NMR spectroscopy and elemental analysis. In the presence of benzyl alcohol, the *rac*-LA polymerization reactions mediated by all complexes proceeded in a controlled manner. Kinetic studies revealed that the polymerization rates decrease in the order H > Ph > ^{i}Pr >> ^{t}Bu. Heterotactic PLA was produced when the bulky substituents were introduced to the phenoxy rings. All complexes also showed a good performance in the polymerization of ε-CL. The copolymerizations between *rac*-LA and ε-CL were well controlled in terms of molecular weight and molecular weight distribution. The block copolymers were produced by this catalystic system.

/ /

Student's signature Thesis Advisor's signature

Copyright by Kasetsart University All rights reserved

ACKNOWLEDGEMENTS

First of all, I would like to express my deepest gratitude to my adviser, Dr. Pimpa Hormnirun for her enthusiastic guidance, inspiration and encouragement throughout the course of my research. Thank you for her supports and understanding. This thesis could not be accomplished without the opportunity she gave. I also owe thanks to her for giving me the chance to find the way back to the right track of my life.

I am deeply grateful to my co-advisors, Dr. Tanin Nanok and Assistant Professor Dr. Pitak Chuawong, for providing valuable opportunities to learn and gain lots of experiences, advices and comments.

A heart-felt gratitude also goes to my colleagues for their providing assistance and sharing useful ideas. I would also like to thank all of the staffs at Department of Chemistry, Faculty of Science, Kasetsart University for research facilities, especially for Mr. Wiriya Traibooth for his kind help in NMR techniques.

During studies, I received full financial support from Faculty of Science Kasetsart University Postgraduate Studentship (ScKUPGS). I also have partial financial supports from the National Center of Excellence in Petroleums, Petrochemical Technology and Advanced Materials (NCE-PPAM) and the graduate school Kasetsart University for the Publication in an approved international journal.

Last, but certainly not least, with great pleasure I would like to express my parents for the inexhaustible and unconditional love and support.

Sittichoke Tabthong

August, 2014

Copyright by Kasetsart University All rights reserved

TABLE OF CONTENTS

Page

TABLE OF CONTENTS	i
LIST OF TABLES	ii
LIST OF FIGURES	iii
LIST OF ABBREVIATIONS	xi
INTRODUCTION	1
OBJECTIVE	22
LITERATURE REVIEW	23
MATERIALS AND METHODS	54
RESULTS AND DISCUSSION	87
CONCLUSIONS	143
LITERATURE CITED	145
APPENDIX	173
CURRICULUM VITAE	183

Copyright by Kasetsart University All rights reserved

LIST OF TABLES

Table		Page
1	Tetrad probabilities of PLA based on Bernoullian statistics.	16
2	The triad assignments of carbonyl peaks of PLA-*co*-PCL.	18
3	Crystal data and refinement parameters for complex **L^{3}AlMe**.	93
4	Polymerizations of *L*-LA using initiators **L^{1}AlMe-L^{7}AlMe** in the presence of benzyl alcohol.	102
5	Polymerization of *rac*-LA using initiators **L^{1}AlMe-L^{7}AlMe** in the presence of benzyl alcohol.	107
6	Kinetic results for *L*-LA polymerization using complexes **L^{1}AlMe-L^{7}AlMe** in the presence of benzyl alcohol.	108
7	Kinetic results for *rac*-LA polymerization using complexes **L^{1}AlMe-L^{7}AlMe** in the presence of benzyl alcohol.	109
8	Polymerization of *rac*-LA using initiator **L^{3}AlMe** in the presence of benzyl alcohol.	113
9	Polymerization data of *rac*-LA for complexes **L^{2A}AlMe-L^{4A}AlMe**, **L^{1B}AlMe-L^{4B}AlMe** and **L^{1C}AlMe-L^{3C}AlMe**.	125
10	Kinetic results for *rac*-LA polymerization using aluminum Salan complexes in the presence of benzyl alcohol.	131
11	The ε-CL polymerization data for aluminum Salan complexes.	137
12	Copolymerization of ε-CL and *rac*-LA with aluminum Salan complexes.	142

Appendix Table

1	Bond lengths (Å) for complex **L^{3}AlMe**.	174
2	Bond angles for complex **L^{3}AlMe**.	175

Copyright by Kasetsart University All rights reserved

LIST OF FIGURES

Figure		Page
1	The life cycle of PLA.	3
2	Stereoisomer of lactides (LA).	3
3	The possible microstructures of PLA.	4
4	Synthesis of ε-caprolactone from renewable resources.	5
5	Example of lactones.	6
6	The mechanism for the ring-opening polymerization of lactide by metal catalyst.	8
7	(a) Intermolecular and (b) intermolecular transesterifications.	9
8	(a) Bimolecular cross chain transfer and (b) alcohol cross chain transfer.	10
9	Epimerization of lactide.	10
10	Proposed mechanicm for CROP of LA.	12
11	Polymerization of lactone according to the activated monomer mechanism.	12
12	Anionic ring-opening polymerization of lactone using alkali metal compounds.	13
13	Proposed mechanism for anionic ring-opening polymerization of lactone by *tert*-butoxybis(dimethylamino) methane and tris(dimethyl amino) methane.	14
14	The microstructure of PLA at tetrad level (m = *meso*, {m ≡ *i*, isotactic}; r = *racemic*, {r ≡ *s*, syndiotactic }).	15
15	Schematic diagram to show chemical shift (in ppm) of the tetrads for PLA in a) homonuclear decoupled ^{1}H NMR from *rac*-LA; b) ^{13}C NMR from *rac*-LA; c) homonuclear decoupled ^{1}H NMR from *meso*-LA; d) ^{13}C NMR from *meso*-LA.	16

Copyright by Kasetsart University All rights reserved

LIST OF FIGURES (Continued)

Figure		Page
16	Full assignment of PLA-*co*-PCL.	17
17	Possible mode of transesterification (C = caproyl unit, L = Lactyl unit and LL = Lactydyl unit).	19
18	The structure of complexes **1-10**.	25
19	The structure of complexes **11-13**.	27
20	The structure of complexes **14-24**.	30
21	The structure of complexes **25-30**.	33
22	The structure of complexes **31-32**.	34
23	The structure of complexes **33-38**.	37
24	The structure of complexes **39-40**.	38
25	The structure of complexes **41-44**.	40
26	The structure of complexes **45-50**.	42
27	The structure of Salen aluminum complexes **51-53**.	43
28	The structure of Salen aluminum complexes **54-65**.	45
29	The structure of Salen aluminum complexes **66-67**.	46
30	The structure of Salen aluminum complexes **68**.	46
31	The structure of Salan aluminum complexes **69-71**.	48
32	The structure of Salalen aluminum complexes **72**.	49
33	The structure of aluminum complexes **73-77**.	49
34	The structure of aluminum complexes **78-79**.	50
35	The structure of aluminum complexes **80-84**.	52
36	The structure of aluminum complexes **85-87**.	53
37	Synthetic pathway for preparation of ligands $\mathbf{H_2L^1}$-$\mathbf{H_2L^7}$.	56
38	Synthetic pathways for the preparation of aluminum complex $\mathbf{L^1AlMe}$-$\mathbf{L^7AlMe}$.	62
39	Synthetic pathway for $\mathbf{H_2L^{1A}}$-$\mathbf{H_2L^{4A}}$, $\mathbf{H_2L^{1B}}$-$\mathbf{H_2L^{4B}}$ and $\mathbf{H_2L^{1C}}$-$\mathbf{H_2L^{3C}}$.	67

Copyright by Kasetsart University All rights reserved

LIST OF FIGURES (Continued)

Figure		Page
40	Synthetic pathway for the preparation of **L^{1A}AlMe-L^{4A}AlMe**, **L^{1B}AlMe-L^{4B}AlMe** and **L^{1C}AlMe-L^{3C}AlMe**.	78
41	Synthetic pathway for ligands **H_2L^1-H_2L^7**.	88
42	The synthetic pathway for **L^1AlMe-L^7AlMe**.	89
43	^{1}H NMR spectrum of complex **L^1AlMe** (400 MHz, DMSO-d_6, 300 K, * = residual DMSO).	90
44	^{1}H NMR spectrum of complex **L^2AlMe** (400 MHz, DMSO-d_6, 300 K, * = residual DMSO).	91
45	^{1}H NMR spectrum of complex **L^3AlMe** (400 MHz, DMSO-d_6, 300 K, * = residual DMSO).	91
46	The molecular structure of complex **L^3AlMe.**	92
47	Square pyramidal (sqp) and trigonal bipyramidal (tbp) geometries of the five-coordinate aluminum methyl Schiff base complexes.	94
48	^{1}H NMR spectrum of complex **L^4AlMe** (400 MHz, DMSO-d_6, 300 K, * = residual DMSO).	96
49	^{1}H NMR spectrum of complex **L^5AlMe** (400 MHz, DMSO-d_6, 300 K, * = residual DMSO).	96
50	^{1}H NMR spectrum of complex **L^6AlMe** (400 MHz, DMSO-d_6, 300 K, * = residual DMSO).	98
51	^{1}H NMR spectrum of complex **L^7AlMe** (400 MHz, DMSO-d_6, 300 K, * = residual DMSO).	98
52	^{1}H NMR spectrum of complex **L^3AlOBn** (400 MHz, DMSO-d_6, 300 K, *i* = impurity, * = residual DMSO).	100
53	The LA polymerization procedure using complexes **L^1AlMe-L^7AlMe**.	100

Copyright by Kasetsart University All rights reserved

LIST OF FIGURES (Continued)

Figure		Page
54	The homonuclear decoupled ^{1}H NMR spectra at the methine region of the resultant PLAs from *rac*-LA using (a) **L^{1}AlMe**/$PhCH_2OH$; (b) **L^{2}AlMe**/$PhCH_2OH$; (c) **L^{3}AlMe**/$PhCH_2OH$; (d) **L^{4}AlMe**/$PhCH_2OH$; (e) **L^{5}AlMe**/$PhCH_2OH$; (f) **L^{6}AlMe**/$PhCH_2OH$; (g) **L^{7}AlMe**/$PhCH_2OH$.	105
55	Semilogarithmic polts of *rac*-LA conversion with time in toluene at 70 ˚C with complex **L^{3}AlMe**/$PhCH_2OH$ as initiator ($[LA]_0$ = 0.42 M, **I**, [Al] = 16.67 mM, [LA]/[Al] = 25; **II**, [Al] = 12.5 mM, [LA]/[Al] = 34; **III**, [Al] = 8.33 mM, [LA]/[Al] = 50; **I**V, [Al] = 6.10 mM, [LA]/[Al] = 69; **V**, [Al] = 4.16 mM, [LA]/[Al] = 100).	106
56	Plot of ln k_{app} *versus* ln [Al] for the polymerization of *rac*-LA with complex **L^{3}AlMe**/$PhCH_2OH$ as an initiator (toluene, 70 ˚C, $[LA]_0$ = 0.42 M).	107
57	Plot of k_{app} *versus* [Al] for the polymerization of *rac*-LA with complex **L^{3}AlMe**/$PhCH_2OH$ as an initiator (toluene, 70 ˚C, $[LA]_0$ = 0.42 M).	107
58	Semilogarithmic plots of *L*-LA conversion with time in toluene at 70 ˚C with complexes **L^{1}AlMe-L^{7}AlMe** ($[LA]_0$/[Al] = 50, [Al]/$[PhCH_2OH]$ = 1, $[LA]_0$ = 0.42 M, [Al] = 8.33 mM). (a) **L^{5}AlMe** (●), **L^{1}AlMe** (▲) and **L^{6}AlMe** (♦); (b) **L^{4}AlMe** (♦), **L^{2}AlMe** (▲), **L^{3}AlMe** (●) and **L^{7}AlMe** (▼).	109
59	Semilogarithmic plots of *rac*-LA conversion with time in toluene at 70 ˚C with complexes **L^{1}AlMe-L^{7}AlMe** ($[LA]_0$/[Al] = 50, [Al]/$[PhCH_2OH]$ = 1, $[LA]_0$ = 0.42 M, [Al] = 8.33 mM). (a) **L^{5}AlMe** (■), **L^{1}AlMe** (●) and **L^{6}AlMe** (♦); (b) **L^{4}AlMe** (▲), **L^{2}AlMe** (●), **L^{3}AlMe** (♦) and **L^{7}AlMe** (▼); (c) **L^{6}AlMe** (♦).	110

Copyright by Kasetsart University All rights reserved

LIST OF FIGURES (Continued)

Figure		Page
60	Plot of M_n as a function of monomer conversion for *rac*-LA polymerization using **L^{3}AlMe**/$PhCH_2OH$ ($[LA]_0/[Al]$ = 50, $[Al]/[PhCH_2OH]$ = 1, $[LA]_0$ = 0.42 M, [Al] = 8.33 mM)**.**	113
61	Plot of the number-average molecular weight (M_n) *versus* the molar ratio of monomer to initiator ($[LA]_0/[Al]$) for the polymerization of *rac*-lactide using **L^{3}AlMe** in toluene at 70 ˚C	114
62	Aluminum complex **14**.	115
63	Synthetic pathway for **H_2L^{1A}-H_2L^{4A}**, **H_2L^{1B}-H_2L^{4B}** and **H_2L^{1C}-H_2L^{3C}**.	116
64	Synthetic pathway for Salan aluminum methyl complex.	116
65	^{1}H NMR spectrum of complex **L^{1A}AlMe** (400 MHz, C_6D_6, 300 K, * = residual C_6D_5H).	117
66	^{1}H NMR spectrum of complex **L^{2A}AlMe** (400 MHz, C_6D_6, 300 K, * = residual C_6D_5H).	118
67	^{1}H NMR spectrum of complex **L^{3A}AlMe** (400 MHz, C_6D_6, 300 K).	118
68	^{1}H NMR spectrum of complex **L^{4A}AlMe** (400 MHz, C_6D_6, 300 K, * = residual C_6D_5H).	119
69	^{1}H NMR spectrum of complex **L^{1B}AlMe** (400 MHz, C_6D_6, 300 K, * = residual C_6D_5H).	120
70	^{1}H NMR spectrum of complex **L^{2B}AlMe** (400 MHz, C_6D_6, 300 K, * = residual C_6D_5H).	120
71	^{1}H NMR spectrum of complex **L^{3B}AlMe** (400 MHz, C_6D_6, 300 K).	121
72	^{1}H NMR spectrum of complex **L^{4B}AlMe** (400 MHz, C_6D_6, 300 K, * = residual C_6D_5H).	121

Copyright by Kasetsart University All rights reserved

LIST OF FIGURES (Continued)

Figure		Page
73	^{1}H NMR spectrum of complex **L^{1C}AlMe** (500 MHz, $C_6D_5CD_3$, 343 K).	122
74	^{1}H NMR spectrum of complex **L^{2C}AlMe** (500 MHz, $C_6D_5CD_3$, 343 K)	123
75	^{1}H NMR spectrum of complex **L^{3C}AlMe** (500 MHz, $C_6D_5CD_3$, 343 K, * = residual $C_6D_5CD_2H$).	123
76	Groups of Salan aluminum methyl complex.	124
77	Aluminum complexes **69b**, **69g** and **69e**.	126
78	Methine region of homonuclear decoupled ^{1}H NMR spectra of resultant PLAs from *rac*-LA using (a) **L^{1A}AlMe**/$PhCH_2OH$; (b) **L^{2A}AlMe**/$PhCH_2OH$; (c) **L^{3A}AlMe**/$PhCH_2OH$; (d) **L^{4A}AlMe**/$PhCH_2$ OH; (e) **L^{1B}AlMe**/$PhCH_2OH$; (f) **L^{2B}AlMe**/$PhCH_2OH$; (g) **L^{3B}AlMe** /$PhCH_2OH$; (h) **L^{4B}AlMe**/$PhCH_2OH$; (i) **L^{1C}AlMe** /$PhCH_2OH$; (j) **L^{2C}AlMe**/$PhCH_2OH$; (k) **L^{3C}AlMe**/$PhCH_2OH$.	128
79	Semilogarithmic polts of *rac*-LA conversion with time in toluene at 70 ˚C with complex **L^{1B}AlMe/**$PhCH_2OH$ as initiator ($[LA]_0$ = 0.42 M, **I**, [Al] = 16.67 mM, [LA]/[Al] = 25; **II**, [Al] = 12.5 mM, [LA]/[Al] = 34; **III**, [Al] = 8.33 mM, [LA]/[Al] = 50; **I**V, [Al] = 6.10 mM, [LA]/[Al] = 69; **V**, [Al] = 4.16 mM, [LA]/[Al] = 100).	129
80	Plot of ln k_{app} *versus* ln [Al] for the polymerization of *rac*-LA with complex **L^{1B}AlMe**/$PhCH_2OH$ as an initiator (toluene, 70 ˚C, $[LA]_0$ = 0.42 M).	130
81	Plot of k_{app} *versus* [Al] for the polymerization of *rac*-LA with complex **L^{1B}AlMe**/$PhCH_2OH$ as an initiator (toluene, 70 ˚C, $[LA]_0$ = 0.42 M).	130

Copyright by Kasetsart University All rights reserved

LIST OF FIGURES (Continued)

Figure		Page
82	Semilogarithmic plots of *rac*-LA conversion with time in toluene at 70 ˚C with aluminum Salan complexes ($[LA]_0/[Al]$ = 50, $[Al]/[PhCH_2OH]$ = 1, $[LA]_0$ = 0.42 M, [Al] = 8.33 mM). (a) **L^{1B}AlMe** (▼), **L^{4A}AlMe** (■), **L^{2A}AlMe** (●), **L^{1C}AlMe** (⬢), **L^{4B}AlMe** (▲); (b) **L^{3A}AlMe** (●), **L^{3B}AlMe** (■); (c) **L^{2C}AlMe** (●), **L^{3C}AlMe** (■).	133
83	Plot of M_n as a function of monomer conversion for *rac*-LA polmeriation using (a) **L^{1B}AlMe**/$PhCH_2OH$, (b) **L^{2B}AlMe**/$PhCH_2$ OH, (c) **L^{3B}AlMe** /$PhCH_2OH$, (d) **L^{4B}AlMe**/$PhCH_2OH$ ($[LA]_0/[Al]$ = 50, $[Al]/[PhCH_2OH]$ = 1, $[LA]_0$ = 0.42 M, [Al] = 8.33 mM)**.**	134
84	Aluminum Salen complexes for ε-CL polymerization.	135
85	Copolymerization of ε-CL and *rac*-LA initiated by aluminum Salan complexes.	138
86	^{1}H NMR spectrum of PLA-*co*-PCL.	139
87	(left) ^{1}H NMR spectrum of ε- and α-methylene protons of PLA-*co*-PCL, (right) ^{13}C NMR spectrum of carbonyl carbons of PLA-*co*-PCL using Group A complex	140
88	Aluminum complexes **(*R*,*R*)-1**, **(*S*,*S*)-1** and **4b**.	140

Appendix Figure

1	The molecular structure of complex **L^3AlMe**	174
2	Plot of M_n as a function of monomer conversion for *rac*-LA polymerization using (a) **L^1AlMe**/$PhCH_2OH$, (b) **L^2AlMe** /$PhCH_2OH$, (c) **L^4AlMe** /$PhCH_2OH$, (d) **L^5AlMe**/$PhCH_2OH$, (e) **L^6AlMe**/$PhCH_2OH$, , (f) **L^7AlMe**/$PhCH_2OH$ ($[LA]_0/[Al]$ = 50, $[Al]/[PhCH_2OH]$ = 1, $[LA]_0$ = 0.42 M, [Al] = 8.33 mM)**.**	176

Copyright by Kasetsart University All rights reserved

LIST OF FIGURES (Continued)

Appendix Figure		Page
3	Plot of M_n as a function of monomer conversion for *rac*-LA polymerization using (a) **L^{2A}AlMe**/PhCH$_2$OH, (b) **L^{3A}AlMe**/PhCH$_2$ OH, (c) **L^{4A}AlMe**/PhCH$_2$OH ([LA]$_0$/[Al] = 50, [Al]/[PhCH$_2$ OH] = 1, [LA]$_0$ = 0.42 M, [Al] = 8.33 mM)**.**	177
4	Plot of M_n as a function of monomer conversion for *rac*-LA polymerization using (a) **L^{1C}AlMe**/PhCH$_2$OH, (b) **L^{2C}AlMe**/PhCH$_2$ OH, (c) **L^{3C}AlMe** /PhCH$_2$OH ([LA]$_0$/[Al] = 50, [Al]/[PhCH$_2$OH] = 1, [LA]$_0$ = 0.42 M, [Al] = 8.33 mM)**.**	178
5	(left) ^{1}H NMR spectrum of ε- and α-methylene protons of PLA-*co*-PCL, (right) ^{13}C NMR spectrum of carbonyl carbons of PLA-*co*-PCL using Group A complexes.	179
6	(left) ^{1}H NMR spectrum of ε- and α-methylene protons of PLA-*co*-PCL, (right) ^{13}C NMR spectrum of carbonyl carbons of PLA-*co*-PCL using Group C complexes.	180
7	DSC thermograms of PLA-*co*-PCL using Group A complexes.	181
8	DSC thermograms of PLA-*co*-PCL using Group A complexes.	181
9	DSC thermograms of PLA-*co*-PCL using Group A complexes.	182

Copyright by Kasetsart University All rights reserved

LIST OF ABBREVIATIONS

BBL	=	*β*-Butyrolactone
br	=	broad signal (NMR)
CEM	=	Chain-End control Mechanism
CROP	=	Cationic polymerization
d	=	doublet
D,L-LA	=	*D,L*-lactide
DCM	=	Dichloromethane
D-LA	=	*D*-lactide
DSC	=	Differential Scanning Calorimetry
Et	=	Ethyl
GPC	=	Gel permeation chromatography
[I]	=	Initiator concentration
i	=	Isotactic
^{i}Pr	=	Isopropyl
J	=	Coupling constant (NMR)
k_{app}	=	Apparaent rate constant
LA	=	Lactide
L_{CL}	=	Average sequence length of the caproyl unit
L_{LA}	=	Average sequence length of the lactidyl unit
L-LA	=	*L*-lactide
L_n	=	Ligand
m	=	*meso* linkage
m	=	multiplet (NMR)
M	=	Metal atom
$[M]_0$	=	Initial monomer concentration
Me	=	Methyl
meso-LA	=	*meso*-lactide
M_n	=	Number average molecular weight
M_n(th)	=	Theoretical number-average molar mass

Copyright by Kasetsart University All rights reserved

LIST OF ABBREVIATIONS (Continued)

M_w	=	Weight average molecular weight
NHCs	=	*N*-Heterocyclic carbenes
OR	=	Alkoxide
PCL	=	Polycaprolactone
PDI	=	Polydispersity index
PDLLA	=	Poly(*D*,*L*-lactide)
PE	=	Polyethylene
PG	=	Polyglycolide
PLA	=	Polylactide
PLLA	=	Poly(*L*-lactide)
PP	=	Polypropylene
ppm	=	Parts per million
PS	=	Polystyrene
P_m	=	Probability of *meso* linakge
P_r	=	Probability of *racemic* linkage
r	=	*racemic* linkage
R	=	Degree of randomness
rac-LA	=	*racemic*-lactide
RO	=	Alkoxide group
RI	=	Refractive Index
ROP	=	Ring-Opening Polymerization
SEM	=	Enantiomorphic Site Control Mechanism
^{t}Bu	=	*tert*-butyl
T_c	=	Crystallization temperature
T_g	=	Glass transition temperature
THF	=	Tetrahydrofuran
T_m	=	Melting temperature
δ-VL	=	*δ*-Valerolactone
ε-CL	=	*ε*-Caprolactone

Copyright by Kasetsart University All rights reserved

ALUMINUM COMPLEXES SUPPORTED BY BIS(PYRROLIDENE) SCHIFF-BASE AND SALAN LIGANDS FOR THE RING-OPENING POLYMERIZATION OF LACTIDES AND ε-CAPROLACTONE

INTRODUCTION

Since the first discovery of synthetic polymers in 1930, these polymers have become one of the most attractive materials in daily life (Gibson, 1964). Many of synthetic polymers, such as polyolefins, are petroleum-based polymers. Polyolefins, such as polyethylene (PE), polypropylene (PP) and polystyrene (PS) are not only easy to synthesize and manufacture, but they also have excellent properties such as lightness, durability and chemical resistance. Therefore they have been used in a variety of applications. However, these polymers become the main cause of pollution because they take a very long time to degrade in nature (Wilesa and Scott, 2006). Furthermore, the cost of their raw material increases continuously due to the depletion of fossil fuels. Thus, with regard to both environmental and economic concerns, an environmental friendly polymer from renewable sources becomes a major point of interest in material sciences (Ragauskas *et al.*, 2006).

Aliphatic polyesters, such as polylactide (PLA), polyglycolide (PG), poly(ε-caprolactone) (PCL) as well as their copolymers are the most important class of environmental-friendly polymers to date. They can be derived from renewable resources, for example, biomass from agricultural products and offered a lower dependence of petroleum-based polymers. The usage of them as a packaging or single-use disposal product resolves the problem of garbage management (Doi and Steinbuchet, 2002). In addition, the hydrolysis of their ester bonds yields non-toxic compounds, such as lactic acid and glycolic acid, which can be eliminated as water and carbon dioxide *via* Krebs cycle (Dechy *et al.*, 2004; Albertsson and Varma, 2003). Due to these particular properties, they can be used in biomedical and

Copyright by Kasetsart University All rights reserved

pharmaceutical applications, *e.g*. sutures, stints, surgical implants, time release control drug, etc (Jérôme and Lecomte, 2008; Gupta and Kumar, 2007; Uhrich *et al.*, 1999).

1. Lactide and polylactide

Polylactide or poly(lactic acid) (PLA) is an aliphatic polyester derived from renewable resources such as corn, sugar beet and sugar cane. The life cycle of PLA is illustrated in **Figure 1** (Ikada and Tsuji, 2000). PLA can be synthesized by either the polycondensation of lactic acid or the ring-opening polymerization (ROP) of lactide (LA). Condensation of lactic acid requires high temperature in order to remove the water from the reaction equilibrium, making the reaction possible to reach the high conversion. This generally limits molecular weight (M_w) of polymer. Moreover, polymer microstructure from polycondensation is random (Dechy *et el*., 2004). On the other hand, the ROP of LA by catalysts overcomes the limitation of polycondensation. This technique allows the polymerization to be controlled in terms of molecular weight (M_n), polydispersity index (PDI), polymer microstructure and the rate of polymerization (Darensbourg and Karroonnirun, 2010; Stéphanie *et al.*, 2006).

Due to the presence of two chiral centers in the LA monomer, three different lactide stereoisomers can be formed, namely (*S*,*S*)-LA or *L*-LA, (*R*,*R*)-LA or *D*-LA, and (*R*,*S*)-LA or *meso*-LA (**Figure 2**). The equimolar mixture of *L*-LA and *D*-LA is referred to *rac*-LA or *DL*-LA which is a commonly employed synthetic substrate.

The stereochemistry of the polymer microstructures has a significant effect on the mechanical, physical and degradation properties of PLA materials. For example, highly isotactic PLA is a crystalline polymer, with melting temperature (T_m) in the range of 170-180 ˚C, and it has good mechanical strength, whereas atactic PLA is an amorphous and brittle polymer. Stereocomplex of poly(*D*-LA) and poly(*L*-LA) shows a high T_m value of 230 ˚C (Biela *et al*., 2006; Coulembier *et al*., 2006). Polymer microstructure can be controlled by a judicious choice of the catalyst, which can invoke stereoselectivity in the resulting polymer.

Copyright by Kasetsart University All rights reserved

When pure *L*-LA or *D*-LA is polymerized, optically pure isotactic poly(*L*-LA) or poly(*D*-LA) is obtained, respectively. Polymerization of *rac*-LA can produce three different types of PLA: isotactic, heterotactic and atactic PLAs. In the case of *meso*-LA, it is possible to have three different stereoregular microstructures: syndiotactic and heterotactic PLA and atactic PLAs. The possible configurations of PLA microstructures are shown in **Figure 3**.

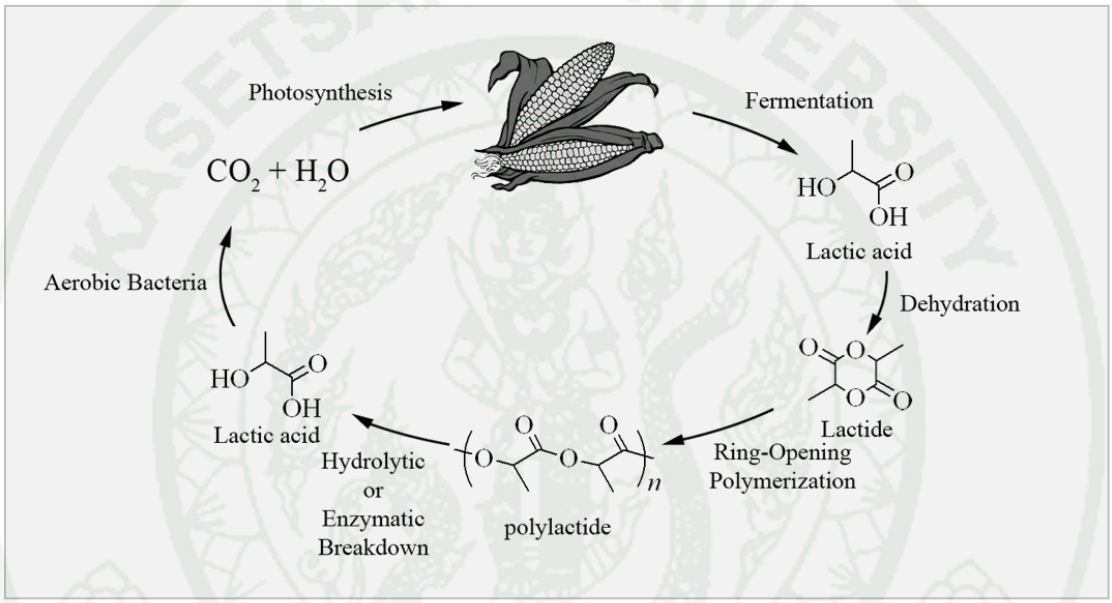

Figure 1 The life cycle of PLA.

Source: Mecking (2009)

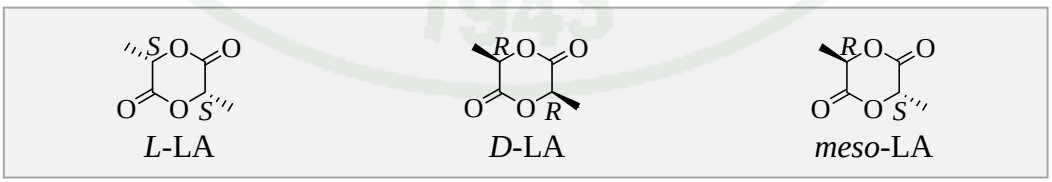

Figure 2 Stereoisomers of lactide (LA).

Copyright by Kasetsart University All rights reserved

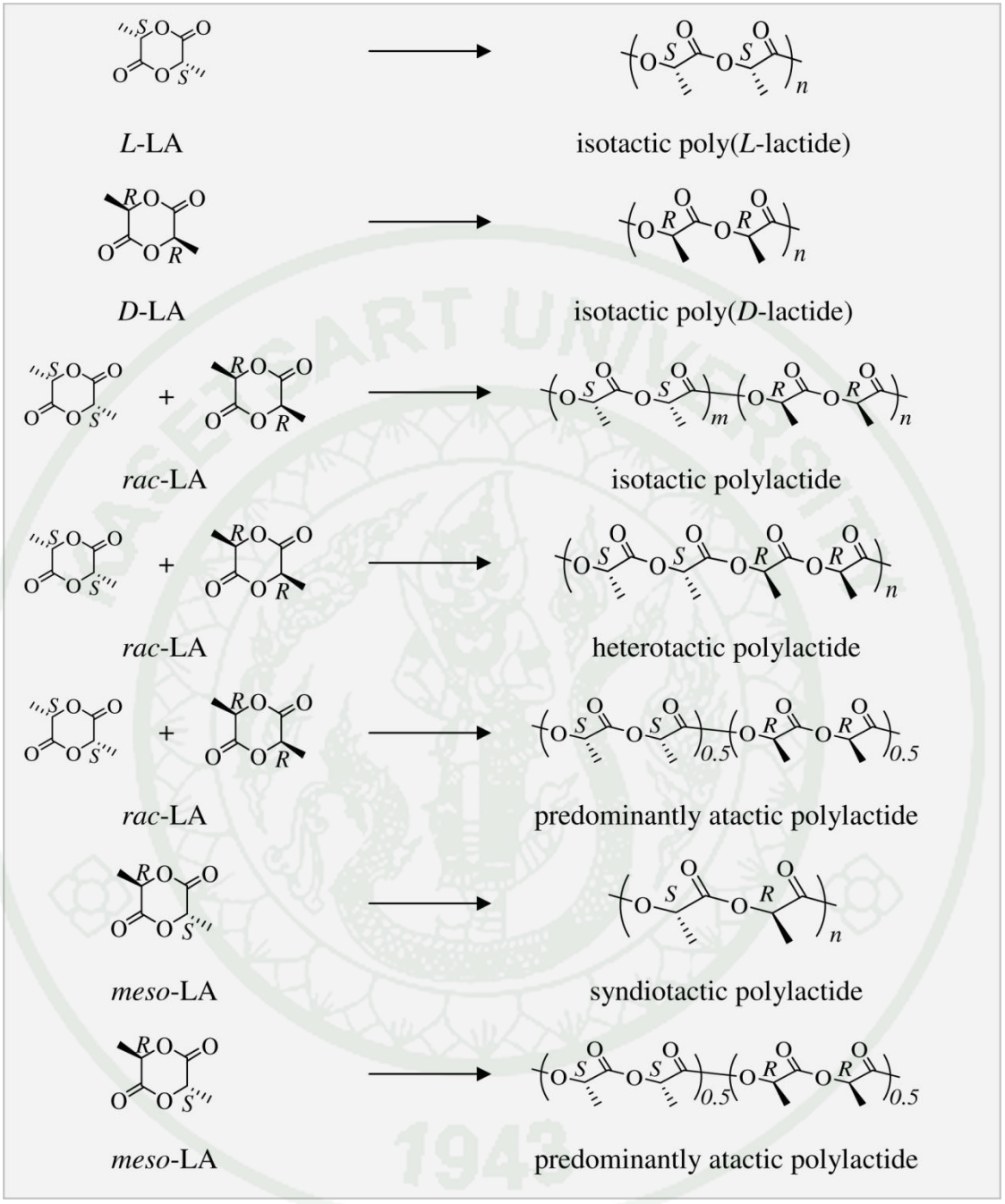

Figure 3 The possible microstructures of PLA.

2. *ε*-Caprolactone and polycaprolactone

Polycaprolactone (PCL) can be synthesized by the ROP of *ε*-caprolactone (*ε*-CL), a seven-membered ring lactone. The monomer *ε*-caprolactone can be obtained

Copyright by Kasetsart University All rights reserved

from renewable resource such as starch as shown in **Figure 4** (Minami and Kozaki, 2003; Gross and Kalra, 2002). The first step is the hydrolysis of starch to obtain glucose. Next, the oxidization of the glucose yields gluconolactone or gluconic acid. Then, the reduction of the gluconolactone or the gluconic acid yields caproic acid. Caproic acid is chlorinated to obtain 6-chlorocaproic acid. The final step is the cyclization of 6-chlorocaproic acid to obtain ε-caprolactone. In general, PCL can be synthesized by the ROP of ε-caprolactone in the presence of the catalyst/initiator utilizing a compound with a desired end-group from the initiator. PCL is a semicrystalline polymer. The melting temperature, T_m, of PCL is in the range of 56-65 ˚C. PCL is biodegradable polyester and it exhibits remarkable drug permeability. However, it takes longer time than PLA to decompose. The degradation rate depends on the molecular weight and the degree of semicrystallinity (Iroh, 1999; Ong and Price, 1978). PCL can be used in both biomedical and pharmaceutical applications (Jenkins *et al.*, 2006).

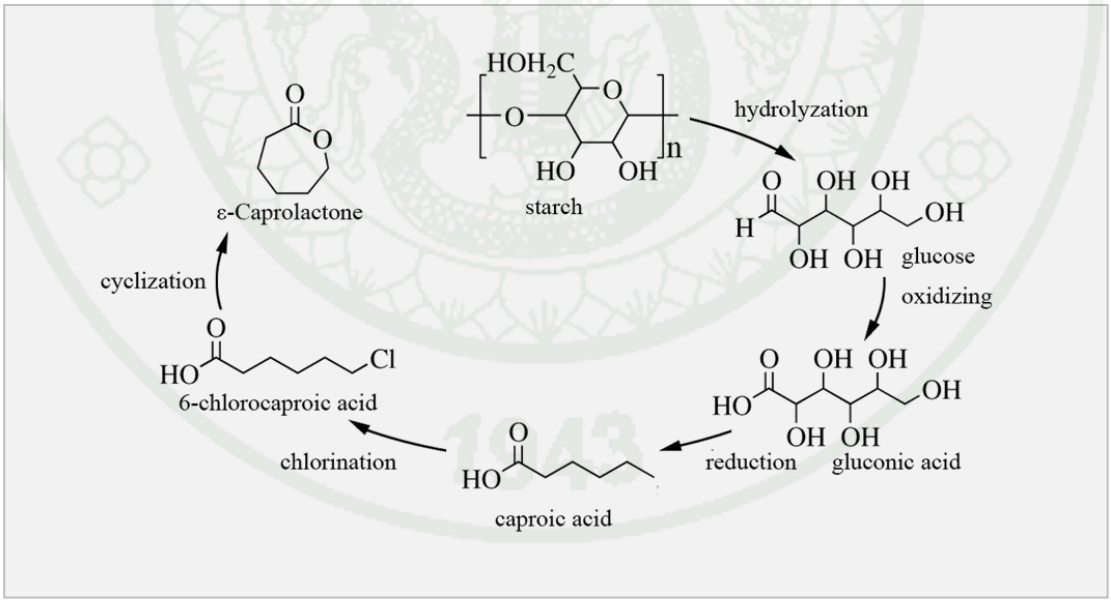

Figure 4 Synthesis of ε-caprolactone from renewable resources.

Source: Minami and Kozaki (2003)

Copyright by Kasetsart University All rights reserved

3. Other lactones and their polymer

Nomenclature of lactones depends on their precursor acid molecules. A prefix is a Greek alphabet representing the number of carbons in the heterocyclic ring and the suffix is a "lactone." Examples of lactones are shown in **Figure 5**. Nowadays, some of lactones such as *γ*-valerolactone and *β*-butylrolactone can be produced from renewable resources (Beek *et al*., 1990; Raupp and Spring, 2013) but the production costs are high (Allen *et al.*, 2010). Therefore, the lactones are normally prepared *via* chemical synthetic pathway (Yong and Zhong, 2010; Carbaj *et al*., 2007).

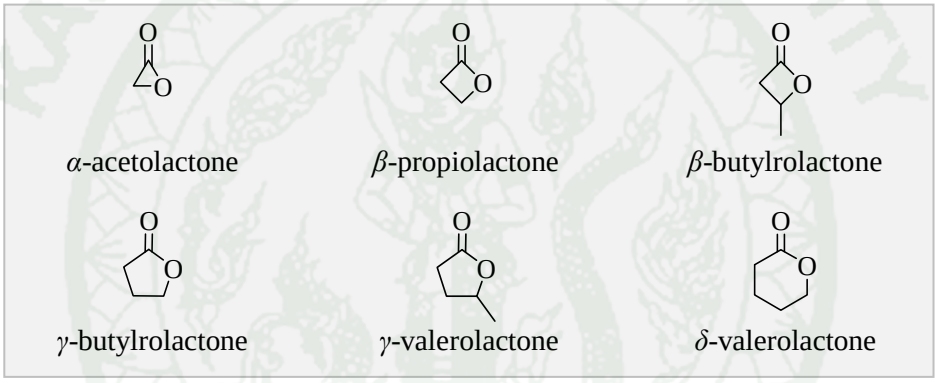

Figure 5 Example of lactones.

Metal alkoxides supported by ancillary ligand were found to be efficient catalysts for the controlled ROP of lactones (Amgoune *et al*., 2006). Although some initiators are able to polymerize lactone with good activity under mild conditions (Rieth *et al.*, 2002), the stereoselective ROP of *racemic β*-butylrolactone (*rac*-BBL) remains a challenge topic for researchers (N. Ajellal *et al*., 2009). The synthesis of poly(*β*-butylrolactone) with different tacticities; *i.e.* isotacticity (Wu and Lenz, 1998), syndiotacticity (Kricheldolf and Eggerstedt, 1997) and atacticity (Moeller *et al*., 2000) was reported.

In comparison, both ring size and substituent of lactones play the major role in the polymerizability. In general, the ability for ROP of lactones is expressed by the free energy of the polymerizing process (Eastmond *et al*., 1989). When the ring size

Copyright by Kasetsart University All rights reserved

increases, the thermodynamic polymerizability and the ring strain also increase. When the ring size is kept constant, substitution on the α-carbon decreases polymerizability. This can be explained by the decreasing of internal energy upon polymerization (ΔH_p) (Chen *et al.*, 2011; Duda and Kowalski, 2009; W. Saiyasombat *et al.*, 1998).

4. Copolymer of lactide and ε-caprolactone

Recently, copolymers of lactide/ε-caprolactone have received much interest in the medical and pharmaceutical fields due to their outstanding biodegradable and bio-compatible properties (Mecking, 2004). PLA exhibits good mechanical properties but poor elasticity because the T_g value of PLA (60 ˚C) is higher than human body's temperature. On the contrary, PCL exhibits poor mechanical properties, but shows good drug permeability, elasticity and thermal property (Ge *et al*., 2000; Kasperczyk, 2001). The copolymer combines advantages and diminishes disadvantages from both polymers. Furthermore, the *in vivo* degradation time can be prolonged by varying the ratio of PLA/PCL in the components from a few weeks of pure PLA to a year of pure PCL (Meretoja *et al.*, 2006). The copolymer properties can be tailored to fulfill the requirements of various applications by varying the copolymer composition, monomer sequencing and molecular weight.

Copolymer can be synthesized by copolymerization of LA/CL or blending of PLA/PCL. However, the blending method has a limitation due to the phase separation of high molecular weight PLA and PCL (Dell'Erba *et al.*, 2001; Na *et al.*, 2002; Sakai *et al.*, 2001). To avoid phase separation, copolymerization of LA/CL is a proper method for the copolymer production. Additionally, this method allows the control of the copolymer properties in terms of composition and morphology (Pappalardo *et al.*, 2009). The synthesis of copolymer has been widely studied focused on either block (Vesna *et al.*, 2000) or random (Purnama *et al.*, 2012; Nomura *et al.*, 2010) copolymer.

Copyright by Kasetsart University All rights reserved

5. Ring-opening polymerization

As mentioned in the previous section, the ring-opening polymerization (ROP) is the promising method to produce polylactones from cyclic lactones. This method can be used for the homopolymerization of lactide and ε-caprolactone and the copolymerization of LA/CL (Wu *et al.*, 2006). In addition, the production of well-controlled molecular weight and low polydispersity polymer using ROP under mild condition can be achieved (Williams, 2007; Lou *et al.*, 2003). Organometallic compounds (Sauer *et al.*, 2013: Chisholm, 2010), organocatalysts (Kamber *et al.*, 2007) and enzymes (Uyama and S. Kobayashi, 1993; Knani *et al.*, 1993) have received attention as initiators for the controlled ROP of cyclic esters. Among these catalysts, organometallic complexes have received considerable attention due to the verities of both activity and selectivity depending on the choice of central metal atoms (**M**), ancillary ligands (**L**) and an initiating nucleophile, most commonly an alkoxide group (**RO**, where R is alkyl or amide). The ROP of cyclic ester is commonly operated by two steps, coordination-insertion mechanism and ring opening polymerization (Marshall *et al.*, 2005; Dove *et al.*, 2006; Chisholm, 2008) as illustrated in **Figure 6**.

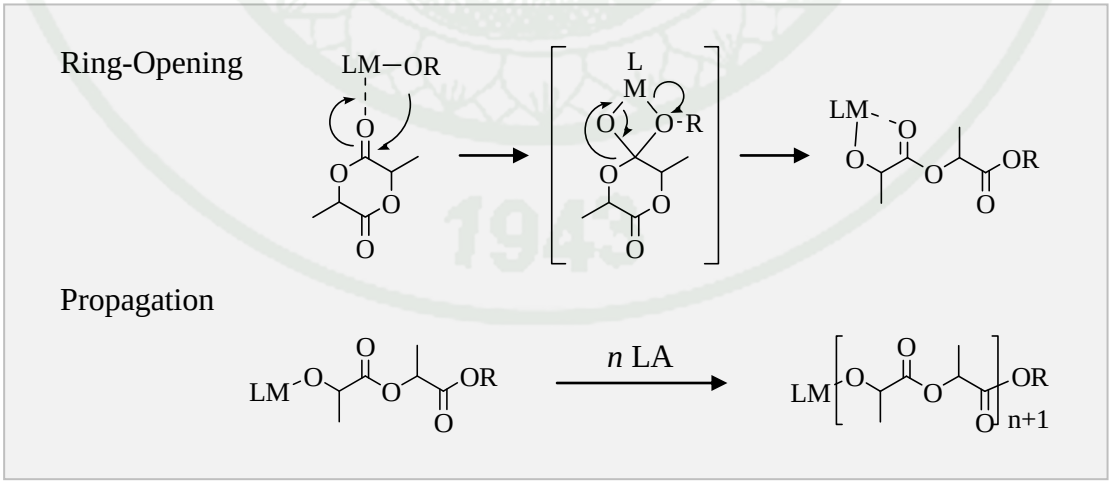

Figure 6 The mechanism for the ring-opening polymerization of lactide by metal catalyst.

Copyright by Kasetsart University All rights reserved

The initiation step involves the coordination of the $O_{carbonyl}$ atom of the monomer to the central metal atom of the catalyst. This activates the $C_{carbonyl}$ atom toward nucleophilic attack by $O_{alkoxide}$, followed by the ester bond breaking. This leads to the formation of the aliphatic ester. The propagation involves the repeat enchainment of monomers and regeneration of the metal-alkoxide bond.

The thermodynamics of ROP is driven by the ring strain of the monomer. The selectivity of the catalyst is significant to assist ring-opening compared to side reactions such as transesterification (Duda and Kowalski, 2009). Generally, the side reactions occur slower than the propagation of the polymer chain, but they become significant when the polymerization reaches a low monomer concentration at high conversion. Transesterifications that take place within the same polymer chain and between two polymer chains are called intramolecular and intermolecular trans-esterifications, respectively (**Figure 7**). Intramolecular transesterification leads to the formation of cyclic ester polymer and shorter propagating chain while intermolecular transesterification is the cause of polymer chain redistribution to both high and low molecular weights. In conclusion, transesterification results in the broadening of the PDI value. In case of *rac*-LA and *meso*-LA polymerizations, transesterification may cause a scrambling of stereocenters along the polymer chain, leading to the loss of stereoselectivity.

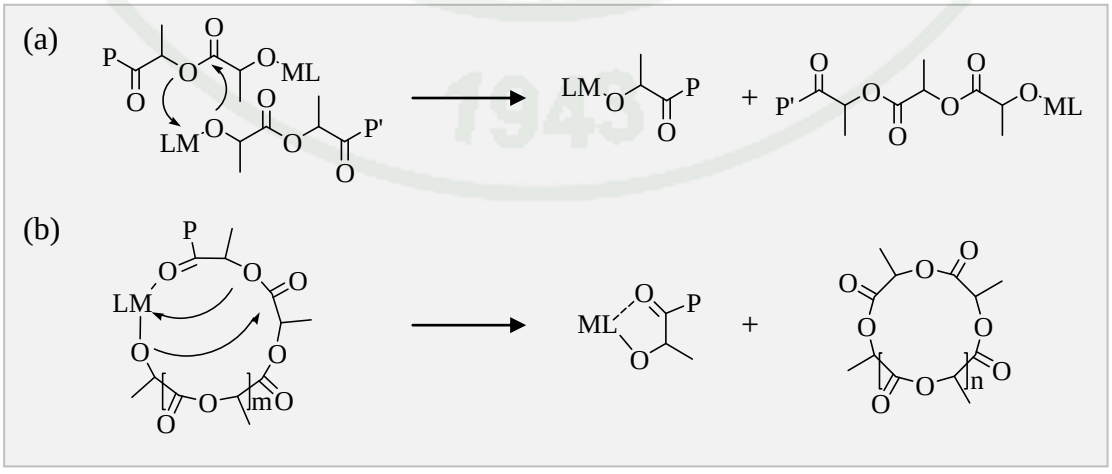

Figure 7 (a) Intermolecular and (b) intramolecular transesterifications.

Copyright by Kasetsart University All rights reserved

In addition to the transesterification reaction, chain transfer and epimerization reactions are common side reactions generally occurring during the polymerization. Chain transfer can be brought by the self-exchange of growing polymer chains between two active metal centers as shown in **Figure 8(a)** or the addition of an excess alcohol to promote the exchange of growing polymer chain and the excess alcohol as shown in **Figure 8(b)**. Since **LMOX** (where **X** is alkyl, amide or polymer chain) represents an active species, the addition of an excess alcohol commonly increases the number of the growing polymer chain. For living polymerization, varying the ratio of **LMOX**/ROH is an alternative method to control molecular weight of resulting polymer (Zhao *et al.*, 2012).

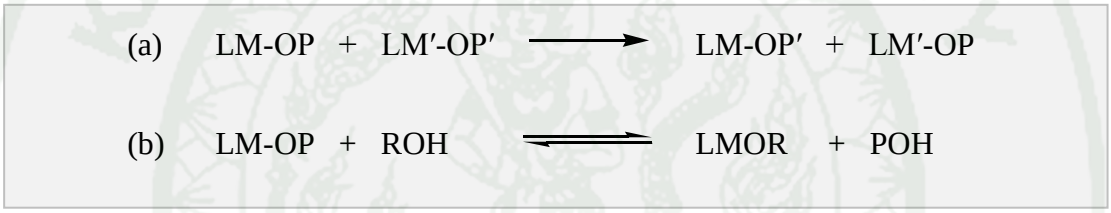

Figure 8 (a) Bimolecular cross chain transfer and (b) alcohol cross chain transfer.

Some electropositive metal can activate the second side reaction called epimerization which is brought by some bases (Shuklov *et al.*, 2010; Whitehorne and Schaper, 2012) according to the mechanism illustrated in **Figure 9**. Epimerization equilibrium leads to the formation of an unsaturated bond in the lactide ring and allows the rearrangement of the methyl group. However, *D*- and *L*-LA are more

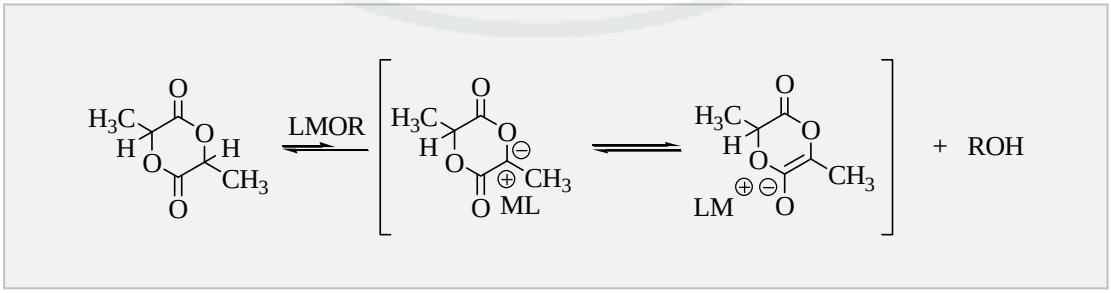

Figure 9 Epimerization of lactide.

Copyright by Kasetsart University All rights reserved

thermodynamically stable than *meso*-LA, so the monomer prefers to reverse to the initial form. The reaction leads to a loss of stereocontrol of the resulting polymer. Additionally, epimerization may cause the formation of the forbidden tetrad such as *rrr* or *mmm* from *rac*-LA or *meso*-LA polymerization, respectively.

6. Cationic ring-opening polymerization

Cationic ring-opening polymerization (CROP) is an efficient method for polymerization of a variety of lactones (Penczek, 2000). The polymerization is achieved in the presence of alkylating agents (Kricheldorf *et al*. 1986; 1987; Kricheldorf and Dunsing, 1986; Kricheldorf and Kreiser, 1987), acylating agents (A. Holfman *et al.*, 1984), Lewis acid (Tang *et al.*, 2003; Albertsson and Palmgren, 1996) and protic acid (Bourissou *et al*., 2005). The use of methyl trifluoromethanesulfonate ($CF_3SO_3CH_3$, CH_3OTf) catalyst/protic acid initiator has found to be an effective method to the production of well-controlled high molecular weight PLAs. The proposed mechanism is illustrated in **Figure 10** (Kricheldorf and Kreiser, 1987). The first step is the activation of the LA monomer by methylation with methyl trifate followed by the nucleophilic attack of the trifate anion (TfO^-) on the positively charged LA ring. Propagation is preceded by the nucleophilic attack by LA on the activated cationic chain end.

The polymerization can be terminated by a monofunctional nucleophile such as water or amine. The polymerization at high temperature may cause the significant epimerization and the loss of controlled character in the resulting polymer. In each system, the detailed mechanisms may slightly different depending on the type of cationic species, lactones, and solvents.

Mechanism of activated cationic polymerization was proposed as described in **Figure 11** (Penczek, 2000). In the initiation step, the reaction occurs in the same fashion noted above for common cationic ring-opening polymerization. The $O_{carboxyl}$ of monomer is activated by the acid, followed by nucleophilic attack either by the initiating alcohol or by the growing polymer chain. Despite the formation of cationic

Copyright by Kasetsart University All rights reserved

chain end of the growing polymer chain, the growing polymer chain with a neutral charge is introduced. Thus, the typicall side-reaction for the cationic polymerization mechanism can be avoided (Basko, 2012). The present of alkyl ester chain end from the initiating alkyl alcohol suggested that the polymerization proceeds by acyl bond cleavage, not by alky bond cleavage.

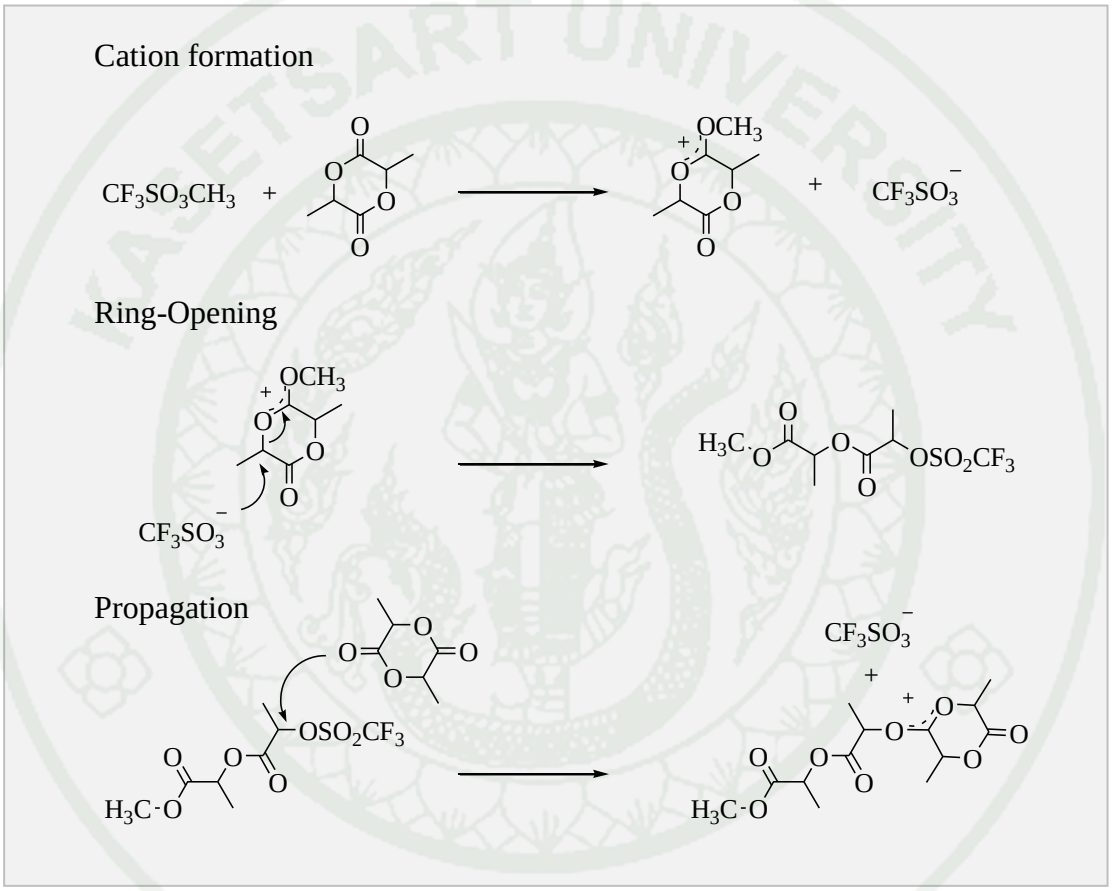

Figure 10 Proposed mechanism for CROP of LA.

Source: Kricheldorf and Kreiser. (1987)

7. Anionic polymerization

Several alkali salts (Xie *et al.*, 1999) and alkali metal compounds (Kricheldorf and Saunders, 1990; Kasperczyk and Bero, 2000; Kasperczyk, 1995) have been applied to polymerize lactones. Alkali metal compounds such as lithium or potassium

Copyright by Kasetsart University All rights reserved

tert-butoxide have been found to be active catalysts for *L*-LA and *rac*-LA. The proposed mechanism for the ROP of lactone using alkali metal compound is shown in **Figure 12**. However, the results showed a significant number of side reactions such as epimerization and back-biting reaction due to their high basicity. A series of bulky ligands were designed to provide a steric barrier around the active anion to minimizing the side reactions (Ko and Lin, 2001).

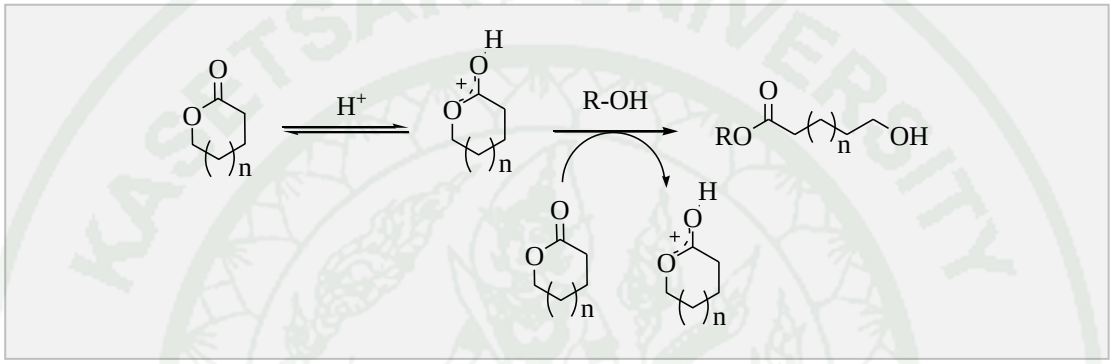

Figure 11 Polymerization of lactone according to the activated monomer mechanism.

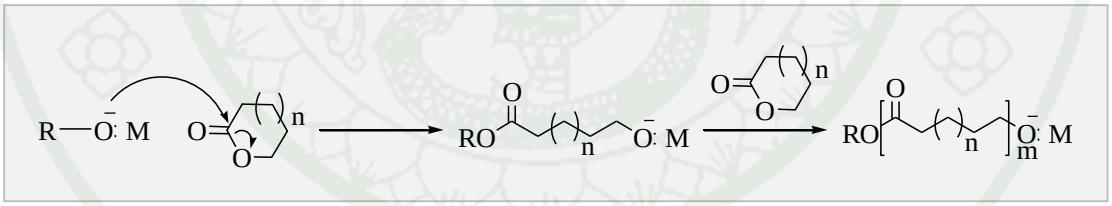

Figure 12 Anionic ring-opening polymerization of lactone using alkali metal compounds.

Commercially available organic compounds such as *tert*-butoxy bis(dimethyl amino)methane and tris(dimethylamino)methane (**Figure 13**) have been used for the ROP of lactone in the presence or absence of alcohol (Wawer and Osek, 1985; Wasserman and Ives, 1978; Trost and Preckel, 1973; Bredereck *et al*., 1967; 1968a; 1968b). The resulting PLAs showed well-controlled molecular weights and narrow PDIs. The mechanism involving heterolytic cleavage to alkoxides was proposed, as shown in **Figure 13** (Csihony *et al*., 2004).

Copyright by Kasetsart University All rights reserved

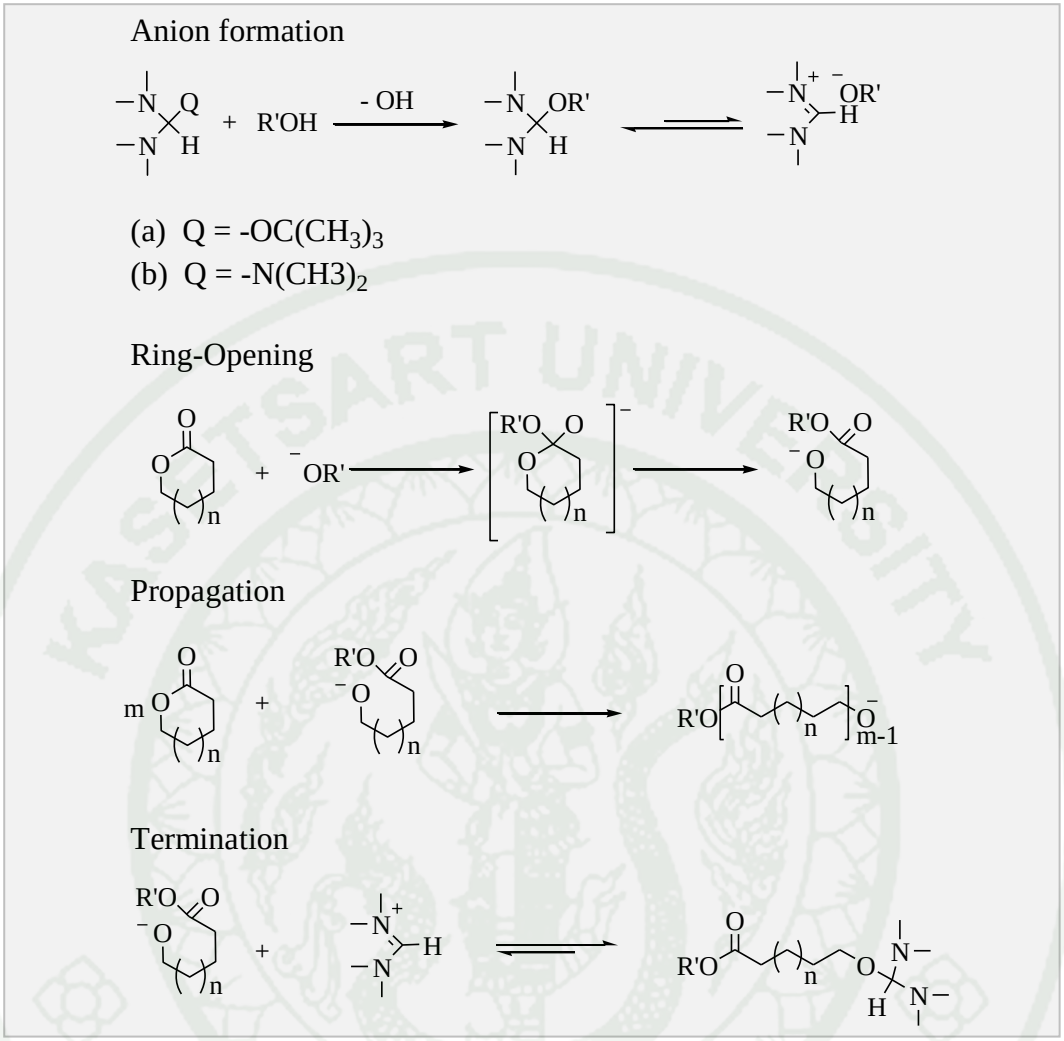

Figure 13 Proposed mechanism for anionic ring-opening polymerization of lactone by *tert*-butoxy bis(dimethylamino) methane and tris(dimethylamino) methane.

It can be seen that many the reagents can function as talent anionic initiators for ROP. The ring-opening of lactone by alkoxide generates a propagating anion, which can continue to ring open lactone through an anionic mechanism. The chain termination from reversible deactivation of the propagation anion by an electrophile or from amidinium counterion is normally observed during the polymerization process.

Copyright by Kasetsart University All rights reserved

8. Characterization

8.1 Characterization of PLA microstructure

The microstructure of PLA can be characterized using homonuclear decoupled ^{1}H NMR and proton decoupled ^{13}C NMR spectroscopy at the tetrad level. Stereoregular tetrad components are shown in **Figure 14** (Chisholm *et al.*, 1997). The letter *r* stands for the *racemic* linkage whereas *m* is noted for the *meso* linkage. The stereoselectivity are determined by the P_r and P_m values according to the probabilities of *racemic* linkage and *meso* linkage between the monomer units, respectively (Thakur *et al.*, 1997; 1998a; 1998b; Kasperczyz, 1995; 1996).

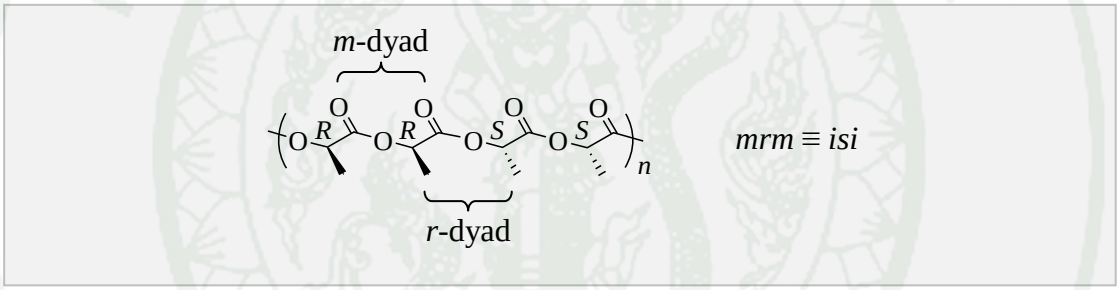

Figure 14 The microstructure of PLA at tetrad level (*m* = *meso*, {*m* ≡ *i*, isotactic}; *r* = *racemic*, {*r* ≡ *s*, syndiotactic}).

The homonuclear decoupled ^{1}H NMR spectrum of PLA from both *rac*-LA and *meso*-LA can exhibit five tetrad sequences as shown in **Table 1** (Chamberlain *et al.*, 2001). All sequences were defined according to Bernoullian statistics (Bovey and Mirau, 1996). The correlation peaks are observed at 5.15 to 5.25 ppm in the ^{1}H NMR spectrum and 69.4 to 69.0 ppm in the ^{13}C NMR spectrum. The assignments are shown in **Figure 15** (Zell *et al.*, 2002). In the case of *rac*-LA polymerization, P_m = 1 represents isotactic enriched PLA whereas P_r = 1 represents heterotactic enriched PLA. For *meso*-LA polymerization, syndiotactic polymer has P_r = 1 whereas a heterotactic polymer has P_m = 1. For both *rac*-LA and *meso*-LA, atactic PLA has P_r = P_m = 0.5 (Stanford and Dove, 2010; Ovitt and Coates, 2002).

Copyright by Kasetsart University All rights reserved

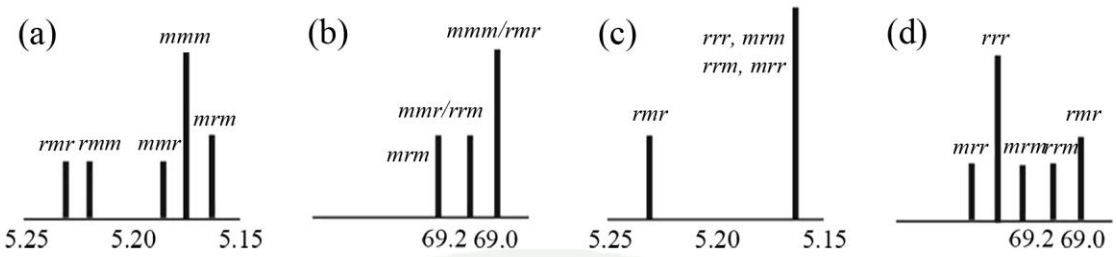

Figure 15 Schematic diagram to show chemical shift (in ppm) of the tetrads for PLA in (a) homonuclear decoupled ^{1}H NMR from *rac*-LA; (b) ^{13}C NMR from *rac*-LA; (c) homonuclear decoupled ^{1}H NMR from *meso*-LA; (d) ^{13}C NMR from *meso*-LA.

Table 1 Tetrad probabilities of PLA based on Bernoullian statistics.

tetrad	Probability	
	rac-LA	*meso*-LA
mmm	$P_m^2 + P_rP_m/2$	0
mmr	$P_rP_m/2$	0
rmm	$P_rP_m/2$	0
rmr	$P_r^2/2$	$(P_m^2 + P_rP_m)/2$
mrm	$(P_r^2 + P_rP_m)/2$	$P_m^2/2$
rrm	0	$P_rP_m/2$
mrr	0	$P_rP_m/2$
rrr	0	$P_r^2 + P_rP_m/2$

8.2 Characterization of polylactide-*co*-polycaprolactone (PLA-*co*-PCL)

The chemical composition of copolymers is determined by ^{1}H NMR spectroscopy through the ratio of the integrated intensity of the methine proton of PLA unit and methylene proton of PCL unit at 4.9-5.2 and 4.0-4.2 ppm, respectively (Nomura *et al.*, 2010). The full assignment of copolymer is shown in **Figure 16**. In the case of PLA-*co*-PCL, each signal relates to 2 protons. Therefore, the integrated intensities of each polymer can be compared directly. The percentage of CL-LA

Copyright by Kasetsart University All rights reserved

heterodiads can also be calculated from ^{1}H NMR by comparing the relative intensity ratio of the signals corresponding to methylene protons assigned as α(CL-CL), (a), or ε(CL-CL), (b), to that of the same methylene protons for the α(CL-LA), (f), or ε(CL-LA), (e), homosequences.

The chain microstructure of copolymer is determined by ^{13}C NMR spectroscopy. This technique is much sensitive to monomer sequencing and can be used to calculate an average length of polymer sequences in the copolymer (Vanhoorne *et al.*, 1992; Kasperczyk and Bero, 1991; 1993). The signals of carbonyl carbon between 165 to 175 ppm are very useful for a quantitative determination. The ^{13}C spectra of carbonyl regions of the copolymer as well as assignment of the peak according to the literature are shown in **Table 2** (Kasperczyk and Bero, 1991; 1993). The average lengths of lactidyl unit ($L_{LA} = L_{LL}$) and caproyl unit (L_C) were calculated from equation 1 and 2.

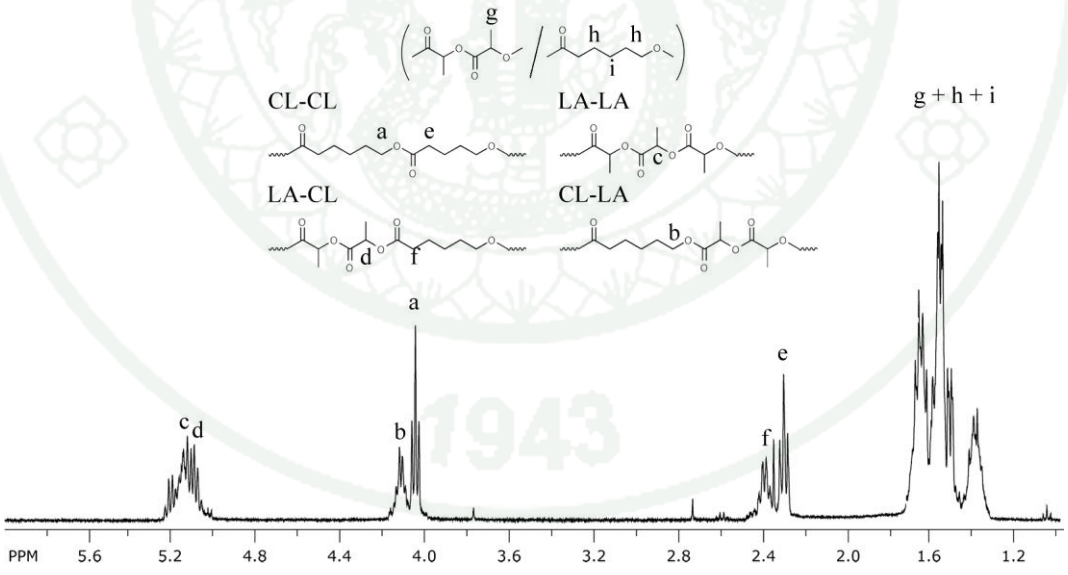

Figure 16 Full assignment of PLA-*co*-PCL.

$$L_{LL} = \frac{(LLLLLL + LLLLC + CLLLL + CLLC)}{(CLLC + {}^{1}/_{2}(LLLLC+CLLLL))} \quad (1)$$

Copyright by Kasetsart University All rights reserved

$$L_C = \frac{(LLCLL + CCLL + LLCC + CCCC)}{(LLCLL + {}^1/_2(CCLL+LLCC))} \quad (2)$$

where LLLLL, LLLLC, CLLLL, CLLC, LLCLL, CCLL, LLCC and CCC corresponding to the integrated values of triad sequence signals. For the synthesis of perfectly random copolymerization, L_{LL} and L_C are equal to 2.

Table 2 The triad assignments of carbonyl peaks of PLA-*co*-PCL.

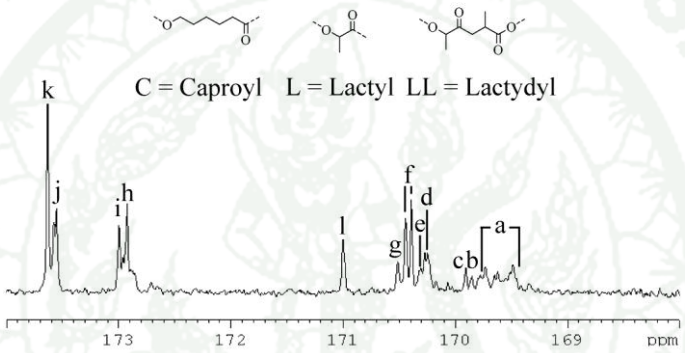

Peaks	δ, ppm	Triad(s)
a	169.1-169.7	LLLLLL
b	169.75	CLLLC
c	169.8	LLLLC
d	170.1	CLLLL
e	170.2	CLLLC
f	170.25-170.35	CLLC
g	170.4	LLLLC
h	172.8	LLCLL
i	172.9	CCLL
j	173.45	LLCC
k	173.55	CCC
l	170.8	CLC

Copyright by Kasetsart University All rights reserved

The peak corresponding to CLC sequence indicates the presence of second mode transesterification as illustrated in **Table 2** and **Figure 17**. The coefficient of second mode of transesterification, T_{II}, can be calculated by equation 3.

$$T_{II} = [CLC]_e / [CLC]_R \quad (3)$$

where $[CLC]_e$ is the experimentally determined concentration of CLC sequence from the ^{13}C NMR spectroscopy, and $[CLC]_R$ is the theoretical concentration for completely random chains calculated via Bernoullian statistic as presented in equation 4.

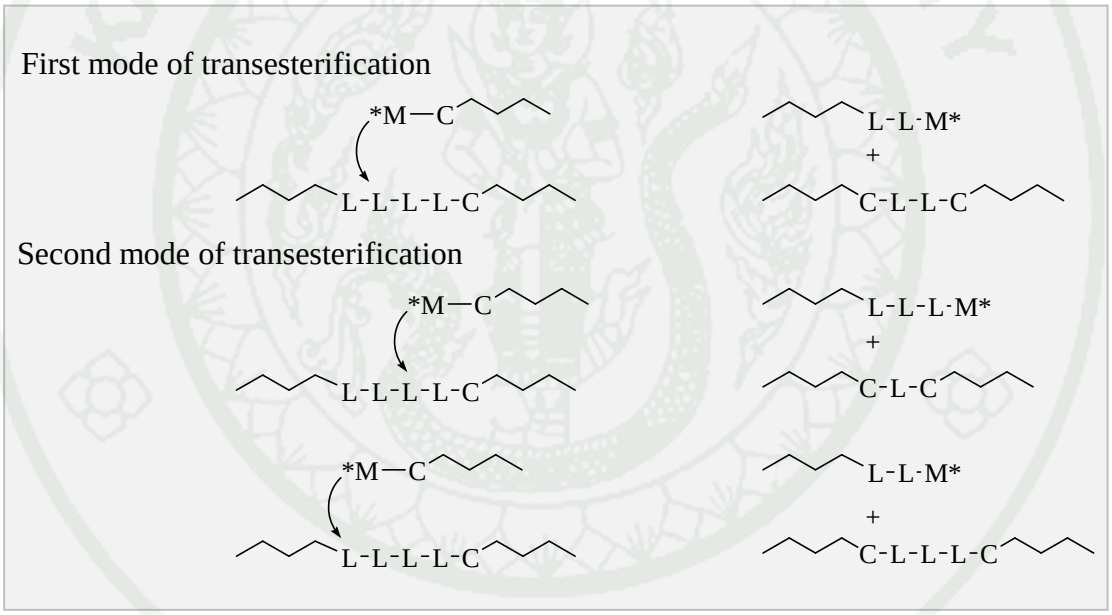

Figure 17 Possible mode of transesterification (C = caproyl unit, L = Lactyl unit and LL = Lactidyl unit).

$$[CLC]_R = k^2/(k+1) \quad (4)$$

where k = [CL]/[L]. The degree of randomness (R) of the copolymer is calculated from equation 5. The R value is in the range of 0 to 1 for block and completely random copolymers, respectively.

Copyright by Kasetsart University All rights reserved

$$R = L^{R}_{LL} / L^{e}_{LL} = L^{R}_{C} / L^{e}_{C} \quad (5)$$

where L^{e}_{LL} and L^{e}_{C} are the average length of the lactidyl and caproyl blocks, respectively, from experiment, L^{R}_{LL} and L^{R}_{C} represent the average length of the lactidyl and caproyl blocks, respectively, for chains with random distribution of units, as would be obtained by the complete transesterification *via* first and second mode. Both L^{R}_{LL} and L^{R}_{C} can be calculated from the following equation:

$$L^{R}_{LL} = (k + 1) / 2k \quad (6)$$

$$L^{R}_{C} = k+1 \quad (7)$$

9. Aluminum catalysts

Metal alkoxide such as aluminum triisopropoxide ($Al(O^{i}Pr)_3$) (Haruo *et al.*, 2005; Wang *et al*., 2006; Yalcin and Asgar, 2012), germanium tetraethoxide ($Ge(OEt)_4$) (Kricheldorf and Langanke, 2002), titanium tetraisopropoxide ($Ti(O^{i}Pr)_4$) (Kim *et al*., 2009), scandium trimethoxide ($Sc(OMe)_3$) (Ling *et al.*, 2009), samarium tri(4-*tert*-butyl-phenoxide) ($Sm(OC_6H_4C_3H_9)_3$) (Peng *et al.*, 2005), stannous di-*n*-butyl diisoproxide ($^{n}Bu_2Sn(O^{i}Pr)_2$) (Yang *et al.*, 2010; Malcolm *et al.*, 2007), zinc diethoxide ($Zn(OEt)_2$) (Mohammed and Robert, 2012; Malgorzata *et al*., 2011; Kathleen and Marc, 2004) and zirconium tetraisopropoxide ($Zr(O^{i}Pr)_4$) (Gamze and Kayan, 2012) are known to be important reagents widely employed as catalysts for the ROP of PLA and PCL.

Among these metal alkoxides, aluminum alkoxide has displayed excellent selectivity but poor activity. Aluminum is a trivalent metal center with Lewis acid properties. Aluminum(III)isopropoxide, $Al(O^{i}Pr)_3$, has been proved to be an active catalyst for the ROP of lactones. On the other hand, $Al(O^{i}Pr)_3$ is known to exist in a form of a mixture of trimer and tetramer aggregates. Due to the aggregation phenomenon, its activity is less active than the activity of $Sn(Oct)_2$ (Kowalski *et al.*,

Copyright by Kasetsart University All rights reserved

1998). Single-site aluminum alkoxide complexes, **LAlOX**, where **X** is alkyl, amide, exhibit better activity and stereoregularity than that of $Al(O^iPr)_3$. Since the breakthrough discovery of stereoselective polylactide polymerization using an enantiomormerically pure (SalBinap)AlEt/EtOH (Spassky and Wisniewski, 1996) and a *racemic* (SalBinap)AlO^iPr, many novel aluminum catalysts have been designed, synthesized and used in the ROP of lactones. The elevated number of single-site aluminum complexes containing bidentate, tridentate and tetradentate ligand(s) have been reported recently (Jianming *et al.*, 2014).

Copyright by Kasetsart University All rights reserved

OBJECTIVE

The overview objective of this research is focused on finding new effective and selective aluminum catalysts for ROP of lactones and their copolymerization. The work in these studies can be separated into two groups of aluminum catalysts. The first one is the aluminum complexes supported by bis(pyrrolidene) Schiff-base ligands and the second one is the aluminum complexes supported by Salan ligands. The synthesis of all aluminum complexes used an air-free technique involving the use of a glovebox and a Schlenk line. All complexes were characterized using NMR spectroscopy and elemental analysis techniques. The synthesized catalysts were examined as active initiators for *L*-LA, *rac*-LA and ε-CL polymerizations. The use of aluminum Salan complexes in the copolymerizations of ε-CL and *rac*-LA was investigated. The polymer characterization techniques, for example, gel permeation chromatography (GPC), differential scanning calorimetry (DSC), homonuclear decoupled and ^{13}C NMR spectroscopy were exploited.

Copyright by Kasetsart University All rights reserved

LITERATURE REVIEW

1. Stereoselective ROP of lactide

The stereoselective ring-opening polymerization of lactides has received much attention in recent years. A large number of investigations have been directed towards the development of efficient metal based initiators. The remarkable efficient initiators were summarized in this section.

1.1 Stereoselective ROP of *rac*-lactide

1.1.1 Synthesis of stereoblock PLA

In 1996, an enantiomorpic-pure binaphthyl Schiff-base aluminum complex **(*R,R*)-1** was found to be a highly selective initiator for the polymerization of *rac*-LA (Spassky *et al.*, 1996) in toluene at 70 ˚C. The chiral nature of the catalyst guided to the highly selective ROP of *L*-LA to give isotactic PLA. The polymerization rate of *L*-LA is 20 times faster than that of *D*-LA (k_L/k_D = 20). On the other hand, a chiral aluminum complex **(*R,R*)-2** based on (*R,R*)-cyclohexanediamine Schiff base showed higher selectivity over *D*-LA (k_D/k_L = 14) (Feijen *et al.*, 2002). In both systems, the chiral ligand induced the enantiomorphic site control of LA polymerization and led to the formation of stereocomplex and stereoblock PLAs with high melting temperature (T_m reached 210 ˚C). For racemic aluminum catalysts ***rac*-1** (Coates and Ovitt, 2000; 2002) and ***rac*-2** (Feijen *et al.*, 2003), isotactic stereoblock PLAs, which had lower melting temperature than that of PLA produced from complex **(*R,R*)-1** and **(*R,R*)-2**, were obtained through a polymer exchange mechanism where the growing polymer chains switch between *L*- and *D*- species. Notably, ***rac*-2** showed excellent isosectivity over *rac*-LA polymerization in the solvent-free condition at 130 ˚C.

Copyright by Kasetsart University All rights reserved

Achiral aluminum complexes **3** and **4a** were discovered by Nomura *et al.* and Chen *et al*., respectively (Nomura *et al.* 2002; Chen *et al*., 2004). In the presence of isopropyl alcohol, both complexes showed highly selective over *rac*-LA polymerization to generate stereoblock PLA *via* chain-end control mechanism. The P_m values are up to 0.91 and 0.90 for complex **3** and **4a**, respectively. In 2008, Nomura *et al*. introduced complex **4b**/isopropyl alcohol system for the production of isotactic stereoblock PLA (P_m = 0.98) with the outstanding T_m value of 210. This is the best stereoselective achiral catalyst/initiator system reported to date (Nomura *et al*. 2008).

It must be emphasized that an aminophenoxide aluminum complex **5** in the presence of benzyl alcohol catalyzed *rac*-LA to afford highly isotactic PLA material with a P_m value of 0.88. The polymerization was well-controlled and living (Hormnirun *et al.*, 2000).

Enolic tetradentate Schiff base aluminum catalyst **6**/isopropyl alcohol (Pang *et al*., 2007), **7** (Bouyahi *et al*., 2007) and **8** (Alaaeddine *et al.*, 2009) showed less dependence on chirality of ligand over the stereoselectivity. The P_m values were in the range of 0.80-0.87 for both chiral and achiral systems suggesting that stereocontrol was determined by a chain-end control mechanism.

Yasuniwa and co-workers synthesized a series of aluminum alkoxides bearing achiral ligands (**9a**-**9b**), chiral tridentate Schiff-base ligand (**9c**) and half-Salen ligand (**9d**) and achieved the controlled stereoselective polymerization of *rac*-LA using these aluminum complexes (Matsubara *et al*., 2012). In particular, the P_m value of the PLA initiated by **9d** was up to 0.9, whereas **9b** initiated the ROP of *rac*-LA efficiently even at room temperature in a pyridine solution with high stereoselectivity (P_m = 0.87). The behavior of these aluminum complexes in solution, including the inversion of the chirality at the aluminum center, was investigated. The detailed identification of PLA showed that the isotactic stereoblock copolymers generated in these processes. These results indicated that the significance of chiral aluminum center in the stereocontrolled polymerization.

Copyright by Kasetsart University All rights reserved

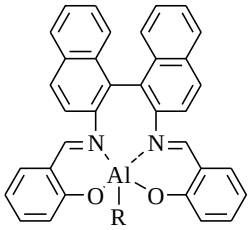

(*R*,*R*)-1: R = OMe
***rac*-1:** R = O^{i}Pr

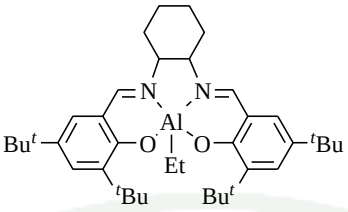

(*R*,*R*)-2
***rac*-2**

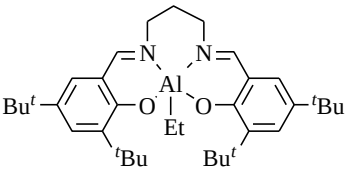

3

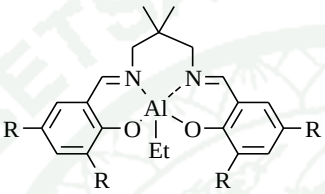

4a: R = ^{t}Bu
4b: R = Si(CH$_3$)$_2$^{t}Bu

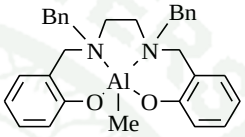

5

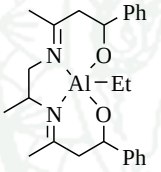

6

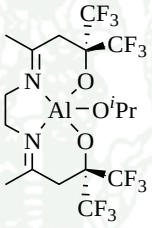

7

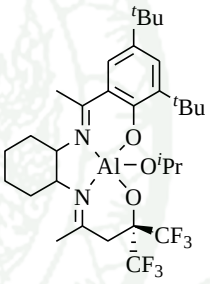

8

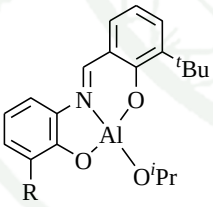

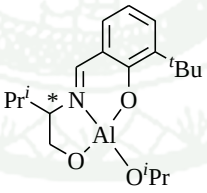

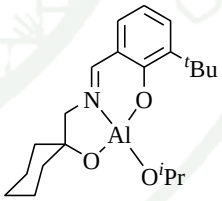

9a: R = H
9b: R = Me

9c

9d

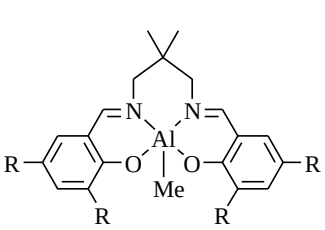

10a: R = CMe$_2$Ph

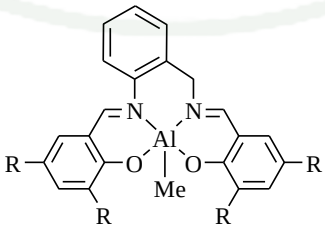

10b: R = CMe$_2$Ph

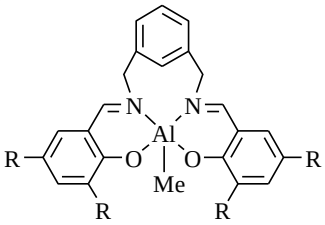

10c: R=CMe$_2$Ph

Figure 18 The structure of complexes **1-10**.

Copyright by Kasetsart University All rights reserved

Recently, Lin and coworkers reported the synthetic route of complexes **10a-10c** (Chen *et al*. 2012). All complexes were evaluated as a catalyst for the ROP of *rac*-LA in the presence of benzyl alcohol at 70 ˚C in toluene. Complexes **10a** and **10b** afforded highly isotactic PLA materials with the P_m values of 0.97 and 0.94, respectively. The difference in the observed P_m values was attributed to the flexibility of the backbone, in which 2,2-dimethyl-1,3-propanediamine linker was more flexible than 2-(aminomethyl)aniline backbone. Complex **10c** showed the same level of isoselectivity as complex **10a**.

Dinuclear zinc complexes comprising monodentate *N*-heterocyclic carbenes (NHCs) was first investigated by Tolman and coworker (Jensen *et al*., 2004). Polymerization of *rac*-LA using these complexes gave heterotactic bias PLA materials with the moderate P_r values of 0.60. These complexes were developed by introducing of more sterically hindered NHCs by Waymounth and coworker. Achiral carbene **11** produced highly isotactic PLA material with a P_m value of 0.90 from *rac*-LA at -70 ˚C.

Lanthanide metal complexes, such as yttrium, europium and erbium, exhibit higher polymerization rate for lactides than aluminum complexes. Among the lanthanide metal complexes, yttrium complex showed a high isoselective property for *rac*-LA polymerization. The homochiral yttrium complex **12** provided a very active initiator for the polymerization of *rac*-lactide. A highly isotactic PLA (P_m = 0.81) at 15 ˚C was produced in dichloromethane (Arnold *et al.*, 2008; 2009).

Recently, yttrium complexes supported by pentadentate iminophosphorane ligands **13a-13b** were explored by the Williams group (Bakewell *et al.*, 2012). Their isoselectivities over *rac*-LA polymerization in THF exceeded up to 0.8 at -15 ˚C. When the polymerization temperature reached the room temperature, the P_m value slightly dropped to 0.7.

Copyright by Kasetsart University. All rights reserved

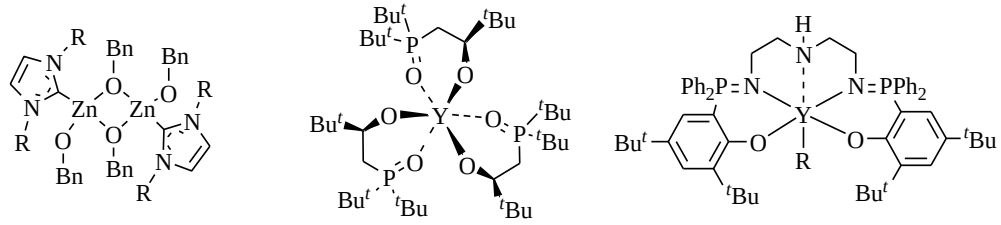

11: R = 2,4,6-trimethylphenyl **12** **13a:** R = O^{t}Bu **13b:** R = OEt

Figure 19 The structure of complexes **11-13**.

1.1.2 Synthesis of heterotactic PLA

The preparation of heterotactic polylactide from the ROP of *rac*-LA results from the alternate incorporation of *D*- and *L*-LA during the chain propagation *via* chain-end control mechanism. The high heteroselectivity can be observed from several metals such as aluminum, zinc, magnesium, gallium or lanthanide metal. Gibson's group found remarkable stereocontrol in the polymerization of *rac*-LA using aluminum complex **14** in toluene at 70 ˚C (P_r = 0.96). This is the first time that aluminum complex was found to furnish a highly heterotactic PLA (Hormnirun *et al.*, 2000).

Coates and co-workers reported a series of *β*-diiminate dinuclear achiral complexes **15a**-**15c** (Chamberlain *et al.*, 2001). Changing the ligand substituent from isopropyl (**15c**, P_r = 0.90) to ethyl (**15a**, P_r = 0.79) or *n*-propyl (**15b**, P_r = 0.76) resulted in a decrease in hetereotacticity (CH_2Cl_2, room temperature).

The monomeric zinc triphenylsalinoxide **16** with a coordinated THF had the same heterotactic selectivity towards *rac*-LA polymerization in THF as complex **15c** (Chisholm *et al.*, 2001). Magnesium complexes **17a-17b** did not show stereoselectivity toward ROP neither in CH_2Cl_2 or benzene but they had the same heteroselectivity in THF as complex **16** (Chisholm *et al.*, 2002; Chisholm and Phomphrai, 2003). For monometallic zinc or magnesium complexes **16, 17a-17b**, it

Copyright by Kasetsart University All rights reserved

was found that the coordinated THF molecule to central metal atom played an important role in enhancing the heteroselectivity of the complexes.

Dinuclear zinc complex **18** was synthesized by Lin and coworker (Chen *et al.*, 2006). This complex furnished heterotactic PLA material from *rac*-LA at -55 ˚C in THF with a P_r value up to 0.91.

The tridentate Schiff base ligand was demonstrated to give high level of hetereocontrol with calcium (Darensbourg *et al*., 2008) and indium (Douglas *et al.*, 2008). However, the reduction in heterospecificity was observed in both catalytic systems due to an equilibrium between an active monomeric species and an inactive dimeric form. A monomeric aryloxide tris-pyrazolyl borate calcium complex **19** showed a high level of hetereocontrol (P_r = 0.90) for *rac*-LA polymerization in THF (Chisholm *et al*., 2004). In addition, polymerization of *rac*-LA was very rapid. A 90% conversion within 5 minutes was achieved.

Germanium complex **20** supported by C_3-symmetric amine(trisphenolate) ligand was reported by Davidson and co-workers (Chmura *et al*., 2007). This complex showed excellent hetereocontrol (P_r = 0.78-0.82) under the solvent-free condition at 130 ˚C. Zirconium and hafnium complexes containing C_3-symmetric amine(trisphenolate) ligands (**21** and **22**) were employed in both solution at ambient temperature and solvent free condition at 130 ˚C. These complexes gave the same level of stereocontrol (**21**, P_r = 0.96; **22,** P_r = 0.88) (Chmura *et al*., 2008).

Okuda and co-workers synthesized a series of scandium complexes supported by 1,ω-dithiaalkanedily-bridged bis(phenolate) ligands. Scandium complex **23** showed excellent heterotactic control in *rac*-LA polymerization. The controlling abilities were improved by the presence of the coordinated THF and the bulky substituents at the *ortho* position of the phenol group (Ma *et al*., 2006; Liu *et al*., 2007). At 25 ˚C in THF, complex **23** afforded heterotactic PLA materials from *rac*-LA with a P_r up to 0.96.

Copyright by Kasetsart University All rights reserved

Yttrium complex **24a** with the bulky and conformationally flexible *α,α*-dimethylbenzyl groups at the *ortho* and *para* positions of the phenol group produced substantial PLAs with the P_r value up to 0.90 at 20 ˚C in THF (Amgoune *et al*. 2006; 2007). Yttrium complexes **24b** and **24c** displayed modest activity but high stereoselectivity in the polymerization of *rac*-LA to give highly heterotactic PLA materials with the P_r values ranking from 0.95 to 0.99 (Amgoune *et al*., 2007).

An investigation by the Tolman group demonstrated that the combination of indium(III) chloride, triethyl amine and benzyl alcohol resulted in highly heterotactic PLA with the P_r value up to 0.90 (Pietrangelo *et a*l., 2009). The stereocontrol in this system was postulated to be a result of the formation of complex species in which lactide bound to the metal was acted as an ancillary ligand.

1.2 Stereoselective ROP of *meso*-lactide

1.2.1 Synthesis of syndiotactic PLA

A high level of syndiotactic PLA materials with the P_r value up to 0.96 was prepared from the ROP of *meso*-LA using complex **(*R*,*R*)-1** in toluene at 70 ˚C. Due to the enantiomerically pure properties of complex **(*R*,*R*)-1**, Coates and Ovitt proposed that the mechanism occurred *via* an enantiomorpic site controlled mechanism. The PLA exhibited a T_g value of 45 ˚C and a T_m value of 153 ˚C. This is the only catalyst that produces syndiotactic PLA with the highest thermal properties. Some of achiral metal complexes were also applied for *meso*-LA polymerization. However, the stereoselectivity of these metal complexes were very poor, for example dinuclear zinc complex **15c** and Yttrium complex **24a** afforded syndiotactic PLAs with the moderate P_r values of 0.76 and 0.75, respectively.

1.2.2 Synthesis of heterotactic PLA

The formation of heterotactic PLA materials from *meso*-LA polymerization is rarely found to date. A few cases have been reported on the

Copyright by Kasetsart University All rights reserved

synthesis of heterotactic PLA materials with fairly P_m values. Complex ***rac*-1** gave heterotactic PLA with a P_m value up to 0.80 from the ROP of *meso*-LA. The polymer exchange mechanism was proposed to explain the novel formation. The fast switching of each individual polymer chain between enantiomeric aluminum centers is a key for the insertion of the next monomer unit. The free carbene of complex **11** was prepared to produce a heterotactic biased PLA with a P_m value of 0.83 in THF at -40 ˚C.

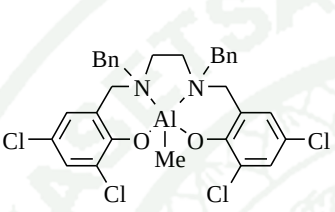

14

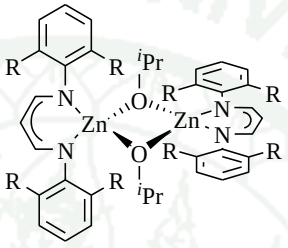

15a: R = Et
15b: R = ^{n}Pr
15c: R = ^{i}Pr

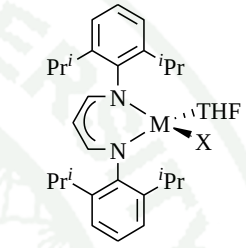

16: M = Zn; X = OSiPh$_3$
17a : M = Mg; X = N^{i}Pr$_2$
17b: M = Mg; X = O^{t}Bu

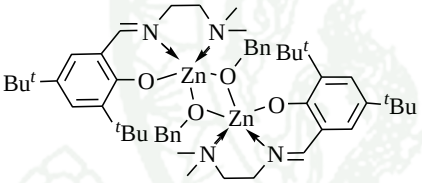

18

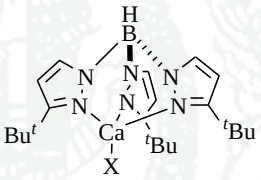

19: X = OC_6H_3-2,6-^{i}Pr

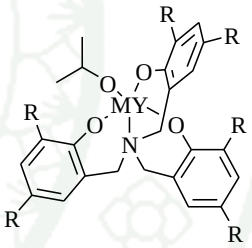

20: M = Ge; R= Me
21: M = Zr; R= ^{t}Bu
22: M = Hf; R= ^{t}Bu

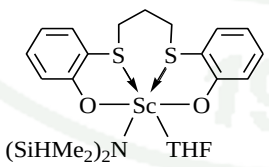

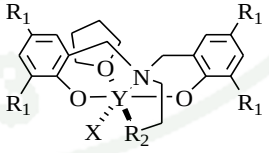

23

24a: R_1 = CMe_2Ph; R_2 = OMe; X= $N(SiHMe_2)_2$
24a: R_1 = CMe_3; R_2 = NMe_2; X= CH_2SiMe_3
24b: R_1 = CMe_3; R_2 = NEt_2; X= CH_2SiMe_3

Figure 20 The structure of complexes **14-24**.

Copyright by Kasetsart University All rights reserved

2. Aluminum metal complexes

Metal alkoxide, metal amine and metal halide have been widely reported to use as initiators for the ROP of cyclic esters. Among the metal alkoxides, aluminum complexes have received considerable attention due to their ability and activity to control the ROP. Selected aluminum complexes reported to date were summarized in this section.

2.1 Bidentate ligands

2.1.1 N,N Ligands

Complexes **25a**-**25d** were synthesized by a treatment of $AlEt_2Cl$ and the corresponding lithium salts. Complexes **25b**-**25c** showed poor activity for *L*-LA polymerization, whereas complex **25a** and **25d** were found to be active catalysts for the ROP of *L*-LA (Liu *et al*., 2010). Complex **26** was synthesized by the Bergman group (Koller and Bergman, 2011). It showed high activities for the ROP of various lactones such as ε-CL, TMC, δ-VL and *rac*-LA in the absence of solvent or alcohol cocatalysts. Gong and Ma synthesized a series of aluminum ethyl complexes **25a**-**25m** bearing symmetrical and asymmetrical β-diketiminate ligands (Gong and Ma, 2008). Aluminum complexes **27a**-**275m** initiated the ROP of ε-CL at 80 ˚C. However, all complexes displayed moderate activities for the polymerization of ε-CL, and produce the polymer with broad molecular weight distributions (PDI = 1.66-3.74). The structure of the ancillary ligands had a significant influence on the polymerization behavior of the corresponding aluminum complexes.

Recently, bis(pyrrolylaldiminato) aluminum methyl complexes **28a**-**28g** were synthesized from the reaction of trimethyl aluminum and two equivalents of the corresponding pyrrolylaldimine ligands (Supathana *et al*., 2013). The ligands were modified to have different steric and electronic contributions. Polymerizations of *L*-LA using complexes **28a**-**28g** in a presence of benzyl alcohol were investigated to reveal to the effects of steric (**28e** < **28d** < **28c** < **28b** < **28a**) and electronic (**28f** < **28g**

Copyright by Kasetsart University All rights reserved

< **28a**) on the polymerization rate. The introduction of the bulky substituents and the electron withdrawing groups was found to suppress the polymerization rate. The presence of substituents also improved the isoselectivity of **28b**-**28d** for the ROP of *rac*-LA polymerization.

Hormnirun and coworkers studied the effects of the ligand structure and the coordination geometry around the aluminum complexes supported by pyrrolylaldiminate ligands on the polymerization activities of *rac*-LA (Tabthong *et al*., 2014). Two series of aluminum alkyl complexes, dimethyl aluminum pyrrolylaldiminates (**29a**-**29g**) and monomethylaluminum pyrrolylaldiminates (**30a**-**30g**), were reported. All complexes promoted the living ring-opening polymerization of *rac*-lactide in the presence of benzyl alcohol with a good control over M_n and PDIs. Complexes **29f** and **29g** were found to efficiently mediate the immortal polymerization in the presence of up to 5 equivalents of benzyl alcohol as evidenced by the narrow PDI values and the good agreement between the experimental M_n values and monomer/benzyl alcohol ratios. The steric and electronic effects of the imine nitrogen substituents played a major role on the polymerization activities both in activity and selectivity. The catalytic activity decreased as follows: **c** > **a** ≈ **b** ≈ **e** > **d** >> **f** > **g**. In comparison, the catalytic activity of the monomethylaluminum complexes **29a**-**29g** is slightly higher than that of the dimethylaluminum counterpart **30a**-**30g**. The polymerization of *rac*-lactide by **30f** furnished heterotactically enriched PLA with the P_r value up to 0.60 whereas **30g** produced the isotactic-enriched polymer with the P_m value of 0.74.

2.1.2 N,O Ligands

Bidentate Schiff base N,O ligands employed in aluminum initiators were reported to have an significant impact on the rate of the ring-opening polymerization. Aluminum complexes containing phenoxy-imine ligand **31a-31r** were synthesized and used for the ROP of ε-CL in the presence of benzyl alcohol at 25 ˚C in toluene (Nomura *et al*., 2005). The imino substituent played an important role for the efficient ROP in a controlled manner. The electron-withdrawing substituents in combination with the steric effect of imine moiety enhanced the

Copyright by Kasetsart University All rights reserved

polymerization rate. The introduction of the bulky substituent on the salicylidene moiety also led to a high activity of the catalyst. Although complex **31a** was also effective for the ROP of δ-VL under the same condition, the polymerization rate of β-BL was much slower even at 70 ˚C. The linear relationship between monomer conversion and M_n with narrow PDI indicated that the ROP proceeded in a living/controlled manner. However, the loss of controlled manner was observed at high conversion of ε-CL as resulted in broadening the PDIs.

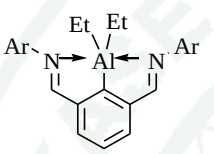

25a: Ar = C_6H_5
25b: Ar = 2,6-Me_2-C_6H_3
25c: Ar = 2,6-Et_2-C_6H_3
25d: Ar =2,6-^{i}Pr$_2$-C_6H_3

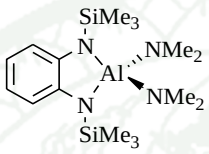

26

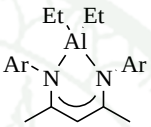

27a: Ar = C_6H_5
27b: Ar = 4-Me-C_6H_4
27c: Ar = 4-OMe-C_6H_4
27d: Ar = 4-Cl-C_6H_4
27e: Ar = 4-F-C_6H_4
27f: Ar = 2-F-C_6H_4
27g: Ar = 4-CF_3-C_6H_4
27h: Ar = 2-CF_3-C_6H_4

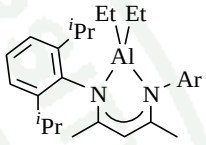

27i: Ar = C_6H_5
27j: Ar = 4-OMe-C_6H_4
27k: Ar = 4-Cl-C_6H_4
27l: Ar = 4-F-C_6H_4
27m: Ar = 2,6-Me_2-C_6H_3

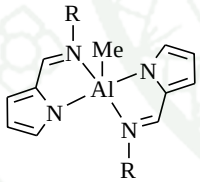

28a: Ar = C_6H_5
28b: Ar = 2,6-$Me_2C_6H_3$
28c: Ar = 2,4,6-$Me_3C_6H_2$
28d: Ar = 2,6-$Et_2C_6H_3$
28e: Ar = 2,6-^{i}Pr$_2$C$_6$H$_3$
28f: Ar = 4-$CF_3C_6H_4$
28g: Ar = 4-OMe-C_6H_4

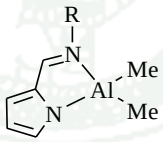

29a: Ar = C_6H_5
29b: Ar = 4-F-C_6H_4
29c: Ar = 4-Me-C_6H_4
29d: Ar = 4-OMe-C_6H_4
29e: Ar = 2-Me-C_6H_4
29f: Ar = 2-^{t}Bu-C_6H_4
29g: Ar = Adamantyl

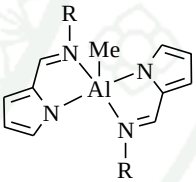

30a: Ar = C_6H_5
30b: Ar = 4-F-C_6H_4
30c: Ar = 4-Me-C_6H_4
30d: Ar = 4-OMe-C_6H_4
30e: Ar = 2-Me-C_6H_4
30f: Ar = 2-^{t}Bu-C_6H_4
30g: Ar = Adamantyl

Figure 21 The structure of complexes **25-30**.

A series of aluminum complexes bearing phenoxy-imine ligand **32a-32i** were further investigated by the Nomura group (Jiu *et al*., 2008). The polymerizations of ε-CL were examined at 25 ˚C in the presence of benzyl alcohol. In each case, the catalytic activity was strongly influenced by the imino substituent. The efficient and

Copyright by Kasetsart University All rights reserved

the living polymerization were achieved using complex **32i** with C_6F_5 unit. Complexes **32c**-**32k** were used for the ROP of *δ*-VL and *rac*-LA (Iwasa *et al.*, 2008). The polymerizations were examined at 60 ˚C in the presence of benzyl alcohol. The results also revealed that the imino substituent had a strongly impact on both catalytic activity and catalytic efficiency. Complexes **32i** and **32l** showed moderate catalytic activity in the ROP of *rac*-LA, but the resulting polymer possessed no stereoregularity. The attempts to polymerize of *β*-BL and *γ*-BL resulted in negligible amount of polymer, suggesting that the system was not suitable for six to seven membered ring cyclic ester. Pellecchia and coworkers tested complexes as an initiator for the ROP of *ε*-CL, *L*-LA and *rac*-LA. Methanol and $B(C_6F_5)_3$ were used an initiator. Polymerizations were carried out in toluene at 25 or 70 ˚C. All complexes were found to be very efficient initiators in the presence of methanol. In contrast, $B(C_6F_5)_3$ led to the low activity and the broad PDI, suggesting a cationic mechanism of polymerization was operative (Pappalardo *et al*., 2009).

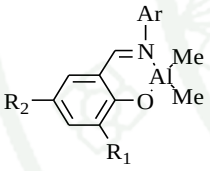

31a: R_1 =R_2 =H Ar = C_6H_5
31b: R_1 =R_2 =H Ar = 2,6-Me_2-C_6H_3
31c: R_1 =R_2 =H Ar = 2,6-^{i}Pr$_2$-C_6H_3
31d: R_1 =R_2 =H Ar = 2,4.6-Ph_3-C_6H_2
31e: R_1 =R_2 =H Ar = 2,4,6-^{t}Bu$_3$-C_6H_2
31f: R_1 =R_2 =H Ar = 2,4.6-F_3-C_6H_2
31g: R_1 =R_2 =H Ar = 4-Cl-C_6H_4
31h: R_1 =R_2 =H Ar = 2,6-Cl_2-C_6H_3
31i: R_1 =R_2 =H Ar = 2,4.6-Cl_3-C_6H_2
31j: R_1 = H;R_2 =Me Ar = 2-^{t}Bu-C_6H_4
31k: R_1 = Me; R_2 =H Ar = 2-^{t}Bu-C_6H_4
31l: R_1 = R_2 = Me Ar = 2-^{t}Bu-C_6H_4
31m: R_1 = ^{i}Pr; R_2 =H Ar = 2-^{t}Bu-C_6H_4
31n: R_1 = Ph;R_2=Me Ar = 2-^{t}Bu-C_6H_4
31o: R_1 = R_2 = ^{t}Bu Ar = 2-^{t}Bu-C_6H_4
31p: R_1 = R_2 = Br Ar = 2-^{t}Bu-C_6H_4
31q: R_1 = R_2 =Me Ar = 2-^{t}Bu-C_6H_4
31r: R_1 = R_2 = ^{t}Bu Ar = C_6H_6

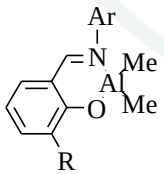

32a: R = Me Ar = 2,6-^{i}Pr$_2$-C_6H_3
32b: R = Me Ar = ^{t}Bu
32c: R = ^{t}Bu Ar = 2,6-^{i}Pr$_2$-C_6H_3
32d: R = ^{t}Bu Ar = ^{t}Bu
32e: R = ^{t}Bu Ar = Cyclohexyl
32f: R = ^{t}Bu Ar = Adamantyl
32g: R = ^{t}Bu Ar = C_6H_5
32h: R = ^{t}Bu Ar = 2,6-Me_2-C_6H_3
32i: R = ^{t}Bu Ar = C_6F_5
32j: R = ^{t}Bu Ar = 2,4.6-Me_3-C_6H_2
32k: R = ^{t}Bu Ar = 2,4.6-^{t}Bu $_3$-C_6H_2

Figure 22 The structure of complexes **31-32**.

The catalytic activities of aluminum alryloxides **33a**-**33e** toward ROP of *rac*-LA and *ε*-CL were studied in the presence of alcohol using toluene as a solvent (Zhang and Wang, 2008). The polymerization using complex **33** proceeded much

Copyright by Kasetsart University All rights reserved

slower than those using complexes **31** and **32** even at the elevated temperature (110 ˚C). In each polymerization reaction, the M_n value was much higher than the calculated value suggesting the small number of active species. Hence, the ROP did not take place in a living manner. In addition, complex **33b** was inactive for the ROP of *rac*-LA under the same condition.

A series of aluminum complexes supported by *β*-ketoamino ligands **34a**-**34d** were synthesized and employed in the ROP of *ε*-CL (Lin *et al.*, 2008). The polymerization temperature was varied in the range of 50-70 ˚C. The 3-position substituents on *β*-ketoamino ligand of the aluminum complexes influenced the catalyst activity remarkably for the ROP of *ε*-CL in the absence of an initiator. The order of catalytic activity was **34a** > **34b** > **34c** > **34d**. The resulting polymers had broad PDIs in the range of 1.92-2.63.

In 2011, Carpentier and co-workers examined the coordination chemistry of the bidentate fluorinated alkoxyimino ligand and the aluminum center (Bouyahyi *et al.*, 2012). The proligands were reached selectively with $AlMe_3$ to give the corresponded monoligand **35a**-**35d** and the bis-ligand complexes **36a**-**36d**. The catalytic abilities of all complexes were evaluated in the ROP of *rac*-LA and *ε*-CL. In the absence of alcohol, complexes did not initiate the ROP of *rac*-LA at 60 ˚C and *ε*-CL at room temperature. In the presence of alcohol, all complexes were found to readily polymerize both *rac*-LA at 60 ˚C and *ε*-CL at room temperature. The reaction proceeded in a control fashion. To demonstrate the living-immortal ROP of **36a**-**36d**, the amount of benzyl alcohol as a chain transfer agent was varied from 1-5 equivalents. Polymer mass analysis by MALDI-TOF showed only a major product of linear polymer. No cyclic isomer was detected. The synthesized PLAs were all essentially atactic.

Williams and coworkers reported the synthetic pathway of a series of bis(8-quinolinato)aluminum ethyl complexes (Bakewell *et al.*, 2012). All complexes were viable initiators for the ROP of *rac*-lactide in the presence of isopropyl alcohol. The first-order rate constants were observed. However, polymerizations using complexes

Copyright by Kasetsart University All rights reserved

37a-**37h** and **37j** were very slow. On the other hand, complex **37i** showed faster rate; k_{obs} was one-order of magnitude higher. There were clear differences in the degree of isoselectivity of these complexes, *i.e*. the degree of stereoselectivity was depending on the size of the R_1 substituent. In the series, the highest isoselectivity was obtained from **37g** (P_m = 0.76).

Aluminum complex **38** was synthesized by Ko and co-worker in 2011 (Li *et al*., 2011). The treatment of **38** with water afforded an air stable oxo-bridge dimer complex. Both complexes **38** and its dimer were tested as catalysts toward the ROP of *L*-LA in the presence and absence of 9-anthracenemethanol under various conditions. The PDIs of PLLA produced were all narrow, ranging from 1.04 to 1.16, and a linear relationship between M_n and $[LA]_0/[9\text{-AnOH}]_0$ existed. The ^{1}H NMR spectrum of PLLA displayed that the polymer chain was capped with one 9-anthracenemethyl ester and one hydroxyl chain end. Surprisingly, aluminum complex **38** was found to be less active than its analogue but had a similar control of PDI toward the ROP of *L*-LA.

2.1.3 S,O Ligands

Lin and co-workers synthesized a series of aluminum complexes bearing 2-methoxybenzenethiol **39a**-**39b** as shown in **Figure 24** (Huang *et al*., 2001). All complexes initiated the ROP of *ε*-CL and *δ*-VL. The polymerization was carried out at 25 ˚C in toluene. The experimental results showed that these aluminum thiolate complexes initiated the ROP of lactones in a controlled fashion, giving polymer with narrow PDIs and thiolate chain end.

A series of aluminum complexes supported by phenoxy-thioether (OS) ligands **40a**-**40d** were synthesized (Lamberti *et al*., 2012). Their catalytic performances in *ε*-CL, *L*-LA, and *rac*-LA ring-opening polymerizations were explored. In all cases, the polymerizations proceeded in a controlled fashion and the immortal character was achieved upon addition of an excess of methanol. End group analyses of the obtained oligomer samples supported a classical coordination-insertion mechanism. The

Copyright by Kasetsart University All rights reserved

substituents at the *ortho* position of the aromatic ring bound to the sulfur atom had a moderate effect on the catalytic behavior of the aluminum complexes. In particular, the presence of a substituent at the *ortho* position of the thiophenol aryl ring resulted in an increase of the catalytic activity in the *ε*-CL polymerization, regardless of the size and the electronic character of the substituent, whereas in the polymerization of LA, a decrease in the catalytic activity was observed by increasing the size of the substituent.

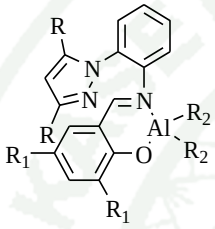

33a: R = Me R_1 = H R_2 = Me
33b: R = Me R_1 = ^{t}Bu R_2 = Me
33c: R = Me R_1 = H R_2 = Me
33d: R = Ph R_1 = ^{t}Bu R_2 = Me
33e: R = Ph R_1 = ^{t}Bu R_2 = Et

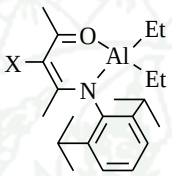

34a: X = Cl
34b: X = H
34c: X = Ph
34d: X = Me

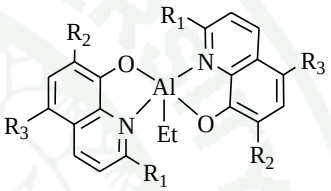

37a: R_1 = Me R_2 = R_3= H
37b: R_1 = Me R_2 = H; R_3 = Me
37c: R_1 = Me R_2 = R_3= Cl
37d: R_1 = Me R_2 = R_3= Br
37e: R_1 = Me R_2 = H; R_3 = Cl
37f: R_1 = Me R_2 = I; R_3 = Cl
37g: R_1 = Me R_2 = R_3= I
37h: R_1 = Me R_2 = Me; R_3 = H
37i: R_1 = ^{t}Bu R_2 = R_3 = H
37j: R_1 = Me R_2 = H; R_3 = OMe

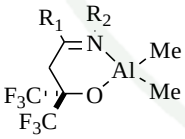

35a: R_1 = Ph R_2 = Bn
35b: R_1 = Me R_2 = Bn
35c: R_1 = Ph R_2 = Ph
35d: R_1 = Ph R_2 = Cy

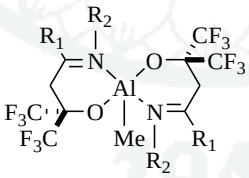

36a: R_1 = Ph R_2 = Bn
36b: R_1 = Me R_2 = Bn
36c: R_1 = Ph R_2 = Ph
36d: R_1 = Ph R_2 = Cy

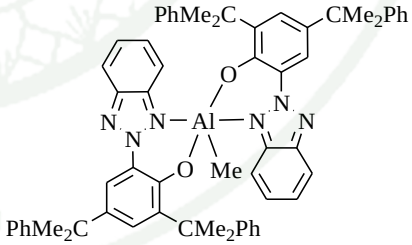

38

Figure 23 The structure of complexes **33-38**.

Copyright by Kasetsart University All rights reserved

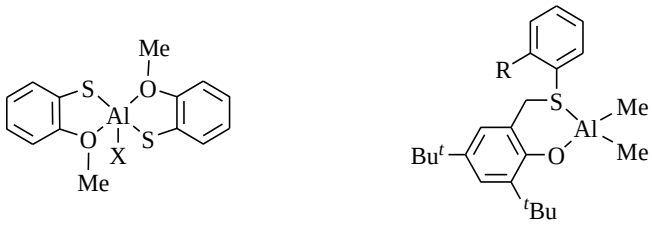

39a: X = Me
39b: X = Cl

40a: R = H
40d: R = Br
40e: R = Me
40f: R = CF_3

Figure 24 The structure of complexes **39-40**.

2.2 Tridentate ligand

2.2.1 N,O,N Ligand

In 2004, Huang and coworkers prepared aluminum complexes bearing dianionic amine bis(phenolate) ligands **41a** and **41b** (Chen *et a*l., 2004). All complexes were used as a catalyst for the ROP of *ε*-CL. The polymerization reactions were carried out in toluene at 50 ˚C in the presence of benzyl alcohol. All complexes showed excellent catalytic activity and behaved in a controlled manner toward the ROP of *ε*-CL. Moreover, the living and immortal characters were also observed even up to 8 equivalents of alcohol was added.

In 2011, Ma and Wang reported the synthesis of aluminum complexes **42a-42c** supported by quinoline-based N,N,O-tridentate ligands (Ma and Wang, 2011). The kinetic studies for the polymerization of *ε*-CL catalyzed by complexes **42a-42c** in the presence of benzyl alcohol indicated that the polymerizations proceeded with the first-order dependence on monomer concentration. The polymerization was well controlled and gave a polymer with narrow molecular weight distribution.

The N,O,N-supported tetracoordinate amidoaluminum complexes **43a** and **43b** were synthesized by Dagorne and coworkers (Hild *et al*., 2011). Both complexes effectively polymerized TMC at room temperature in a highly controlled manner to

Copyright by Kasetsart University All rights reserved

yielded narrowly PDI polymeric materials in either presence or absence of benzyl alcohol. The molecular weight results supported that the ROP polymerization by **43a** and **43b**/BnOH proceeded in an immortal manner, with benzyl alcohol acting as a chain transfer agent.

The mono-adduct aluminum methyl complexes **44a**-**44d** showed the potential to perform as catalysts toward the ROP of *L*-LA in the presence of benzyl alcohol (Chuang *et al*., 2012). It was found that a great catalytic activity and a "controlled" character were achieved with a **44**:BnOH molar ratio of 1:2 in toluene at 110 ˚C. Experimental results indicated that all complexes exhibited good activities. Among them, complex **44b** showed the greater "controlled" character than other complexes. As a result, polymerizations catalyzed by **44b** were systematically investigated the "living" character. The ^{1}H NMR spectrum of PLLA displayed that the PLLA chain was capped by benzyl ester one of chain end and hydroxyl at another chain end. The "immortal" character of complex **44b** was further investigated using excess equivalent BnOH (up to 50 equivalents) as the chain transfer agent. It was worthy of note that complex **44b** in the presence of excess amounts of BnOH (>10 equivalents) showed the improved catalytic activity and the better controlled behavior (PDI ≈ 1.20) at 110 ˚C.

2.2.2 N,N,N Ligand

The synthesis of methyl- and hydridoaluminum complexes, **45a**-**45b**, was reported by Bertrand and coworkers (Emig *et al.*, 1998). All complexes initiated the polymerization of *rac*-LA in benzene at 80 ˚C. The hydride complex **45b** showed about two times active than the methyl aluminum derivative **45a**. Carrying out the reaction at 100 ˚C led to the higher catalytic activities but the PDI value became broader. High molecular weight polymers were obtained in good yields. However, the PDI values were relatively broad (PDI = 1.61-1.79).

Catalysis of complexes **46**-**47** for the ROP of ε-CL was tested (Chai *et al.*, 2008). At room temperature, the polymerization was very slow, but at 60 ˚C the

Copyright by Kasetsart University All rights reserved

polymerization become faster. The results of the polymerizations catalyzed by **46-47** showed that both monomer conversion and the polymer molecular weight increased with time. It was also noted that in each polymerization reaction the observed M_n of polymer was higher than the calculated value suggesting the significant number of intermolecular chain transfer occurred during the polymerization.

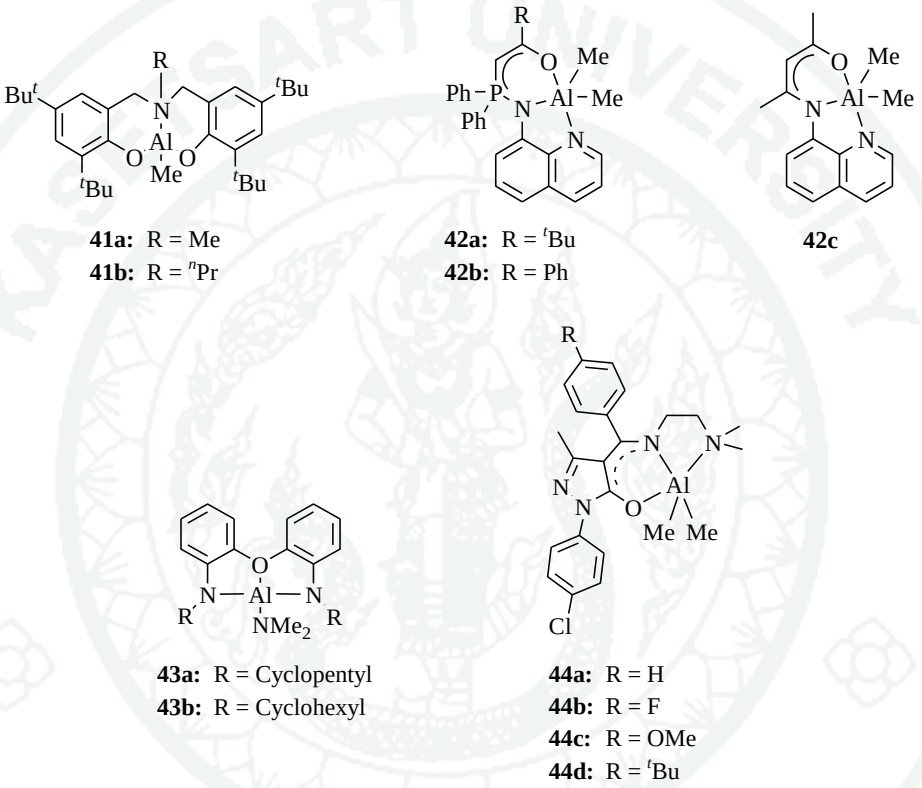

Figure 25 The structure of complexes **41-44**.

A series of aluminum complexes containing tridentate pyrrolyl ligands **48a-48c** were synthesized by Changa *et al.* (Changa *et al.*, 2011). All complexes showed activity in the ROP of *ε*-CL and produced high molecular weight PCL. However, the PDI values of PCL were relatively broad ranging from 1.12 to 1.41. This may be attributed to the side reactions or the multiple reacting sites (Al-H or Al-R). Steric effect was considered as the main reason for the observed different activities of these complexes toward the ROP of *ε*-CL. The short Al-H bond lengths prevents the monomer from coordinating to the aluminum center and blocks the polymerization, whereas the longer Al-N and Al-S bond lengths allow the polymerization to proceed.

Copyright by Kasetsart University All rights reserved

Ma and Wang investigated a series of aluminum complexes supported by quinoline-based *N*,*N*,*N*-chelate ligands **49a**-**49c** (Ma and Wang, 2011). All complexes initiated the ROP of 200 equivalents of ε-CL at an elevated temperature in the presence of benzyl alcohol. All complexes exhibited almost the same activity at 70 ˚C. However, at 30 ˚C complex **49b** was slightly more active than **49c** and **49a**. The M_n closely matched the calculated values. The PDIs were relatively narrow, ranging from 1.08 to 1.38. These results implied that the polymerizations were well controlled. In addition, the aluminum complexes **49a**-**49c** showed higher catalytic activity and better control than the *N*,*N*,*O*-chelate aluminum complexes **49a**-**49b**. However, all complexes were inactive toward the ROP of *rac*-LA in the presence or absence of benzyl alcohol.

The aluminum complexes **50a**-**50c** were investigated as initiators for the ring-opening polymerization of *L*-LA (Yang *et al*., 2012). The polymerizations were carried out in toluene at 70 ˚C. In an absence of alcohol, all aluminum complexes were almost inert for lactide polymerization and no polymer was obtained even at high temperature. However, when activated with benzyl alcohol, the activities were improved and full conversions were achieved in 24 h. The activities and M_w of the resulted polymer showed independence on the bulkiness of the *ortho* groups of *N*-aryl moieties.

2.3 Tetradentate ligand

2.3.1 N,N,O,O Ligand

An achiral aluminum Schiff base methoxide complex **51a** was discovered by Spassky and co-workers (Spassky *et al*., 1993). This complex showed the abilities to control the ROP polymerization of *rac*-lactide. Aluminum complexes supported by tetradentate ligands have been received much attention since then. Further studies by Montaudo *et al.* indicated that the polymerization using **51a** showed the first order kinetic in both LA and catalyst (Montaudo *et al.*, 1996). However, transesterifications always occur during the course of polymerization.

Copyright by Kasetsart University All rights reserved

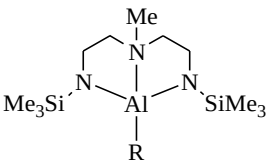

45a: R = Me
45b: R = H

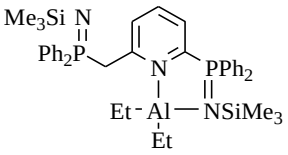

46

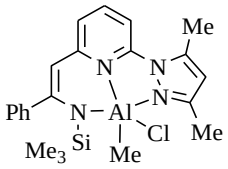

47

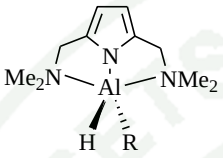

48a: R = H
48b: R = $SCPh_3$
48c: R = NH-2,6-^{i}Pr-C_6H_3

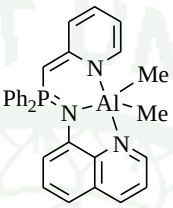

49a

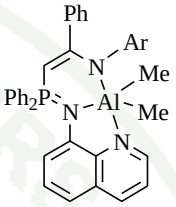

49b: R = C_6H_5
49c: R = 4-Me-C_6H_4

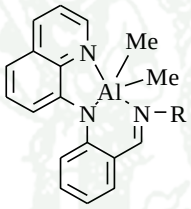

50a: R = 2,6-Me_2-C_6H_3
50b: R = 2,6-Et_2-C_6H_3
50c: R = 2,6-$^{i}Pr_2$-C_6H_3

Figure 26 The structure of complexes **45-50**.

Gibson and co-workers reported the synthesis of a aluminium methyl complex supported by Schiff base of *N*,*N*′-bis(salicylidene)-1,2-ethylenediamine **51b** and used of this complex as an initiator for ROP of *rac*-LA in CH_2Cl_2 (Cameron *et al*., 1999). It was found that the polymerization at ambient temperature showed living characteristic. Furthermore, the transesterification was not observed during the course of polymerization. In 2000, Spassky and co-workers reported the modification of Salen ligand at the imine position by introducing the methyl group on both imine carbons (Bhaw-Luximon *et al*., 2000). The modified initiator called Al(Happen)OMe (**45c**) displayed higher activity than **51a** and **51b**. The living polymerizations without

Copyright by Kasetsart University All rights reserved

transesterification reactions were also observed in both CH_2Cl_2 at 25˚C and toluene at 70 ˚C.

Nomura and co-workers examined two series of substituted catalysts with difference number of methylene group on the ligand backbone as shown in **Figure 27** (Nomura *et al.,* 2002). The polymerizations of *rac*-LA were carried out in toluene in the presence of **52** or **53** at 70˚C. The catalytic reactivities of **53a**-**53e** were higher than those of **52a**-**52e**. In agreement with the previous results, the larger R_1 generally induced a higher isotacticity.

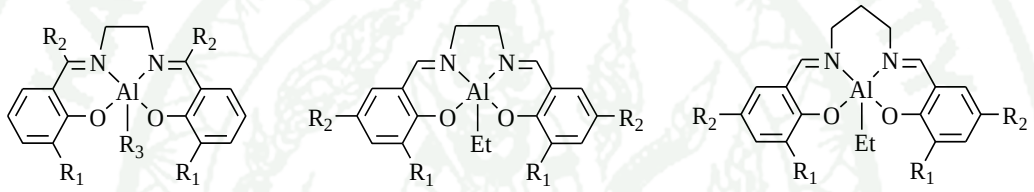

51a: R_1 = H, R_2 = H, R_3 = OMe
51b: R_1 = Cl, R_2 = H, R_3 = OMe
51c: R_1 = H, R_2 = Me, R_3 = OMe

52a: $R_1 = R_2$ = H
52b: $R_1 = R_2$ = Me
52c: $R_1 = {}^{i}$Pr, R_2 = H
52d: R_1 = Ph, R_2 = H
52e: $R_1 = R_2 = {}^{t}$Bu

53a: $R_1 = R_2$ = H
53b: $R_1 = R_2$ = Me
53c: $R_1 = {}^{i}$Pr, R_2 = H
53d: R_1 = Ph, R_2 = H
53e: $R_1 = R_2 = {}^{t}$Bu

Figure 27 The structure of Salen aluminum complexes **51**-**53**.

The steric effect of methylene-bridge was investigated by Jing and coworkers in 2004 (Tang *et al*., 2004). Various substituents were introduced to the backbone. Complex **54a** showed high catalytic activity and good stereoselectivity whereas complex **54b** revealed a low catalytic activity. The presence of two bulky benzyl substituents on the backbone of complex **54c** reduced the stereoselectivity as well as the catalytic activity. The kinetic study using complex **54a** showed the first order in both monomer and initiator. A linear relationship between *rac*-LA conversion and molecular weight of poly(*rac*-LA) was observed. The molecular weight distribution data were very narrow throughout the course of polymerization.

In 2006, the synthesis of aluminum Salen complexes **55**-**62** containing various types of diamino-bridge linkage and different substituents on the phenoxy rings was

Copyright by Kasetsart University All rights reserved

reported by Gibson and co-workers (Hormnirun *et al.*, 2006). Both the phenoxy substituents and the backbone linkers have a significant influence on the polymerization activities. For complexes **55**-**57** the apparent rate constants (k_{app}) were increased in the presence of chloro substituent group. The introducing bulky *tert*-butyl group resulted in an increase of P_m values. However, the polymerization rate was slower. In the cases of complexes **57**-**60**, the use of aromatic backbone linkers caused the reduction of polymerization rate and the decrease of stereoselectivity for the *rac*-LA polymerization. The P_m values were increased by introducing the bulky *tert*-butyl group but the polymerizations were retarded. For complexes **61** and **62**, the polymerization rates were relatively slow and poor stereoselectivity was observed.

In 2007, a series of achiral and chiral-Salen aluminum complexes **63**-**65** were described by Nomura and co-workers (Nomura *et al*., 2007). All complexes were used for the polymerization of *rac*-LA in toluene at 70 ˚C. The results showed that the high stereoselectivity PLAs (P_{meso} = 0.86-0.97) and low PDIs (1.05-1.08) were observed at high conversion. The highest reactivity and selectivity in this system was obtained with complex **64e**. The isotactic selectivity was produced *via* a chain-end controlled mechanism.

Aluminum complexes **66** and **67** were reported by Jing and coworkers (Du *et al.*, 2007). Both complexes showed high efficiency for *rac*-LA polymerization. The observed molecular weights were very close to the calculated values and the PDIs were also narrow (1.08-1.10). Additionally, both complexes showed relatively high steroselectivity for *rac*-LA polymerization (P_m = 0.62-0.71).

In 2012, a series of achiral and chiral-Salen aluminum complexes **68a-68f** were described by Lin and co-workers (Chen *et al*., 2012). Ring-opening polymerization of *L*-LA and *rac*-LA using complexes **68a**-**68f** as an initiator were systematically studied at 70 ˚C in toluene. Each of these complexes displayed good activities for the polymerizations of both *L*-LA and *rac*-LA with a good correlation between the observed molecular weight and the calculated value. The narrow

Copyright by Kasetsart University All rights reserved

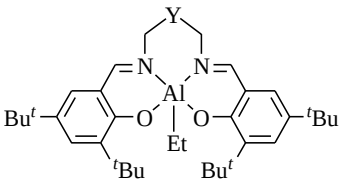

54a: Y = $C(CH_3)_2$
54b: Y = $C(CH_2CH_3)_2$
54c: Y = $C(Bn)_2$

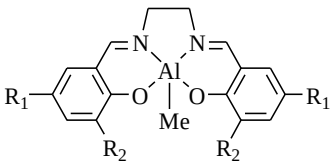

55a: $R_1 = R_2 = H$
55b: R_1 = Cl, R_2 = H
55c: $R_1 = R_2$ = Cl
55d: $R_1 = R_2 = {}^t$Bu

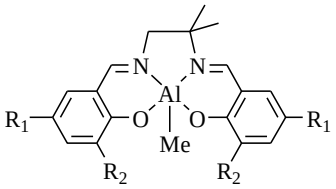

56a: $R_1 = R_2 = H$
56b: $R_1 = R_2$ = Cl
56c: $R_1 = R_2 = {}^t$Bu

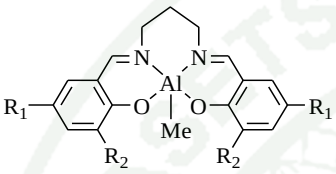

57a: $R_1 = R_2$ = H
57b: $R_1 = R_2$ = Cl
57c: $R_1 = R_2 = {}^t$Bu

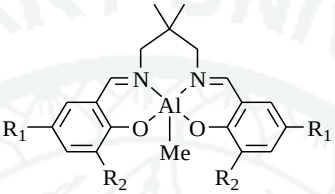

58a: $R_1 = R_2$ = H
58b: $R_1 = R_2$ = Cl
58c: $R_1 = R_2 = {}^t$Bu
58d: $R_1 = R_2$ = Br

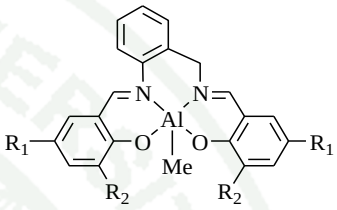

59a: $R_1 = R_2$ = H
59b: $R_1 = R_2$ = Cl
59c: $R_1 = R_2 = {}^t$Bu

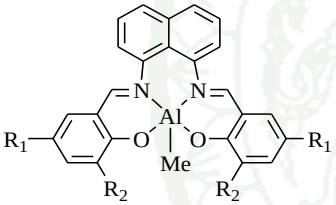

60: $R_1 = R_2 = {}^t$Bu

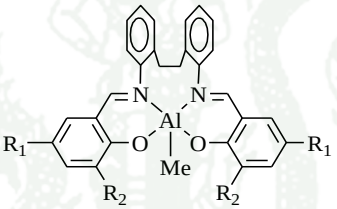

61a: $R_1 = R_2$ = H
61b: $R_1 = R_2$ = Cl
61c: $R_1 = R_2 = {}^t$Bu

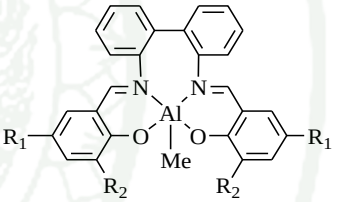

62a: $R_1 = R_2$ = H
62b: $R_1 = R_2$ = Cl
62c: $R_1 = R_2 = {}^t$Bu

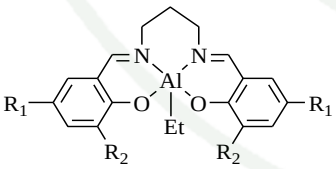

63a: R_1 =H, $R_2 = {}^t BuC_6H_3$
63b: R_1= H, $R_2 = Me_3Si$
63c: R_1= Ph, $R_2 = Me_3Si$

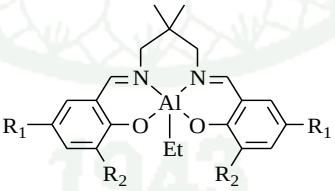

64a: R_1= H, $R_2 = Me_3Si$
64b: R_1= Ph, $R_2 = Me_3Si$
64c: R_1= H, $R_2 = Et_3Si$
64d: $R_1 = CF_3$, $R_2 = Et_3Si$
64e: R_1= H, $R_2 = {}^t BuMe_2Si$
64f: R_1= H, $R_2 = Ph_3Si$
64g: R_1= H, $R_2 = {}^i Pr_3Si$
64h: R_1= H, $R_2 = {}^t BuPh_2Si$
64i: R_1= H, $R_2 = {}^n Bu_3Sn$

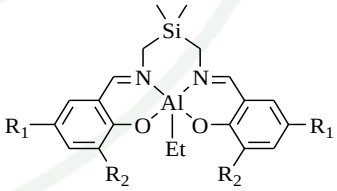

65: R_1 = Ph, $R_2 = Me_3Si$

Figure 28 The structure of Salen aluminum complexes **54-65**.

Copyright by Kasetsart University All rights reserved

molecular weight distributions ranging from 1.06 to 1.10 were also observed. For complexes **68a** and **68b**, a linear relationship between the M_n and $[M]_0/[I]_0$ ratio and the low PDIs of the polymer indicated the highly controlled and "living" character of the polymerization process. Further investigation of **68f** by varying the monomer to initiator ratio showed that the living polymerization characteristic was maintained even at different ratios. However, complexes **68d** and **68e** had less catalytic activity, probably due to the presence of bulky substituents on the diamine backbone.

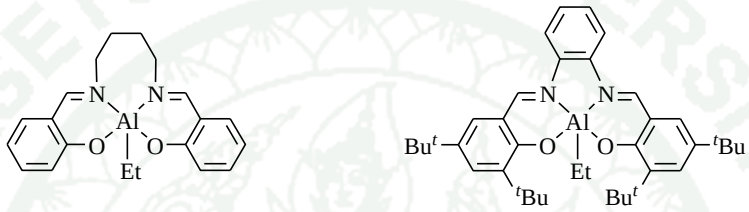

66 **67**

Figure 29 The structure of Salen aluminum complexes **66-67**.

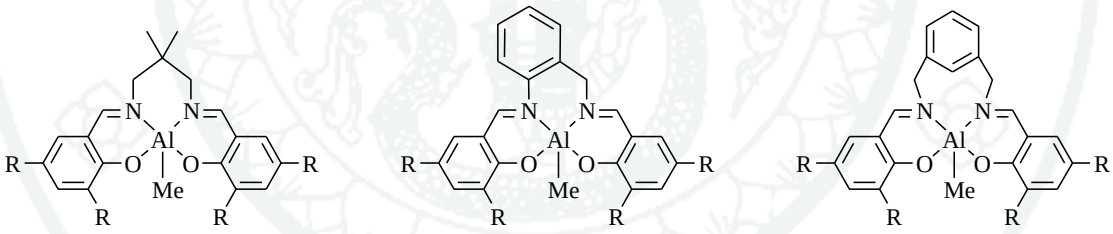

68a: R = CMe_2Ph **68b:** R = CMe_2Ph **68c:** R = CMe_2Ph

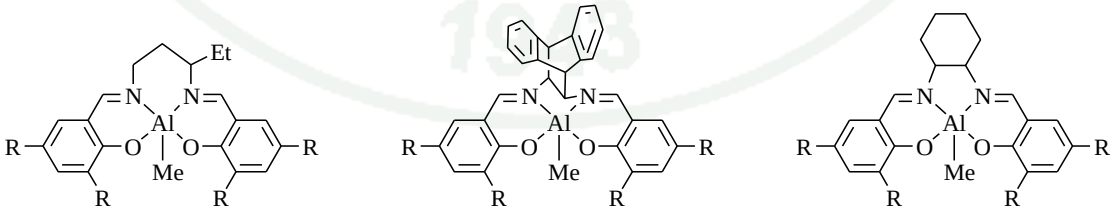

68d: R = CMe_2Ph **68e:** R = CMe_2Ph **68f:** R = CMe_2Ph

Figure 30 The structure of Salen aluminum complexes **68**.

Copyright by Kasetsart University All rights reserved

Aluminum complexes supported by "Salan" type ligand were reported by Gibson and co-worker (Hormnirun *et al.*, 2004). In comparison, Salan ligand has higher flexibility due to the presence of sp^3 hybridized nitrogen donors in the Salan derivatives. Structures of complex **69a-69h** were shown in **Figure 31**. Polymerizations were carried out in toluene at 70 ˚C. In all cases, aluminum complexes showed high controlled fashion (PDI = 1.04-1.11) at high conversion. Moreover, the molecular weights were in close agreement with the calculated values. An increase in the size of ligand substituents resulted in the reduction of polymerization rate whereas the introduction of electron-withdrawing substituents caused the increase of polymerization rate. High levels of isoselectivity were observed from polymerizations using complexes **69a** and **69e**. In the case of complex **69g**, heterotactic PLA was obtained.

Chen, Feijen and co-workers have reported the synthesis of aluminum ethyl complexes supported by chiral tetradentate phenoxyamine ligands (Du *et al*., 2007). In the presence of isopropanol, enantiomerically pure (*R,R*) complexes **70a-70c** and their racemic mixtures, ***rac*-70a**-***rac*-70c,** were efficient catalysts for the ring-opening polymerization of *rac*-LA, as evidenced by the resulting PLAs having the number average molecular weights corresponding to the theoretical values and narrow molecular weight distributions. Isotactic biased PLAs were obtained from polymerizations using **(*R,R*)-70a** and ***rac*-70a** (P_m = 0.66 and 0.62, respectively), whereas **(*R,R*)-70c** and ***rac*-70c** furnished atactic PLAs with P_r values of 0.55 and 0.57, respectively. Complex **(*R,R*)-70b** afforded heterotactic biased PLA (P_r = 0.64) by a chain-end control mechanism. The P_m value was increased to 0.73 when *rac*-LA was polymerized using complex ***rac*-70a**.

Hormnirum and co-workers had reported the preparation of aluminum methyl complexes supported by achiral tetradentate phenoxyamine ligands **71a-71d** (Sumrit and Hormnirun, 2013). In the presence of benzyl alcohol, all complexes displayed heteroselective polymerization to give heterotactic-enriched PLAs with P_r values ranging from 0.64 to 0.74. The character of the ligand substituents from the two different phenolic rings and the complex fluxionality arising from the ligand

Copyright by Kasetsart University All rights reserved

interconversion were suggested to be responsible for the different levels of stereoselectivity and activity.

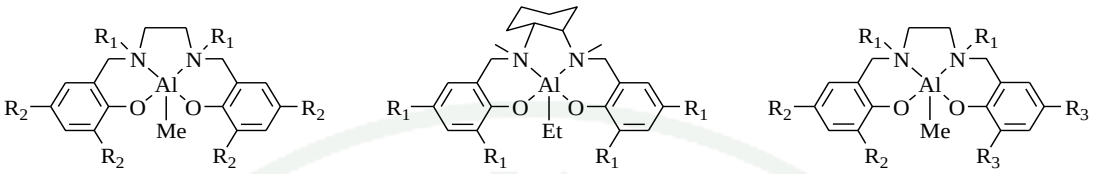

69a: R_1 = Me; R_2 = H
69b: R_1 = Me; R_2 = Me
69c: R_1 = Me; R_2 = ^{t}Bu
69d: R_1 = Me; R_2 = Cl
69e: R_1 = Bn; R_2 = H
69f: R_1 = Bn; R_2 = Me
69g: R_1 = Bn; R_2 = ^{t}Bu
69h: R_1 = Bn; R_2 = Cl

R_1 = H: **(*R*,*R*)-70a**, ***rac*-70a**
R_1 = Cl: **(*R*,*R*)-70b**, ***rac*-70b**
R_1 = Me: **(*R*,*R*)-70c**, ***rac*-70c**

71a: R_1 = Me; R_2 = ^{t}Bu; R_3 = H
71b: R_1 = Me; R_2 = ^{t}Bu; R_3 = Me
71c: R_1 = Me; R_2 = ^{t}Bu; R_3 = Cl
71d: R_1 = Bn; R_2 = ^{t}Bu; R_3 = Cl

Figure 31 The structure of Salan aluminum complexes **69-71**.

In 2011, Jones and co-workers reported the first use of aluminum Salalen complexes **72a-72h** for the ring opening polymerization of *rac*-LA in a presence of benzyl alcohol (Whitelaw *et al*., 2011). At 80 and 100 ˚C, polylactides with narrows PDIs (1.04-1.56) and moderate degree of stereoselectivity (P_r in the range of 0.39-0.74) were formed. Polylactide synthesized from **72d** revealed the presence of benzyl alkoxide end group. The repeating unit of the polymer was 144 mass units suggesting that only a small degree of transesterification taking place.

A series of aluminum complexes supported by *N*,*N*,*O*,*O*-tetradentate enolic Schiff-base ligands were reported by Jing and co-workers (Pang *et al.,* 2007). Complexes **73a-73b** have identical diimine linker but different enol substituents while complexes **73b** and **74** have the same enol structure but different imine bridge moieties. Polymerizations of *rac*-LA were carried out in the presence of isopropanol. In all cases, first-order kinetics in monomer were observed. All the three complexes provided the characteristic features of the living polymerization as shown by the linear relationship between number-average molecular weight and the percentage of LA conversion. The k_{app} values for **73a-73b** and **74** were 0.085 h^{-1}, 0.047 h^{-1} and 0.046 h^{-1}, respectively. Polymerization using **73a** showed higher stereoselectivity (P_m = 0.77) when compared with **73b** and **74**.

Copyright by Kasetsart University All rights reserved

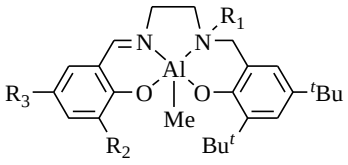

72a: R_1 = Me; R_2 = R_3 = ^{t}Bu
72b: R_1 = Ph; R_2 = R_3 = ^{t}Bu
72c: R_1 = Me; R_2 = Me; R_3 = H
72d: R_1 = Ph; R_2 = Me; R_3 = H
72e: R_1 = Me; R_2 = R_3 = H
72f: R_1 = Ph; R_2 = R_3 = H
72g: R_1 = Me; R_2 = R_3 = Cl
72h: R_1 = Ph; R_2 = R_3 = Cl

Figure 32 The structure of Salalen aluminum complexes **72**.

Jing and co-workers reported a series of enolic Schiff base aluminum complexes with different steric and electronic properties (Pang *et al.*, 2008). Polymerizations using aliphatic diimine backbone complexes **75-76** and aryl diimine backbone complexes **77a-77b** were carried out in toluene at 70 ˚C. In all cases, the first order kinetics in monomer were observed. The molecular weight also followed a linear relationship in monomer conversion. Lengthening the backbone from C_2 alkylene to C_3 alkylene gave rise to significant increase in activity. In this series, complex **76b** had the highest activity and the stereoselectivity owing to the C_3 alkylene backbone and the two gem-methyl groups on the middle carbon atom.

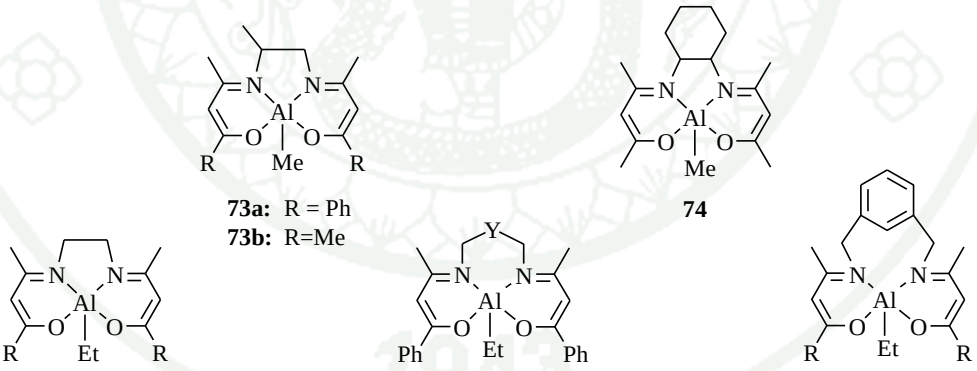

73a: R = Ph
73b: R=Me

74

75a: R = Me
75b: R= Ph
75c: R = CF_3

76a: Y = CH_2
76b: Y= $C(CH_3)_2$

77a: R = Ph
77b: R=Me

Figure 33 The structure of aluminum complexes **73-77**.

A family of aluminum methyl complexes supported by tetradentate phenoxy-amine ligands was prepared by Gibson and co-workers in 2007 (Tang *et al.*, 2007). Complexes **78a-78d** were employed in the ring-opening polymerization of *rac*-LA at

Copyright by Kasetsart University All rights reserved

70 ˚C in toluene. Active complexes were generated by *in situ* alcoholysis with benzyl alcohol. Complexes **78a** and **78c** afforded well controlled fashion of PLA with moderate isotactic bias. The P_m values of **78a** and **78b** were 0.73 and 0.65, respectively. However, complexes **78c** and **78d** afforded atactic PLA.

In 2007, Wu reported the synthesis of aluminum complexes supported by a sulfonamide/Schiff base ligands (Wu *et al.*, 2007). Complex **79** was used to prepare alkoxide species by alcoholysis with benzyl alcohol. The polymerization of *L*-LA using complex **79** showed narrow PDIs (1.05-1.10). Hence, the living character of the polymerization was proved. However, complex **79** had slightly lower selectivity for the polymerization of *rac*-LA (P_m = 0.60) than aluminum alkoxide complexes supported by Salen ligand. This was attributed to the less bulky of the sulfonamide/Schiff base ligand.

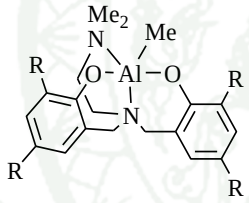

78a: R = Me
78b: R = ^{i}Pr
78c: R = Cl
78d: R = ^{t}Bu

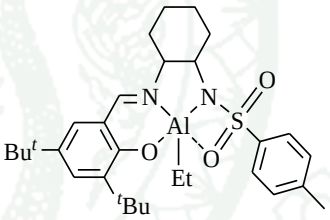

79

Figure 34 The structure of aluminum complexes **78-79**.

2.3.2 N,N,N,N Ligand

Chen and Feijen reported a series of achiral bis(pyrrolidene) Schiff base aluminum complexes **80a-80c** (Du *et al*., 2009). Aluminum isopropoxide species were generated by *in situ* alcoholysis and then used as initiators for *rac*-LA polymerization. The observed molecular weights closed to the calculated values and the narrow PDIs indicated of a living polymerization. All aluminum complexes polymerized *L*-LA to give isotactic PLLA without epimerization. The polymerization

Copyright by Kasetsart University All rights reserved

of *rac*-LA produced isotactic polymer whereas atactic PLA was obtained from the polymerization of *meso*-LA. The activity of *rac*-LA polymerization decreases in the following order: **80a** > **80b** > **80c**.

Phomphrai and co-workers have reported a series of aluminium complexes supported by N_2O_2 bis(phenoxy)-amine ligands (Phomphrai *et al.*, 2010). Complexes **81a-81c** had a different arrangement of N_2O_2 moieties around aluminum canter. All complexes were tested for the polymerization of *rac*-LA in toluene at 70 ˚C. The polymerization catalyzed by **81a** reached 92% conversion in 16 hours, affording isotactic polymer with enhanced isotactic bias. The resulting PLAs had a closed-to-calculated molecular weight with slightly narrow PDI (PDI = 1.28). In comparison, complexes **81b** and **81c** were much less active for the ROP of *rac*-LA.

The ROP capability of a sulphonamide-supported aluminum alkoxide and alkyl complexes were reported by Mountford and co-workers (Schwarz *et al*., 2010). Complexes **82a**-**82b** were accessed for their ROP performance for *rac*-LA in toluene at 70 ˚C. The kinetic studies of both complexes showed the first order consumption of *rac*-LA and well-controlled polymerization process (PDI = 1.11-1.14). Polymerizations using **83a**-**83b** gave PLAs with molecular weights higher than the calculated values and broader PDIs. In contrast, complex **84** showed reasonably well-controlled ROP.

2.3.3 S,S,O,O Ligand

Aluminum alkyl complexes supported by [OSSO] type bisphenolato ligands **85-86** were reported by Okuda and coworker in 2005 (Ma *et al.*, 2005). All complexes were reacted with isopropanol to generate alkoxide initiators for the ROP of *rac*-LA. Polymerizations were carried out in toluene at 70 ˚C. The first order dependence on monomer concentration was observed for **85a** with k_{app} = 9.57x10^{-5} s^{-1}. For comparison, complex **85b** had lower polymerization rate (k_{app} = 0.83x10^{-5} s^{-1}) when compared with complex **85a**. In all cases, PDIs were narrow at high conversion (1.04-1.08) and heterotactic-enriched PLA were obtained.

Copyright by Kasetsart University All rights reserved

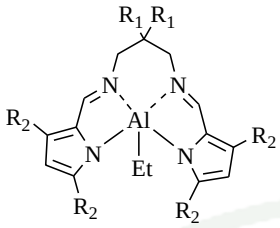

80a: $R_1 = R_2 = H$
80b: $R_1 = Me$, $R_2 = H$
80c: $R_1 = Me$, $R_2 = Me$

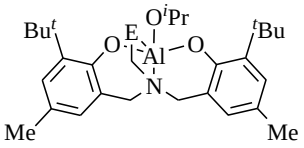

81a: E = Py
81b: E = CH_2NMe_2
81c: E = CH_2NEt_2

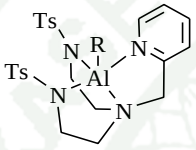

82a: R = O^{i}Pr
82b: R = OBn

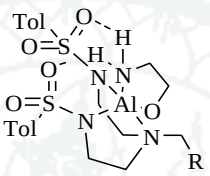

83a: R = Ph
83b: R = CH_2OMe

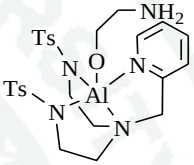

84

Figure 35 The structure of aluminum complexes **80-84**.

The racemic chiral methyl aluminum complex **87** was synthesized and used for the polymerization of *rac*-LA in the presence of isopropanol (B. Lian *et al.*, 2009). Preliminary kinetic studies indicated a first order dependence in monomer concentration with k_{app} = 1.70 x10^{-4} s^{-1}. Over the entire conversion range, M_w increased linearly with the conversion up to 95%. The results suggested a controlled-living polymerization. The PLAs showed narrow molecular weight distribution (PDI = 1.05-1.11) and the experimental M_w values were closed to the calculated values. The homonuclear decoupled ^{1}H NMR spectra at the methine region of PLAs showed an atactic microstructure.

Copyright by Kasetsart University All rights reserved

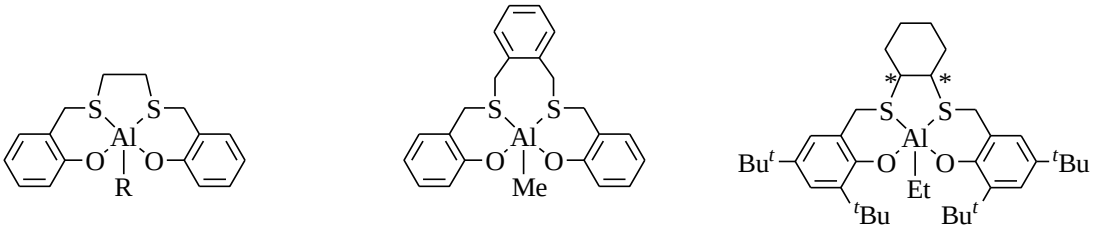

85a: R = Me
85b: R = Et

86

87

Figure 36 The structure of aluminum complexes **85-87**.

Copyright by Kasetsart University All rights reserved

MATERIALS AND METHODS

1. General considerations

All manipulations with air- and/or moisture-sensitive compounds were carried out under a dry nitrogen atmosphere using standard Schlenk and cannula techniques. Toluene was distilled from Na-benzophenone and stored over activated 4 Å molecular sieves. Hexane and pentane were distilled from CaH_2 under nitrogen and stored over activated 4 Å molecular sieves. Benzyl alcohol was refluxed over sodium and then freshly distilled to an ampoule. All solvents were degassed prior to use unless stated otherwise. NMR solvents were dried over 4 Å molecular sieves and were freeze-pump-thaw degassed three times. A 2.0 M solution of trimethylaluminum in toluene (Aldrich) was used without purification. 1,2-Ethylenediamine (99%), 1,3-propanediamine (99%), 2,2-dimethyl-1,3-propanediamine (99%), 2-(aminomethyl) benzenamine (98%) , 1,4-butanediamine (99%), 1,2-phenylenediamine (99.5%), *rac*-1,2-diaminocyclohexane (99%), pyrrole-2-carboxaldehyde (98%), salicylaldehyde (98%), sodium borohydride (98%), *N*,*N*′-dimethylethylenediamine (99%), *N*,*N*′-diethylethylenediamine (95%) and *N*,*N*′-diisopropylethylenediamine (99%) were purchased from Aldrich and used as received. 3-Isopropylsalicylaldehyde, 3-*tert*-butylsalicylaldehyde, 3-phenylsalicylaldehyde were prepared by procedures analogous to those described in literature (N. Matsukawa, 2000). *Rac*-lactide and *L*-lactide (Aldrich) were recrystallized from anhydrous toluene, and were then sublimed three times prior to use. The ε-caprolactone was stirred with CaH_2 overnight and then distilled under reduced pressure prior to use. All other chemicals were commercially available and used as received unless otherwise stated.

^1H (399.87 MHz) and ^{13}C (100.55 MHz) nuclear magnetic resonance (NMR) spectra were recorded on a Varian Unity Inova 400 MHz spectrometer at 300 K. Homonuclear decoupled ^1H NMR experiments were performed on Bruker Advance 500 MHz spectrometer. ^1H NMR spectra were referenced internally to the residual protio impurity peaks in the deuterated solvent (^1H: δ $CDCl_3$, 7.26; C_6D_6, 7.16; $(CD_3)_2SO$, 2.54; toluene-d_8, 2.08, 6.97, 7.01, 7.09). ^{13}C NMR spectra were referenced

Copyright by Kasetsart University All rights reserved

to the solvent as follows: $CDCl_3$, δ 77.0; C_6D_6, 128.06; $(CD_3)_2SO$, 39.52 and toluene-d_8, 20.43, 125.13, 127.96, 128.87, 137.48. The following abbreviations have been used for multiplicities: s (singlet); d (doublet); t (triplet); q (quartet); sept (septet); dd (doublet of doublets); dt (doublet of triplets); td (triplet of doublets); m (unresolved multiplet); br (board). Elemental analysis data (C, H, N) were obtained from a LECO Elemental Analyzer CS-932H. Gel permeation chromatography (GPC) measurements were conducted on a Polymer Laboratories PL-GPC-220 instrument equipped with PLgel 10 μm MIXED-D 300 × 7.5 mm columns and tetrahydrofuran (THF) was used as the eluent (flow rate: 1 ml min^{-1} at 40 ˚C). The number average molecular weight (M_n) and polydispersity index (M_w/M_n) were calibrated against polystyrene (PS) standards. M_n values of polymer were corrected with a Mark–Houwink factor of 0.58 for polylactide and 0.56 for polycaprolactone according to the literature (R. Alfred and L. W. H. Howard, 1972; R. D. John, 2005). X-ray diffraction data were measured on a Bruker-Nonius kappaCCD diffractometer with graphite monochromated MoKα radiation (λ = 0.71073 Å) at 150(2) K. The structure was solved by direct methods by SIR97 (A. Altomare, 1999), and refined with full-matrix least-squares calculations on F^2 using SHELXL-97 (G. M. Sheldrick, 2008). Glass transition temperatures (T_g), the crystallization temperature (T_c) and melting temperature (T_m) of the copolymers were measured by differential scanning calorimetry (DSC) using a NETZSCH DSC 204F1 Phoenix Instruments in nitrogen flow. Samples were first heated to 200 ˚C at a rate of 10˚C min^{-1} and cooled to 20 ˚C for two cycles. The samples were then cooled to -100 ˚C, by liquid nitrogen, followed by heating to 200 ˚C at a heating rate of 5 ˚C per minute to determine their thermal properties.

2. Synthesis of bis(pyrrolidene) Schiff-base ligands (H_2L^1-H_2L^7)

The reaction was performed according to the procedure previously reported in the literature (Azpeitia *et al*., 2011; Mu *et al*., 2011). The bis(pyrrolidene) Schiff-base ligands were prepared by the condensation reaction between two equivalents of pyrrole-2-carboxaldehyde and one equivalent of appropriate diamine in ethanol at

Copyright by Kasetsart University. All rights reserved

room temperature as shown in **Figure 37**. In all cases, the desired ligands were obtained in quantitative yields.

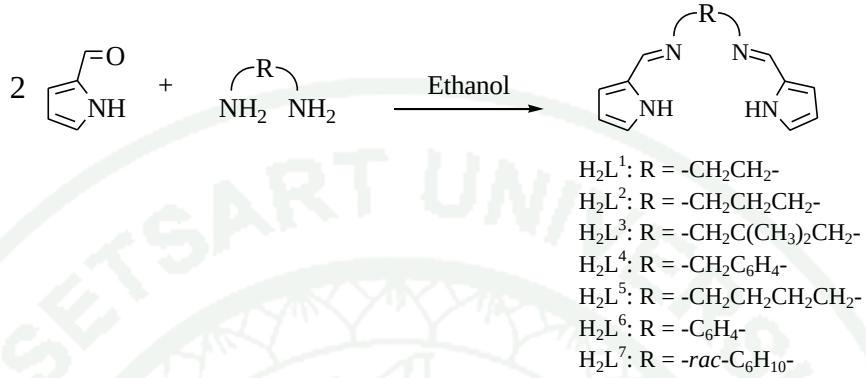

Figure 37 Synthetic pathway for preparation of ligands **H_2L^1-H_2L^7**.

2.1 Synthesis of *N*,*N*′- bis((1H-pyrrol-2-yl)methylene)ethane-1,2-diamine (H_2L^1) (Azpeitia *et al*., 2011; Bacchi *et al*., 2003; Bhowon *et al*., 2004; Burness *et al*., 1976; Biel and Hoya, 1965; Che *et al*., 2005; Clarke and JWeber, 1968; Dillard and Taylor, 1974; Franceschi *et al*., 2001; Grigoras *et al*., 1997; Jones *et al*., 2001; Male *et al*., 1997; McCleverty and Jones, 1971; Mohamadou and Barbier, 1990; Mu *et al*., 2011; Li *et al*., 2007; Munro *et al*., 2011; Pfeiffer *et al*., 1937; Pui *et al*., 2000; 2002; 2003; Robertson *et al*., 1963; Saito *et al*., 1963; Srivastava and Mishra, 1995; Srivastava and Singh, 1999; Srivastava *et al*., 2002; Stackelberg, 1947; Stern *et al*., 2000; van den Ancker *et al*., 2006; van Stein *et al*., 1984; Wawschinek and Weiss, 1964; Weber, 1967; Xiang *et al*., 2005; Yang *et al*., 2003; 2004)

To a stirred solution of pyrrole-2-carboxaldehyde (3.00 g, 31.55 mmol) in ethanol (50 ml) was slowly added 1,2-ethylenediamine (0.95 g, 15.78 mmol). The reaction mixture was stirred and a catalytic amount of formic acid was added. The reaction mixture was stirred at room temperature for 4 hours and during which time, a white precipitate formed. The white solid was collected by filtration and dried under vacuum. Yield: 3.01 g; 89%.

Copyright by Kasetsart University All rights reserved

^{1}H NMR data (399.87 MHz, d_6-DMSO, 300 K): δ 11.42 (br s, 2H, N*H*), 8.11 (s, 2H, N=C*H*), 6.90-6.87 (m, 2H, Pyrrole-*H*), 6.45 (dd, $^{4}J_{HH}$ = 1.4 Hz, $^{3}J_{HH}$ = 3.5 Hz, 2H, Pyrrole-*H*), 6.12 (dd, $^{3}J_{HH}$ = 2.6 Hz, $^{3}J_{HH}$ = 3.5 Hz, 2H, Pyrrole-*H*), 3.76 (s, 4H, N(CH_2CH_2)N).

^{13}C NMR data (100.55 MHz, d_6-DMSO, 300 K): δ 152.6 (N=*C*H), 130.0 (Pyrrole-*C*), 121.9 (Pyrrole-*C*H), 113.4 (Pyrrole-*C*H), 108.8 (Pyrrole-*C*H), 61.4 (N(*C*H_2*C*H_2)N).

Elemental analysis for $C_{12}H_{14}N_4$: C, 67.27; H, 6.59; N, 26.15 %. Found C, 67.07; H, 6.68; N, 26.47 %.

2.2 Synthesis of *N*,*N*′-bis((1H-pyrrol-2-yl)methylene)propane-1,3-diamine (H_2L^2) (Bacchi *et al.*, 2003; Bhowon *et al*., 2004; Clarke and Weber, 1968; Datta *et al.*, 2003; Du *et al*., 2009; Ganjali *et al*., 2004; Grigoras *et al.*, 1997; Jones *et al*., 2001; Li *et al.*, 2007; McCleverty and Christopher, 1971; Mohamadou and Barbier, 1990; Munro and Camp, 2003; Munro *et al.*, 2011; Swiegers, 1994; Weber, 1967; Yang *et al*., 2004; Zhang *et al*., 2004; 2005)

To a stirred solution of pyrrole-2-carboxaldehyde (3.00 g, 31.55 mmol) in ethanol (50 ml) was added 1,3-propylenediamine (1.17 g, 15.78 mmol). The reaction mixture was stirred at room temperature for 4 hours. White solid crystals was collected by filtration and dried under vacuum. Yield: 3.32 g; 92%.

^{1}H NMR data (399.87 MHz, d_6-DMSO, 300 K): δ 11.38 (br s, 2H, N*H*), 8.11 (s, 2H, N=C*H*), 6.91-6.88 (m, 2H, Pyrrole-*H*), 6.46 (dd, $^{4}J_{HH}$ = 1.5 Hz, $^{3}J_{HH}$ = 3.5 Hz, 2H, Pyrrole-*H*), 6.14 (dd, $^{3}J_{HH}$ = 2.6 Hz, $^{3}J_{HH}$ = 3.5 Hz, 2H, Pyrrole-*H*), 3.56 (dt, $^{3}J_{HH}$ = 6.5 Hz, $^{4}J_{HH}$ = 0.8 Hz, 4H, NCH_2CH_2CH_2N), 1.93 (q, $^{3}J_{HH}$ = 6.9 Hz, 2H, NCH_2CH_2CH_2N).

^{13}C NMR data (100.55 MHz, d_6-DMSO, 300 K): δ 151.8 (N=*C*H), 130.0 (Pyrrole-*C*), 121.9 (Pyrrole-*C*H), 113.2 (Pyrrole-*C*H), 108.7 (Pyrrole-*C*H), 58.1 (N*C*H_2CH_2*C*H_2N), 32.5 (NCH_2*C*H_2CH_2N).

Copyright by Kasetsart University All rights reserved

Elemental analysis for $C_{13}H_{16}N_4$: C, 68.39; H, 7.06; N, 24.54 %. Found C, 68.25; H, 7.32; N, 24.77 %.

2.3 Synthesis of *N*,*N*′- bis((1H-pyrrol-2-yl)methylene)-2,2-dimethylpropane-1,3-diamine (H_2L^3) (Du *et al*., 2009; Grigoras *et al*., 1997; Munro *et al*., 2011; Yang *et al*., 2007)

To a stirred solution of pyrrole-2-carboxaldehyde (1.50 g, 15.78 mmol) in ethanol (25 ml) at room temperature was added 2,2-dimethyl-1,3-propylenediamine (0.81 g, 7.89 mmol). After stirred for 3 days at room temperature, a yellow solid precipitated. The product was collected by filtration and dried under vacuum. Yield: 1.17 g, 57%.

^{1}H NMR data (399.87 MHz, d_6-DMSO, 300 K): δ 11.25 (br s, 2H, N*H*), 8.08 (s, 2H, N=C*H*), 6.91-6.89 (m, 2H, Pyrrole-*H*), 6.46 (dd, $^4J_{HH}$ = 1.5 Hz, $^3J_{HH}$ = 3.5 Hz, 2H, Pyrrole-*H*), 6.14 (dd, $^3J_{HH}$ = 2.6 Hz, $^3J_{HH}$ = 3.5 Hz, 2H, Pyrrole-*H*), 3.38 (d, $^4J_{HH}$ = 1.0 Hz, 4H, NCH_2C$(CH_3)_2$CH_2N), 0.97 (s, 6H, NCH_2C(C$H_3)_2$CH_2N).

^{13}C NMR data (100.55 MHz, d_6-DMSO, 300 K): δ 151.8 (N=*C*H), 130.1 (Pyrrole-*C*), 121.7 (Pyrrole-*C*H), 112.9 (Pyrrole-*C*H), 108.7 (Pyrrole-*C*H), 69.4 (N*C*H_2C$(CH_3)_2$ *C*H_2N), 36.7 (NCH_2*C*$(CH_3)_2$CH_2N), 24.3 (NCH_2C(*C*$H_3)_2$CH_2N)

Elemental analysis for $C_{15}H_{20}N_4$: C, 70.28; H, 7.86; N, 21.86 %. Found C, 70.20; H, 7.95; N, 22.18 %.

Copyright by Kasetsart University. All rights reserved

2.4 Synthesis of *N*,*N*'-bis((1H-pyrrol-2-yl)methylene)-2-aminobenzylamine (**H_2L^4**) (Meghdadi *et al*., 2011; Zamani *et al.*, 201)

To a stirred solution of 2-pyrrolecarboxaldehyde (2.00 g, 21.03 mmol) in 40 ml of ethanol in a round bottom flask was added 1.29 g (10.52 mmol) of 2-aminobenzylamine. The mixture was stirred for 3 h at room temperature to give a yellow power which was filtered off, washed with cold ethanol and dried under vacuum. Yield: 2.49 g; 83%.

^{1}H NMR data (399.87 MHz, d_6-DMSO, 300 K): δ 11.69 (br S, 1H, N*H*), 11.41 (br S, 1H, N*H*), 8.25 (s, 1H, N=C*H*), 8.23 (s, 1H, N=C*H*), 7.33-7.36 (m, 1H Ar-*H*), 7.25-7.31 (m, 1H Ar-*H*), 7.13-7.19 (m, 1H Ar-*H*), 7.07-7.09 (m, 1H, Pyrole-*H*), 7.01-7.05 (m, 1H, Ar-*H*), 6.84-6.88 (m, 1H, Pyrrole-*H*), 6.69-6.74 (m, 1H, Pyrrole-*H*), 6.36-6.40 (m, 1H, Pyrrole-*H*), 6.21-6.25 (m, 1H, Pyrrole-*H*), 6.07-6.12 (m, 1H, Pyrrole-*H*), 4.88 (s, 2H, ArC*H*$_2$).

^{13}C NMR data (100.55 MHz, DMSO-d_6, 300 K): *δ* 152.9 (*C*NH), 150.3 (Ar*C*), 150.1 (*C*NH),133.5 (Ar*C*CH$_2$), 130.9 (Pyrrole-*C*), 130.2 (Pyrrole-*C*), 128.9 (Ar*C*H), 127.9 (Ar*C*H), 124.9 (Ar*C*H), 123.8 (Pyrrole-*C*H), 122.1 (Pyrrole-*C*H), 117.8 (Ar*C*H), 116.1 (Pyrrole-*C*H), 113.7 (Pyrrole-*C*H), 10.9.8 (Pyrrole-*C*H), 109.0 (Pyrrole-*C*H), 59.5 (Ar*C*H$_2$).

Elemental analysis for $C_{17}H_{16}N_4$: C, 73.89; H, 5.84; N, 20.27 %. Found: C, 73.92; H, 6.06; N, 20.74 %.

2.5 Synthesis of *N*,*N*′-bis((1H-pyrrol-2-yl)methylene)butane-1,4-diamine (H_2L^5) (Clarke and Weber, 1968; 1967; Grigoras *et al*., 1997; Holland *et al*., 2009; Li *et al*., 2007; Mohamadou *et al*., 1990; Yang *et al*., 2003; 2004; Yuan and Wan, 2006; Zhang *et al*., 2005)

To a stirred solution of pyrrole-2-carboxaldehyde (1.50 g, 15.77 mmol) in ethanol (25 ml) at room temperature was added 1,4-butylenediamine (0.70 g, 7.89

Copyright by Kasetsart University All rights reserved

mmol). After being stirred for 3 days at room temperature, a white solid precipitated. The product was collected by filtration and dried under vacuum. Yield: 1.89 g; 99%.

^{1}H NMR data (399.87 MHz, d_6-DMSO, 300 K): δ 11.37 (br s, 2H, N*H*), 8.09 (s, 2H, N=C*H*), 6.89-6.86 (m, 2H, Pyrrole-*H*), 6.45 (dd, $^{4}J_{HH}$ = 1.5 Hz, $^{3}J_{HH}$ = 3.5 Hz, 2H, Pyrrole-*H*), 6.12 (dd, $^{3}J_{HH}$ = 2.6 Hz, $^{3}J_{HH}$ = 3.5 Hz, 2H, Pyrrole-*H*), 3.56-3.50 (m, 4H, NC*H*$_2$CH$_2$CH$_2$C*H*$_2$N), 1.68-1.63 (m, 4H, NCH$_2$C*H*$_2$C*H*$_2$CH$_2$N).

^{13}C NMR data (100.55 MHz, d_6-DMSO, 300 K): δ 152.2 (N=*C*H), 130.8 (Pyrrole-*C*), 122.5 (Pyrrole-*C*H), 113.8 (Pyrrole-*C*H), 109.4 (Pyrrole-*C*H), 60.8 (N*C*H$_2$CH$_2$ CH$_2$*C*H$_2$N), 29.2 (NCH$_2$*C*H$_2$*C*H$_2$CH$_2$N).

Elemental analysis for $C_{14}H_{18}N_4$: C, 69.39; H, 7.49; N, 23.12 %. Found C, 69.29; H, 7.66; N, 23.41 %.

2.6 Synthesis of *N*,*N*′- bis((1H-pyrrol-2-yl)methylene)-1,2-phenylenediamine (H_2L^6) **(**Azpeitia *et al.*, 2011; Bacchi *et al.*, 2003; Berube *et al*., 2003; Bhowon *et al*., 2004; Chen *et al*., 2008; Clarke and Weber, 1968; Dezelic and Dolibic, 1957; Franceschi *et al.*, 2001; Ganjali *et al.*, 2005; Grigoras *et al*., 1997; Han *et al.*, 2007; Jones *et al*., 2000; McCleverty and Christopher, 1971; Mohamadou and Barbier, 1990; Mu *et al*., 2011; Munro *et al*., 2006; Pfeiffer *et al.*, 1937; Rao *et al*., 2010; Srivastava and Kalam, 2002; Srivastava and Mishra, 1995; Srivastava and Singh, 1999a; 1999b; Wang *et al.*, 2007; Weber, 1967)

To a stirred solution of pyrrole-2-carboxaldehyde (3.00 g, 31.55 mmol) in ethanol (25 ml) was added 1,2-phenylenediamine (1.71 g, 15.77 mmol). The reaction mixture was stirred at room temperature for 3 days. Pale yellow crystals was collected by filtration and dried under vacuum. Yield: 1.12 g; 26%.

^{1}H NMR data (399.87 MHz, d_6-DMSO, 300 K): δ 11.62 (br s, 2H, N*H*), 8.25 (s, 2H, N=C*H*), 7.20-7.17 (m, 2H, Ar*H*),7.08-7.05 (m, 2H, Ar*H*), 7.04-7.01 (m, 2H, Pyrrole-*H*), 6.69-6.67 (m, 2H, Pyrrole-*H*), 6.24-6.21 (m, 2H, Pyrrole-*H*).

Copyright by Kasetsart University All rights reserved

^{13}C NMR data (100.55 MHz, d_6-DMSO, 300 K): δ 152.2 (N=*C*H), 145.2 (Ar*C*), 131.3 (Pyrrole-*C*), 125.7 (Ar*C*H), 124.0 (Ar*C*H), 121.5 (Pyrrole-*C*H), 116.2 (Pyrrole-*C*H), 110.0 (Pyrrole-*C*H).

Elemental analysis for $C_{16}H_{14}N_4$: C, 73.26; H, 5.38; N, 21.36 %. Found C, 72.85; H, 5.70; N, 21.40 %.

2.7 Synthesis of *N*,*N*′-bis((1H-pyrrol-2-yl)methylene)cyclohexyl-1,2-diamine (H_2L^7) (Bhowon *et al*., 2004; Gupta *et al*., 2009; van den Ancker *et al*., 2006; Zhang *et al*., 2008)

To a stirred solution of pyrrole-2-carboxaldehyde (1.50 g, 15.77 mmol) in ethanol (25 ml) at room temperature was added cyclohexane-1,2-diamine (0.90 g, 7.89 mmol). After being stirred for 3 days at room temperature, a white solid was collected by filtration and dried under vacuum. Yield: 1.54 g; 73%.

^{1}H NMR data (399.87 MHz, d_6-DMSO, 300 K): δ 11.19 (br s, 2H, N*H*), 7.98 (s, 2H, N=C*H*), 6.81-6.79 (m, 2H, Pyrrole-*H*), 6.34 (dd, $^3J_{HH}$ = 3.5 Hz, $^4J_{HH}$ = 1.4 Hz, 2H, Pyrrole-*H*), 6.05 (dd, $^3J_{HH}$ = 3.5 Hz, $^4J_{HH}$ = 2.6 Hz, 2H, Pyrrole-*H*), 3.24-3.18 (m, 2H, N(Cyclohexyl-C*H*)N), 1.84-1.40 (m, 8H, N(cyclohexyl-CH_2)N).

^{13}C NMR data (100.55 MHz, d_6-DMSO, 300 K): δ 151.6 (N=*C*H), 130.6 (Pyrrole-*C*H), 122.3 (Pyrrole-*C*), 113.9 (Pyrrole-*C*H), 109.4 (Pyrrole-*C*H), 74.4 (Cyclohexyl-*C*H), 34.1 (cyclohexyl-*C*H_2), 25.0 (cyclohexyl-*C*H_2).

Elemental analysis for $C_{16}H_{20}N_4$: C, 71.61; H, 7.51; N, 20.88 %. Found C, 71.47; H, 7.81; N, 20.58 %.

Copyright by Kasetsart University All rights reserved

3. Synthesis of bis(pyrrolidene) Schiff-base aluminum complexes

The aluminum complexes **L^1AlMe-L^7AlMe** were prepared by treating the relevant tetradentate bis(pyrrolidene) Schiff-base ligand **H_2L^1-H_2L^7** with trimethyl aluminum. The reactions were carried out in toluene at 110 ˚C for the desired reaction time, according to **Figure 38**.

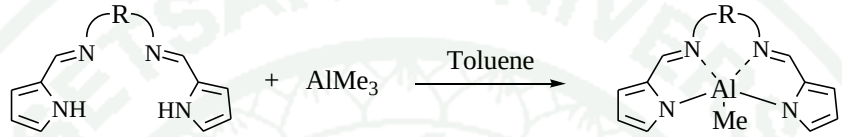

H_2L^1: R = -CH_2CH_2-
H_2L^2: R = -$CH_2CH_2CH_2$-
H_2L^3: R = -$CH_2C(CH_3)_2CH_2$-
H_2L^4: R = -$CH_2C_6H_4$-
H_2L^5: R = -*rac*-C_6H_{10}-
H_2L^6: R = -C_6H_4-
H_2L^7: R = -$CH_2CH_2CH_2CH_2$-

L^1AlMe: R = -CH_2CH_2-
L^2AlMe: R = -$CH_2CH_2CH_2$-
L^3AlMe: R = -$CH_2C(CH_3)_2CH_2$-
L^4AlMe: R = -$CH_2C_6H_4$-
L^5AlMe: R = - $CH_2CH_2CH_2CH_2$ -
L^6AlMe: R = -C_6H_4-
L^7AlMe: R = -*rac*-C_6H_{10}-

Figure 38 Synthetic pathway for the preparation of aluminum complexes **L^1AlMe-L^7AlMe**.

3.1 Synthesis of **L^1AlMe** (Azpeitia *et al*., 2011).

To a stirred suspension of **H_2L^1** (1.00 g, 4.67 mmol) in toluene (30 ml) was slowly added $AlMe_3$ (2.33 ml of a 2.0 M solution in toluene, 4.67 mmol). The reaction mixture was stirred at 110 ˚C for 24 hours and during which time, a white solid precipitated. The white solid was collected by filtration and dried under vacuum. Yield: 0.86 g; 83%.

^{1}H NMR data (399.87 MHz, d_6-DMSO, 298 K): δ 8.33 (s, 2H, N=C*H*), 7.30 (s, 2H, Pyrrole-*H*), 6.62 (d, $^3J_{HH}$ = 3.3 Hz, 2H, Pyrrole-*H*), 6.18 (dd, $^3J_{HH}$ = 3.3 Hz, $^3J_{HH}$ = 1.9 Hz, 2H, Pyrrole-*H*), 4.00-3.93 (m, 2H, NCH_2), 3.74-3.66 (m, 2H, NCH_2), -0.97 (s, 3H, AlCH_3).

Copyright by Kasetsart University All rights reserved

^{13}C NMR data (100.55 MHz, d_6-DMSO, 298 K): δ 158.6 (N=*C*H), 136.2 (Pyrrole-*C*), 133.7 (Pyrrole-*C*H), 115.6 (Pyrrole-*C*H), 112.8 (Pyrrole-*C*H), 46.9 (N(*C*H_2*C*H_2)N).

Elemental analysis for $C_{13}H_{15}N_4Al$ (254.27): C, 61.41; H, 5.95; N, 22.03 %. Found C, 61.38; H, 6.14; N, 22.00 %.

3.2 Synthesis of **L^2AlMe**

To a stirred suspension of **H_2L^2** (1.00 g, 4.38 mmol) in toluene (30 ml) was slowly added $AlMe_3$ (2.19 ml of a 2.0 M solution in toluene, 4.38 mmol). The reaction mixture was stirred at 110 ˚C for 24 hours. After cooling to -20 ˚C, colorless crystals formed. The crystals were collected by filtration and dried under vacuum. Yield: 0.33 g; 28%.

^{1}H NMR data (399.87 MHz, d_6-DMSO, 298 K): δ 8.28 (s, 2H, N=C*H*), 7.34-7.32 (m, 2H, Pyrrole-*H*), 6.67 (dd, $^4J_{HH}$ = 0.8 Hz, $^3J_{HH}$ = 3.4 Hz, 2H, Pyrrole-*H*), 6.25 (dd, $^3J_{HH}$ = 3.4 Hz, $^3J_{HH}$ = 1.9 Hz, 2H, Pyrrole-*H*), 3.88-3.76 (m, 4H, NC*H*$_2$CH$_2$C*H*$_2$N), 2.12-2.01 (m, 1H, NCH$_2$C*H*H′CH$_2$N), 1.86-1.74 (m, 1H, NCH$_2$CH*H*′CH$_2$N), -0.90 (s, 3H, AlC*H*$_3$).

^{13}C NMR data (100.55 MHz, d_6-DMSO, 298 K): δ 160.3 (N=*C*H), 135.5 (Pyrrole-*C*), 134.8 (Pyrrole-*C*H), 116.7 (Pyrrole-*C*H), 113.8 (Pyrrole-*C*H), 55.6 (N*C*H$_2$CH$_2$*C*H$_2$N), 30.2 (NCH$_2$*C*H$_2$CH$_2$N).

Elemental analysis for $C_{14}H_{17}N_4Al$ (268.29): C, 62.67; H, 6.39; N, 20.88 %. Found C, 62.05; H, 6.35; N, 20.30 %.

3.3 Synthesis of **L^3AlMe**

To a stirred suspension of **H_2L^3** (0.80 g, 3.12 mmol) in toluene (30 ml) was slowly added $AlMe_3$ (1.60 ml of a 2.0 M solution in toluene, 3.20 mmol). The reaction mixture was stirred at 110 ˚C for 24 hours. After cooling to -20 ˚C, colorless

Copyright by Kasetsart University All rights reserved

crystals formed. The crystals were collected by filtration and dried under vacuum. Yield: 0.47 g; 57%.

^{1}H NMR data (399.87 MHz, d_6-DMSO, 298 K): δ 8.24 (s, 2H, N=C*H*), 7.39-7.36 (m, 2H, Pyrrole-*H*), 6.68 (dd, $^{4}J_{HH}$ = 0.8 Hz, $^{3}J_{HH}$ = 3.4 Hz, 2H, Pyrrole-*H*), 6.26 (dd, $^{3}J_{HH}$ = 3.4 Hz, $^{3}J_{HH}$ = 1.9 Hz, 2H, Pyrrole-*H*), 3.76 (d, $^{1}J_{HH}$ = 12.0 Hz, 2H, NC*H*$_2$C(CH$_3$)$_2$CH$_2$N), 3.45 (d, $^{1}J_{HH}$ = 12.2 Hz, 2H, NC*H*$_2$C(CH$_3$)$_2$C*H*$_2$N), 1.05 (s, 3H, NCH$_2$C(C*H*$_3$)(CH$_3$)CH$_2$N), 0.84 (s, 3H, NCH$_2$C(CH$_3$)(C*H*$_3$)CH$_2$N), -0.89 (s, 3H, AlC*H*$_3$).

^{13}C NMR data (100.55 MHz, d_6-DMSO, 298 K): δ 160.8 (N=*C*H), 135.1 (Pyrrole-*C*), 134.9 (Pyrrole-*C*H), 116.6 (Pyrrole-*C*H), 113.8 (Pyrrole-*C*H), 66.8 (N(*C*H$_2$C(CH$_3$)$_2$ *C*H$_2$)N), 35.8 (NCH$_2$*C*(CH$_3$)$_2$CH$_2$N), 25.9 (NCH$_2$C(CH$_3$)(*C*H$_3$)CH$_2$N), 22.0 (NCH$_2$C (*C*H$_3$)(CH$_3$)CH$_2$N).

Elemental analysis for $C_{16}H_{21}N_4Al$ (296.35): C, 64.35; H, 7.14; N, 18.91 %. Found C, 64.26; H, 7.35; N, 18.72 %.

3.4 Synthesis of **L^{4}AlMe**

To a stirred solution of **H$_2$L^4** (1.00, 3.62 mmol) in toluene (50 ml) was added a TMA (1.81 ml of a 2.0 M in toluene, 3.62 mmol). A pale yellow precipitate was isolated by filtration and dried under reduced pressure. Yield: 0.67 g, 59%.

^{1}H NMR data (399.87 MHz, d_6-DMSO, 300 K): δ 8.57 (s, 1H, N=C*H*), 8.49 (s, 1H, N=C*H*), 7.42 (s, 1H Pyrrole-*H*), 7.41 (s, 1H Pyrrole-*H*), 7.32-7.38 (m, 2H, Ar-*H*), 7.31-7.33 (m, 1H, Ar-*H*), 7.23-7.30 (m, 1H Ar-*H*), 6.93-6.94 (m, 2H Pyrrole-*H*), 6.95 (d, $^{4}J_{HH}$ = 1.5 Hz, 2H, Pyrrole-*H*), 6.80 (d, $^{3}J_{HH}$ = 1.5 Hz, 2H, Pyrrole-*H*), 6.35-6.36 (m, 2H, Pyrrole-*H*), 6.30-6.33 (m, 2H, Pyrrole-*H*), 4.94 (d, $^{2}J_{HH}$ = 16.3 Hz, 1H, N(ArC*H*H)N), 4.80 (d, $^{2}J_{HH}$ = 16.3 Hz, 1H, N(ArC*H*H)N), -1.21 (s, 3H, AlC*H*$_3$).

Copyright by Kasetsart University All rights reserved

^{13}C NMR data (*100.55 MHz, d_6-DMSO, 298 K*): δ 161.4 (*C*NH), 153.5 (*C*NH), 144.2 (Ar*C*), 136.4 (Pyrrole-*C*), 135.8 (Ar*C*H), 134.6 (Pyrrole-*C*), 134.5 (Ar*C*H), 130.2 (Ar*C*CH_2), 129.0 (Pyrrole-*C*H), 128.5 (Pyrrole-*C*H), 126.2 (Ar*C*H), 119.8 (Ar*C*H), 119.2 (Pyrrole-*C*H), 117.3 (Pyrrole-*C*H), 114.2 (Pyrrole-*C*H), 113.8 (Pyrrole-*C*H), 56.1 (Ar*C*H_2).

Elemental analysis for $C_{18}H_{17}AlN_4$: C, 68.34; H, 5.42; Al, 8.53; N, 17.71 %. Found C, 67.58; H, 5.55; N, 18.02 %.

3.5 Synthesis of **L^5AlMe**

To a stirred suspension of **H_2L^5** (0.60 g, 2.48 mmol) in toluene (20 ml) was slowly added $AlMe_3$ (1.40 ml of a 2.0 M solution in toluene, 2.80 mmol). The reaction mixture was stirred at 110 ˚C for 24 hours after which a white solid precipitated. The solid was collected by filtration and dried under vacuum. Yield: 0.53 g; 81%.

^{1}H NMR data (399.87 MHz, d_6-DMSO, 298 K): δ 8.32 (s, 2H, N=C*H*), 6.92-6.88 (m, 2H, Pyrrole-*H*), 6.66 (dd, $^4J_{HH}$ = 1.0 Hz, $^3J_{HH}$ = 3.3 Hz, 2H, Pyrrole-*H*), 6.22 (dd, $^3J_{HH}$ = 3.4 Hz, $^3J_{HH}$ = 1.8 Hz, 2H, Pyrrole-*H*), 3.80-3.67 (m, 2H, NC*H*$_2$CH$_2$CH$_2$CH$_2$N), 3.57-3.46 (NCH$_2$CH$_2$CH$_2$C*H*$_2$N), 2.05-1.92 (NCH$_2$C*H*$_2$CH$_2$CH$_2$N), 1.89-1.77 (NCH$_2$CH$_2$C*H*$_2$ CH$_2$N), -0.81 (s, 3H, AlC*H*$_3$).

^{13}C NMR data: data are not available due to the limited solubility of complex.

Elemental analysis for $C_{15}H_{19}N_4Al$ (282.32): C, 63.81; H, 6.78; N, 19.85 %. Found C, 64.11; H, 6.72; N, 19.63 %.

3.6 Synthesis of L^6AlMe (Azpeitia *et al*., 2011)

To a stirred solution of **H_2L^6** (1.10 g, 4.19 mmol) in toluene (30 ml) was slowly added $AlMe_3$ (2.09 ml of a 2.0 M solution in toluene, 4.19 mmol). The

Copyright by Kasetsart University All rights reserved

reaction mixture was stirred at 110 ˚C for 24 hours. After cooling to -20 ˚C, a pale yellow solid precipitated. The solid was collected by filtration and dried under vacuum. Yield: 0.33 g; 26%.

^{1}H NMR data (399.87 MHz, d_6-DMSO, 300 K): δ 8.94 (s, 2H, N=C*H*), 7.80 (dd, $^{3}J_{HH}$ = 5.9, $^{4}J_{HH}$ = 3.4, 2H, Ar*H*), 7.69 (m, 2H, Pyrrole-*H*), 7.33 (dd, $^{3}J_{HH}$ = 5.9 Hz, $^{4}J_{HH}$ = 3.3 Hz, 2H, Ar*H*), 7.05-7.01(m, 2H, Pyrrole-*H*), 6.45 (dd, $^{3}J_{HH}$ = 3.6 Hz, $^{4}J_{HH}$ = 1.4 Hz, 2H, Pyrrole-*H*), -1.13 (s, 3H, AlCH_3).

^{13}C NMR data (100.55 MHz, d_6-DMSO, 300 K): δ 151.0 (N=*C*H), 138.3 (Pyrrole-*C*), 137.4 (Ar*C*), 137.2 (Pyrrole-*C*H), 127.4 (Ar*C*H), 120.5 (Ar*C*H), 117.2 (Pyrrole-*C*H), 115.7 (Pyrrole-*C*H).

Elemental analysis for $C_{17}H_{15}N_4Al$ (302.31): C, 67.54; H, 5.00; N, 18.53 %. Found C, 67.42; H, 5.24; N, 18.32 %.

3.5 Synthesis of **L^7AlMe**

To a stirred suspension of **H_2L^7** (0.60 g, 2.24 mmol) in toluene (30 ml) was slowly added $AlMe_3$ (1.12 ml of a 2.0 M solution in toluene, 2.24mmol). The reaction mixture was stirred at 110 ˚C for 24 hours. After cooling to -20 ˚C, a pale yellow solid precipitated. The solid was collected by filtration and dried under vacuum. Yield: 0.14 g; 20%.

^{1}H NMR data (399.87 MHz, d_6-DMSO, 298 K): *δ* 8.48 (s, 1H, N=C*H*), 8.48 (s, 1H, N=C*H*), 7.43-7.41 (m, 1H, Pyrrole-*H*), 7.22-7.21 (m, 1H, Pyrrole-*H*), 6.75-6.73 (m, 1H, Pyrrole-*H*), 6.67-6.65 (m, 1H, Pyrrole-*H*), 6.30-6.27 (m, 1H, Pyrrole-*H*), 6.22-6.20 (m, 1H, Pyrrole-*H*), 3.11-3.01 (m, 2H, N(Cyclohexyl-C*H*)N), 2.70-1.40 (m, 8H, N(cyclohexyl-CH_2)N), -0.95 (s, 3H, AlCH_3).

Copyright by Kasetsart University All rights reserved

^{13}C NMR data (100.55 MHz, d_6-DMSO, 300 K): δ 150.8 (N=*C*H), 129.9 (Pyrrole-*C*), 121.6 (Pyrrole-*C*H), 113.1 (Pyrrole-*C*H), 108.6 (Pyrrole-*C*H), 73.7 (Cyclohexyl-*C*H), 34.4 (cyclohexyl-*C*H_2), 24.2 (cyclohexyl-*C*H_2).

Elemental analysis for $C_{17}H_{21}N_4Al$ (308.36): C, 66.22; H, 6.86; N, 18.17 %. Found C, 66.51; H, 7.11; N, 17.90 %.

4. Synthesis of tetradentate bis(phenoxy-amine) ligands

The bis(phenoxy-amine) ligands used in this work were synthesized by a two-step procedure according to the literature, as shown in **Figure 39** (Gibson *et al.*, 2004; Hormnirun *et al.*, 2004).

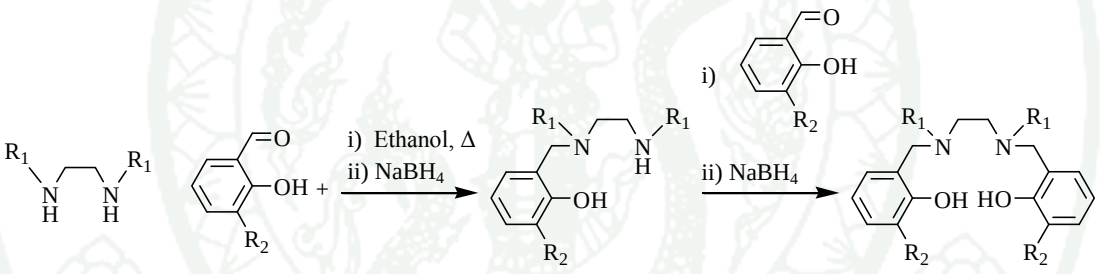

Group A: R_1 = Me	Group B: R_1 = Et	Group C: R_1 = ^{i}Pr
H_2L^{1A}: R_2 = H	H_2L^{1B}: R_2 = H	H_2L^{1C}: R_2 = H
H_2L^{2A}: R_2 = ^{i}Pr	H_2L^{2B}: R_2 = ^{i}Pr	H_2L^{2C}: R_2 = ^{i}Pr
H_2L^{3A}: R_2 = ^{t}Bu	H_2L^{3B}: R_2 = ^{t}Bu	H_2L^{4C}: R_2 = Ph
H_2L^{4A}: R_2 = Ph	H_2L^{4B}: R_2 = Ph	

Figure 39 Synthetic pathway for **H_2L^{1A}- H_2L^{4A}**, **H_2L^{1B}- H_2L^{4B}** and **H_2L^{1C}- H_2L^{3C}**.

4.1 Synthesis of *N*,*N*'-dimethyl-*N*,*N*'-bis[(1-hydroxyphenyl)methylene]-1,2-diaminoethane (**H_2L^{1A}**)

To a solution of *N*,*N*'-dimethyl-1,2-ethylenediamine (1.00 g, 11.35 mmol) in ethanol (125 ml) was added salicylaldehyde (1.39 g, 11.35 mmol), and the resulting

Copyright by Kasetsart University All rights reserved

mixture was stirred for 3 hours at reflux temperature. After cooling to room temperature, sodium borohydride (1.87 g, 50.00 mmol) was slowly added to the solution and stirred for another 2 hours at room temperature. The reaction was quenched with water (100 ml), and the aqueous phase was extracted 3 times with dichloromethane (100 ml). The organic phases were combined and dried over $MgSO_4$. The solution was concentrated *in vacuo* and redissolved in ethanol (125 ml). To the solution was added salicylaldehyde (1.39 g, 11.35 mmol) at room temperature and the reaction mixture was stirred at 70 ˚C overnight. Reduction using $NaBH_4$ (1.87 g, 50.00 mmol) and extraction into dichloromethane was repeated as described above. After removing the solvent, a colorless oil was obtained and this was recrystallized from methanol. Colorless crystals were obtained. Yield: 2.80 g; 62%.

^{1}H NMR data (399.87 MHz, $CDCl_3$, 300 K): δ 10.64 (br s, 2H, O*H*), 7.17 (td, 2H, $^{4}J_{HH}$ = 1.8 Hz, $^{3}J_{HH}$ = 6.4 Hz, Ar*H*), 6.96 (dd, 2H, $^{4}J_{HH}$ = 1.5 Hz, $^{3}J_{HH}$ = 7.4 Hz, Ar*H*), 6.84 (dd, 2H, $^{4}J_{HH}$ = 1.0 Hz, $^{3}J_{HH}$ = 8.1 Hz, Ar*H*), 6.77 (td, 2H, $^{4}J_{HH}$ = 1.2 Hz, $^{3}J_{HH}$ = 7.4 Hz, Ar*H*), 3.70 (s, 4H, ArCH_2), 2.67 (s, 4H, N(CH_2CH_2)N), 2.29 (s, 6H, NCH_3).

^{13}C NMR data (100.55 MHz, $CDCl_3$, 300 K): δ 158.2 (*C*OH), 129.3 (Ar*C*H), 128.9 (Ar*C*H), 122.0 (Ar*C*CH_2N), 119.6 (Ar*C*H), 116.6 (Ar*C*H), 62.2 (Ar*C*H_2N), 54.5 (N(*C*H_2*C*H_2)N), 42.1 (N*C*H_3).

4.2 Synthesis of *N*,*N*′-dimethyl-*N*,*N*′-bis[(4-isopropyl-1-hydroxyphenyl) methylene]-1,2-diaminoethane (**H_2L^{2A}**)

To a solution of *N*,*N*′-dimethyl-1,2-ethylenediamine (1.00 g, 11.35 mmol) in ethanol (125 ml) was added 3-isopropylsalicylaldehyde (1.86 g, 11.35 mmol), and the resulting mixture was stirred for 3 hours at reflux temperature. After cooling to room temperature, sodium borohydride (1.87 g, 50.00 mmol) was slowly added to the solution and stirred for another 2 hours at room temperature. The reaction was quenched with water (100 ml), and the aqueous phase was extracted 3 times with dichloromethane (100 ml). The organic phases were combined and dried over $MgSO_4$. The solution was concentrated *in vacuo* and redissolved in ethanol (125 ml). To the

Copyright by Kasetsart University All rights reserved

solution was added 3-isopropylsalicylaldehyde (1.86 g, 11.35 mmol) at room temperature and the reaction mixture was stirred at 70 ˚C overnight. Reduction using $NaBH_4$ (1.87 g, 50.00 mmol) and extraction into dichloromethane was repeated as described above. After removing the solvent, a colorless oil was obtained and this was recrystallized from methanol. Colorless crystals were obtained. Yield: 3.84 g; 81%.

^{1}H NMR data (399.87 MHz, $CDCl_3$, 298 K): δ 7.13 (dd, $^4J_{HH}$ = 1.7 Hz, $^3J_{HH}$ = 7.8 Hz, 2H, Ar*H*), 6.80 (dd, $^4J_{HH}$ = 1.9 Hz, $^3J_{HH}$ = 7.6 Hz, 2H, Ar*H*), 6.75 (m, 2H, Ar*H*), 3.68 (s, 4H, ArCH_2N), 3.32 (q, $^3J_{HH}$ = 6.9 Hz, 2H, C*H*$(CH_3)_2$), 2.66 (s, 4H, NCH_2CH_2N), 2.27 (s, 6H, NCH_3), 1.22 (d, $^3J_{HH}$ = 6.9 Hz, 12H, CH(CH_3)$_2$).

^{13}C NMR data (100.56 MHz, $CDCl_3$, 298 K): δ 154.9 (*C*-OH), 135.5 (Ar*C*), 126.0 (ArC*H*), 125.5 (Ar*C*H), 121.1 (Ar*C*CH_2N), 118.8 (Ar*C*H), 62.0 (Ar*C*H_2), 53.9 (N*C*H_2*C*H_2N), 41.6 (N*C*H_3), 26.6 (*C*H$(CH_3)_2$), 22.6 (CH(*C*H_3)$_2$).

Elemental analysis for $C_{25}H_{37}N_2O_2$ (384.55): C, 74.96; H, 9.44; N, 7.28 %. Found C, 75.12; H, 9.45; N, 7.30 %.

4.3 Synthesis of *N*,*N*'-dimethyl-*N*,*N*'-bis[(4-*tert*-butyl-1-hydroxyphenyl)methy lene]-1,2-diaminoethane (**H_2L^{3A}**) (Baxter *et al.*, 2002; Hinshaw *et al.*, 1989; Liu *et al.*, 2008)

To a solution of *N*,*N*′-dimethyl-1,2-ethylenediamine (1.00 g, 11.35 mmol) in ethanol (125 ml) was added 3-*tert*-butylsalicylaldehyde (2.02 g, 11.35 mmol), and the resulting mixture was stirred for 3 hours at reflux temperature. After cooling to room temperature, sodium borohydride (1.87 g, 50.00 mmol) was slowly added to the solution and stirred for another 2 hours at room temperature. The reaction was quenched with water (100 ml), and the aqueous phase was extracted 3 times with dichloromethane (100 ml). The organic phases were combined and dried over $MgSO_4$. The solution was concentrated *in vacuo* and redissolved in ethanol (125 ml). To the solution was added 3-*tert*-butylsalicylaldehyde (2.02 g, 11.35 mmol) at room temperature and the reaction mixture was stirred at 70 ˚C overnight. Reduction using

Copyright by Kasetsart University All rights reserved

$NaBH_4$ (1.87 g, 50.00 mmol) and extraction into dichloromethane was repeated as described above. After removing the solvent, a colorless oil was obtained and this was recrystallized from methanol. Colorless crystals were obtained. Yield: 3.15 g; 62%.

^{1}H NMR data (399.87 MHz, $CDCl_3$, 298 K): δ 7.19 (dd, $^4J_{HH}$ = 1.6 Hz, $^3J_{HH}$ = 6.4 Hz, 2H, Ar*H*), 6.82 (dd, $^4J_{HH}$ = 1.6 Hz, $^3J_{HH}$ = 6.6 Hz, 2H, Ar*H*), 6.71 (m, 2H, Ar*H*), 3.67 (s, 4H, ArCH_2N), 2.62 (s, 4H, NCH_2CH_2N), 2.25 (s, 6H, NCH_3), 1.40 (s, 18H, C(CH_3)$_3$).

^{13}C NMR data (100.56 MHz, $CDCl_3$, 298 K): δ 156.8 (*C*-OH), 136.7 (Ar*C*), 126.7 (ArC*H*), 126.0 (Ar*C*H), 121.9 (Ar*C*CH_2N), 118.3 (Ar*C*H), 62.3 (Ar*C*H_2), 53.5 (N*C*H_2*C*H_2N), 41.4 (N*C*H_3), 34.7 (*C*CH_3), 29.5 (C(*C*H_3)$_3$).

Elemental analysis for $C_{26}H_{40}N_2O_2$ (412.61): C, 75.68; H, 9.77; N, 6.79 %. Found C, 75.94; H, 9.90; N, 6.80 %.

4.4 Synthesis of *N*,*N*′-dimethyl-*N*,*N*′-bis[(4-phenyl-1-hydroxyphenyl)methyl ene]-1,2-diaminoethane (**H_2L^{4A}**)

To a solution of *N*,*N*′-dimethyl-1,2-ethylenediamine (1.00 g, 11.35 mmol) in ethanol (125 ml) was added 3-phenylsalicylaldehyde (2.25 g, 11.35 mmol), and the resulting mixture was stirred for 3 hours at reflux temperature. After cooling to room temperature, sodium borohydride (1.87 g, 50.00 mmol) was slowly added to the solution and stirred for another 2 hours at room temperature. The reaction was quenched with water (100 ml), and the aqueous phase was extracted 3 times with dichloromethane (100 ml). The organic phases were combined and dried over $MgSO_4$. The solution was concentrated *in vacuo* and redissolved in ethanol (125 ml). To the solution was added 3-phenylsalicylaldehyde (2.25 g, 11.35 mmol) at room temperature and the reaction mixture was stirred at 70 ˚C overnight. Reduction using $NaBH_4$ (1.87 g, 50.00 mmol) and extraction into dichloromethane was repeated as described above. After removing the solvent, colorless oil was obtained and this was recrystallized from methanol. Colorless crystals were obtained. Yield: 3.18 g; 57%.

Copyright by Kasetsart University All rights reserved

^{1}H NMR data (399.87 MHz, $CDCl_3$, 298 K): δ 7.59 (m, 4H, Ar*H*), 7.40 (m 4H, Ar*H*), 7.31 (dt, $^{4}J_{HH}$ = 2.0 Hz, $^{3}J_{HH}$ = 5.9 Hz, 2H, Ar*H*), 7.27 (dd, $^{4}J_{HH}$ = 2.0 Hz, $^{3}J_{HH}$ = 6.1 Hz, 2H, Ar*H*), 6.95 (dd, $^{4}J_{HH}$ = 1.4 Hz, $^{3}J_{HH}$ = 6.4 Hz, 2H, Ar*H*), 6.85 (m, 2H, Ar*H*), 3.75 (s, 4H, ArCH_2N), 2.73 (s, 4H, NCH_2CH_2N), 2.31 (s, 6H, NCH_3).

^{13}C NMR data (100.56 MHz, $CDCl_3$, 298 K): δ 154.8 (*C*-OH), 138.4 (Ar*C*), 130.0 (ArC*H*), 129.3 (Ar*C*H), 128.9 (Ar*C*H), 128.0 (Ar*C*H), 127.9 (Ar*C*H), 126.7 (Ar*C*H), 121.9 (Ar*C*CH_2N), 119.2 (Ar*C*H), 61.8 (Ar*C*H_2), 54.2 (N*C*H_2*C*H_2N), 41.7 (N*C*H_3).

Elemental analysis for $C_{30}H_{32}N_2O_2$ (452.53): C, 79.61; H, 7.13; N, 6.19%. Found C, 79.44; H, 7.54; N, 5.96.

4.5 Synthesis of *N*,*N*'-diethyl-*N*,*N*'-bis[(1-hydroxyphenyl)methylene]-1,2-di aminoethane (**H_2L^{1B}**) (Baxter *et al.*, 2002; Djebbar-Sid *et al.*, 1989; Giacomelli *et al.*, 1989; Hinshaw *et al.*, 1989)

To a solution of *N*,*N*'-diethyl-1,2-ethylenediamine (1.25 g, 10.76 mmol) in ethanol (125 ml) was added salicylaldehyde (1.21 g, 10.76 mmol), and the resulting mixture was stirred for 3 hours at reflux temperature. After cooling to room temperature, sodium borohydride (2.00 g, 52.87 mmol) was slowly added to the solution and stirred for another 2 hours at room temperature. The reaction was quenched with water (100 ml), and the aqueous phase was extracted 3 times with dichloromethane (100 ml). The organic phases were combined and dried over $MgSO_4$. The solution was concentrated *in vacuo* and redissolved in ethanol (125 ml). To the solution was added salicylaldehyde (1.21 g, 10.76 mmol) at room temperature and the reaction mixture was stirred at 70 ˚C overnight. Reduction using $NaBH_4$ (2.00 g, 52.87 mmol) and extraction into dichloromethane was repeated as described above. After removing the solvent, a colorless oil was obtained and this was recrystallized from methanol. Colorless crystals were obtained. Yield: 2.30 g; 65%.

^{1}H NMR data (399.87 MHz, $CDCl_3$, 298 K): δ 7.16 (dt, $^{4}J_{HH}$ = 1.7 Hz, $^{3}J_{HH}$ =7.5 Hz, 2H, Ar*H*), 6.93 (dd, $^{4}J_{HH}$ = 1.4 Hz, $^{3}J_{HH}$ =7.2 Hz, 2H, Ar*H*), 6.80 (m, 2H, Ar*H*), 6.76

Copyright by Kasetsart University All rights reserved

(dt, $^{4}J_{HH}$ = 1.7 Hz, $^{3}J_{HH}$ = 7.1 Hz, 2H, Ar*H*), 3.73 (s, 4H, ArCH_2N), 2.70 (s, 4H, NCH_2CH_2N), 2.57 (q, $^{3}J_{HH}$ = 7.2 Hz, 4H, NCH_2CH_3), 1.07 (t, $^{3}J_{HH}$ = 7.2 Hz, 6H, NCH_2CH_3).

^{13}C NMR data (100.56 MHz, $CDCl_3$, 298 K): δ 157.7 (*C*-OH), 128.7 (Ar*C*H), 128.4 (Ar*C*H), 121.7 (Ar*C*CH_2N), 119.0 (Ar*C*H), 116.1 (Ar*C*H), 57.7 (Ar*C*H_2), 50.2 (NCH_2*C*H_2N), 47.4 (NCH_2CH$_3$), 10.9 (NCH_2*C*H_3).

Elemental analysis for $C_{20}H_{28}N_2O_2$ (328.45): C, 73.14; H, 8.59; N, 8.53 %. Found C, 72.97; H, 8.65; N, 8.60 %.

4.6 Synthesis of *N*,*N*'-diethyl-*N*,*N*'-bis[(4-isopropyl-1-hydroxyphenyl)methyl ene]-1,2-diaminoethane (**H_2L^{2B}**)

To a solution of *N*,*N*′-diethyl-1,2-ethylenediamine (1.25 g, 10.76 mmol) in ethanol (125 ml) was added 3-isopropylsalicylaldehyde (1.77 g, 10.76 mmol), and the resulting mixture was stirred for 3 hours at reflux temperature. After cooling to room temperature, sodium borohydride (2.00 g, 52.87 mmol) was slowly added to the solution and stirred for another 2 hours at room temperature. The reaction was quenched with water (100 ml), and the aqueous phase was extracted 3 times with dichloromethane (100 ml). The organic phases were combined and dried over $MgSO_4$. The solution was concentrated *in vacuo* and redissolved in ethanol (125 ml). To the solution was added 3-isopropylsalicylaldehyde (1.77 g, 10.76 mmol) at room temperature and the reaction mixture was stirred at 70 ˚C overnight. Reduction using $NaBH_4$ (2.00 g, 52.87 mmol) and extraction into dichloromethane was repeated as described above. After removing the solvent, a colorless oil was obtained and this was recrystallized from methanol. Colorless crystals were obtained. Yield: 3.06 g; 69%.

^{1}H NMR data (399.87 MHz, $CDCl_3$, 298 K): δ 7.11 (dd, $^{4}J_{HH}$ = 2.0 Hz, $^{3}J_{HH}$ = 7.8 Hz, 2H, Ar*H*), 6.78 (dd, $^{4}J_{HH}$ = 2.0 Hz, $^{3}J_{HH}$ = 7.6 Hz, 2H, Ar*H*), 6.75 (m, 2H, Ar*H*), 3.72 (s, 4H, ArCH_2N), 3.31 (q, $^{3}J_{HH}$ = 6.9 Hz, 2H, C*H*$(CH_3)_2$), 2.70 (s, 4H, NCH_2CH_2N),

Copyright by Kasetsart University All rights reserved

2.57 (q, $^{3}J_{HH}$ = 7.2 Hz, 4H, NCH_2CH$_3$), 1.24 (d, $^{3}J_{HH}$ = 6.9 Hz, 12H, CH(CH_3)$_2$), 1.05 (t, $^{3}J_{HH}$ = 7.2 Hz, 6H, NCH$_2$CH_3).

^{13}C NMR data (100.56 MHz, $CDCl_3$, 298 K): δ 155.0 (*C*-OH), 135.3 (Ar*C*), 126.0 (Ar*CH*), 125.3 (Ar*C*H), 121.2 (Ar*C*CH$_2$N), 118.8 (Ar*C*H), 58.0 (Ar*C*H$_2$), 50.3 (NCH_2*C*H$_2$N), 47.5 (N*C*H$_2$CH$_3$), 26.5 (*C*H(CH$_3$)$_2$), 22.6 (CH(*C*H$_3$)2), 11.0 (NCH$_2$*C*H$_3$).

Elemental analysis for $C_{26}H_{40}N_2O_2$ (412.61): C, 75.68; H, 9.779; N, 6.79 %. Found C, 75.34; H, 9.15; N, 6.91 %.

4.7 Synthesis of *N*,*N*'-diethyl-*N*,*N*'-bis[(4-*tert*-butyl-1-hydroxyphenyl)methyl ene]-1,2-diaminoethane (**H_2L^{3B}**)

To a solution of *N*,*N*′-diethyl-1,2-ethylenediamine (1.25 g, 10.76 mmol) in ethanol (125 ml) was added 3-*tert*-butylsalicylaldehyde (1.92 g, 10.76 mmol), and the resulting mixture was stirred for 3 hours at reflux temperature. After cooling to room temperature, sodium borohydride (2.00 g, 52.87 mmol) was slowly added to the solution and stirred for another 2 hours at room temperature. The reaction was quenched with water (100 ml), and the aqueous phase was extracted 3 times with dichloromethane (100 ml). The organic phases were combined and dried over $MgSO_4$. The solution was concentrated *in vacuo* and redissolved in ethanol (125 ml). To the solution was added 3-*tert*-butylsalicylaldehyde (1.92 g, 10.76 mmol) at room temperature and the reaction mixture was stirred at 70 ˚C overnight. Reduction using $NaBH_4$ (2.00 g, 52.87 mmol) and extraction into dichloromethane was repeated as described above. After removing the solvent, a colorless oil was obtained and this was recrystallized from methanol. Colorless crystals were obtained. Yield: 2.46 g; 52%

^{1}H NMR data (399.87 MHz, $CDCl_3$, 298 K): δ 7.18 (dd, $^{4}J_{HH}$ = 1.4 Hz, $^{3}J_{HH}$ = 6.4 Hz, 2H, Ar*H*), 6.80 (dd, $^{4}J_{HH}$ = 1.4 Hz, $^{3}J_{HH}$ = 6.6 Hz, 2H, Ar*H*), 6.70 (m, 2H, Ar*H*), 3.71 (s, 4H, ArCH_2N), 2.67 (s, 4H, NCH_2CH_2N), 2.57 (q, $^{3}J_{HH}$ = 7.16 Hz, 4H, NCH_2CH$_3$), 1.40 (s, 18H, CH(CH_3)$_2$), 1.03 (t, $^{3}J_{HH}$ = 7.16 Hz, 6H, NCH$_2$CH_3).

Copyright by Kasetsart University All rights reserved

^{13}C NMR data (100.56 MHz, $CDCl_3$, 298 K): δ 156.8 (*C*-OH), 136.6 (Ar*C*), 126.7 (ArC*H*), 125.9 (Ar*C*H), 122.0 (Ar*C*CH_2N), 118.3 (Ar*C*H), 58.3 (Ar*C*H_2), 50.2 (N*C*H_2*C*H_2N), 47.5 (N*C*H_2CH$_3$), 34.6 (*C*CH_3), 29.4 (C(*C*H_3)$_3$), 10.9 (NCH$_2$*C*H_3).

Elemental analysis for $C_{28}H_{44}N_2O_2$ (440.66): C, 76.32; H, 10.06; N, 6.36 %. Found C, 76.43; H, 10.04; N, 6.91 %.

4.8 Synthesis of *N*,*N*'-diethyl-*N*,*N*'-bis[(4-phenyl-1-hydroxyphenyl)methyl ene]-1,2-diaminoethane (**H_2L^{4B}**)

To a solution of *N*,*N*′-diethyl-1,2-ethylenediamine (1.25 g, 10.76 mmol) in ethanol (125 ml) was added 3-phenylsalicylaldehyde (2.13 g, 10.76 mmol), and the resulting mixture was stirred for 3 hours at reflux temperature. After cooling to room temperature, sodium borohydride (2.00 g, 52.87 mmol) was slowly added to the solution and stirred for another 2 hours at room temperature. The reaction was quenched with water (100 ml), and the aqueous phase was extracted 3 times with dichloromethane (100 ml). The organic phases were combined and dried over $MgSO_4$. The solution was concentrated *in vacuo* and redissolved in ethanol (125 ml). To the solution was added 3-phenylsalicylaldehyde (2.13 g, 10.76 mmol) at room temperature and the reaction mixture was stirred at 70 ˚C overnight. Reduction using $NaBH_4$ (2.00 g, 52.87 mmol) and extraction into dichloromethane was repeated as described above. After removing the solvent, a colorless oil was obtained and this was recrystallized from methanol. Colorless crystals were obtained. Yield: 3.77 g; 73%.

^{1}H NMR data (399.87 MHz, $CDCl_3$, 298 K): δ 7.56 (m, 4H, Ar*H*), 7.41 (m, 4H, Ar*H*), 7.31 (dt, $^4J_{HH}$ = 2.0 Hz, $^3J_{HH}$ = 5.9 Hz, 2H, Ar*H*), 7.24 (dd, $^4J_{HH}$ = 2.0 Hz, $^3J_{HH}$ = 6.1 Hz, 2H, Ar*H*), 6.92 (dd, $^4J_{HH}$ = 1.4 Hz, $^3J_{HH}$ = 6.4 Hz, 2H, Ar*H*), 6.83 (m, 2H, Ar*H*), 3.79 (s, 4H, ArCH_2N), 2.74 (s, 4H, NCH_2CH_2N), 1.60 (q, $^3J_{HH}$ = 7.2 Hz, 4H, NCH_2CH$_3$), 1.06 (t, $^3J_{HH}$ = 7.2 Hz, 6H, NCH$_2$CH_3).

^{13}C NMR data (100.56 MHz, $CDCl_3$, 298 K): δ 154.9 (*C*-OH), 138.5 (Ar*C*), 129.9 (ArC*H*), 129.3 (Ar*C*H), 128.9 (Ar*C*H), 128.0 (Ar*C*H), 127.9 (Ar*C*H), 126.7 (Ar*C*H),

Copyright by Kasetsart University All rights reserved

122.1 (Ar*C*CH_2N), 119.2 (Ar*C*H), 109.8 (Ar*C*H), 58.0 (Ar*C*H_2), 50.2 (N*C*H_2*C*H_2N), 47.7 (N*C*$H_2$$CH_3$), 10.0 ($NCH_2$*C*$H_3$).

Elemental analysis for $C_{28}H_{44}N_2O_2$ (480.64): C, 79.96; H, 7.55; N, 5.83 %. Found C, 79.99; H, 7.22; N, 5.78 %.

4.9 Synthesis of *N*,*N*'-diisopropyl-*N*,*N*'-bis[(1-hydroxyphenyl)methylene]-1,2-diaminoethane (**H_2L^{1C}**)

To a solution of *N*,*N*′-diisopropyl-1,2-ethylenediamine (1.50 g, 10.41 mmol) in ethanol (125 ml) was added salicylaldehyde (1.27 g, 10.41 mmol), and the resulting mixture was stirred for 3 hours at reflux temperature. After cooling to room temperature, sodium borohydride (1.87 g, 50.00 mmol) was slowly added to the solution and stirred for another 2 hours at room temperature. The reaction was quenched with water (100 ml), and the aqueous phase was extracted 3 times with dichloromethane (100 ml). The organic phases were combined and dried over $MgSO_4$. The solution was concentrated *in vacuo* and redissolved in ethanol (125 ml). To the solution was added salicylaldehyde (1.27 g, 10.41 mmol) at room temperature and the reaction mixture was stirred at 70 ˚C overnight. Reduction using $NaBH_4$ (1.87 g, 50.00 mmol) and extraction into dichloromethane was repeated as described above. After removing the solvent, a colorless oil was obtained and this was recrystallized from methanol. Colorless crystals were obtained. Yield: 1.97 g; 53%.

^{1}H NMR data (399.87 MHz, $CDCl_3$, 298 K): δ 7.16 (dt, $^4J_{HH}$ = 1.7 Hz, $^3J_{HH}$ = 7.5 Hz, 2H, Ar*H*), 6.93 (dd, $^4J_{HH}$ = 1.4 Hz, $^3J_{HH}$ =7.2 Hz, 2H, Ar*H*), 6.80 (m, 2H, Ar*H*), 6.76 (dt, $^4J_{HH}$ = 1.7 Hz, $^3J_{HH}$ =7.1 Hz, 2H, Ar*H*), 3.73 (s, 4H, ArC*H*$_2$N), 2.94 (q, $^3J_{HH}$ = 6.9 Hz, 2H, NC*H*$(CH_3)_2$), 2.70 (s, 4H, NCH_2CH_2N), 0.97 (d, $^3J_{HH}$ = 6.6 Hz, 6H, NCH(C*H*$_3)_2$).

^{13}C NMR data (100.56 MHz, $CDCl_3$, 298 K): δ 157.7 (*C*-OH), 128.7 (Ar*C*H), 128.4 (Ar*C*H), 121.7 (Ar*C*CH_2N), 119.0 (Ar*C*H), 116.0 (Ar*C*H), 57.7 (Ar*C*H_2), 50.2 (N*C*H_2*C*H_2N), 47.4 (N*C*$H_2$$CH_3$), 10.9 ($NCH_2$*C*$H_3$).

Copyright by Kasetsart University All rights reserved

Elemental analysis for $C_{22}H_{32}N_2O_2$ (356.25): C, 74.12; H, 9.05; N, 7.86 %. Found C, 74.23; H, 9.20; N, 7.86 %.

4.10 Synthesis of *N*,*N*'-diisopropyl-*N*,*N*'-bis[(4-isopropyl-1-hydroxyphenyl) methylene]-1,2-diaminoethane (**H_2L^{2C}**)

To a solution of *N*,*N*'-diisopropyl-1,2-ethylenediamine (1.50 g, 10.41 mmol) in ethanol (125 ml) was added 3-isopropylsalicylaldehyde (1.71 g, 10.41 mmol), and the resulting mixture was stirred for 3 hours at reflux temperature. After cooling to room temperature, sodium borohydride (1.87 g, 50.00 mmol) was slowly added to the solution and stirred for another 2 hours at room temperature. The reaction was quenched with water (100 ml), and the aqueous phase was extracted 3 times with dichloromethane (100 ml). The organic phases were combined and dried over $MgSO_4$. The solution was concentrated *in vacuo* and redissolved in ethanol (125 ml). To the solution was added 3-isopropylsalicylaldehyde (1.71 g, 10.41 mmol) at room temperature and the reaction mixture was stirred at 70 ˚C overnight. Reduction using $NaBH_4$ (1.87 g, 50.00 mmol) and extraction into dichloromethane was repeated as described above. After removing the solvent, a colorless oil was obtained and this was recrystallized from methanol. Colorless crystals were obtained. Yield: 3.57 g; 78%.

^{1}H NMR data (399.87 MHz, $CDCl_3$, 298 K): δ 7.09 (dd, $^4J_{HH}$ = 2.2 Hz, $^3J_{HH}$ = 7.8 Hz, 2H, Ar*H*), 6.78 (dd, $^4J_{HH}$ = 2.0 Hz, $^3J_{HH}$ = 7.6 Hz, 2H, Ar*H*), 6.73 (m, 2H, Ar*H*), 3.70 (s, 4H, ArCH_2N), 3.29 (q, $^3J_{HH}$ = 6.9 Hz, 2H, ArC*H*$(CH_3)_2$), 2.94 (q, $^3J_{HH}$ = 6.9 Hz, 2H, NC*H*$(CH_3)_2$), 2.55 (s, 4H, NCH_2CH_2N), 1.23 (d, $^3J_{HH}$ = 6.9 Hz, 12H, ArCH(C$H_3)_2$), 0.97 (d, $^3J_{HH}$ = 6.6 Hz, 6H, NCH(C$H_3)_2$).

^{13}C NMR data (100.56 MHz, $CDCl_3$, 298 K): δ 154.6 (*C*-OH), 136.5 (Ar*C*), 135.4 (Ar*C*), 129.4 (ArC*H*), 128.6 (Ar*C*H), 127.7 (Ar*C*H), 126.2 (Ar*C*H), 125.5 (Ar*C*H), 121.1 (Ar*C*CH_2N), 119.1 (Ar*C*H), 58.4 (Ar*C*H_2), 58.5 (Ar*C*H_2),49.8 (N*C*H_2*C*H_2N), 26.6 (*C*H$(CH_3)_2$), 22.6 (CH(*C*$H_3)_2$).

Copyright by Kasetsart University All rights reserved

Elemental analysis for $C_{28}H_{44}N_2O_2$ (440.66): C, 76.32; H, 10.06; N, 6.36 %. Found C, 76.05; H, 9.75; N, 5.94 %.

4.11 Synthesis of *N*,*N*'-diethyl-*N*,*N*'-bis[(4-phenyl-1-hydroxyphenyl)methyl ene]-1,2-diaminoethane (**H_2L^{3C}**)

To a solution of *N*,*N*'-diisopropyl-1,2-ethylenediamine (1.50 g, 10.41 mmol) in ethanol (125 ml) was added 3-phenylsalicylaldehyde (2.06g, 10.4 mmol), and the resulting mixture was stirred for 3 hours at reflux temperature. After cooling to room temperature, sodium borohydride (1.87 g, 50.00 mmol) was slowly added to the solution and stirred for another 2 hours at room temperature. The reaction was quenched with water (100 ml), and the aqueous phase was extracted 3 times with dichloromethane (100 ml). The organic phases were combined and dried over $MgSO_4$. The solution was concentrated *in vacuo* and redissolved in ethanol (125 ml). To the solution was added 3-phenylsalicylaldehyde (2.06 g, 10.41 mmol) at room temperature and the reaction mixture was stirred at 70 ˚C overnight. Reduction using $NaBH_4$ (1.87 g, 50.00 mmol) and extraction into dichloromethane was repeated as described above. After removing the solvent, a colorless oil was obtained and this was recrystallized from methanol. Colorless crystals were obtained. Yield: 3.28 g; 62%.

^{1}H NMR data (399.87 MHz, $CDCl_3$, 298 K): δ 7.55-7.59 (m, 4H, Ar*H*), 7.39-7.45 (m, 4H, Ar*H*), 7.29-7.34 (m, 2H, Ar*H*), 7.23 (dd, $^4J_{HH}$ = 1.7 Hz, $^3J_{HH}$ = 6.3 Hz, 2H, Ar*H*), 6.91-6.95 (m, 2H, Ar*H*), 6.83 (m, 2H, Ar*H*), 3.77 (s, 4H, ArCH_2N), 2.99 (q, $^3J_{HH}$ = 6.9 Hz, 2H, NC*H*$(CH_3)_2$), 2.61 (s, 4H, NCH_2CH_2N), 0.99 (d, $^3J_{HH}$ = 6.6 Hz, 6H, NCH(C$H_3)_2$).

^{13}C NMR data (100.56 MHz, $CDCl_3$, 298 K): δ 154.6 (*C*-OH), 158.5 (Ar*C*), 135.5 (Ar*C*), 130.1 (ArC*H*), 129.5 (Ar*C*H), 129.4 (Ar*C*H), 128.9 (Ar*C*), 128.6 (Ar*C*H), 128.1 (Ar*C*H), 128.0 (Ar*C*H), 127.7 (Ar*C*H), 122.0 (Ar*C*CH_2N), 119.4 (Ar*C*H), 58.5 (Ar*C*H_2), 58.4 (Ar*C*H_2), 49.9 (N*C*H_2*C*H_2N).

Copyright by Kasetsart University All rights reserved

Elemental analysis for $C_{34}H_{40}N_2O_2$ (508.69): C, 80.28; H, 7.93; N, 5.51 %. Found C, 80.27; H, 7.43; N, 5.50 %.

5. Synthesis of tetradentate bis(phenoxy-amine) aluminum complexes

Treatment of ligands **H_2L^{1A}- H_2L^{4A}**, **H_2L^{1B}- H_2L^{4B}** and **H_2L^{1C}- H_2L^{3C}** with an equimolar amount of trimethyl aluminum in toluene at 70 ˚C resulted in the formation of Salan aluminum methyl complexes **L^{1A}AlMe-L^{4A}AlMe**, **L^{1B}AlMe-L^{4B}AlMe** and **L^{1C}AlMe-L^{3C}AlMe**, respectively (**Figure 40**). All complexes were obtained in moderate to good *yields.*

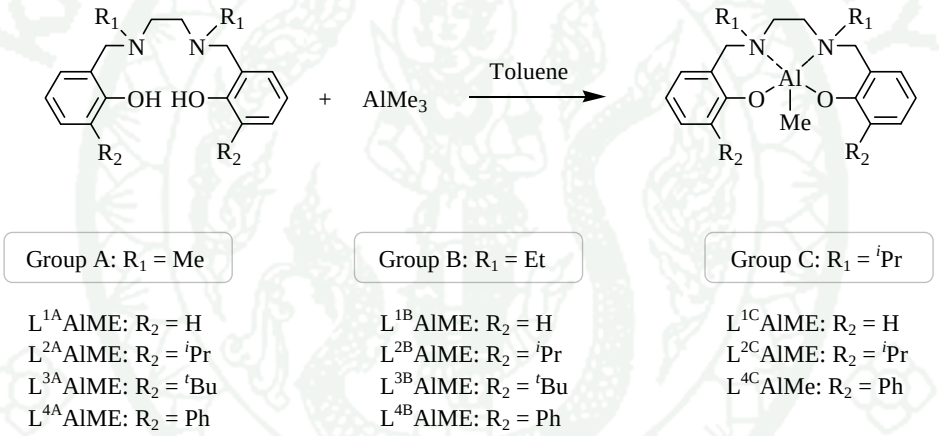

Figure 40 Synthetic pathway for the preparation of **L^{1A}AlMe-L^{4A}AlMe**, **L^{1B}AlMe-L^{4B}AlMe** and **L^{1C}AlMe-L^{3C}AlMe**.

5.1 Synthesis of **L^{1A}AlMe** (Milione *et al.*, 2012; Gibson *et al.*, 2004; Hormnirun *et al.*, 2004)

To a stirred solution of **H_2L^{1A}** (2.00 g, 6.67 mmol) in toluene (30 ml) was slowly added $AlMe_3$ (3.33 ml of a 2.0 M solution in toluene, 6.66 mmol). The reaction mixture was stirred at 70 ˚C for 24 hours. After cooling to room temperature, a white solid precipitated. The solid was collected by filtration and dried under vacuum. Yield: 1.58 g; 70%.

Copyright by Kasetsart University All rights reserved

^{1}H NMR data (399.87MHz, C_6D_6, 298 K): δ 7.23-7.19 (m, 4H, Ar*H*), 6.83 (m, 4H, Ar*H*), 3.76 (br s, 2H, ArCH_2), 2.53 (br s, 2H, ArCH_2), 1.90 (br s, 2H, N(CH_2CH_2)N), 1.68 (s, 6H, NCH_3), 1.61 (br s, 2H, N(CH_2CH_2)N), -0.53 (s, 3H, AlCH_3).

^{13}C *NMR data (100.58 MHz, C_6D_6, 298 K)*: δ 160.9 (*C*OAl), 130.5 (Ar*C*H), 128.9 (Ar*C*H), 121.8 (Ar*C*CH$_2$N), 120.5 (Ar*C*H), 116.6 (Ar*C*H), 61.3 (Ar*C*H$_2$N), 54.3 (N(*C*H$_2$*C*H$_2$)N), 43.6 (N*C*H$_3$), -10.8 (Al*C*H$_3$).

5.2 Synthesis of $\mathbf{L^{2A}AlMe}$

To a stirred solution of $\mathbf{H_2L^{2A}}$ (2.00 g, 5.20 mmol) in toluene (30 ml) was slowly added $AlMe_3$ (2.60 ml of a 2.0 M solution in toluene, 5.20 mmol). The reaction mixture was stirred at 70 ˚C for 24 hours. After cooling to room temperature, the solvent was removed under reduced pressure to leave a colorless sticky oil. The product was recrystallized from hexane, collected by filtration and dried under vacuum. Yield: 1.73 g; 78%.

^{1}H NMR data (399.87 MHz, C_6D_6, 298 K): δ 7.16 (dd, $^{4}J_{HH}$= 1.6 Hz, $^{3}J_{HH}$= 7.6 Hz, 2H, Ar*H*), 6.79-6.81 (m, 2H, Ar*H*), 6.65 (t, $^{3}J_{HH}$ = 6.9 Hz, 2H, Ar*H*), 4.44 (d, $^{3}J_{HH}$ = 12.2 Hz, 2H, ArCH_2N), 3.33-3.62 (m, 2H, C*H*(CH$_3$)$_2$), 3.19 (d, $^{3}J_{HH}$ = 12.2 Hz, 2H, ArCH_2N), 2.75-2.84 (m, 2H, NCH_2CH$_2$N), 2.45-2.62 (m, 2H, NCH$_2$CH_2N), 2.29-2.34 (s, 6H, NCH_3), 1.26 (d, $^{3}J_{HH}$ = 6.7 Hz, 12H, CH(CH_3)$_2$), -0.91 (s, 3H, AlCH_3).

^{13}C NMR data (100.56 MHz, C_6D_6, 298 K): δ 157.3 (*C*-OAl), 138.4 (Ar*C*), 126.3 (ArC*H*), 126.2 (Ar*C*H), 121.3 (Ar*C*CH$_2$N), 116.2 (Ar*C*H), 61.8 (Ar*C*H$_2$), 55.2 (NCH$_2$*C*H$_2$N), 44.0 (N*C*H$_3$), 27.2 (*C*H(CH$_3$)$_2$), 22.9 (CH(*C*H$_3$)$_2$), 22.3 (CH(*C*H$_3$)$_2$).

Elemental analysis for $C_{23}H_{37}N_2O_2Al$ (424.56): C, 70.73; H, 8.78; N, 6.60 %. Found C, 70.61; H, 8.77; N, 6.60 %.

Copyright by Kasetsart University. All rights reserved

5.3 Synthesis of **$L^{3A}AlMe$**

To a stirred solution of **H_2L^{3A}** (2.00 g, 4.85 mmol) in toluene (30 ml) was slowly added $AlMe_3$ (2.42 ml of a 2.0 M solution in toluene, 4.85 mmol). The reaction mixture was stirred at 70 ˚C for 24 hours. After cooling to room temperature, a white solid precipitated. The solid was collected by filtration and dried under vacuum. Yield: 1.30 g; 59%.

^1H NMR data (399.87 MHz, C_6D_6, 298 K): δ 7.27 (dd, $^4J_{HH}$ = 1.6 Hz, $^3J_{HH}$ = 6.0 Hz, 2H, Ar*H*), 6.85 (dd, $^4J_{HH}$ = 1.6 Hz, $^3J_{HH}$ = 7.3 Hz, 2H, Ar*H*), 6.61 (t, $^3J_{HH}$ = 7.5 Hz, 2H, Ar*H*), 4.47 (d, $^3J_{HH}$ = 12.2 Hz, 2H, ArCH_2N), 3.14 (d, $^3J_{HH}$ = 12.2 Hz, 2H, ArCH_2N), 3.01-3.09 (m, 2H, NCH_2CH_2N), 2.80-2.90 (m, 2H, NCH_2CH_2N), 2.25 (s, 6H, NCH_3), 1.47 (s, 18H, C(CH_3)$_3$), -0.83 (s, 3H, AlCH_3).

^{13}C NMR data (100.56 MHz, C_6D_6, 298 K): δ 158.8 (*C*-OAl), 139.1 (Ar*C*), 127.1 (ArC*H*), 126.9 (Ar*C*H), 121.8 (Ar*C*CH_2N), 115.5 (Ar*C*H), 61.7 (Ar*C*H_2), 55.2 (N*C*H_2*C*H_2N), 43.9 (N*C*H_3), 34.89 (*C*CH_3), 29.89 (C(*C*H_3)$_3$).

Elemental analysis for $C_{27}H_{41}N_2O_2Al$ (452.61): C, 71.65; H, 9.13; N, 6.19 %. Found C, 71.63; H, 9.00; N, 6.16 %.

5.4 Synthesis of **$L^{4A}AlMe$**

To a stirred solution of **H_2L^{4A}** (2.00 g, 4.42 mmol) in toluene (30 ml) was slowly added $AlMe_3$ (2.21 ml of a 2.0 M solution in toluene, 4.42 mmol). The reaction mixture was stirred at 70 ˚C for 24 hours. After cooling to room temperature, a white solid precipitated. The solid was collected by filtration and dried under vacuum. Yield: 1.10 g; 50%.

^1H NMR data (399.87 MHz, C_6D_6, 298 K): δ 7.66 (m, 4H, Ar*H*), 7.34 (dd, $^4J_{HH}$ = 1.8 Hz, $^3J_{HH}$ = 7.6 Hz, 2H, Ar*H*), 7.02-7.14 (m, 6H, Ar*H*), 6.87 (dd, $^4J_{HH}$ = 1.8 Hz, $^3J_{HH}$ = 7.3 Hz, 2H, Ar*H*), 6.70 (m, 2H, Ar*H*), 4.30 (d, $^3J_{HH}$ = 12.2 Hz, 2H, ArCH_2N), 3.23 (d,

Copyright by Kasetsart University All rights reserved

$^{3}J_{HH}$ = 12.2 Hz, 2H, ArCH_2N), 2.94-3.06 (m, 2H, NCH_2CH_2N), 2.71-2.83 (m, 2H, NCH_2CH_2N), 2.34 (s, 6H, NCH_3), -0.75 (s, 3H, AlCH_3).

^{13}C NMR data (100.56 MHz, C_6D_6, 298 K): δ 159.7 (*C*-OAl), 139.2 (Ar*C*), 130.8 (ArC*H*), 129.4 (Ar*C*H), 128.2 (Ar*C*), 127.5 (Ar*C*H), 125.9 (Ar*C*H), 116.5 (Ar*C*H), 109.8 (Ar*C*H), 61.4 (Ar*C*H_2), 54.8 (NCH_2*C*H_2N), 44.1 (N*C*H_3).

Elemental analysis for $C_{31}H_{33}N_2O_2Al$ (492.59): C, 75.59; H, 6.75; N, 5.69 %. Found C, 75.63; H, 6.56; N, 5.67 %.

5.5 Synthesis of **L^{1B}AlMe**.

To a stirred solution of **H_2L^{1B}** (2.00 g, 6.09 mmol) in toluene (30 ml) was slowly added $AlMe_3$ (3.05 ml of a 2.0 M solution in toluene, 6.09 mmol). The reaction mixture was stirred at 70 ˚C for 24 hours. After cooling to room temperature, the solvent was removed to leave a colorless sticky oil. The product was recrystallized from hexane, collected by filtration and dried under vacuum. Yield: 1.58 g; 70%.

^{1}H NMR data (399.87 MHz, C_6D_6, 298 K): δ 7.13-7.20 (m, 2H, Ar*H*), 6.90-6.96 (m, 2H, Ar*H*), 6.61-6.67 (m, 2H, Ar*H*), 4.00-4.16 (s br, 2H, ArCH_2N), 3.38-3.54 (s br, 2H, ArCH_2N), 2.98-2.80 (s br, 2H, NCH_2CH_2N), 2.56-2.64 (s br, 2H, NCH_2CH_3), 0.99 (t, $^{3}J_{HH}$ = 7.2 Hz, 6H, NCH$_3$CH_3), -0.81 (s, 3H, AlCH_3).

^{13}C NMR data (100.56 MHz, C_6D_6, 298 K): δ 160.3 (*C*-OAl), 129.7 (Ar*C*H), 128.5 (ArC*H*), 121.4 (Ar*C*H), 119.9 (Ar*C*H), 116.7 (Ar*C*H), 125.9 (Ar*C*H), 116.5 (Ar*C*H), 55.4 (Ar*C*H_2), 48.7 (NCH_2*C*H_2N), 45.8 (NCH_2CH_3), 14.1 (NCH_2*C*H_3).

Elemental analysis for $C_{21}H_{29}N_2O_2Al$ (368.45): C, 68.46; H, 7.93; N, 7.60 %. Found C, 68.44; H, 8.25; N, 7.56 %.

Copyright by Kasetsart University All rights reserved

5.6 Synthesis of **$L^{2B}AlMe$**

To a stirred solution of **H_2L^{2B}** (2.00 g, 4.85 mmol) in toluene (30 ml) was slowly added $AlMe_3$ (2.42 ml of a 2.0 M solution in toluene, 4.85 mmol). The reaction mixture was stirred at 70 ˚C for 24 hours. After cooling to room temperature, the solvent was removed to leave colorless sticky oil. The product was recrystallized from hexane, collected by filtration and dried under vacuum. Yield: 1.17 g; 53%.

^1H NMR data (399.87 MHz, C_6D_6, 298 K): δ 7.16 (dd, $^4J_{HH}$ = 1.7 Hz, $^3J_{HH}$ = 7.6 Hz, 2H, Ar*H*), 6.82-6.85 (m, 2H, Ar*H*), 6.63-6.67 (t, $^3J_{HH}$ = 7.4 Hz, 2H, Ar*H*), 4.08-4.25 (s br, 2H, ArCH_2N), 3.38-3.62 (s br, 4H, ArCH_2N and ArC$H(CH_3)_2$), 2.83-3.08 (s br, 2H, NCH_2CH_2N), 2.59-2.81 (s br, 2H, NCH_2CH_3), 1.26 (d, $^3J_{HH}$ = 6.9 Hz, 12H, CH(CH_3)$_2$), 1.02 (t, $^3J_{HH}$ = 7.1 Hz, 6H, NCH$_3$CH_3), -0.81 (s, 3H, AlCH_3).

^{13}C NMR data (100.56 MHz, C_6D_6, 298 K): δ 157.7 (*C*-OAl), 138.4 (Ar*C*), 126.2 (ArC*H*), 126.0 (Ar*C*H), 121.3 (Ar*C*H), 116.2 (Ar*C*H), 55.3 (Ar*C*H_2), 49.2 (Ar*C*H(CH$_3$)$_2$), 44.1 (N*C*H_2*C*H_2N), 22.9 (ArCH(*C*H$_3$)$_2$), 22.49 Ar*C*H(CH$_3$)$_2$, 5.3 ArCH(*C*H$_3$)$_2$.

Elemental analysis for $C_{27}H_{41}N_2O_2Al$ (452.61): C, 71.65; H, 9.13; N, 6.19 %. Found C, 71.64; H, 9.25; N, 6.18 %.

5.7 Synthesis of **$L^{3B}AlMe$**

To a stirred solution of **H_2L^{3B}** (2.00 g, 4.54 mmol) in toluene (30 ml) was slowly added $AlMe_3$ (2.27 ml of a 2.0 M solution in toluene, 4.54 mmol). The reaction mixture was stirred at 70 ˚C for 24 hours. After cooling to room temperature, a white solid precipitated. The solid was collected by filtration and dried under vacuum. Yield: 1.46 g; 67%.

^1H NMR data (399.87 MHz, C_6D_6, 298 K): δ 7.27 (dd, $^4J_{HH}$ = 1.6 Hz, $^3J_{HH}$ = 7.3 Hz, 2H, Ar*H*), 6.88 (dd, $^4J_{HH}$ = 1.5 Hz, $^3J_{HH}$ = 5.6 Hz, 2H, Ar*H*), 6.61 (t, $^3J_{HH}$ = 7.4 Hz,

Copyright by Kasetsart University All rights reserved

2H, Ar*H*), 4.24 (d, $^{3}J_{HH}$ = 12.6 Hz, 2H, ArCH_2N), 3.45 (d, $^{3}J_{HH}$ = 12.6 Hz, 2H, ArCH_2N), 2.96 (s, 2H, NCH_2CH_2N), 2.65-2.82 (m, 2H, NCH_2CH$_3$), 1.47 (s, 18H, C(CH_3)$_3$), 1.01 (t, $^{3}J_{HH}$ = 7.2 Hz, 6H, NCH$_3$CH_3), -0.80 (s, 3H, AlCH_3).

^{13}C NMR data (100.56 MHz, C_6D_6, 298 K): δ 159.3 (*C*-OAl), 138.9 (Ar*C*), 127.0 (ArC*H*), 126.8 (Ar*C*H), 121.5 (Ar*C*H), 115.4 (Ar*C*H), 55.7 (Ar*C*H$_2$), 48.9 (Ar*C*H(CH$_3$)$_2$), 45.4 (N*C*H$_2$*C*H$_2$N), 29.8 (ArCH$_2$*C*H$_3$), 5.4 ArC(*C*H$_3$)$_2$.

Elemental analysis for $C_{29}H_{45}N_2O_2Al$ (480.66): C, 72.46; H, 9.44; N, 5.83 %. Found C, 72.68; H, 9.43; N, 5.85 %.

5.8 Synthesis of **L^{4B}AlMe**

To a stirred solution of **H$_2$L^{4B}** (2.00 g, 4.16 mmol) in toluene (30 ml) was slowly added AlMe$_3$ (2.08 ml of a 2.0 M solution in toluene, 4.16 mmol). The reaction mixture was stirred at 70 ˚C for 24 hours. After cooling to room temperature, a white solid precipitated. The solid was collected by filtration and dried under vacuum. Yield: 1.55 g; 72%.

^{1}H NMR data (399.87 MHz, C_6D_6, 298 K): δ 7.63-7.69 (m, 4H, Ar*H*), 7.32-7.36 (m, 2H, Ar*H*), 7.02-7.13 (m, 6H, Ar*H*), 6.87-6.91 (dd, $^{4}J_{HH}$ = 1.7 Hz, $^{3}J_{HH}$ = 7.3 Hz, 2H, Ar*H*), 6.67-6.73 (m, 2H, Ar*H*), 4.03-4.30 (s br, 2H, ArCH_2N), 3.38-3.61 (s br, 2H, ArCH_2N), 2.89 (m, 4H, NCH_2CH_2N), 2.68-3.00 (m, 2H, NCH_2CH$_3$), 1.05 (t, $^{3}J_{HH}$ = 7.1 Hz, 6H, NCH$_2$CH_3), -0.74 (s, 3H, AlCH_3).

^{13}C NMR data (100.56 MHz, C_6D_6, 298 K): δ 157.4 (*C*-OAl), 139.3 (Ar*C*), 130.8 (ArC*H*), 129.4 (Ar*C*H), 128.0 (Ar*C*H), 127.5 (Ar*C*H), 125.9 (Ar*C*H), 116.5 (Ar*C*H), 74.0 (Ar*C*H$_2$), 55.7 (N*C*H$_2$*C*H$_2$N), 48.5 (Ar*C*H$_2$CH$_3$), 29.8 Ar(CH$_2$*C*H$_3$).
Elemental analysis for $C_{33}H_{37}N_2O_2Al$ (520.64): C, 76.13; H, 7.16 N, 5.38 %. Found C, 76.59; H, 6.93; N, 5.42 %.

Copyright by Kasetsart University All rights reserved

5.9 Synthesis of **L^{1C}AlMe**

To a stirred solution of **H_2L^{1C}** (1.50 g, 3.78 mmol) in toluene (30 ml) was slowly added $AlMe_3$ (1.89 ml of a 2.0 M solution in toluene, 3.78 mmol). The reaction mixture was stirred at 70 ˚C for 24 hours. After cooling to room temperature, the solvent was removed to leave colorless sticky oil. The product was recrystallized from hexane, collected by filtration and dried under vacuum. Yield: 1.31 g; 87%.

^{1}H NMR data (500.13 MHz, toluene-d_8*, 368 K)*: δ 6.94 (td, 2H, $^4J_{HH}$ = 1.8 Hz, $^3J_{HH}$ = 6.4 Hz, Ar*H*), 6.82 (dd, 2H, $^4J_{HH}$ = 1.5 Hz, $^3J_{HH}$ = 7.4 Hz, Ar*H*), 6.68 (dd, 2H, $^4J_{HH}$ = 1.0 Hz, $^3J_{HH}$ = 8.1 Hz, Ar*H*), 6.66 (td, 2H, $^4J_{HH}$ = 1.2 Hz, $^3J_{HH}$ = 7.4 Hz, Ar*H*), 3.55 (s, 4H, ArCH_2), 3.14 (q, $^3J_{HH}$ = 5.4 Hz, 2H, NC*H*$(CH_3)_2$), 2.350 (s, 4H, N(CH_2CH_2)N), 0.82 (d, $^3J_{HH}$ = 5.4 Hz, 12H, NC*H*$(CH_3)_2$), -0.43 (s, 3H, AlCH_3)

^{13}C NMR data (100.56 MHz, toluene-d_8*, 368)*: δ 160.9 (*C*-OAl), 137.3 (Ar*C*H), 129.6 (ArC*H*), 128.6 (Ar*C*H), 120.6 (Ar*C*H), 117.0 (Ar*C*H), 57.7 (ArCH_2), 53.1 (NCH_2CH_2N), 48.9 (NCH$(CH_3)_2$), 14.1 (NCH$(CH_3)_2$).

Elemental analysis for $C_{23}H_{33}N_2O_2Al$ (396.50): C, 69.67; H, 8.39; N, 7.07 %. Found C, 69.67; H, 8.63; N, 7.05 %.

5.10 Synthesis of **L^{2C}AlMe**

To a stirred solution of **H_2L^{2C}** (1.50 g, 3.12 mmol) in toluene (30 ml) was slowly added $AlMe_3$ (1.56 ml of a 2.0 M solution in toluene, 3.12 mmol). The reaction mixture was stirred at 70 ˚C for 24 hours. After cooling to room temperature, a white solid precipitated. The solid was collected by filtration and dried under vacuum. Yield: 1.10 g; 73%.

^{1}H NMR data (500.13 MHz, toluene-d_8*, 368 K)*: δ 7.19 (m, 2H, Ar*H*), 6.63-6.74 (m, 6H, Ar*H*), 3.68 (q, $^3J_{HH}$ = 5.5 Hz, 2H, ArC*H*$(CH_3)_2$), 3.57 (s, 4H, ArCH_2), 3.18 (q,

Copyright by Kasetsart University All rights reserved

$^{3}J_{HH}$ = 5.3 Hz, 2H, NC*H*(CH_3)$_2$), 2.38 (s, 4H, N(CH_2CH_2)N), 1.38 (d, $^{3}J_{HH}$ = 5.1 Hz, 12H, CH(CH_3)$_2$), 0.85 (d, $^{3}J_{HH}$ = 5.3 Hz, 12H, NCH(CH_3)$_2$), -0.43 (s, 3H, AlCH_3).

^{13}C NMR data (100.56 MHz, toluene-d_8, *368K)*: δ 158.0 (*C*-OAl), 137.3 (Ar*C*H), 126.4 (ArC*H*), 126.0 (Ar*C*H), 125.4 (Ar*C*H), 117.0 (Ar*C*H), 55.4 (Ar*C*H_2), 52.7 (N*C*H_2*C*H_2N), 49.0 (N*C*H(CH_3)$_2$), 22.6 (Ar*C*H(CH_3)$_2$),14.1 (NCH(*C*H_3)$_2$).

Elemental analysis for $C_{29}H_{45}N_2O_2Al$ (480.66): C, 72.46; H, 9.44; N, 5.83 %. Found C, 72.91; H, 9.54; N, 8.56 %.

5.11 Synthesis of **L^{3C}AlMe**

To a stirred solution of **H_2L^{3C}** (1.50 g, 2.73 mmol) in toluene (30 ml) was slowly added $AlMe_3$ (1.37 ml of a 2.0 M solution in toluene, 2.73 mmol). The reaction mixture was stirred at 70 ˚C for 24 hours. After cooling to room temperature, a white solid precipitated. The solid was collected by filtration and dried under vacuum. Yield: 1.33 g; 89%.

^{1}H NMR data (500.13 MHz, toluene-d_8, *368 K)*: δ 7.38 (m, 2H, Ar*H*), 7.06 (m, 2H, Ar*H*), 6.65-6.92 (m, 8H, Ar*H*), 6.31-6.54 (m, 4H, Ar*H*), 3.37 (s, 4H, ArCH_2), 2.87 (q, $^{3}J_{HH}$ = 5.1 Hz, 2H, NC*H*(CH_3)$_2$), 2.15 (s, 4H, N(CH_2CH_2)N), 0.63 (d, $^{3}J_{HH}$ = 5.1 Hz, 12H, NCH(CH_3)$_2$), -0.81 (s, 3H, AlCH_3).

^{13}C NMR data (100.56 MHz, toluene-d_8, *368 K)*: δ 157.5 (*C*-OAl), 139.3 (Ar*C*), 130.8 (ArC*H*), 129.4 (Ar*C*H), 128.0 (Ar*C*H), 127.5 (Ar*C*H), 125.9 (Ar*C*H), 116.5 (Ar*C*H), 74.0 (Ar*C*H_2), 55.4 (N*C*H_2*C*H_2N), 49.1 (Ar*C*H_2CH$_3$), 17.2 Ar(CH(*C*H_3)2).

Elemental analysis for $C_{35}H_{41}N_2O_2Al$ (548.69): C, 76.61; H, 7.53; N, 5.11 %. Found C, 76.60; H, 7.68; N, 5.10 %.

Copyright by Kasetsart University All rights reserved

6. General procedure for *rac*-LA, *L*-LA and ε-caprolactone polymerizations

In a nitrogen-filled glove box, an ampoule was charged with a 720 mg for *rac*-LA and *L*-LA or 570 mg for ε-caprolactone (5.00 mmol) and 5.2 μL of benzyl alcohol (50 μmol) was added a solution of catalyst (50 μmol) in 6 ml of toluene ([monomer]:[benzyl alcohol]:[catalyst] = 100:1:1). The reaction mixture was stirred at 70 ˚C for the desired reaction time. After an aliquot was removed for characterization, the reaction was quenched with small drop of methanol. The polymer was precipitated with excess methanol and was then dried *in vacuo* to constant weight.

7. General kinetic procedure for *rac*-LA and *L*-LA polymerization

In a nitrogen-filled glove box, a solution of catalyst (50 μmol) in toluene (6 ml) was added to an ampoule which was charged with a 360 mg of monomer (2.50 mmol) and 5.2 μL of benzyl alcohol (50 μmol) (resulting [monomer]:[benzyl alcohol]:[catalyst] = 50:1:1). The mixture was then stirred at 70 ˚C. At appropriate time intervals, aliquots were removed and quenched with 1 ml of hexane. The aliquots were then dried *in vacuo* and analyzed by ^{1}H NMR spectroscopy.

8. General procedure for *rac*-LA and ε-caprolactone copolymerization

In nitrogen-filled glove box, an ampoule containing *rac*-LA (360 mg), ε-CL (290 mg), and benzyl alcohol (5.2 μL) was added a solution of catalyst (50 μmol) in toluene (6 ml) ([*rac*-LA]:[ε-CL]:[benzyl alcohol]:[catalyst] = 50:50:1:1). The reaction was then stirred at 70 ˚C. The samples were withdrawn at appropriate time intervals. Characterization of products was performed after drying under vacuum.

Copyright by Kasetsart University All rights reserved

RESULTS AND DISCUSSION

1. Aluminum complexes supported by bis(pyrrolidene) Schiff-base ligands

Since the first discovery of the well-controlled and stereoselective polymerization of lactides using the enantiomerically pure (*R*)-(SalBinap)-$AlOCH_3$ (**(*R*,*R*)-1**) by Spassky and coworkers, the five-coordinate aluminum alkoxide complexes have become promising catalysts for the ring-opening polymerization of lactones (Spassky *et al*., 1996). The efficiency of many chiral and achiral bis(salicylidene) Schiff-base aluminum complexes as catalysts for the ROP of lactones have been reported since then. However, most of bis(salicylidene) Schiff-base aluminum complexes have lower activities than the other reported metal catalyst systems (Chisholm *et al.*, 2004; Chamberlian *et al.*, 2001; Williams *et al.*, 2003). Compared with the existing aluminum catalysts with a bis(salicylidene) Schiff-base ligand system (Spassky *et al.*, 1996; Randano *et al*., 2000; Ovitt and Coates, 2000; Zhong and Feijen, 2002), the five-coordinate aluminum complexes ligated by bis(pyrrolidene) Schiff-base ligands showed not only an excellent activity but also exhibited a good stereoselectivity over the ROP of lactides (Du *et al.*, 2009). According to the work reported by Du and coworkers, the results showed that both activity and selectivity were enhanced for initiators bearing the flexible C_3 linkers. However, the introduction of dimethyl substituents on the pyrrole rings was found to decrease both activity and selectivity. With regard of the fact that the ability over ROP of bis(salicylidene) Schiff-base aluminum complexes is strongly dependence on the flexibility of the linker (Nomura *et al.*, 2002; 2004; Hormnirun *et al.*, 2006), this work focused on the architecture of backbone that linked between the two pyrrole units. This investigation was included the length and the flexibility of the backbone linkers. The chiral nature of aluminum complex was also in the point of concern.

Copyright by Kasetsart University. All rights reserved

1.1 Synthesis of tetradentate bis(pyrrolidene) Schiff-base ligands

The bis(pyrrolidine) Schiff base ligands **H_2L^1-H_2L^7** with different backbone structures illustrated in **Figure 41** were obtained in good yields (57-99%) by reacting two equivalents of the pyrrole-2-carboxaldehyde with the relevant diamine in ethanol at room temperature. The synthesis of all ligands was described in Materials and Methods. NMR spectroscopic technique and elemental analysis were used to characterize the synthesized ligands.

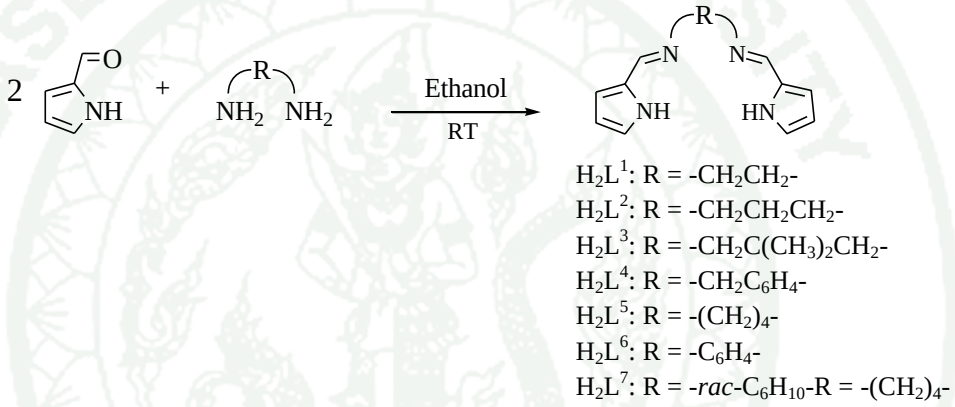

Figure 41 The synthetic pathway for ligands **H_2L^1-H_2L^7**.

Satisfactory elemental analyses were obtained on all compounds (see 2.1-2.7 in Materials and Methods) and spectroscopic data were consistent with the formulae depicted in **Figure 41**. The ^{1}H NMR spectra of all compounds except **H_2L^4** show one peak of the imine proton (N=C*H*), three peaks of the pyrrolic protons and a set of the backbone protons. For **H_2L^4**, an asymmetrical nature of this ligand was indicated by the observation of two imine resonances and two sets of pyrrolic protons.

1.2 Synthesis of aluminum bis(pyrrolidine) Schiff-base complexes

The aluminum methyl complexes **L^1AlMe-L^7AlMe** were prepared by treating the relevant tetradentate Schiff-base with trimethylaluminum in toluene as shown in **Figure 42**. Complexes **L^1AlMe** and **L^5AlMe** rapidly precipitated from the reaction

Copyright by Kasetsart University All rights reserved

solution after the addition of trimethyl aluminum. Complexes **L[2]AlMe** and **L[3]AlMe** were obtained directly from the cooled reaction mixture as off-white solids, whereas complexes **L[4]AlMe** and **L[6]AlMe** were obtained as pale yellow solids. X-ray quality crystal of complex **L[3]AlMe** was grown from the low-rate cooling of the crude reaction product from 110 ˚C to room temperature. Reaction of **H_2L[7]** and trimethyl aluminum took several days to fully convert all the Schiff-Base to **L[7]AlMe**. The synthesis of complexes **L[1]AlMe** and **L[6]AlMe** has been reported in the literature (Azpeitia *et al*., 2011).

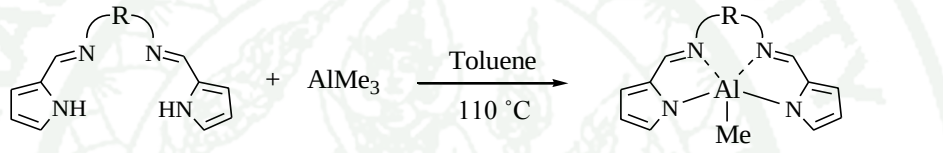

H_2L^1: R = -CH_2CH_2-
H_2L^2: R = -$CH_2CH_2CH_2$-
H_2L^3: R = -$CH_2C(CH_3)_2CH_2$-
H_2L^4: R = -$CH_2C_6H_4$-
H_2L^5: R = -*rac*-C_6H_{10}-
H_2L^6: R = -C_6H_4-
H_2L^7: R = -$(CH_2)_4$-

L^1AlMe: R = -CH_2CH_2-
L^2AlMe: R = -$CH_2CH_2CH_2$-
L^3AlMe: R = -$CH_2C(CH_3)_2CH_2$-
L^4AlMe: R = -$CH_2C_6H_4$-
L^5AlMe: R = -$(CH_2)_4$-
L^6AlMe: R = -C_6H_4-
L^7AlMe: R = -*rac*-C_6H_{10}-

Figure 42 The synthetic pathway for **L[1]AlMe-L[7]AlMe**.

The ^{1}H NMR spectrum of complex **L[1]AlMe** (**Figure 43**) shows a signal at δ -0.97 ppm, which is attributed to the protons of the aluminum methyl group. The pyrrole protons display one multiplet and two double doublets at δ 7.30, 6.62 and 6.18, respectively. The signal of imine protons appears as a singlet at δ 8.33 ppm. The signal of four methylene protons of backbone appears as two multiplets at δ 4.00-3.93 and δ 3.74-3.66 ppm, which indicated a monomeric structure with a five-coordinate aluminum center.

The ^{1}H NMR spectrum of complex **L[2]AlMe** is shown in **Figure 44**. A singlet of imine protons, a set of pyrrole protons and aluminum methyl protons were observed in the same fashion with complex **L[1]AlMe**. The four NCH_2 protons show

Copyright by Kasetsart University All rights reserved

two overlapping multiplets at δ 3.88-3.76 ppm. Two multiplets at δ 2.12-2.01 and δ 1.86-1.74 ppm arise from the diastertereotopic methylene protons of the ligand backbone. All intensities of the peaks and a symmetric pattern indicate a monomeric structure with a five coordinate aluminum center for **L^{2}AlMe**.

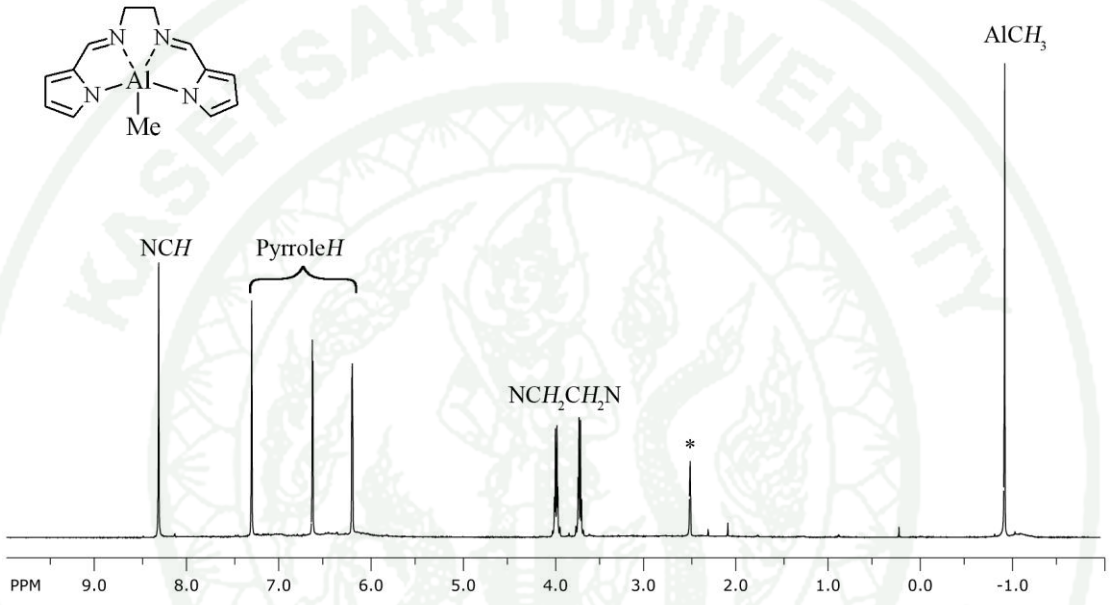

Figure 43 ^{1}H NMR spectrum of complex **L^{1}AlMe** (400 MHz, DMSO-d_6, 300 K, * = residual DMSO).

Figure 45 illustrates the ^{1}H NMR spectrum of complex **L^{3}AlMe**. The characteristic signal at δ -0.89 is attributed to the protons of the aluminum methyl group and the signal of imine protons appears as a singlet at δ 8.24 ppm. The pyrrole protons display one multiplet and two double doublets at δ 7.39-7.36, 6.68 and 6.26, respectively. The four NCH_2 protons show two doublets centered at δ 3.76 and δ 3.45 with the $^2J_{HH}$ coupling constants of 12.2 Hz. Two methyl protons from backbone display two singlets at δ 1.05 and δ 0.84 ppm. All the peaks indicate a monomeric structure for **L^{3}AlMe** with a five coordinated aluminum center.

Copyright by Kasetsart University All rights reserved

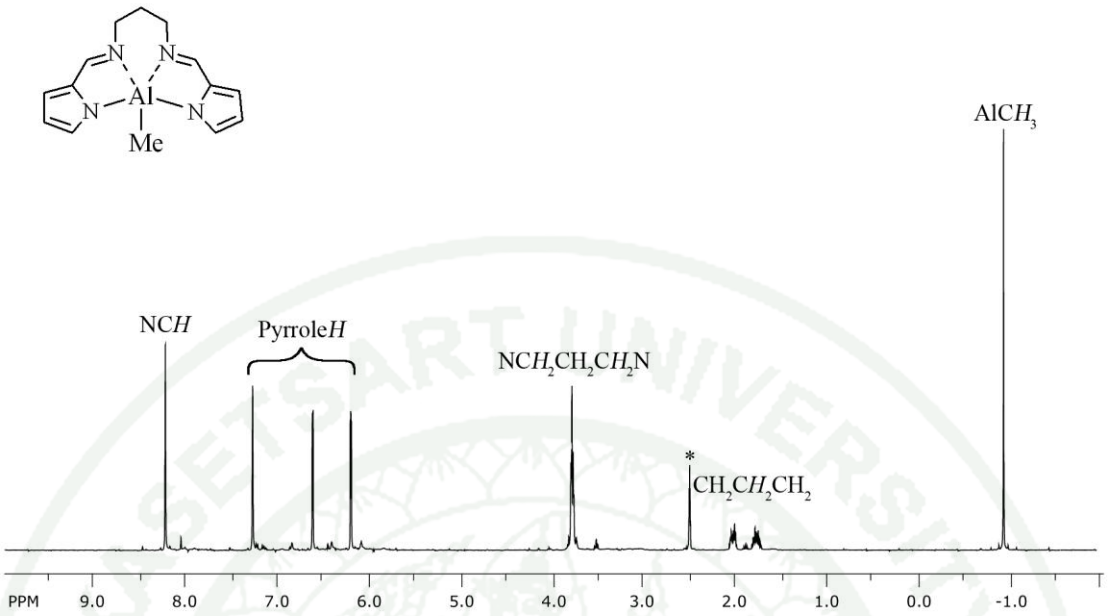

Figure 44 ^{1}H NMR spectrum of complex **L^{2}AlMe** (400 MHz, DMSO-d_6, 300 K, * = residual DMSO).

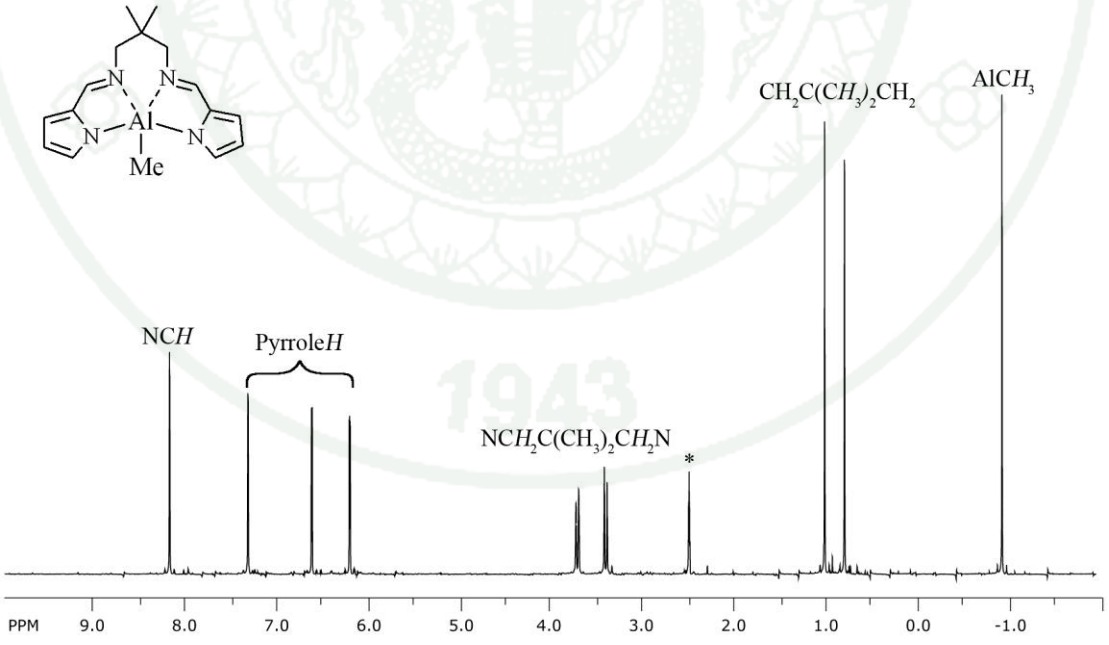

Figure 45 ^{1}H NMR spectrum of complex **L^{3}AlMe** (400 MHz, DMSO-d_6, 300 K, * = residual DMSO).

Copyright by Kasetsart University All rights reserved

Single crystals of complex **L^{3}AlMe** were grown by cooling a concentrated toluene solution from 110 ˚C to room temperature. X-ray diffraction analysis revealed that this complex is monomeric with well defined geometry of the ligand around the central aluminum atom. The molecular structure is shown the **Figure 46**. The unit cell parameters are summarized in **Table 3** and the refinement details are given in **Appendix Tables 1** and **2**.

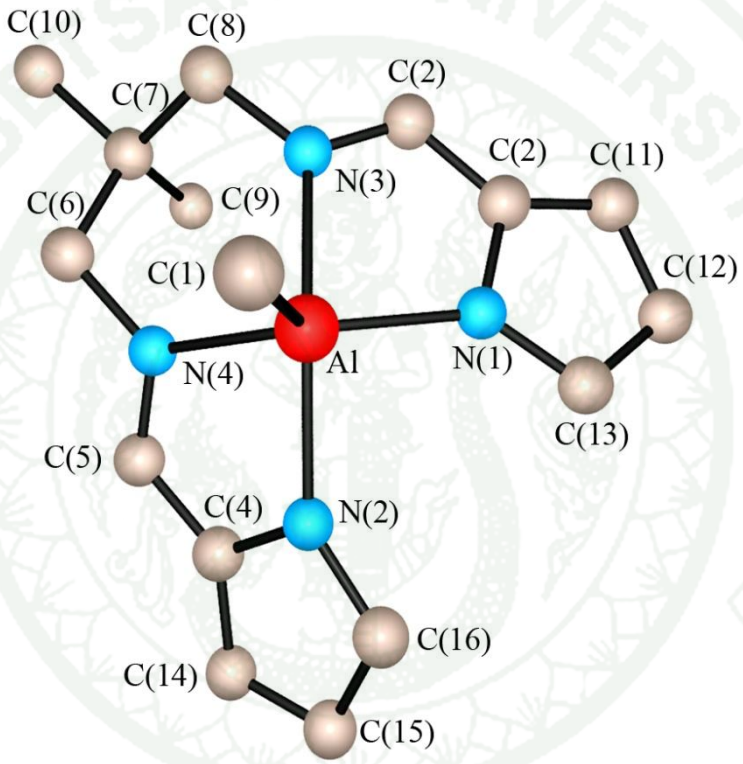

Figure 46 The molecular structure of complex **L^{3}AlMe.** Selected bond lengths (Å) and angles (°) are as follows: Al-C(1), 1.967(2); Al-N(1), 1.976(1); Al-N(2), 1.959(1); Al-N(3), 2.033(1); Al-N(4), 2.054(1); N(3)-C(6), 1.289(2); N(4)-C(5), 1.291(2); C(1)-Al-N(1), 108.95(7); C(1)-Al-N(2), 115.41(7); C(1)-Al-N(3), 106.27(7); C(1)-Al-N(4), 102.07(7); N(1)-Al-N(2), 92.86(6); N(1)-Al-N(3), 80.43(5); N(1)-Al-N(4), 148.16(6); N(2)-Al-N(3), 137.59(6); N(2)-Al-N(4), 79.92(6); N(3)-Al-N(4), 84.28(5).

Copyright by Kasetsart University All rights reserved

Table 3 Crystal data and refinement parameters for complex **L^3AlMe.**

Crystal data and refinement parameters	**L^3AlMe**
Empirical formula	$C_{16}H_{21}AlN_4$
Formula weight	296.354
Temperature (K)	150
Dimension (mm)	0.25 × 0.20 × 0.10
Crystal system	Orthorhombic
Space group	$Pna2_1$
a (Å)	9.5878(4)
b (Å)	14.6264(6)
c (Å)	11.4569(3)
α (deg)	90.00
β (deg)	90.00
γ (deg)	90.00
V (Å^3)	1606.66(10)
Z	4
Absorption coefficient (mm^{-1})	0.126
Calculated density (mg/m^3)	1.225
Reflections collected/unique	11,799/3650
Number of observations [>2σ(*I*)]	3397
Goodness of fit on F^2	1.020
R_1 [$I > 2\sigma(I)$]	0.0344
Largest difference in peak and hole (e/Å^3)	0.170/-0.173
Final R indices [$I > 2\sigma(I)$]	R_1 = 0.0382
	wR_2 = 0.0916

Copyright by Kasetsart University All rights reserved

The geometry of **L^{3}AlMe** can be defined by the τ and χ values. The τ value is expressed as (β-α)/60, where α and β are the two largest N-Al-N angles in the diagonal direction in the *xy* plane with the Al-Me group oriented along the *z*-axis as shown in **Figure 47**. The geometry of five coordinate aluminum complex can be classified as either square pyramidal (sqp) or trigonal bipyramidal (tbp) (Atwood and Harvey, 2001). The *τ* value ranges from 0 for an ideal square pyramid to 1 for an ideal trigonal bipyrimid (Addison *et al.*, 1984; Munoz-Hernadez *et al*., 2001).



Figure 47 Square pyramidal (sqp) and trigonal bipyramidal (tbp) geometries of the five-coordinate aluminum methyl Schiff base complexes.

The geometry χ parameter was developed by Konno *et al.* (Matsuo *et al*., 2003; Konno *et al*., 2000). The parameter can be used to define the geometry of five-coordinate metal complex. The χ is calculated by the equation 8.

$$\chi = (\beta+\gamma+\delta-2\alpha)/180 \quad (8)$$

where α and β represent the two largest bond angles defined by four of five donor atoms N_1-N_4, γ and δ represent the angles concerning the remaining donor atom C. For $\chi = 0$, the coordination geometry is a perfect sqp, and for $\chi = 1$ is a perfect tbp.

Although, the τ parameter is more favorable for identifying the geometry of five-coordinate metal complexes, it declines to adequately quantify the tbp distortions for complexes with rigid ligand frameworks. For the identification of the geometry

Copyright by Kasetsart University All rights reserved

around metal center with severe rigid ligand framework, a modified index parameter, χ, has been proposed to describe the trigonality of the complexes (Watanabe *et al.*, 2011). The χ parameter is more reliable according to the fact that it is based on more bond angles to determine the deviations from the tbp geometry (HAzpeitia *et al.*, 2011).

For **L^{3}AlMe**, the calculated τ and χ values are 0.18 and 0.36, respectively, indicating of distorted square pyramidal geometry. The bite angle, $N_{(pyrrole)}$-Al-$N_{(pyrrole)}$ is 72.86(6)˚. The average Al-$N_{(imino)}$ bond length is 2.044 Å, which is slightly larger than those observed in **L^{1}AlMe** (average Al-$N_{(imino)}$ bond length is 2.003 Å). However, the average Al-$N_{(pyrrole)}$ bond length (1.968 Å) is closed to those observed in **L^{1}AlMe** (1.960 Å) (H.F. Azpeitia *et al.*, 2011).

The ^{1}H NMR spectrum of complex **L^{4}AlMe** is illustrated in **Figure 48**. The spectrum shows a singlet at -1.21 ppm which is attributed to the aluminum methyl protons. The signal due to the diastereotopic methylene protons occurs as two doublets centered at 3.76 and 3.45 ppm with the $^2J_{HH}$ value of 12.2 Hz. Notably, the protons corresponding to pyrrole rings display as two set of signals. The amine protons also appear as two singlets, indicating of the asymmetric structure of the complex in the solution.

Complex **L^{5}AlMe** has poor solubility in most common NMR solvents. However, it is slightly soluble in DMSO-d_6 at room temperature and the ^{1}H NMR spectrum of this complex is shown in **Figure 49**. The spectrum displays an equal intensity of two Al-CH_3 characteristic peaks but shows only one set of pyrrole and backbone protons. The peaks of NCH_2CH_2 protons at δ 3.40-3.70 are related to the backbone methylene protons of **L^{1}AlMe**. This result suggests the presence of at least two isomers at room temperature. The intensity ratio of the peaks and the elemental analysis result, which consistent with the stoichiometry $C_{15}H_{19}AlN_4$, suggest the formation of a five coordinated aluminum complex. Based on this information, either

Copyright by Kasetsart University All rights reserved

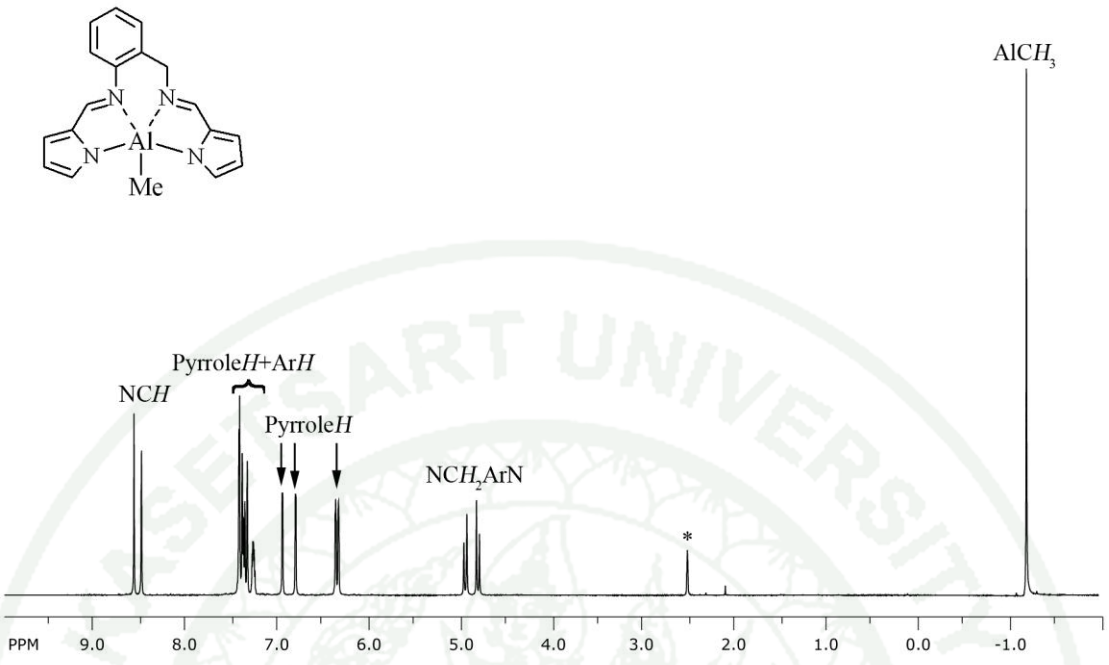

Figure 48 ^{1}H NMR spectrum of complex **L^{4}AlMe** (400 MHz, DMSO-d_6, 300 K , * = residual DMSO).

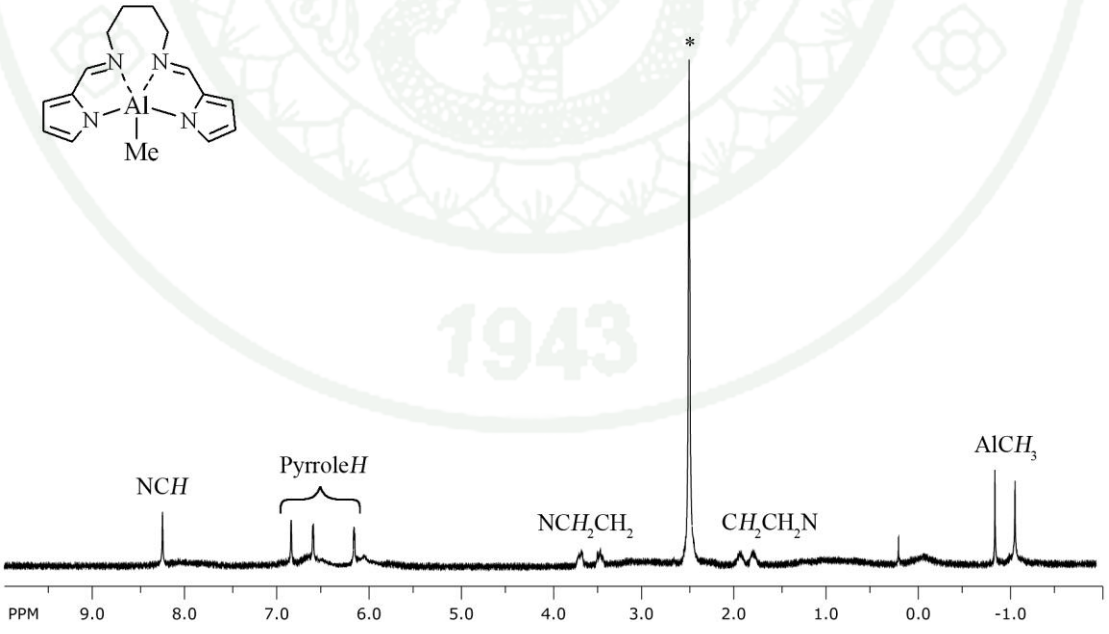

Figure 49 ^{1}H NMR spectrum of complex **L^{5}AlMe** (400 MHz, DMSO-d_6, 300 K , * = residual DMSO).

Copyright by Kasetsart University All rights reserved

the fast transformation between two possible geometries, sqp and tbp, or the formation of two diastereoisomers is considered. However, with the lack of spectroscopic information, it is inconceivably to conclude whether reasons with respect to this complex.

Synthesis of complex **L^{6}AlMe** was reported by Azpeitia and coworkers (Azpeitia *et al.*, 2011). The complex was prepared from the treatment of ligand precursor with an equimolar of $AlMe_3$. The complex was obtained from the cooled reaction mixture as a pale yellow solid in a moderate yield (26%). The ^{1}H NMR spectrum of complex **L^{6}AlMe** is shown in **Figure 50**. The characteristic signal at δ -1.13 ppm is attributed to the protons of the aluminum methyl group whereas the signal of imine protons appears as a singlet at δ 8.94 ppm. The pyrrole protons display one multiplet and two double doublets at δ 7.69, 7.05 and 6.45, respectively. The signal of aromatic protons of backbone appears as two doublets at δ 7.80 and δ 7.33 ppm with the $^3J_{HH}$ and $^4J_{HH}$ value of 5.9 and 3.4 Hz, respectively. Recently, the synthesis and the X-ray structures of aluminum complexes with different alkyl groups (**L^{6}AlEt** and **L^{6}Al^{t}Bu**) were reported (Azpeitia *et al.*, 2011). For **L^{6}AlEt,** the τ and χ values are calculated to be 0.03 and 0.41, respectively, indicating of the distorted square pyramidal geometry. The bite angle is 102.86(16)˚. However, in the case of **L^{6}Al^{t}Bu**, the τ and χ values for are 0.16 and 0.50, respectively. These two parameters suggested the possible geometry of this complex can be either a distorted square pyramidal or an intermediate between tbp and sqp. The bite angle is 101.78(7)˚. According to this geometrical parameter, the molecular geometry of **L^{6}AlEt** and **L^{6}Al^{t}Bu** is an intermediate between tbp and sqp. Comparing to the structure of **L^{6}AlEt** and **L^{6}Al^{t}Bu**, the possible structure of **L^{6}AlMe** is a distorted square pyramidal.

Complex **L^{7}AlMe** is prepared from the treatment of racemic ligand precursor with an equimolar amount of $AlMe_3$ in toluene at 110 ˚C. The ^{1}H NMR spectrum in DMSO-d_6, as illustrated in **Figure 51**, clearly revealed the presence of two stereoisomers in solution. The molar ratio of the characteristic both imine peaks is 1:1.

Copyright by Kasetsart University All rights reserved

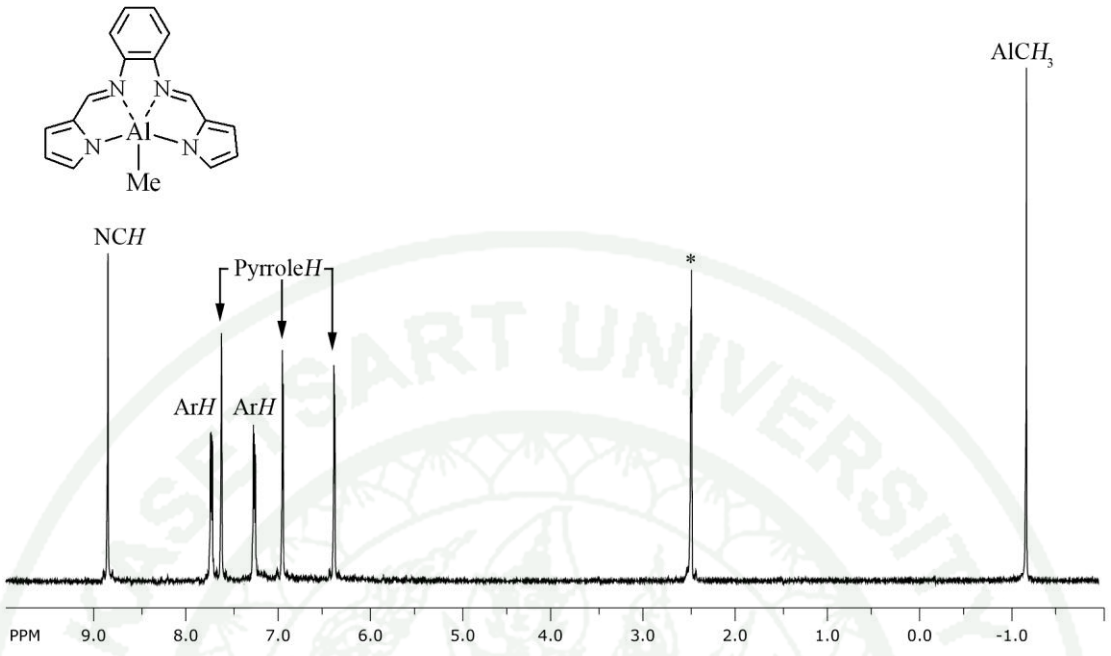

Figure 50 ^{1}H NMR spectrum of complex **L^{6}AlMe** (400 MHz, DMSO-d_6, 300 K , * = residual DMSO).

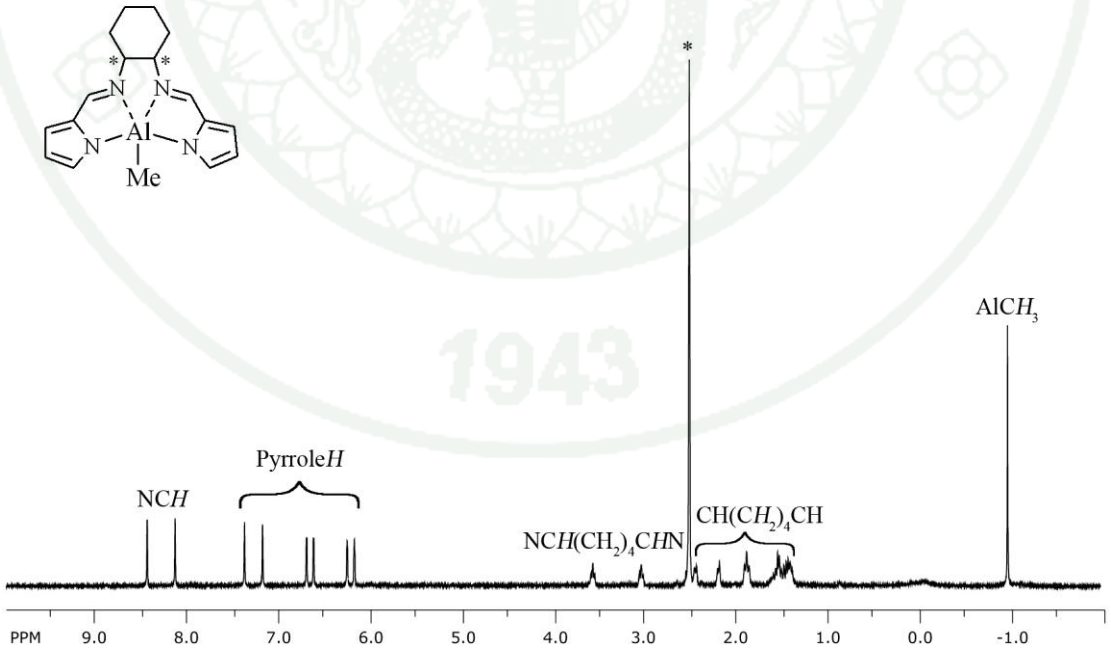

Figure 51 ^{1}H NMR spectrum of complex **L^{7}AlMe** (400 MHz, DMSO-d_6, 300 K , * = residual DMSO).

Copyright by Kasetsart University All rights reserved

1.3 Synthesis of aluminum benzyloxide complex

It is well known that the aluminum alkoxide complex is the most active species for the ROP of lactones (Duda *et al*., 1990 ; Balasanthiran *et al*., 2013). Benzyl alcohol is normally used *in situ* to generate the aluminum alkoxide complex (Ovitt and Coates, 2012). The formation of the aluminum alkoxide species can be confirmed by the isolation of complex **L^{3}AlOBn** synthesized by the reaction between **L^{3}AlMe** and an equimolar amount of benzyl alcohol in anhydrous toluene at 70 ˚C. The appearance of the methylene protons from benzyloxy group (OCH_2PH) as a singlet resonance at δ 4.47 as well as the absence of the aluminum methyl signal indicated the complex conversion to the corresponding aluminum benzyloxide complex. The ^{1}H NMR spectrum of **L^{3}AlOBn** in DMSO-d_6 reveals a symmetric structure of this complex. The imine proton appears as a singlet at δ 8.21 ppm and the methylene protons from the backbone appear as two doublets at δ 3.45 and δ 3.54 ppm.

1.4 LA polymerization studies using complexes **L^{1}AlMe- L^{7}AlMe**

Complexes **L^{1}AlMe- L^{7}AlMe** were examined as initiators for the ROP of *L*-LA and *rac*-LA. The aluminum alkoxide species were generated *in situ* by alcoholysis of the aluminum methyl complexes with one equivalent of benzyl alcohol, according to **Figure 53**.

Copyright by Kasetsart University All rights reserved

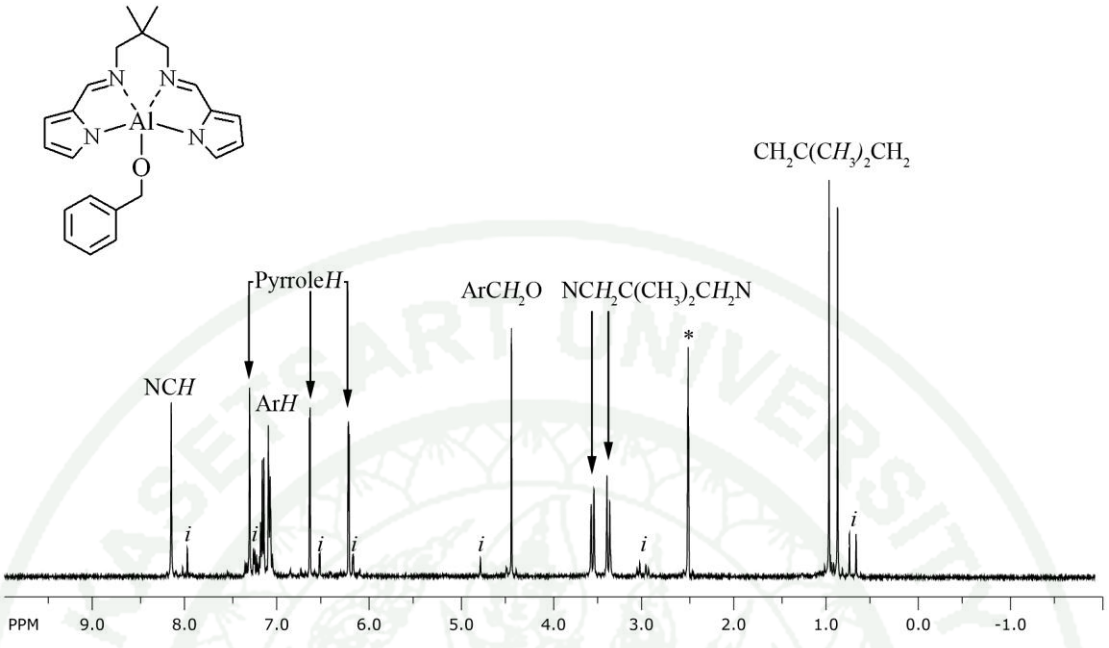

Figure 52 ^{1}H NMR spectrum of complex **L^{3}AlOBn** (400 MHz, DMSO-d_6, 300K, *i* = impurity, * = residual DMSO).

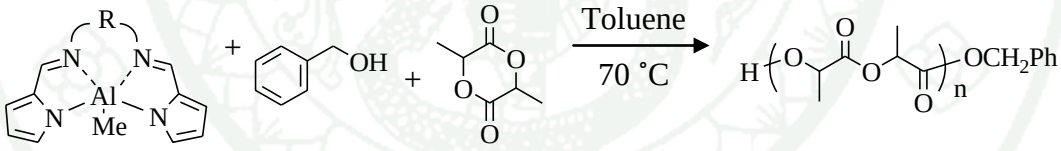

in situ alcoholysis

Figure 53 The LA polymerization procedure using complexes **L^{1}AlMe- L^{7}AlMe**.

In typical polymerization experiment, LA (720 mg, 5.00 mmol), aluminum complex (0.05 mmol) and benzyl alcohol (5.2 μL, 0.05 mmol) were dissolved in 6 ml of toluene and introduced to a polymerization tube equipped with a magnetic bar. The molar ratio of *rac*-LA or *L*-LA to an initiator was fixed at 100:1 ($[LA]_0/[Al]$ = 100; $[LA]_0$ = 0.83 M; [Al] = 8.33 mM; M_n (theory) =14,400). The experiments were carried out at 70 ˚C. After a certain time, aliquot was taken from the polymerization mixture to determine the monomer conversion by comparing the methine signal intensity of monomer (δ 5.05-5.11 ppm) and the polymer (δ 5.11-5.27 ppm). The

Copyright by Kasetsart University All rights reserved

polymers were precipitated from cold methanol. The resultant polymers were isolated by filtration and dried under vacuum. The polymer molecular weights and polydispersity indices were determined form GPC analysis in THF calibrated with polystyrene standards. The molecular weight was corrected using the correction coefficient according to literature (Kricheldorf and Rost, 2005; Palard *et al.*, 2007).

Preliminary polymerization experiments were conducted using the optically pure *L*-LA. Independently of the catalyst being used, an isotactic polylactide was expected. The results are summarized in **Table 4**. All complexes were found to be active under the polymerization conditions. Molecular weight distributions are in the range of 1.02-1.08. These relatively narrow PDI values supported the controlled polymerization catalysis. Moreover, the M_n(GPC) values were in good agreement with the theoretical ones (M_n(th)) suggesting the growth of one polymer chain per an initiator. Complexes **L^2AlMe-L^4AlMe**, with C_3 backbone, showed remarkably high conversion up to 80% of monomer within 1 hour. Complexes with C_2 backbone (**L^1AlMe**, **L^6AlMe** and **L^7AlMe**) took longer time to reach high conversion of monomer. In the C_2 backbone series, complex **L^1AlMe** showed lower activity than complex **L^7AlMe**, which has a racemic cyclohexyl backbone**.** Complex **L^6AlMe** took about ten days to achieve 92% conversion of monomer or 10 times slower than complex **L^7AlMe**. According to the fact that the polymerization reaction proceeds *via* a coordination-insertion mechanism, the complex rearranges itself to form six-coordinate complex in transition stage(s). Hence, the lack of backbone flexibility may cause the dramatically activity drop (P. Hormnirun *et al*., 2006). Complex **L^5AlMe** which has the butylene backbone showed slightly higher activity than **L^1AlMe.** In the C_3 backbone series, the polymerizations using **L^2AlMe-L^4AlMe** were relatively fast. (Borgne *et al*., 1993, Wisniewski *et al*., 1997; Bhaw-Luximon *et al*., 2000; Jhurry *et al*., 2001; Radano *et al*., 2000). The complexes required about an hour to proceed to full conversion.

Polymerization of *rac*-LA was explored to evaluate the stereospecificity of the polymerization system. The results are summarized in **Table 5**. The narrow molecular weight distributions were also observed. The molecular weights measured by GPC

Copyright by Kasetsart University All rights reserved

(M_n(GPC)) were in good agreement with the calculated values. This reflects the well-controlled and living fashion of the catalysts.

Table 4 Polymerizations of *L*-LA using initiators **L[1]AlMe-L[7]AlMe** in the presence of benzyl alcohol[a]

Initiator	Time (h)	Conversion[b] (%)	M_n(th)[c] (g mol^{-1})	M_n(GPC)[d] (g mol^{-1})	PDI[d]
L[1]AlMe	48	73	10573	10140	1.08
L[2]AlMe	1	92	13238	10590	1.04
L[3]AlMe	1	83	11974	11190	1.06
L[4]AlMe	0.5	99	14251	12810	1.07
L[5]AlMe	24	94	13548	12720	1.05
L[6]AlMe	240	82	11818	12480	1.15
L[7]AlMe	24	94	13548	11230	1.02

87

[a]$[LA]_0/[Al]$ = 100, $[Al]/[PhCH_2OH]$ = 1, $[LA]_0$ = 0.42 M, toluene, 70 ˚C. [b]As determined *via* integration of the methine resonances (^{1}H NMR) of LA and PLA ($CDCl_3$, 400 MHz). [c]Calculated by $([LA]_0/[I]) \times 144.13 \times$ conversion. [d]Determined by gel permeation chromatography (GPC) calibrated with polystyrene standards in THF and corrected by a factor of 0.58 for PLA.

According to the results, it can be seen that the flexibility of backbone has an influence on the polymerization activity. Comparing the polymerization time between **L[3]AlMe** and **L[1]AlMe** or **L[6]AlMe** revealed that the introduction of more flexible backbone could accelerate the polymerization reaction. In the C_3 backbone group, complex **L[4]AlMe** showed highest activity. It converted 100 equivalents of both *L*-LA and *rac*-LA to polylactide within 30 minutes. The conjugate molecular structure resulting from incorporation of benzene ring in the backbone and more rigid planar geometry leads to a decrease of stereoselectivity (Du *et al*., 2007). Increasing the number of carbon atoms to four as in **L[5]AlMe** also gives a decrease in stereoselectivity.

Copyright by Kasetsart University All rights reserved

Table 5 Polymerizations of *rac*-LA using initiators **L[1]AlMe-L[7]AlMe** in the presence of benzyl alcohol[a]

Initiator	Time (h)	Conversion[b] (%)	M_n(th)[c] (g mol^{-1})	M_n(GPC)[d] (g mol^{-1})	PDI[d]	P_m
L[1]AlMe	48	77	11088	8481	1.06	0.61
L[2]AlMe	1	98	14112	10424	1.05	0.69
L[3]AlMe	1	95	13680	12817	1.03	0.80
L[4]AlMe	0.5	99	14251	13723	1.07	0.74
L[5]AlMe	24	82	11808	99077	1.02	0.52
L[6]AlMe	200	86	12384	11628	1.11	0.64
L[7]AlMe	24	82	11808	1088	1.09	0.73

[a]$[LA]_0/[Al]$ = 100, $[Al]/[PhCH_2OH]$ = 1, $[LA]_0$ = 0.42 M, toluene, 70 ˚C. [b]As determined *via* integration of the methine resonances (^{1}H NMR) of LA and PLA ($CDCl_3$, 400 MHz). [c]Calculated by $([LA]_0/[I]) \times 144.13 \times$ conversion. [d]Determined by gel permeation chromatography (GPC) calibrated with polystyrene standards in THF and corrected by a factor of 0.58 for PLA. [e]P_m and P_r are the probability of *meso* and *racemic* linkages between monomer units, respectively. $P_r = 1 - P_m$.

The tacticity of the resultant polymer was investigated using the homonuclear decoupled ^{1}H NMR spectroscopic technique. The homonuclear decoupled ^{1}H NMR spectra of the polymer produced from **L[1]AlMe-L[7]AlMe** are shown in **Figure 54**. Complex **L[3]AlMe**/$PhCH_2OH$ exhibits the highest isoselectivity among other complexes in the series. In a presence of benzyl alcohol, **L[2]AlMe**, **L[4]AlMe** and **L[7]AlMe** polymerized *rac*-LA to form isotactic biased polymers with the P_m values of 0.69, 0.74 and 0.73, respectively. The uses of complex **L[1]AlMe**/$PhCH_2OH$ and **L[6]AlMe**/$PhCH_2OH$ resulted in moderate isoselectivity (**L[1]AlMe**, P_m = 0.61; **L[6]AlMe**, P_m = 0.64). PLA produced by **L[5]AlMe** is atactic with the P_m value of 0.52.

The stereoselectivity can be controlled by either a site control mechanism (SCM) or a chain-end control mechanism (CEM). To achieve high degree of

Copyright by Kasetsart University All rights reserved

isoselectivity, the geometry of the ligand should be flexible enough to be controlled by the chirallity of living group (Nomura *et al.*, 2007). In the series, complex **L^{3}AlMe** showed the highest P_m value of 0.80 regardless of the distorted trigonal-bipyramidal geometry in the crystal structure. It can be assumed that the **L^{3}AlMe** has high flexibility in solution due to its dimethyl propylene backbone. The stereocontrol mechanism is operating in the propagation step (Radano *et al.*, 2000). After the first monomer is inserted into the Al-OBn bond of achiral complex **L^{3}AlOBn**, a chirality derived from the monomer is introduced into the complex. If the chiral environment around the metal center is rigid, the catalytic activity should be drastically diminished as can be observed in complexes with C_2 backbone. In case of high flexibility C_3 backbone complexes **L^{2}AlMe-L^{4}AlMe,** the propagation reaction of both *L*-LA and *D*-LA take place simultaneously *via* a CEM. In the set C_3 backbone complexes, **L^{3}AlMe** showed lowest rate but highest stereoselectivity. The steric repulsion between gem-dimethyl substituted backbone of **L^{3}AlMe** and monomer should increase the stereoselectivity but decrease the polymerization rate. For the same reason, complex **L^{4}AlMe** also showed the steric repulsion from it phenylene containing backbone and displays higher P_m than **L^{2}AlMe**.

1.5 Kinetic studies of *L*-LA and *rac*-LA polymerization

To gain further insight into polymerization mechanism, the kinetics studies toward *rac*-LA polymerization using **L^{3}AlMe** in the presence of benzyl alcohol were performed. The *rac*-LA concentration was fixed ($[LA]_0$ = 0.42 M) and the concentration of **L^{3}AlMe** was varied from 4.16 mM to 12.50 mM. The reactions were carried out in toluene at 70 ˚C and monitored by ^{1}H NMR spectroscopy. In each case, the first order kinetics in monomer was observed. The appropriate semilogarithmic plots are shown in **Figure 55**. The polymerization of *rac*-LA using **L^{3}AlMe/** $PhCH_2OH$ as catalyst/initiator proceeds according to:

$$-d[LA]/dt = k_{app}[LA] \quad (9)$$

Copyright by Kasetsart University All rights reserved

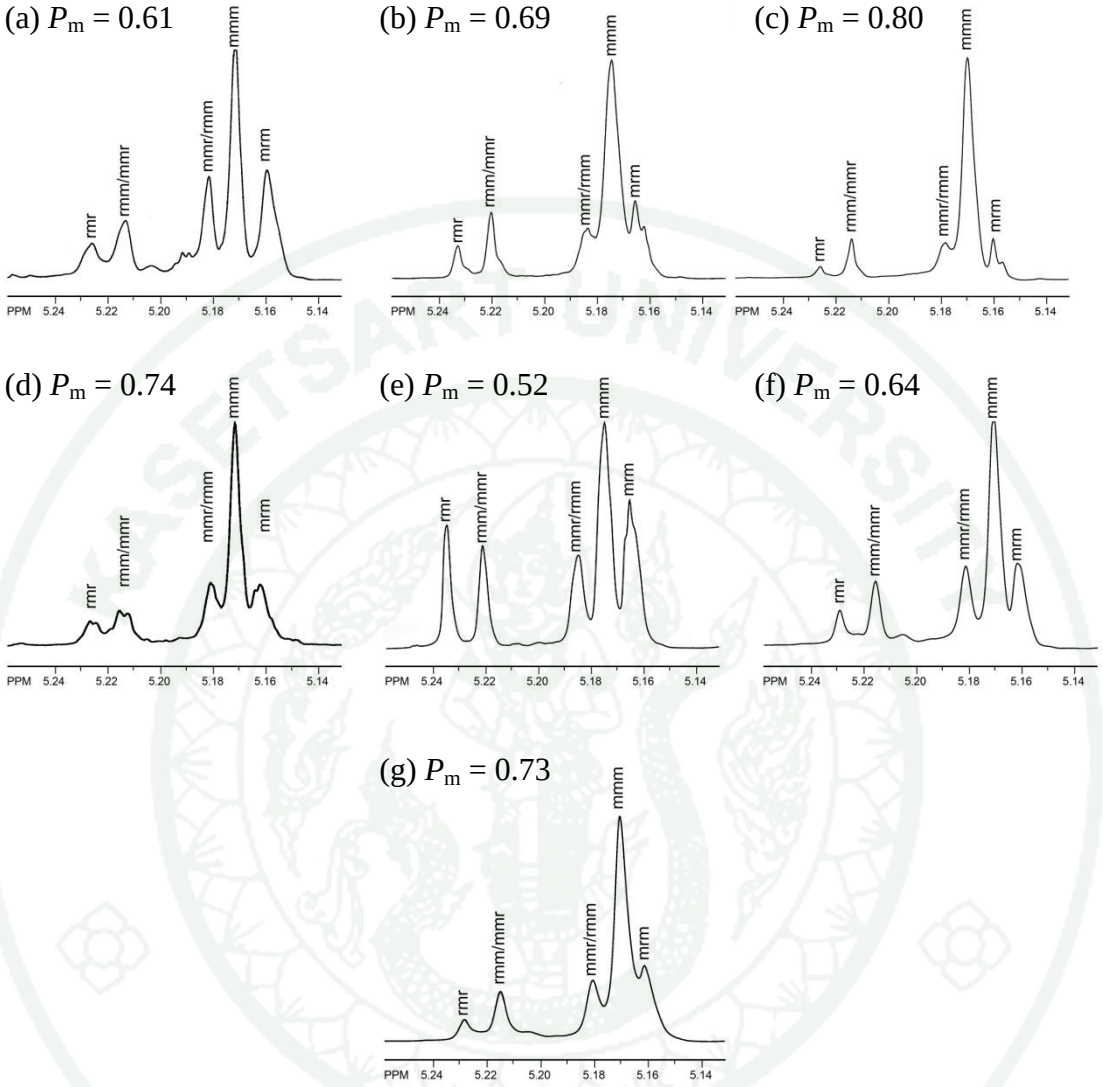

Figure 54 The homonuclear decoupled ^{1}H NMR spectra at the methine region of the resultant PLAs from *rac*-LA using (a) **L^{1}AlMe**/PhCH$_2$OH; (b) **L^{2}AlMe**/PhCH$_2$OH; (c) **L^{3}AlMe**/PhCH$_2$OH; (d) **L^{4}AlMe**/PhCH$_2$OH; (e) **L^{5}AlMe**/PhCH$_2$OH; (f) **L^{6}AlMe**/PhCH$_2$OH; (g) **L^{7}AlMe**/PhCH$_2$OH.

where $k_{app} = k_p[Al^x$, and k_p is the propagating rate constant. To determine the order in aluminum (x), ln k_{app} was plotted against ln [Al] as illustrated in **Figure 56**. The slope of the plot increases linearly with the aluminum concentration. The order in the aluminum (slope, x) is 1.39. Therefore, the polymerization of *rac*-LA using **L^{3}AlMe**/PhCH$_2$OH follows the overall kinetic equation:

Copyright by Kasetsart University All rights reserved

$$-d[LA]/dt = k_p[Al]^{1.39}[LA] \quad (10)$$

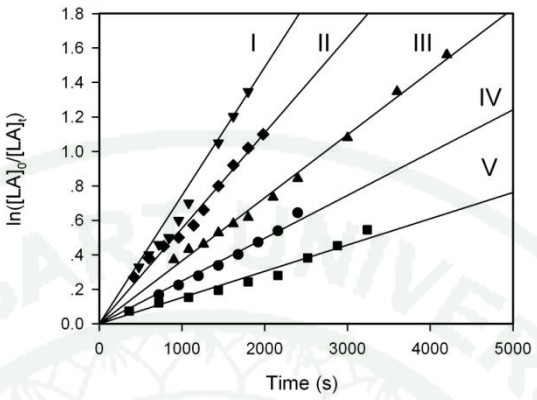

Figure 55 Semilogarithmic plots of *rac*-LA conversion with time in toluene at 70 ˚C with complex **L^{3}AlMe/**$PhCH_2OH$ as initiator ($[LA]_0$ = 0.42 M, **I**, [Al] = 16.67 mM, [LA]/[Al] = 25; **II**, [Al] = 12.5 mM, [LA]/[Al] = 34; **III**, [Al] = 8.33 mM, [LA]/[Al] = 50; **I**V, [Al] = 6.10 mM, [LA]/[Al] = 69; **V**, [Al] = 4.16 mM, [LA]/[Al] = 100).

Fractional dependencies upon initiator concentration has been previously observed for zinc (Williams *et al.*, 2003; D'Auria *et al.*, 2012), ferrous (O'Keefe *et al.*, 2002), stannous (Kowalski *et al.*, 2000), yttrium (Chamberlain *et al.*, 2000), and aluminum alkoxides (Dubis *et al*., 1991; Duda and Penczek, 1994; Ouhadi, 1976; Alcazar-Roman *et al*., 2003). The nonintegral x value was postulated to arise from the aggregation of the active species (Williams *et al.*, 2003; Nomura *et al.*, 2007) or an equilibrium between monomeric and dimeric species in the polymerization medium (Ropson *et al.*, 1995). Nevertheless, the propagation rate constant (k_p) can be alternatively obtained from the gradient of the k_{app} *versus* [Al] plot, as depicted in **Figure 57**. The linear relationship between k_{app} and [Al] demonstrates the first order kinetics in aluminum concentration, with the k_p value of 6.78×10^{-2} $s^{-1}mol^{-1}L$ at 70 ˚C. This k_p value is higher than that obtained from the kinetic study using the analogous aluminum ethyl complex ($k_p = 4.95 \times 10^{-2}$ $s^{-1}mol^{-1}L$) (Du *et al.*, 2009). According to the nonzero x-intercept as shown in **Figure 57**, it indicates that there is a threshold catalyst concentration for the polymerization to take place (Williams *et al.*,

Copyright by Kasetsart University All rights reserved

2003; O'Keefe *et al*., 2001; Tharkur, 1998a), which is 2.34 mM for **L^{3}AlMe**/PhCH$_2$OH initiation system.

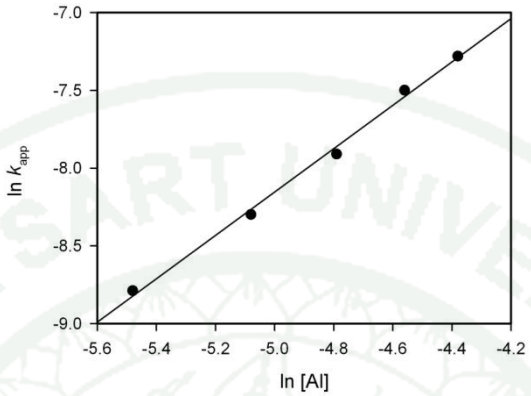

Figure 56 Plot of ln k_{app} *versus* ln [Al] for the polymerization of *rac*-LA with complex **L^{3}AlMe**/PhCH$_2$OH as an initiator (toluene, 70 ˚C, $[LA]_0$ = 0.42 M).

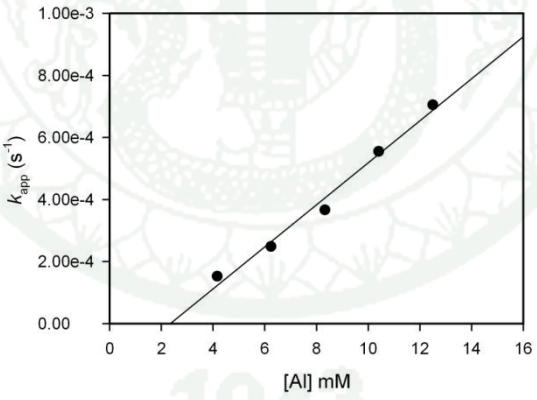

Figure 57 Plot of k_{app} *versus* [Al] for the polymerization of *rac*-LA with complex **L^{3}AlMe**/PhCH$_2$OH as an initiator (toluene, 70 ˚C, $[LA]_0$ = 0.42 M).

The kinetics studies of *L*-LA and *rac*-LA polymerizations using all complexes were carried out with the molar ratio of monomer to initiator of 50:1. The concentration of aluminum complexes **L^{1}AlMe**-**L^{7}AlMe** was fixes at 8.33 mM. Polymerizations were carried out in toluene at 70 ˚C. The polymerization kinetic

Copyright by Kasetsart University All rights reserved

results for *L*-LA and *rac*-LA were summarized in **Table 6** and **7**, respectively. Semilogarithmic plots of the monomer conversion *versus* time for *L*-LA and *rac*-LA were shown in **Figures 58a-b** and **59a-c**, respectively.

Table 6 Kinetic results for *L*-LA polymerization using complexes **L[1]AlMe- L[7]AlMe** in the presence of benzyl alcohol[a]**.**

Initiator	k_{app} (s^{-1})[b]
L[1]AlMe	37.7×10^{-6}
L[2]AlMe	1397.5×10^{-6}
L[3]AlMe	517.0×10^{-6}
L[4]AlMe	3499.7×10^{-6}
L[5]AlMe	41.8×10^{-6}
L[6]AlMe	3.8×10^{-6}
L[7]AlMe	412.9×10^{-6}

[a]All polymerizations were carried out in toluene at 70 ˚C, $[LA]_0$ = 0.43 M, [Al] = 8.33 mM. [b]Measured by ^{1}H NMR from methine region of polymer and monomer.

In the case of *L*-LA polymerization, complexes **L[1]AlMe**, **L[6]AlMe** and **L[7]AlMe**, which have two carbons on the bridge, **L[6]AlMe** showed the lowest polymerization rates (3.8×10^{-6} s^{-1}). The k_{app} of **L[6]AlMe** are one magnitude lower than that of **L[1]AlMe** (37.7×10^{-6} s^{-1}). The k_{app} of **L[7]AlMe** with *rac*-1,2-cyclohexyl bridge is one magnitude higher (360.3×10^{-6} s^{-1}) than that of **L[1]AlMe**. Changing the diimine backbone from ethylene to propylene results in an increase in the apparent kinetic rate (k_{app}**(L[2]AlMe)** = 1397.5×10^{-6} s^{-1}). The introduction of gem alkyl substituents on the diimine bridge diminishes the activity of catalysts, which was shown by slightly drop of k_{app} of **L[3]AlMe** (517.0×10^{-6} s^{-1}). Notably, th*e* *o*-$C_6H_4CH_2$ bridge exhibits the highest k_{app} among all complexes in the series. These results are related to the flexibility of the diimine linker, allowing suitably adaption to the next incoming monomer which causes to a high activity of the

Copyright by Kasetsart University All rights reserved

catalyst. Lengthening the backbone to a butylene linker as complex **L^{5}AlMe** shows a comparable k_{app} (360.3×10^{-6} s^{-1}) to the k_{app} of **L^{3}AlMe**.

Table 7 Kinetic results for *rac*-LA polymerization using complexes **L^{1}AlMe-L^{7}AlMe** in the presence of benzyl alcohol[a].

Initiator	k_{app} (s^{-1})[b]
L^{1}AlMe	38.2×10^{-6}
L^{2}AlMe	778.9×10^{-6}
L^{3}AlMe	366.5×10^{-6}
L^{4}AlMe	2844.6×10^{-6}
L^{5}AlMe	302.2×10^{-6}
L^{6}AlMe	3.5×10^{-6}
L^{7}AlMe	124.7×10^{-6}

[a]All polymerizations were carried out in toluene at 70 ˚C, $[LA]_0$ = 0.43 M, [Al] = 8.33 mM. [b]Measureed by ^{1}H NMR from methine region of polymer and monomer.

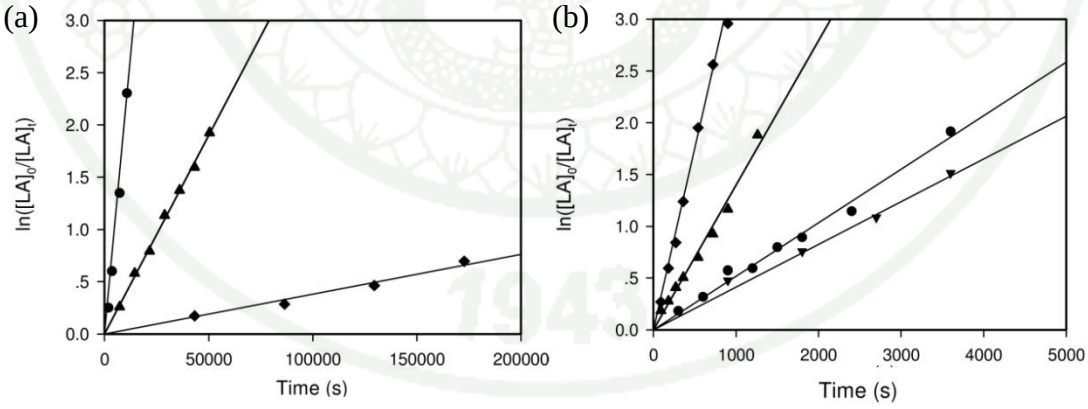

Figure 58 Semilogarithmic plots of *L*-LA conversion with time in toluene at 70 ˚C with complexes **L^{1}AlMe-L^{7}AlMe** ($[LA]_0/[Al]$ = 50, $[Al]/[PhCH_2OH]$ = 1, $[LA]_0$ = 0.42 M, [Al] = 8.33 mM). (a) **L^{5}AlMe** (●), **L^{1}AlMe** (▲) and **L^{6}AlMe** (♦)**;** (b) **L^{4}AlMe** (♦), **L^{2}AlMe** (▲), **L^{3}AlMe** (●) and **L^{7}AlMe** (▼).

Copyright by Kasetsart University All rights reserved

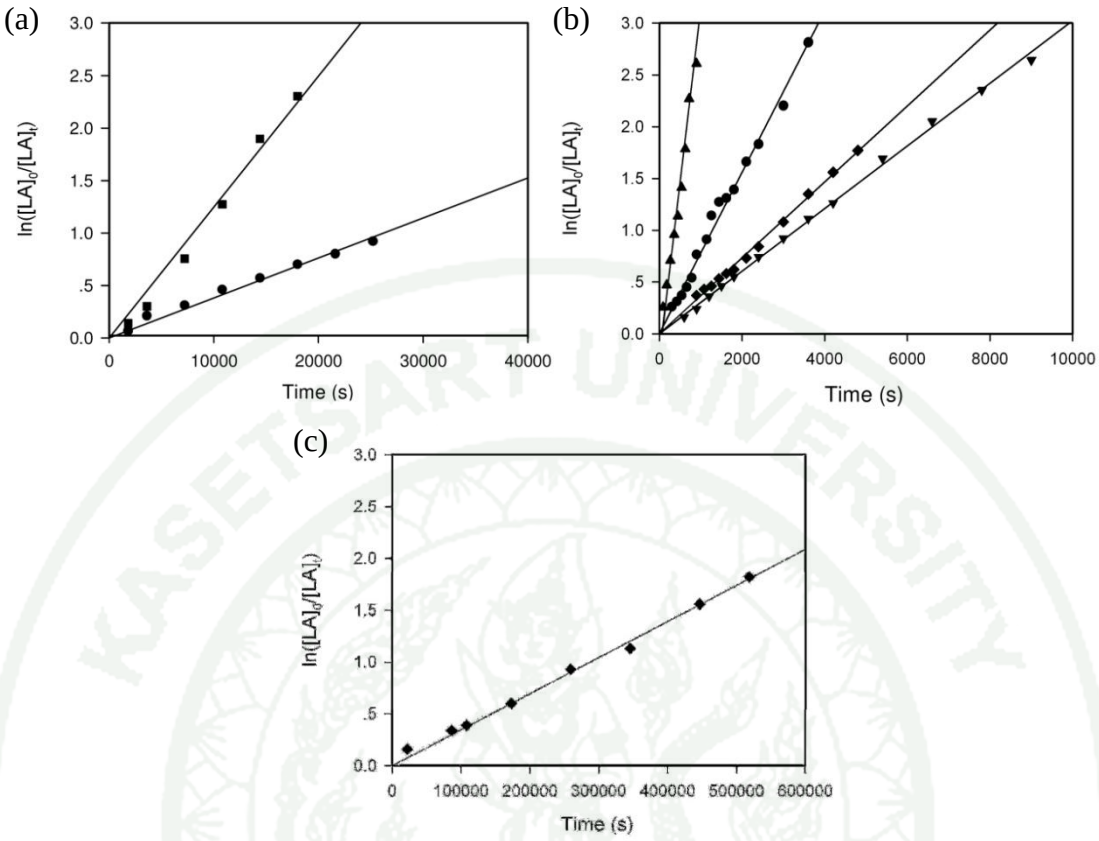

Figure 59 Semilogarithmic plots of *rac*-LA conversion with time in toluene at 70 ˚C with complexes **L^{1}AlMe-L^{7}AlMe** ([LA]$_0$/[Al] = 50, [Al]/[PhCH$_2$OH] = 1, [LA]$_0$ = 0.42 M, [Al] = 8.33 mM). (a) **L^{5}AlMe** (■) and **L^{1}AlMe** (●); (b) **L^{4}AlMe** (▲), **L^{2}AlMe** (●), **L^{3}AlMe** (♦) and **L^{7}AlMe** (▼); (c) **L^{6}AlMe** (♦).

For *rac*-LA polymerizations, the trend of activity was the same as for *L*-LA polymerizations. The rigid C_2 backbone complexes show low polymerization rates. The k_{app} of **L^{1}AlMe**, **L^{6}AlMe** and **L^{7}AlMe** are 38.2 $\times 10^{-6}$, 3.5 $\times 10^{-6}$ and 124.7 $\times 10^{-6}$ s^{-1}, respectively. The polymerization rates for *rac*-LA are relatively close to the *L*-LA polymerization using **L^{1}AlMe** and **L^{6}AlMe**. For set of C_3 backbone complexes, **L^{4}AlMe** appeared to process the highest polymerization activity. The k_{app} is 2844.6 $\times 10^{-6}$ s^{-1}. The k_{app} of **L^{2}AlMe** and **L^{3}AlMe** are 778.9 $\times 10^{-6}$ and 336.5 s^{-1}, respectively. The polymerization rates for *rac*-LA using C_3 complexes are all lower than that for *L*-LA polymerization. In conclusion, the rates of polymerization decrease in the order of **L^{4}AlMe** > **L^{2}AlMe** > **L^{3}AlMe** > **L^{5}AlMe** > **L^{7}AlMe** > **L^{1}AlMe** >> **L^{6}AlMe**.

Copyright by Kasetsart University All rights reserved

The diminishment of the k_{app} value for *rac*-LA polymerizations compared to those of for *L*-LA polymerization is considered under the assumption that the polymerization occurs *via* the chain-end control (CEM) mechanism. In the initiation step, the complex initiates both *L*-LA and *D*-LA without differentiation between the two enantiomers. In the propagation step, the complex has incorporated *L*-LA or *D*-LA and the chain-end chirality strongly differentiates an enantiomer with the same chiral sense from another one. The monomer with the same chiral sense preferentially enters the reaction site for the polymerization reaction. Hence, the kinetic equation can be rewritten as shown in equations 11-14 (Nomura *et al*. 2007).

$$-d[L\text{-LA}]/dt = k_{(L\text{-}L)p}[Al\text{-}L][L\text{-LA}]_t + k_{(D\text{-}L)p}[Al\text{-}D][L\text{-LA}]_t \quad (11)$$

$$-d[D\text{-LA}]/dt = k_{(D\text{-}D)p}[Al\text{-}D][D\text{-LA}]_t + k_{(D\text{-}L)p}[Al\text{-}L][D\text{-LA}]_t \quad (12)$$

where $k_{(L\text{-}L)p}$ and $k_{(D\text{-}D)p}$ are the propagating rate constant of *L*-LA and *D*-LA, respectively. The $k_{(D\text{-}L)p}$ is stand for the propagation rate constant that the mismatch monomer has been incorporated. The total rate of ROP of *rac*-LA is given by the summation of equation 11 and 12 as shown in equation 13.

$$-d[rac\text{-LA}]/dt = k_{(L\text{-}L)p}[Al\text{-}L][L\text{-LA}]_t + k_{(D\text{-}D)p}[Al\text{-}D][D\text{-LA}]_t + k_{(D\text{-}L)p}[Al\text{-}D][L\text{-LA}] + k_{(D\text{-}L)p}[Al\text{-}L][D\text{-LA}]_t \quad (13)$$

In the ROP of *rac*-LA, $k_{(L\text{-}L)p} = k_{(D\text{-}D)p}$, [Al-L] = [Al-D] = ½[Al] and [*L*-LA] = [*D*-LA]. Taking into consideration these relationships, equation 13 can be reduced to equation 14.

$$-d[rac\text{-LA}]/dt = \tfrac{1}{2}\,(k_{(L\text{-}L)p} + k_{(D\text{-}L)p})[Al][rac\text{-LA}]_t \quad (14)$$

In the case of *rac*-LA polymerization using rigid C_2 backbone complexes, the rearrangement of ligand geometry is difficult and independent on the type of monomer enantiomers. This was represented by the comparable k_{app} values from *L*-LA and *rac*-LA polymerizations. The kinetic equation can be written in common

Copyright by Kasetsart University All rights reserved

form as described in equation 10. When the ultimate stereoselectivity is achieved, $k_{(D\text{-}L)p}$ converges to zero and the $k_{(rac)p}$ is $\frac{1}{2}k_{(L\text{-}L)p}$.

For the *rac*-LA polymerization using the flexible C_3 backbone complexes, $k_{(D\text{-}L)p}$ is lower than $k_{(L\text{-}L)p}$ due to the rearrangement of ligand geometry for mismatched monomer insertion requests further energy. This results in the diminishment of $k_{(rac)p}$ and k_{app} as the direct variation a function of $k_{(rac)p}$ is also diminished. This eventually culminates in the lower polymerization rate of *rac*-LA than that of *L*-LA polymerizations using complexes **L^{2}AlMe**-**L^{4}AlMe**.

The plot of M_n *versus rac*-LA conversion using **L^{3}AlMe**/$PhCH_2OH$ as an initiator is shown in **Figure 60**. From the plot, the M_n increased linearly with respect to the monomer conversion indicating that the polymerization is well controlled. The molecular weight distribution remained narrow until 95% of monomer conversion. This implies the absence of transesterification reaction. The plots of M_n versus *rac*-LA conversion using complexes in the series are shown in the **Appendix Figure 2**.

Further evidence for the well-controlled character of polymerization was observed by changing the molar ratio of monomer to initiator ($[LA]_0/[Al]$). As can be seen in **Table 8**, initiator **L^{3}AlMe** was able to polymerize *rac*-LA at a high loading of monomer to initiator ratio ($[LA]_0/[Al]$ = 1600:1). A linear relationship between M_n and $[LA]_0/[Al]$ for initiator **L^{3}AlMe** was illustrated in **Figure 61**. The number-averaged molecular weights M_n are relatively close to the theoretical values, indicative of a well-controlled polymerization process. The living characteristic is further elucidated by the low molecular weight distributions observed. In addition, a high degree of isotacticity in polymerization of *rac*-LA using initiator **L^{3}AlMe** was still observed at high monomer to initiator ratio. The P_m values of resulting polymers remained almost unchanged, in the range of 0.78 to 0.80 (**Table 8**, entries 1-5).

Copyright by Kasetsart University All rights reserved

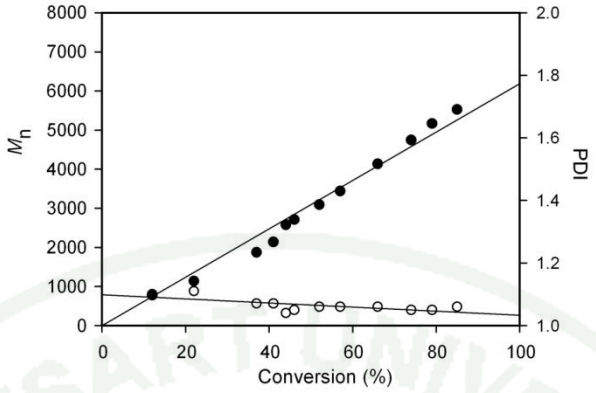

Figure 60 Plot of M_n as a function of monomer conversion for *rac*-LA polymerization using **L^{3}AlMe**/PhCH$_2$OH ([LA]$_0$/[Al] = 50, [Al]/[PhCH$_2$OH] = 1, [LA]$_0$ = 0.42 M, [Al] = 8.33 mM)**.**

Table 8 Polymerization of *rac*-LA using initiator **L^{3}AlMe** in the presence of benzyl alcohol[a].

entry	[LA]$_0$/[Al]	Time (h)	conversion[b] (%)	M_n(th)[c] (g mol^{-1})	M_n(GPC)[d] (g mol^{-1})	PDI[d]	P_m[e]
1	**100**	3	95	13692	12915	1.04	0.80
2	**200**	6	93	26808	26102	1.02	0.78
3	**400**	12	96	55346	59260	1.18	0.80
4	**800**	48	93	10723	106418	1.11	0.78
5	**1600**	60	95	219078	233616	1.17	0.78

[a]General polymerization conditions: toluene as a solvent, 70 ˚C. [b]As determined *via* integration of the methine resonances (^{1}H NMR) of LA and PLA ($CDCl_3$, 400 MHz). [c]Calculated by ([LA]$_0$/[I]) × 144.13 × conversion. [d]Determined by gel permeation-chromatography (GPC) calibrated with polystyrene standards in THF and corrected by a factor of 0.58 for PLA. [e]P_m and P_r are the probability of *meso* and *racemic* linkages between monomer units, respectively.

Copyright by Kasetsart University All rights reserved

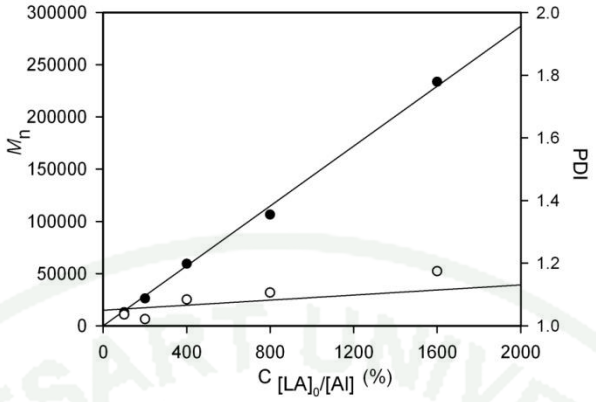

Figure 61 Plot of the number-averaged molecular weight (M_n) *versus* the molar ratio of monomer to initiator ([LA]$_0$/[Al]) for the polymerization of *rac*-lactide using **L^{3}AlMe** in toluene at 70 ˚C.

2. Aluminum complexes supported by Salan ligand

The term Salan ligand is commonly used to simplify the tetradentate phenoxyamine ligand, which can be considered as a fully reduced bis(salicylidene) Schiff-base or Salen ligand (Atwood *et al*, 1995). Compared to Salen ligand, the Salan-type ligand has more flexible structure due to the sp^3 hybridization of amine nitrogen atoms (Hornmirun *et al.*, 2004). Various types of metal complexes supported with Salan ligand, *e.g.* yttrium (Pappalardo *et al*., 2013), magnesium (Song *et al*., 2013) and aluminum (Shaver *et al.*, 2013; Sumrit and Hormnirun, 2013; Cross *et al.*, 2013) for the ROP of lactones have been reported. Among these metal Salan complexes, aluminum Salan complexes exhibited an excellent stereocontrol for the polymerization of lactones, while other metals bearing the same ligand did not show the stereocontrol in the polymerization of *meso*-LA and *rac*-LA (Pappalardo *et al*., 2013). Although, aluminum Salan complexes were found to be versatile catalysts for the polymerization of lactones such as β-BL and ε-CL, the use of these complexes for lactone copolymerization is very limited. Recently, Shaver and coworker examined the use of aluminum Salan complex **14** for β-BL/*rac*-LA copolymerization (Shaver and Cross, 2013). The results showed that complex **14** can be used to produce a gradient copolymer with narrow PDI.

Copyright by Kasetsart University All rights reserved

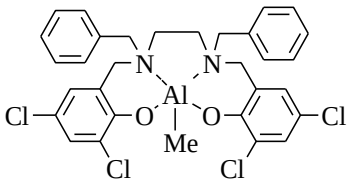

Figure 62 Aluminum complex **14**.

Herein, we described the use of aluminum Salan complexes for both homo- and copolymerization for lactones. The research in this section is particularly related to the fact that both activity and stereoselectivity of aluminum Salan complexes are strongly dependent on both the substituent on nitrogen donors (R_1) and the size of the substituent especially on the *ortho* position of phenoxide units (R_2). The series of aluminum complexes with various sizes of R_1 and R_2 were investigated for homopolymerizations of *rac*-LA and ε-CL.

2.1 Synthesis of aluminum complexes supported by Salan ligands

The Salan ligand can be synthesizes by a stepwise Schiff-base condensation and reduction or a modified Mannich condensation (Wong *et al*., 1998; Tshuva *et al.*, 2001). In this study, all ligands were successfully synthesized by the stepwise condensation as illustrated in **Figure 63**. (Glasner and Tshuva, 2014; Hormnirun *et al*., 2004). All Salan ligands were isolated as white solids. Satisfactory elemental analyses were obtained on all ligands (see 4.1-4.11 in Materials and Methods) and all spectroscopic data were consistent with the formulation as shown in **Figure 63**.

Treatment of the ligand precursors with an equimolar amount of $AlMe_3$ in toluene at 110 ˚C resulted in the formation of Salan aluminum methyl complexes (**Figure 64**). For clarity, these complexes are divided in three different groups depending upon the substituents attached to the nitrogen atoms: Group A: *N*-methyl ethylene backbone complexes (**L^{1A}AlMe-L^{4A}AlMe)**; Group B: *N*-ethyl ethylene backbone complexes (**L^{1B}AlMe-L^{4B}AlMe)**; and Group C: *N*-isopropyl ethylene backbone complexes (**L^{1C}AlMe-L^{4C}AlMe)**. The synthesis and subsequent characteristic of these complexes are briefly described in the following section.

Copyright by Kasetsart University All rights reserved

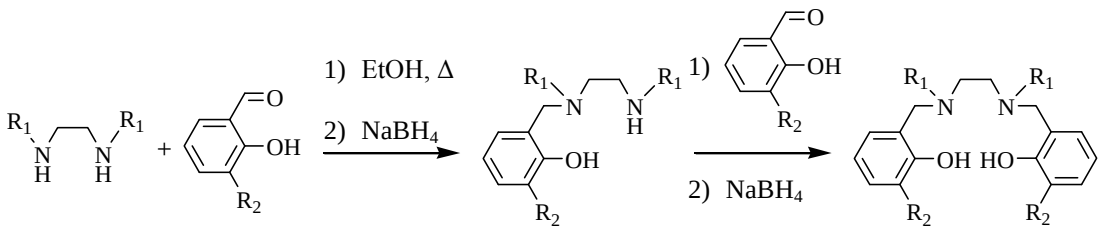

Group A: R_1 = Me

H_2L^{1A}: R_2 = H
H_2L^{2A}: R_2 = ^{i}Pr
H_2L^{3A}: R_2 = ^{t}Bu
H_2L^{4A}: R_2 = Ph

Group B: R_1 = Et

H_2L^{1B}: R_2 = H
H_2L^{2B}: R_2 = ^{i}Pr
H_2L^{3B}: R_2 = ^{t}Bu
H_2L^{4B}: R_2 = Ph

Group C: R_1 = ^{i}Pr

H_2L^{1C}: R_2 = H
H_2L^{2C}: R_2 = ^{i}Pr
H_2L^{4C}: R_2 = Ph

Figure 63 Synthetic pathway for **H_2L^{1A}- H_2L^{4A}**, **H_2L^{1B}- H_2L^{4B}** and **H_2L^{1C}- H_2L^{3C}**.

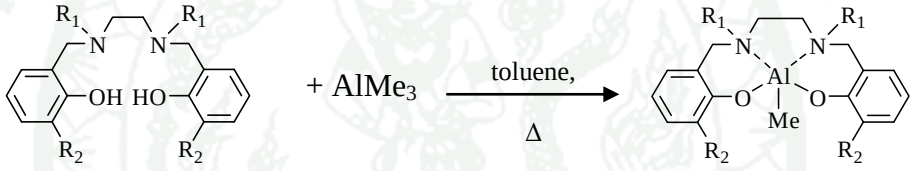

Group A: R_1 = Me

H_2L^{1A}: R_2 = H
H_2L^{2A}: R_2 = ^{i}Pr
H_2L^{3A}: R_2 = ^{t}Bu
H_2L^{4A}: R_2 = Ph

Group B: R_1 = Et

H_2L^{1B}: R_2 = H
H_2L^{2B}: R_2 = ^{i}Pr
H_2L^{3B}: R_2 = ^{t}Bu
H_2L^{4B}: R_2 = Ph

Group C: R_1 = ^{i}Pr

H_2L^{1C}: R_2 = H
H_2L^{2C}: R_2 = ^{i}Pr
H_2L^{4C}: R_2 = Ph

Figure 64 Synthetic pathway for Salan aluminum methyl complexes.

The synthesis of aluminum complex **L^{1A}AlMe** was reported by Gibson and co-workers (Hormnirun *et al.*, 2004). Complex **L^{1A}AlMe** was obtained as a white solid after recrystallization from toluene at room temperature whereas complexes **L^{2A}AlMe-L^{4A}AlMe** were recrystallized from hexane at -20 ˚C. Elemental analyses of **L^{2A}AlMe-L^{4A}AlMe** were consistent with the stoichiometries $C_{25}H_{37}AlN_2O_2$ (**L^{2A}AlMe**), $C_{27}H_{41}AlN_2O_2$ (**L^{3A}AlMe**) and $C_{31}H_{33}AlN_2O_2$ (**L^{4A}AlMe**).

The ^{1}H NMR spectrum of **L^{1A}AlMe** was assigned according to the literature. The fully assignment of **L^{1A}AlMe** and **L^{2A}AlMe** are shown in **Figures 65** and **66**. Both spectra contain broad resonances due to the flexible nature of Salan ligand

Copyright by Kasetsart University All rights reserved

framework. Unlike the ^{1}H NMR spectra of complexes **L^{1A}AlMe** and **L^{2A}AlMe,** the phenoxymethylene protons (ArCH_2N) of **L^{3A}AlMe** and **L^{4A}AlMe,** show the diastereotopic split pattern as two doublets as illustrated in **Figure 67** and **68**. It is perceptible that as the phenoxy substituents become bulkier, the diminishing of complex flexibility is denoted. This phenomenon was also observed from aluminum Salan complexes with a cyclohexyl backbone (Du *et al*., 2007). Either bulky phenoxy substituents or uncompromising backbone slows down the exchange between two diastereoisomers of Salan aluminum complex in solution. The first diastereoisomer adopts a *cis*-(O,O) and *cis*-(Me,Me), whereas the second isomer is an intermediate between square pyramidal (*cis*-(O,O) and *trans*-(Me,Me)) and trigonal bipyramidal (*trans*-(O,O) and *trans*-(Me,Me)) (Du *et al*., 2007).

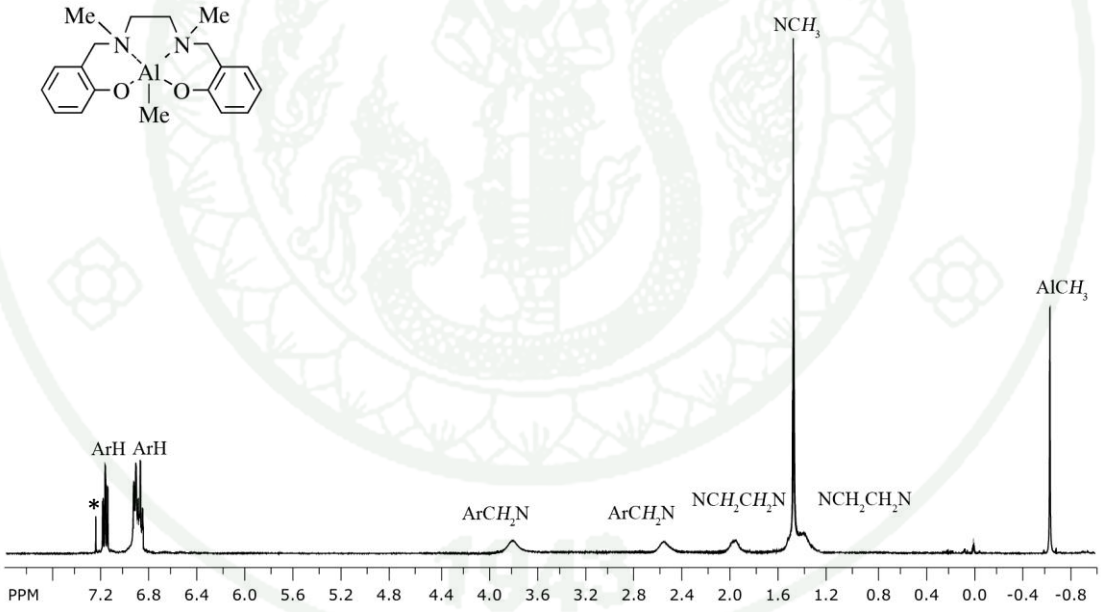

Figure 65 ^{1}H NMR spectrum of complex **L^{1A}AlMe** (400 MHz, C_6D_6, 300 K, * = residual C_6D_5H).

Copyright by Kasetsart University All rights reserved

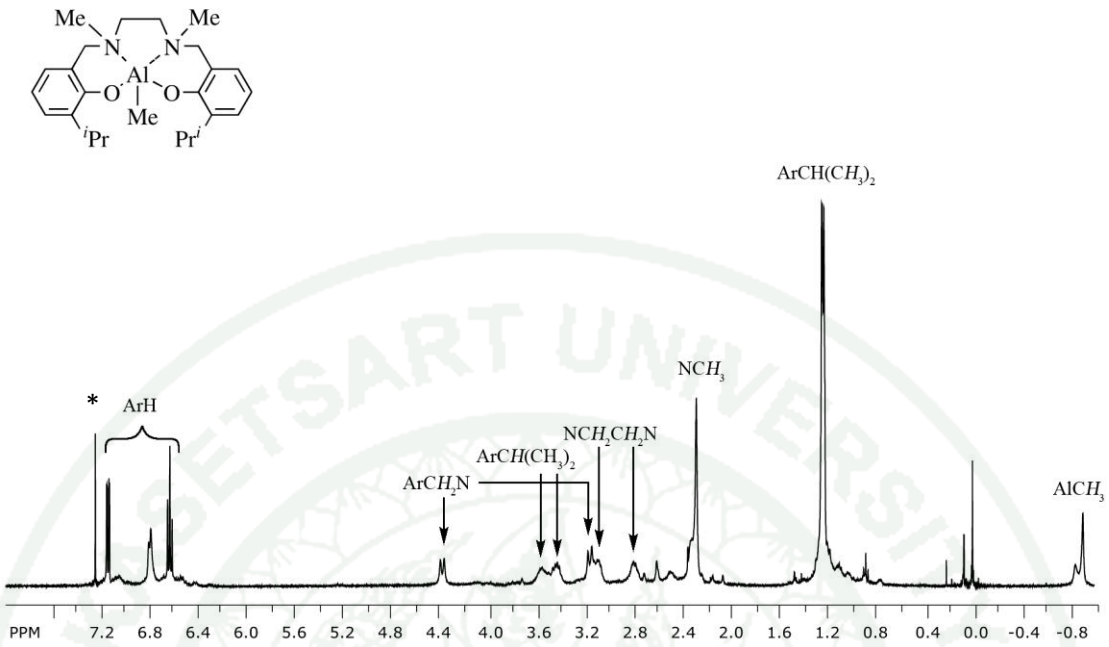

Figure 66 ^{1}H NMR spectrum of complex **L^{2A}AlMe** (400 MHz, C_6D_6, 300 K, * = residual C_6D_5H).

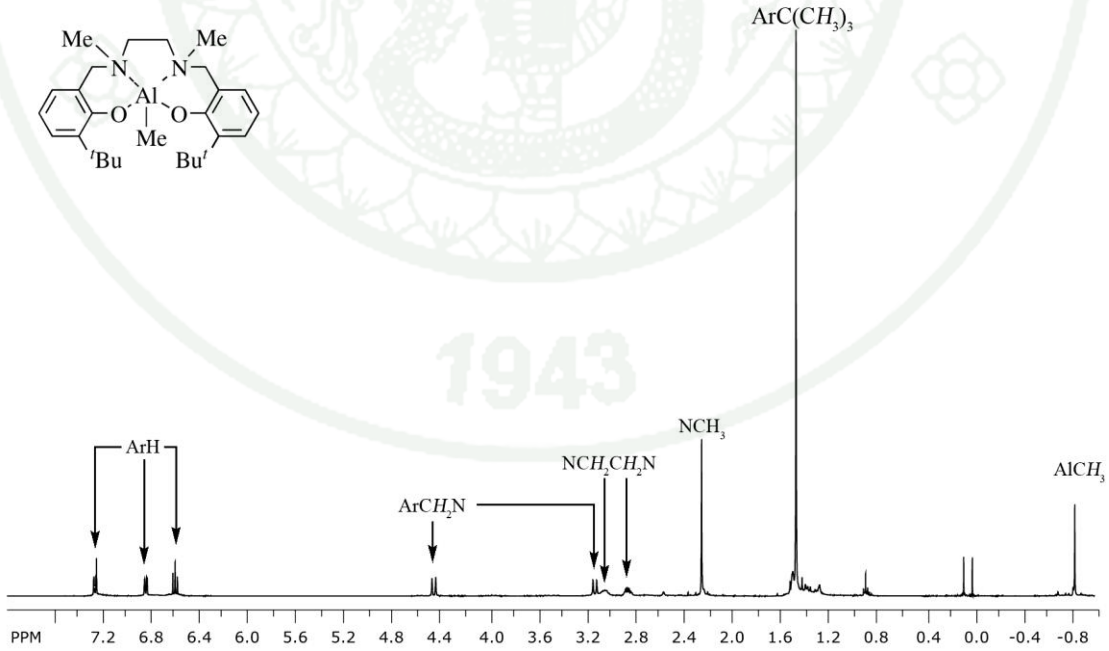

Figure 67 ^{1}H NMR spectrum of complex **L^{3A}AlMe** (400 MHz, C_6D_6, 300 K).

Copyright by Kasetsart University All rights reserved

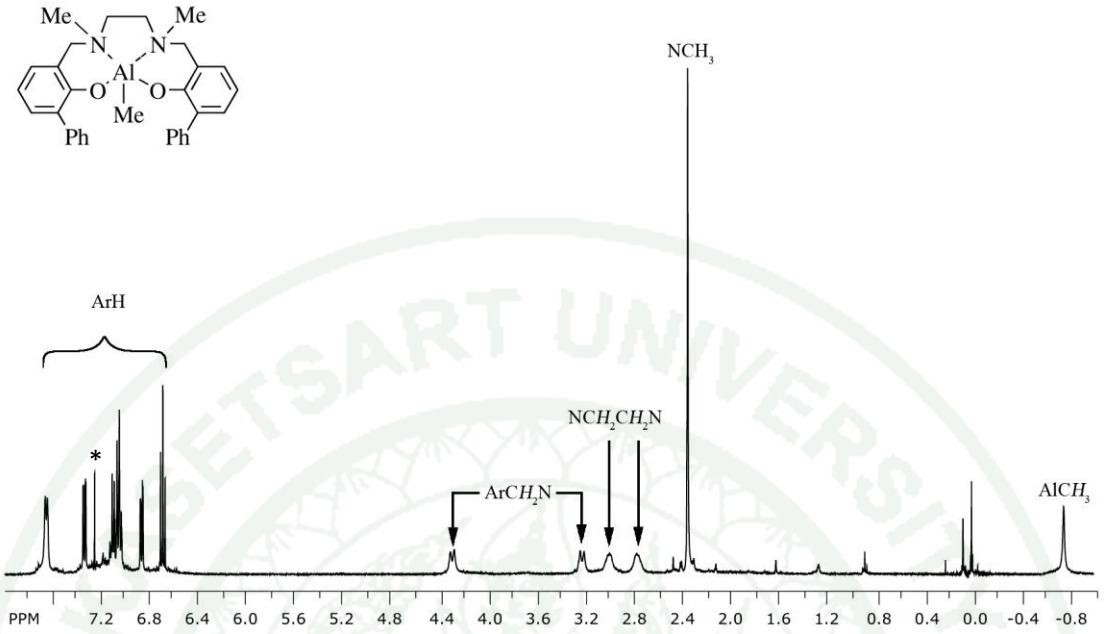

Figure 68 ^{1}H NMR spectrum of complex **L^{4A}AlMe** (400 MHz, C_6D_6, 300 K, * = residual C_6D_5H).

The *N*-ethyl complexes **L^{1B}AlMe-L^{4B}AlMe** (Group B) were all obtained in high yields after recrystallization from cold hexane. Complexes **L^{1B}AlMe-L^{3B}AlMe** were obtained as white powders whereas complex **L^{4B}AlMe** was obtained as a pale yellow solid. The ^{1}H NMR spectra of all complexes with full assignment were shown in **Figures 69**-**72**. Complexes **L^{1B}AlMe**, **L^{2B}AlMe** and **L^{4B}AlMe**, with unsubstituent, isopropyl and phenyl substituents on the *ortho*-positions of the phenoxy rings, respectively, showed peaks corresponded to both the phenoxymethylene protons (CH_2ArOAl) and the backbone methylene protons (NCH_2CH_2N) as broad signals. In the case of **L^{3B}AlMe**, the phenoxymethylene protons and backbone protons appear as two doublets and a sharp singlet, respectively (**Figure 71**). The formation of these complexes was supported by elemental analyses which were consistent with the stoichiometries $C_{21}H_{29}AlN_2O_2$ (**L^{1B}AlMe**), $C_{27}H_{41}AlN_2O_2$ (**L^{2B}AlMe**), $C_{29}H_{45}AlN_2O_2$ (**L^{3B}AlMe**) and $C_{33}H_{37}AlN_2O_2$ (**L^{4B}AlMe**).

Copyright by Kasetsart University All rights reserved

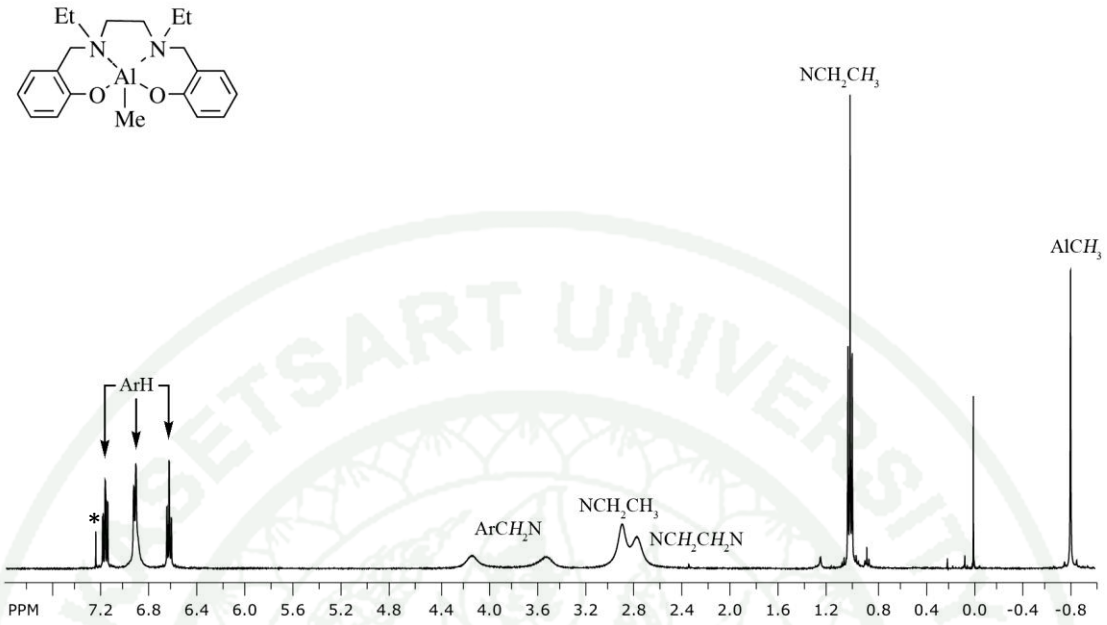

Figure 69 ^{1}H NMR spectrum of complex **L^{1B}AlMe** (400 MHz, C_6D_6, 300 K, * = residual C_6D_5H).

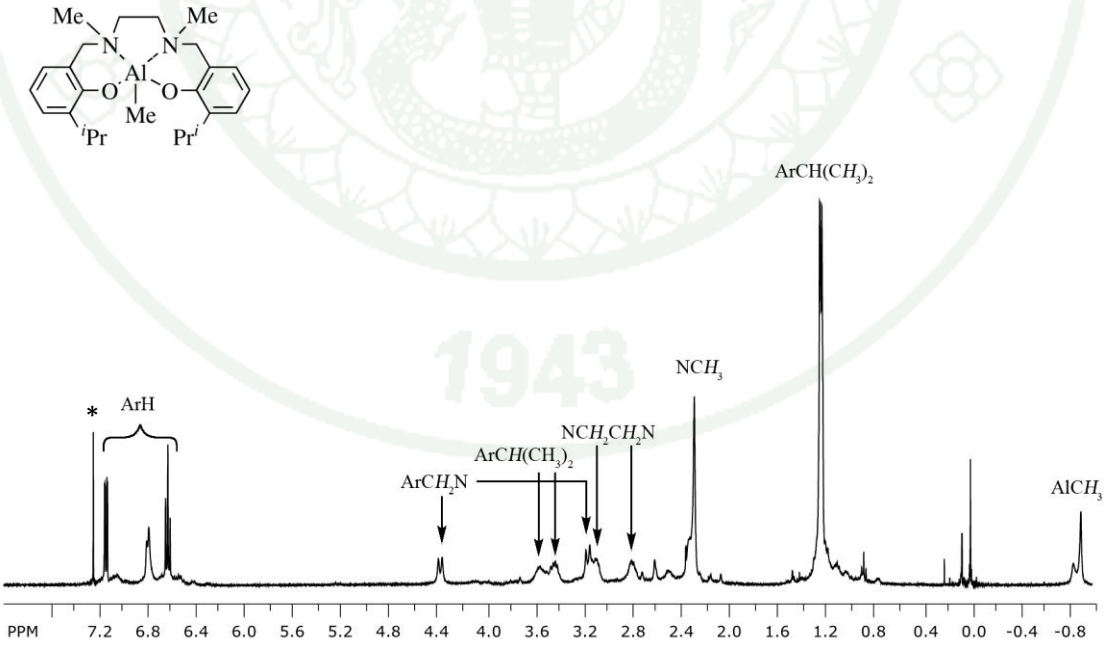

Figure 70 ^{1}H NMR spectrum of complex **L^{2B}AlMe** (400 MHz, C_6D_6, 300 K, * = residual C_6D_5H).

Copyright by Kasetsart University All rights reserved

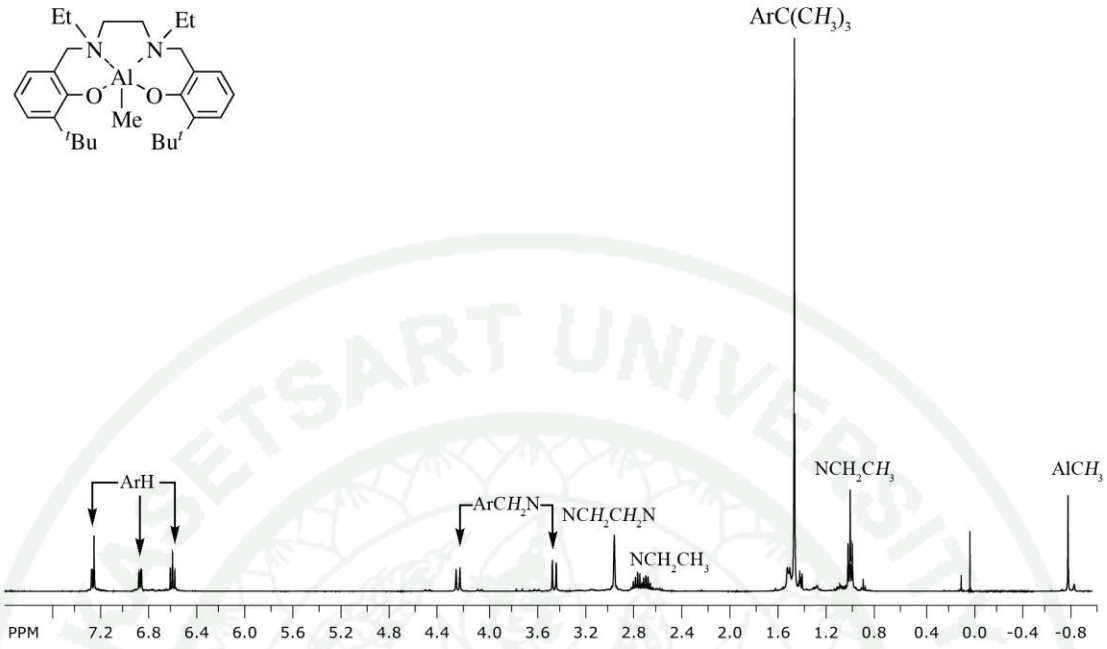

Figure 71 ^{1}H NMR spectrum of complex **L^{3B}AlMe** (400 MHz, C_6D_6, 300 K).

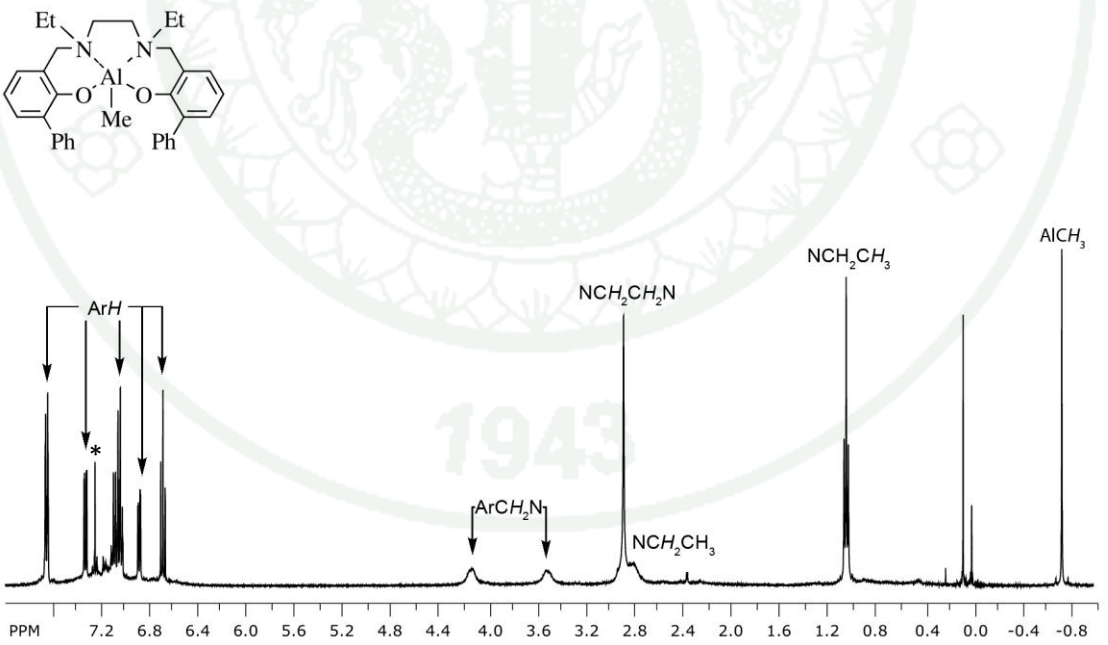

Figure 72 ^{1}H NMR spectrum of complex **L^{4B}AlMe** (400 MHz, C_6D_6, 300 K, * = residual C_6D_5H).

Copyright by Kasetsart University All rights reserved

All the Group C complexes **L^{1C}AlMe-L^{3C}AlMe** were obtained in high yields. Complexes **L^{1C}AlMe** and **L^{2C}AlMe** were obtained as colorless crystals after recrystallization from hexane. Complex **L^{3C}AlMe** precipitated from the reaction medium during the addition of TMA. Elemental analyses were consistent with the stoichiometries $C_{23}H_{33}AlN_2O_2$ (**L^{1C}AlMe**), $C_{30}H_{48}AlN_2O_2$ (**L^{2C}AlMe**) and $C_{36}H_{44}AlN_2O_2$ (**L^{3C}AlMe**).

The complexes in this group were found to be insoluble in C_6D_6 and precipitated from toluene-d_8 at room temperature. Therefore, the NMR experiments for Group C complexes were carried out in toluene-d_8 at 70 ˚C. In all cases, both phenoxymethylene protons (CH_2ArOAl) and backbone methylene protons (NCH_2CH_2N) appear as two sharp singlets. The signals coresponding to the NCH(CH$_3$)$_2$ and NCH(CH_3)$_2$ appear as a quartet and a doublet, respectively. The characteristic AlCH_3 peaks are observed as a singlet at *ca.* -0.4 ppm for **L^{1C}AlMe** and **L^{2C}AlMe** and δ -0.8 ppm for **L^{3C}AlMe.** NMR results reveal that all complexes exist as a conformational stereoisomer at an investigated temperature.

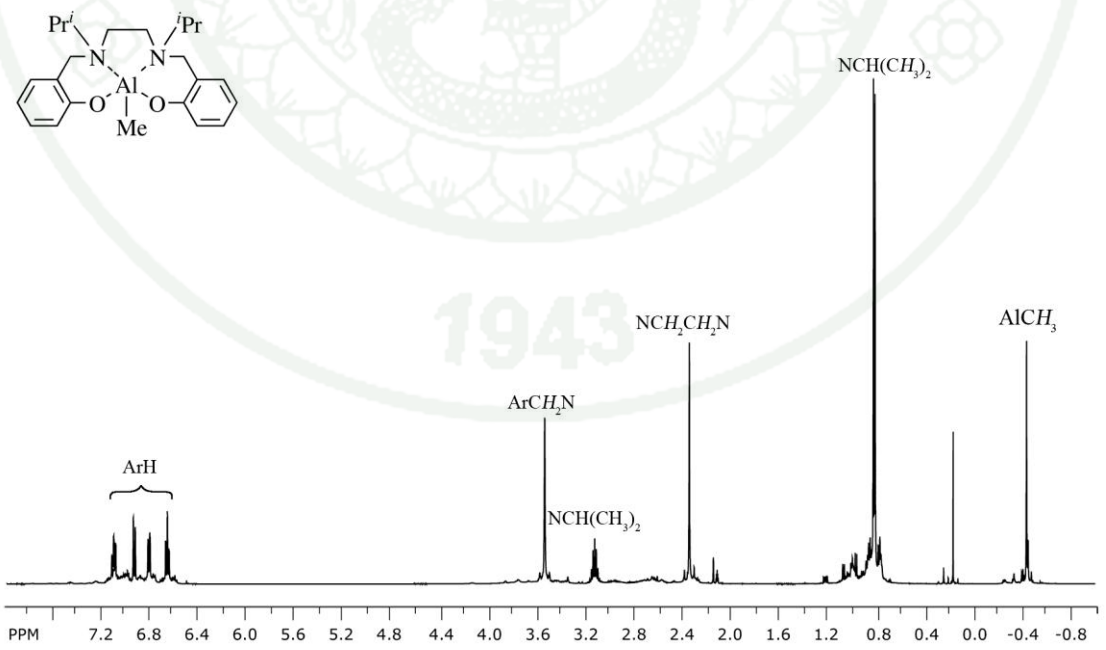

Figure 73 ^{1}H NMR spectrum of complex **L^{1C}AlMe** (500 MHz, $C_6D_5CD_3$, 343 K).

Copyright by Kasetsart University All rights reserved

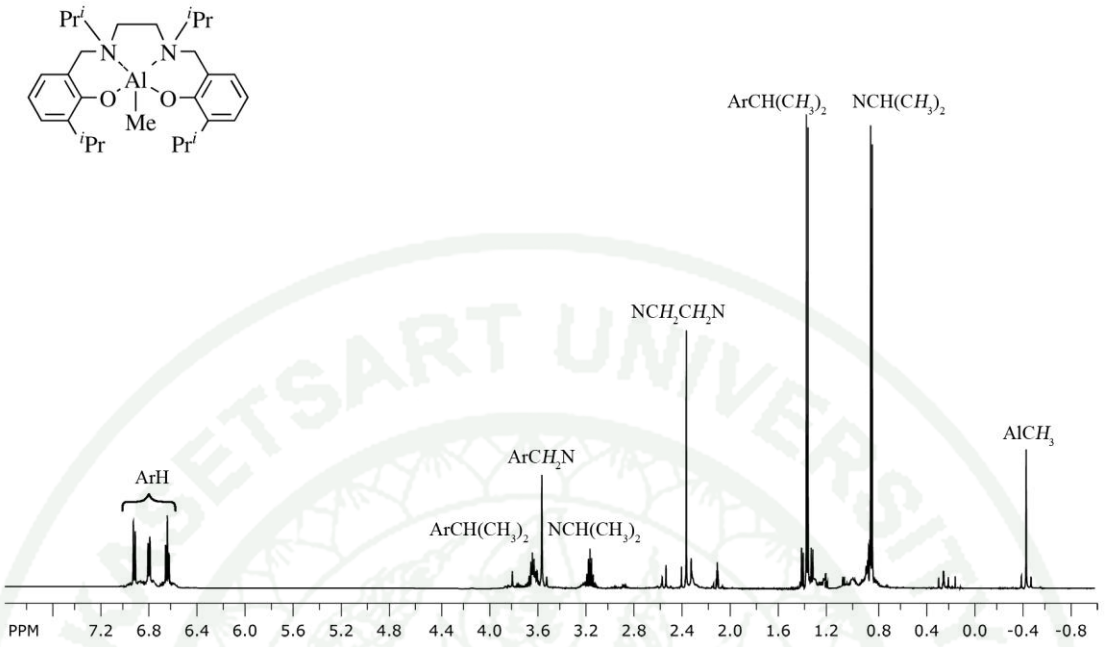

Figure 74 ^{1}H NMR spectrum of complex **L^{2C}AlMe** (500 MHz, $C_6D_5CD_3$, 343 K).

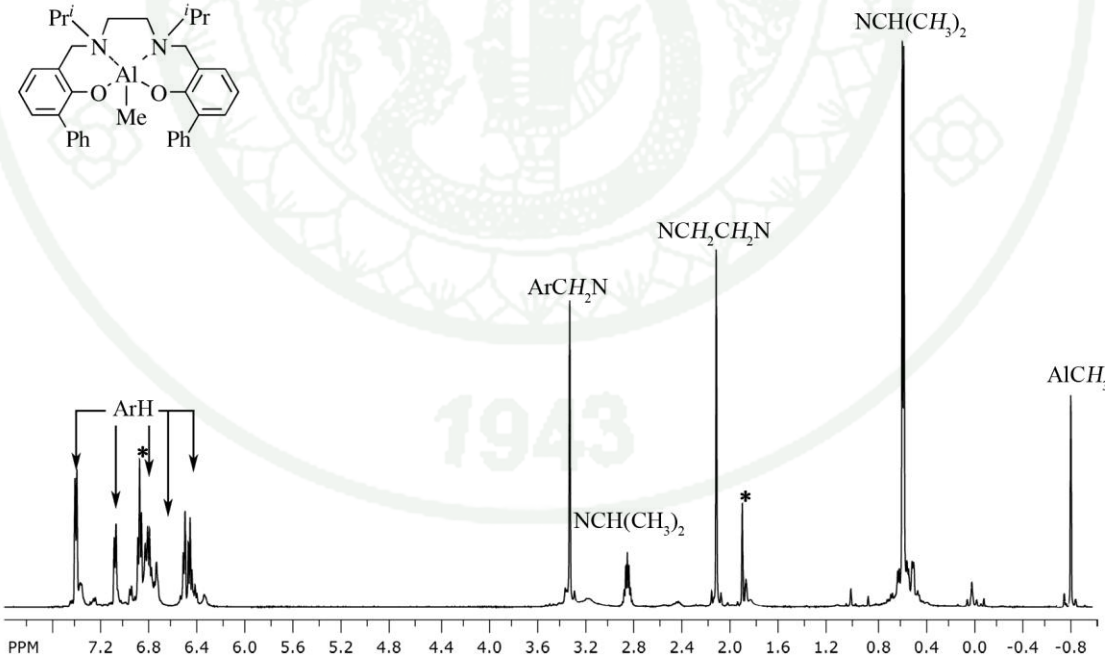

Figure 75 ^{1}H NMR spectrum of complex **L^{3C}AlMe** (500 MHz, $C_6D_5CD_3$, 343 K , * = residual $C_6D_5CD_2H$).

Copyright by Kasetsart University All rights reserved

2.2 LA polymerization results using aluminum methyl complexes

All aluminum Salan complexes were used as an initiator for the ring-opening polymerization of *rac*-Lactide in toluene at 70 ˚C in a presence of an equimolar of benzyl alcohol. The molar ratio of *rac*-LA to initiator was fixed at 100:1 ($[LA]_0/[Al]$ = 100; $[LA]_0$ = 0.83 M; [Al] = 8.33 mM; M_n(theory) = 14400). All complexes were found to be effective catalysts for the ring opening polymerization of *rac*-lactide. The polymerization results are shown in **Table 9**. All complexes yielded PLA with the molecular weights close to the theoretical numbers and narrow molecular weight distribution.

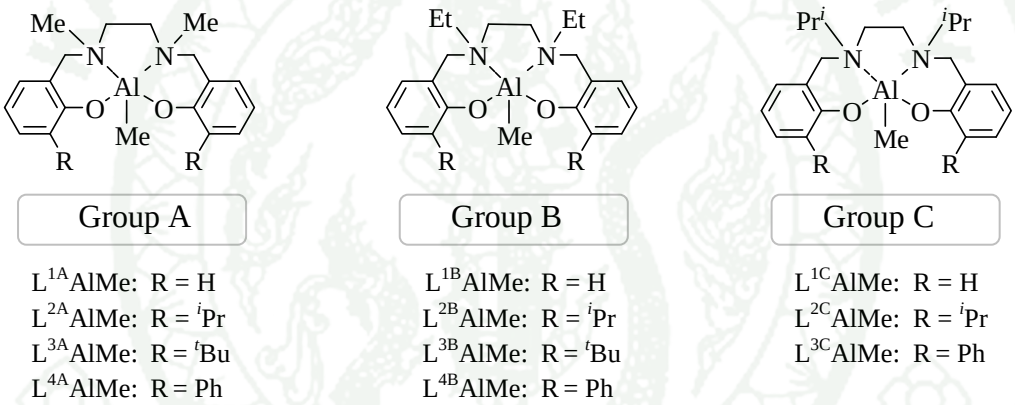

Figure 76 Groups of Salan aluminum methyl complex.

For Group A complexes with the methyl groups attached on the nitrogen donors, the ROP of *rac*-LA using complex **L^{1A}AlMe** required 24 hours to reach to 98% conversion. Its activity was comparable to the previous report by Hormnirun (Hormnirun *et al.*, 2004). Complex **L^{2A}AlMe** and **L^{4A}AlMe** converted *rac*-LA to polymer over 98% within 48 hours which were slower than that of complex **L^{1A}AlMe**. The polymerization using complex **L^{3A}AlMe** required longer time (about 60 days) to reach the full conversion. In comparison, this complex showed faster rate than 4,6-di-*tert*-butylphenoxide complex **69g** which required 61 days to reach 66% conversion under the same condition (Hormnirun *et al.*, 2004). In the case of all complexes except **L^{3A}AlMe**, the PDI values were narrow (PDI values are in the range of 1.03-1.07). The broad molecular weight distribution was observed for **L^{3A}AlMe**

Copyright by Kasetsart University All rights reserved

(PDI = 1.33). The broad PDI may be due to transesterification reaction occurring competitively to the propagation and these may also explain the slow polymerization rate.

Table 9 Polymerization data of *rac*-LA for complexes **L^{2A}AlMe-L^{4A}AlMe**, **L^{1B}AlMe-L^{4B}AlMe** and **L^{1C}AlMe-L^{3C}AlMe**[a].

Initiator	Time (h)	conversion[b] (%)	M_n(th) (g mol^{-1})[c]	M_n(GPC) (g mol^{-1})[d]	PDI[d]	P_r/P_m[e]
L^{1A}AlMe	24	98	14110	12100	1.07	0.32:0.68
L^{2A}AlMe	48	98	14110	13200	1.05	0.76:0.24
L^{3A}AlMe	2160	98	14180	15450	1.33	0.40:0.60
L^{4A}AlMe	48	96	13870	11530	1.03	0.74:0.26
L^{1B}AlMe	24	99	14230	16550	1.04	0.22:0.78
L^{2B}AlMe	96	92	13230	13480	1.04	0.66:0.34
L^{3B}AlMe	2160	87	12540	13190	1.11	0.45:0.55
L^{4B}AlMe	96	96	13880	12910	1.05	0.65:0.35
L^{1C}AlMe	96	97	14000	12930	1.10	0.55:0.45
L^{2C}AlMe	288	87	12580	11510	1.12	0.61:0.39
L^{3C}AlMe	288	81	11750	11240	1.09	0.59:0.40

[a]Polymerizations were carried out in toluene at 70 ˚C in the presence of benzyl alcohol, $[LA]_0$=83.3 mM, [Al]=0.83 mM. $[LA]_0$/[Al]=100. [b]Monomer conversion determined by ^{1}H NMR spectroscopy. [c]Calculated by ([M]/[Al]) × 144.14 × (% conv.) + 107.13.[d]Determined by GPC (THF), relative to PS standards, the value of M_n was calculated according to M_n=0.58M_n(GPC). [e]The parameters P_r and P_m are the probabilities of *meso* and *racemic* enrichments of monomer units, respectively.

Copyright by Kasetsart University All rights reserved

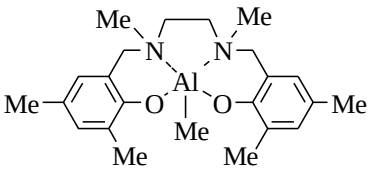

69b

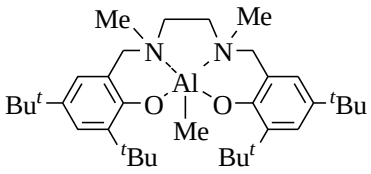

69g

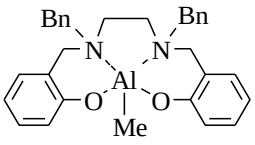

69e

Figure 77 Aluminum complexes **69b**, **69g** and **69e**.

In the case of *N*-ethyl Group B complexes, complex **L^{1B}AlMe** exhibits the same catalytic activity (99% conversion within 24 hours) as complex **L^{1A}AlMe**. Complex **L^{2B}AlMe** and **L^{4B}AlMe** required 96 hours to attain conversion of 92% and 96%, respectively which were two times slower than their Group A analogue. Compared to complex **L^{3A}AlMe**, complex **L^{3B}AlMe** exhibited slightly difference in the catalytic activity. The polymerization proceeded to 87% conversion in the same period of time (60 days) and slightly board PDI value about 1.11 was also observed. The slightly board PDI value most likely arises from transesterification reactions.

Changing the size of the substituent on the nitrogen donor atoms from ethyl to isopropyl group resulted in a dramaticall decrease of the catalytic activity. Complex **L^{1C}AlMe**/BnOH converted 97% of *rac*-LA to PLA within 96 hours. Complexes **L^{2C}AlMe-L^{3C}AlMe** showed four times slower in term of catalytic activity than complexes **L^{2B}AlMe** and **L^{4B}AlMe**. The results showed that the polymerizations of **L^{2C}AlMe** and **L^{3C}AlMe** proceeded to 81% and 87% conversions, respectively, within 12 days. In addition, the large substituent on the nitrogen donor may cause transesterification reaction as indicated by all the PDI values in this group are in the range of 1.09-1.12 which are slightly broad. Consistent with these observations, the activity of the aluminum complexes depends on the substituent size on the nitrogen donor.

The stereochemistry of the obtained PLA samples produced by all complexes was determined by analyzing the homonuclear decoupled ^{1}H NMR spectra. **Figure 78** shows the methine region of homonuclear decoupled ^{1}H NMR spectra of resulting PLAs from *rac*-LA.

Copyright by Kasetsart University All rights reserved

The polymerization of *rac*-LA using unsubstituted complexes **L^{1A}AlMe**, **L^{1B}AlMe** and **L^{1C}AlMe** yielded isotactically enriched PLAs with P_m values of 0.68, 0.78 and 0.55 respectively. In the series, the highest P_m value was obtained from **L^{1B}AlMe**, which has ethyl group attached on the nitrogen donors. The larger size of the substituent group was found to increase an isoselectivity control of catalyst (Sumrit and Hormnirun, 2013; Hormnirun *et al*., 2007). For example, the replacement of the methyl with benzyl substituent on nitrogen donors increased the isoselectivity of complex **69e** (P_m = 0.79). However, when the substituent on nitrogen donors were replaced with isopropyl group, the isoselectivity was dramatically dropped. The selectivity drop from the large substituent group on nitrogen donor is the influence of the steric shielding of the aluminum center which was reported recently in aluminum Salalen system (Whitelaw *et al.*, 2011; Vieira *et al*., 2013).

The fluxionality of aluminum complexes played a major role in the heterotacticity control (Sumrit and Hormnirun, 2013; Pappalardo *et al.*, 2013; Du *et al.*, 2007). According to the recent studies, the presence of bulky substituents on phenolic the ring makes the complex structure more rigid and turns the tacticity content from heterotactic bias to isotactic bias. In the series, the size of substituents on the *ortho* position is as follows: H < ^{i}Pr < ^{t}Bu < Ph. While isotactic PLA can be prepared by **L^{1A}AlMe,** the heterotactic PLAs can be prepared by complexes which have isopropyl groups or phenyl groups at the *ortho* position of phenolic ring such as **L^{2A}AlMe** and **L^{4A}AlMe**. The use of complexes **L^{2A}AlMe** and **L^{4A}AlMe** afforded heterotactic PLAs with P_r of 0.76 and 0.74, respectively. Their P_r values are comparable to that of complex **69b** (P_r = 0.80). The steric effect of the *tert*-butyl group involved the formations of atactic PLA. Both **L^{3A}AlMe** and **69g** produced atactic PLAs with P_m of 0.60 and 0.42, respectively. Consistent with this observation, both activity and selectivity of the aluminum complex strongly depend on the substituent on the *ortho* position of the phenoxy ring (Du *et al*., 2007).

Copyright by Kasetsart University All rights reserved

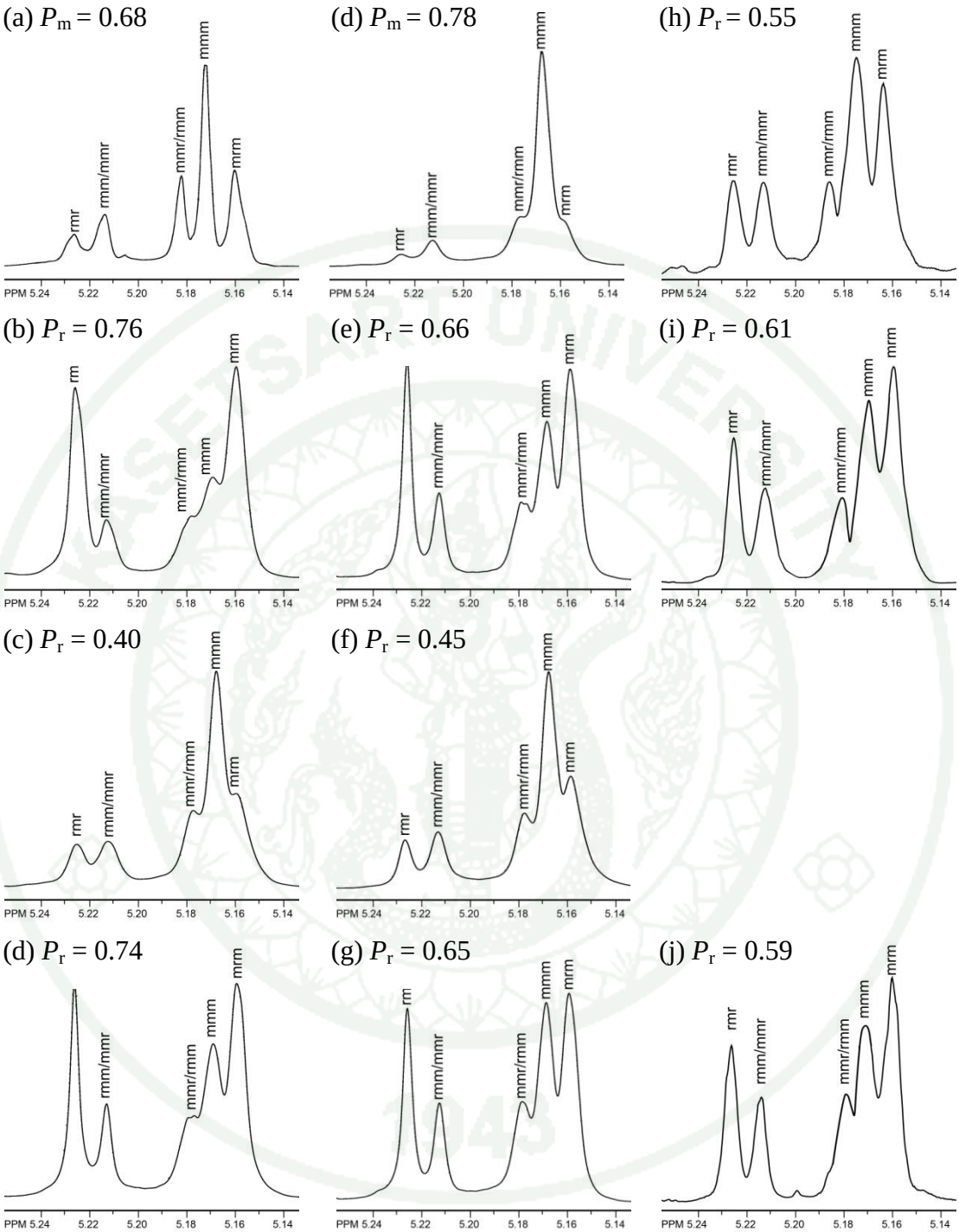

Figure 78 Methine region of homonuclear decoupled ^{1}H NMR spectra of resultant PLAs from *rac*-LA using (a) **L^{1A}AlMe**/PhCH$_2$OH; (b) **L^{2A}AlMe** /PhCH$_2$OH; (c) **L^{3A}AlMe**/PhCH$_2$OH; (d) **L^{4A}AlMe**/PhCH$_2$OH; (e) **L^{1B}AlMe**/PhCH$_2$OH; (f) **L^{2B}AlMe**/PhCH$_2$OH; (g) **L^{3B}AlMe**/PhCH$_2$OH; (h) **L^{4B}AlMe**/PhCH$_2$OH; (i) **L^{1C}AlMe**/PhCH$_2$OH; (j) **L^{2C}AlMe**/PhCH$_2$OH; (k) **L^{3C}AlMe**/PhCH$_2$OH.

Copyright by Kasetsart University All rights reserved

To obtain the polymerization rate equation, kinetic studies of **L^{1B}AlMe** were investigated using various concentrations of catalyst (4.16, 6.24, 8.33, 12.49, and 16.65 mM). The monomer concentration was fixed at 0.42 mM. In each case, the first order kinetics in monomer were observed from the linear plot of $\ln([LA]_0/[LA]_t)$ *versus* time (**Figure 79**). No significant induction period was observed in each case.

Thus, the polymerization of *rac*-LA by **L^{1B}AlMe** is presumably denoted as $-d[LA]/dt = k_{app}[LA]^1$ where $k_{app} = k_p[\mathbf{L^{1B}AlMe}]^x$, in which k_p is the propagation rate constant. To classify the order in the catalyts, ln k_{app} was plotted against ln [**L^{1B}AlMe**] (**Figure 80**). The slope of the plot is *ca.*1.0 (0.997) which means the order x is equal to 1. Therefore the overall rate equation is $-d[LA]/dt = k_p[\mathbf{L^{1B}AlMe}][LA]$.

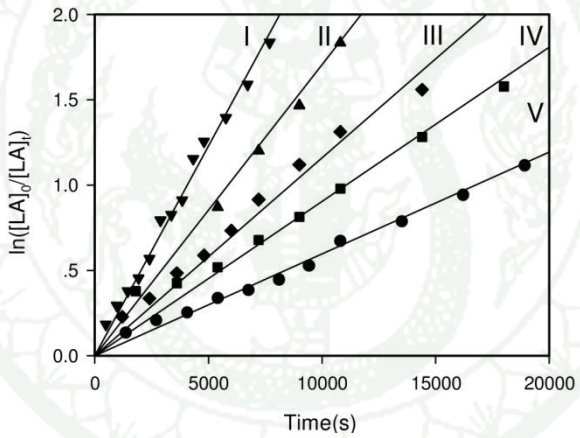

Figure 79 Semilogarithmic plots of *rac*-LA conversion with time in toluene at 70 ˚C with complex **L^{1B}AlMe**/$PhCH_2OH$ as initiator ($[LA]_0$ = 0.42 M, **I**, [Al] = 16.67 mM, [LA]/[Al] = 25; **II**, [Al] = 12.5 mM, [LA]/[Al] = 34; **III**, [Al] = 8.33 mM, [LA]/[Al] = 50; **I**V, [Al] = 6.10 mM, [LA]/[Al] = 69; **V**, [Al] = 4.16 mM, [LA]/[Al] = 100).

The polymerization rate constant, k_p, of **L^{1B}AlMe** obtained from the plot of k_{app} *versus* [**L^{1B}AlMe**] is 1.4×10^{-5} M^{-2} s^{-1} (**Figure 81**). No significant catalyst threshold concentration was observed. This rate raw is consistent with the mechanism involving coordinative insertion at a single aluminum site (Chen *et al*., 2012)

Copyright by Kasetsart University All rights reserved

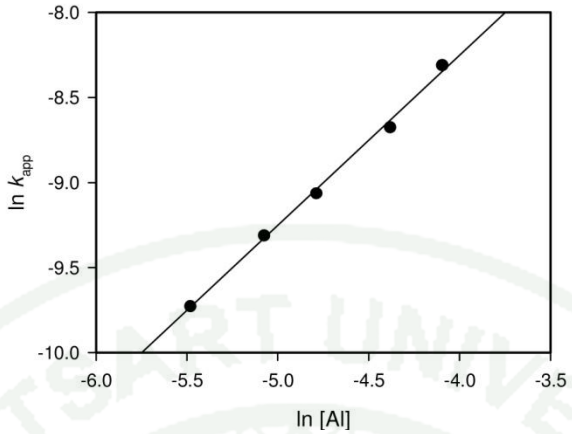

Figure 80 Plot of ln k_{app} *versus* ln [Al] for the polymerization of *rac*-LA with complex **L^{1B}AlMe**/PhCH$_2$OH as an initiator (toluene, 70 ˚C, [LA]$_0$ = 0.42 M).

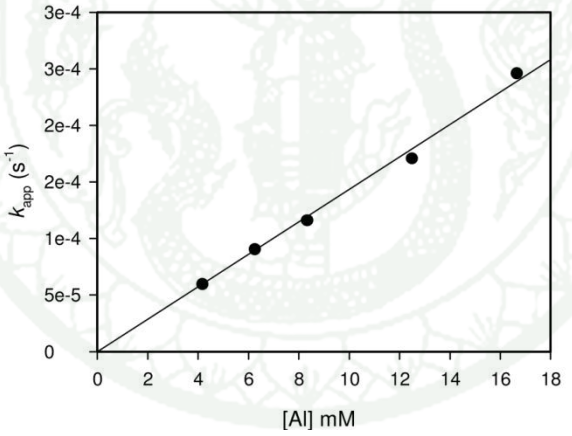

Figure 81 Plot of k_{app} *versus* [Al] for the polymerization of *rac*-LA with complex **L^{1B}AlMe**/PhCH$_2$OH as an initiator (toluene, 70 ˚C, [LA]$_0$ = 0.42 M).

Kinetic studies of *rac*-LA polymerization initiated by complexes **L^{2A}AlMe**-**L^{4A}AlMe**, **L^{1B}AlMe**-**L^{4B}AlMe** and **L^{1C}AlMe**-**L^{3C}AlMe** in the presence of benzyl alcohol were carried out in the toluene at 70 ˚C ([LA]$_0$/[Al] = 50; [LA]$_0$ = 0.83 M; [Al] = 8.33 mM). The monomer conversion was monitored by ^{1}H NMR spectroscopy in CDCl$_3$. The kinetic results are shown in **Table 10**.

Copyright by Kasetsart University All rights reserved

Table 10 Kinetic results for *rac*-LA polymerization using aluminum Salan complexes in the presence of benzyl alcohol.

Initiator	k_{app} (s^{-1})
L^{1A}AlMe	188.0×10^{-6}
L^{2A}AlMe	26.5×10^{-6}
L^{3A}AlMe	0.3×10^{-6}
L^{4A}AlMe	44.8×10^{-6}
L^{1B}AlMe	116.0×10^{-6}
L^{2B}AlMe	11.9×10^{-6}
L^{3B}AlMe	0.2×10^{-6}
L^{4B}AlMe	13.1×10^{-6}
L^{1C}AlMe	17.6×10^{-6}
L^{2B}AlMe	4.3×10^{-6}
L^{3C}AlMe	3.4×10^{-6}

In all cases, the polymerization obeyed first-order kinetics in monomer with no induction period (**Figure 82a-c**). For Group A complexes, it is apparent that the substituents on the phenoxy ring significantly affect the polymerization rate. The decrease of polymerization rate caused by the bulky substituent was observed for the *ortho*-substituted complex. For example, the *tert*-butyl substituted complex **L^{3A}AlMe** exhibited a first order rate constant (k_{app}) of 0.3×10^{-6} s^{-1}, whereas the unsubstituted complex **L^{1A}AlMe** exhibited the value k_{app} of 188.0×10^{-6} s^{-1}. The rate of the isopropyl substituted complex **L^{2A}AlMe** ($k_{app} = 26.5 \times 10^{-6}$ s^{-1}) is slower than that of the phenyl substituted complex **L^{4A}AlMe** ($k_{app} = 44.8 \times 10^{-6}$ s^{-1}). This observation may be consistent with the higher Lewis acidicity of the aluminum centre due to the presence of the electron withdrawing substituent as has been noted previously with its Salen counterparts (Nomura *et al.*, 2007).

Kinetic analyses show that the data obtained on Group B complexes are similar to those obtained from Group A complexes. The kinetic rate order is as

Copyright by Kasetsart University All rights reserved

follows: H > Ph > ^{i}Pr >> ^{t}Bu. The k_{app} obtained from Group B complexes are generally slower than those obtained from Group A complexes. The fastest polymerization was observed for **L^{1B}AlMe** which exhibited the k_{app} of 116.0 × 10^{-6} s^{-1}. The k_{app} of **L^{2B}AlMe** and **L^{4B}AlMe** were 11.9 and 13.1 × 10^{-6} s^{-1}, respectively. The polymerization rate of **L^{3B}AlMe** (0.2 × 10^{-6} s^{-1}) was slightly slower than that obtained from **L^{3A}AlMe**. In addition, the rate constants of **L^{3A}AlMe** and **L^{3B}AlMe** were comparable to 4,6-di-*tert*-butylphenoxide counterparts (0.2 × 10^{-6} s^{-1}) (Hormnirun *et al*., 2004).

For Group C complexes, the rates of *rac*-LA polymerization are certainly slower than those obtained from Group A and Group B complexes. The k_{app} values of **L^{1A}AlMe**, **L^{1B}AlMe** and **L^{1C}AlMe** were 17.6, 4.3 and 3.4 × 10^{-6} s^{-1}, respectively. The results revealed that an increase in the steric bulk of the substituents on the nitrogen donors generally resulted in a lower k_{app} value. For example, the rate of polymerization of complex with unsubstituent on the phenolic rings were in the order as follows: **L^{1A}AlMe** (182 × 10^{-6} s^{-1}) > **L^{1B}AlMe** (116.0 × 10^{-6} s^{-1}) >> **L^{1C}AlMe** (17.6 × 10^{-6} s^{-1}).

In conclusion, the size of the substituents on the phenoxy rings and on the nitrogen donor has a marked influence on the rate of polymerization. A decrease in the polymerization rate was observed when employing more bulky substituted complexes. The presence of phenyl substituents on the phenoxy rings resulted in an increase in the polymerization rate. The substituents at the *ortho* position on the phenoxy ring significantly affect the ability of the catalyst to control the PLA tacticity. The unsubstituted aluminum complexes produced isotactic PLAs, whereas the isopropyl and phenyl substituents produced heterotactic PLAs. The PLA materials prepared by *tert*-butyl substituents complexes were atactic. The lower stereoselectivity of Group B and Group C complexes compare to Group A complexes were attributed to the size of substituents on nitrogen donor.

Copyright by Kasetsart University All rights reserved

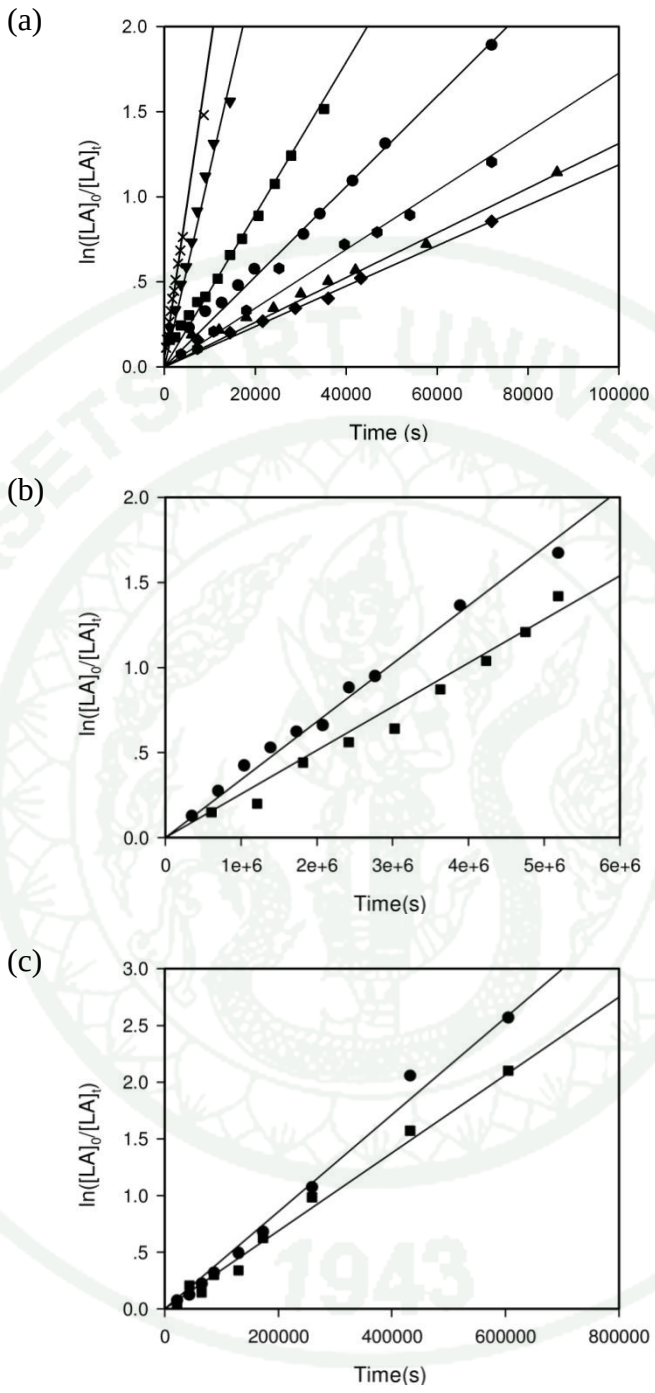

Figure 82 Semilogarithmic plots of *rac*-LA conversion with time in toluene at 70 ˚C with aluminum Salan complexes ($[LA]_0/[Al]$ = 50, $[Al]/[PhCH_2OH]$ = 1, $[LA]_0$ = 0.42 M, [Al] = 8.33 mM). (a) **L^{1A}AlMe** (×), **L^{1B}AlMe** (▼), **L^{4A}AlMe** (■), **L^{2A}AlMe** (●), **L^{1C}AlMe** (⬢), **L^{4B}AlMe** (▲), **L^{2B}AlMe** (◆) ; (b) **L^{3A}AlMe** (●), **L^{3B}AlMe** (■); (c) **L^{2C}AlMe** (●), **L^{3C}AlMe** (■).

Copyright by Kasetsart University All rights reserved

A linear correlation between M_n and monomer conversion was observed for all polymerization. Examples of the plots of M_n using Group B complexes are shown in **Figure 83a-c**. The molecular weight distributions remained low at *ca.* 1.1 throughout the course of all the polymerizations indicative of well-controlled systems. The plots of M_n using Group A and Group B complexes are shown in the **Appendix Figures 2-3**.

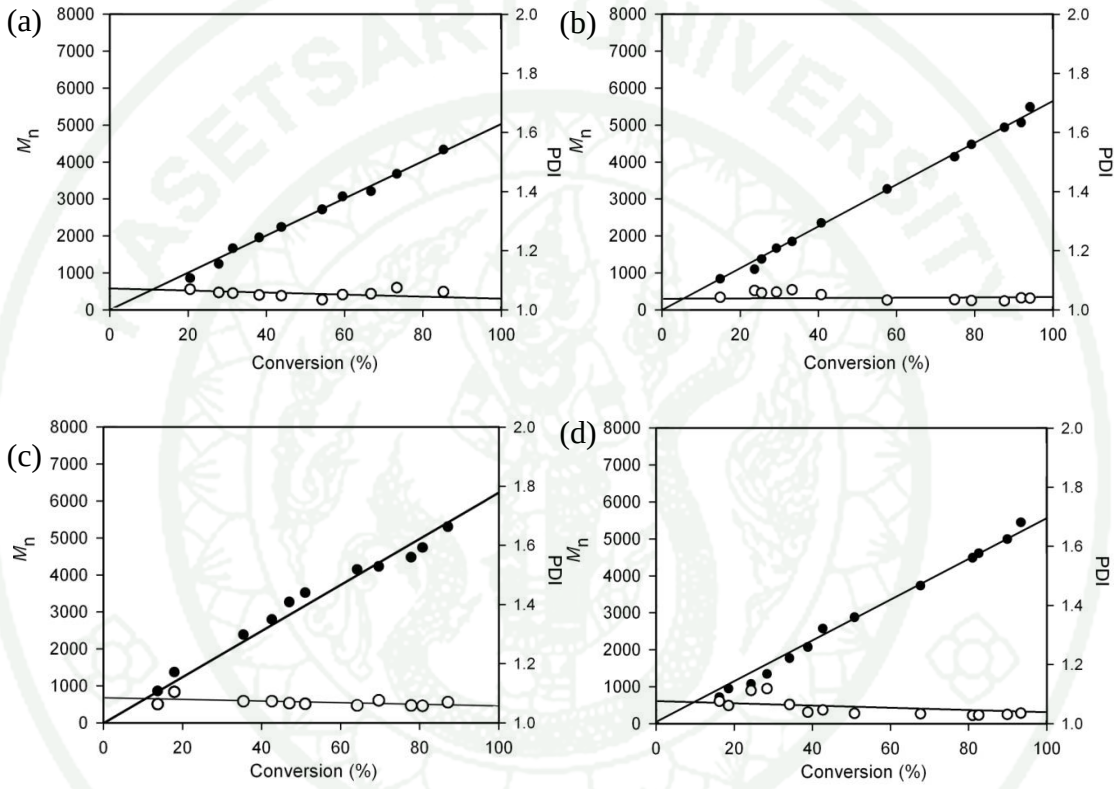

Figure 83 Plot of M_n as a function of monomer conversion for *rac*-LA polymerization using (a) **L^{1B}AlMe**/PhCH$_2$OH, (b) **L^{2B}AlMe**/PhCH$_2$OH, (c) **L^{3B}AlMe**/PhCH$_2$OH, (d) **L^{4B}AlMe**/PhCH$_2$OH ([LA]$_0$/[Al] = 50, [Al]/[PhCH$_2$OH] = 1, [LA]$_0$ = 0.42 M, [Al] = 8.33 mM)**.**

2.3 Ring-opening polymerization of ε-Caprolactone

Aluminum complexes have been received considerable attention as a catalyst for ROP of ε-CL due to their low toxicity and the possibility to control molecular weight with relatively narrow PDI of polymer. One of the most studied

Copyright by Kasetsart University All rights reserved

aluminum based catalysts is aluminum isopropoxide (Mingotaud *et al*., 2000; Duda *et al.*, 1996). Unlike other metal alkoxides, aluminum isopropoxide did not induce degradation of the PCL by intramolecular transesterification or backbiting (Kricheldorf *et al*., 1988). The $Al(O^iPr)_3$ catalyzed ROP of *ε*-CL was reported to be more controlled at lower temperature (0-25 ˚C in comparison to ~100 ˚C) (Jacob *et al*., 1991). Many aluminum Schiff base complexes were investigated in the ROP of *ε*-CL. For example, the HAPENAlOiPr showed an ability to polymerize *ε*-CL in dichloromethane at 25 ˚C (**Figure 84**) and the polymerization occurred through a coordination-insertion mechanism (Bhaw-Luximon *et al*., 2005). Taden and co-workers studied the polymerizations of *ε*-CL using different aluminum Schiff bases on Salen, **I**, and Salcen, **II**, ligands (Taden *et al*., 1997). The polymerizations were carried out in toluene at 50 ˚C. It was found that only aluminum Salen **I** polymerized *ε*-CL within 20 hours while the other complexes only produced oligomers.

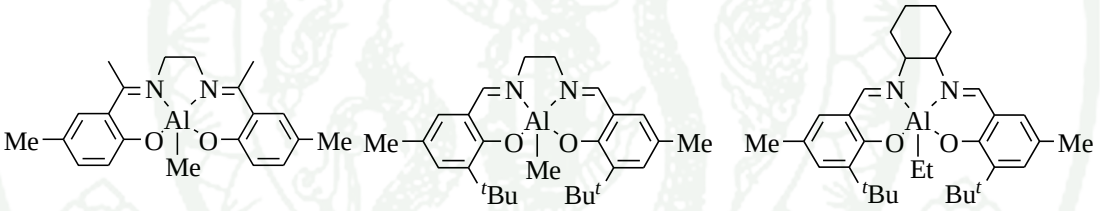

Figure 84 Aluminum Salen complexes for *ε*-CL polymerization.

Although aluminum Salen complexes were investigated for the ROP of *ε*-CL, the reports of aluminum Salan complexes for ROP of *ε*-caprolactone were found to be very limited. In this section, all aluminum Salan complexes synthesized in this work were utilized for the ROP of *ε*-CL. The influence of the catalytic structure on the polymerization activities (M_n and PDI) was investigated using the same polymerization condition as for the ROP of LA.

All complexes were highly active in the ROP of *ε*-CL under the same condition for *rac*-LA polymerization ($[CL]_0/[Al] = 100$; $[CL]_0 = 0.83$ M; [Al] = 8.33

Copyright by Kasetsart University All rights reserved

mM; M_n(theory) = 11400). The 80% conversion was obtained within 6 hours in all cases. The rates were faster than those of *rac*-LA polymerizations under the same condition. The polymers were analyzed by ^{1}H NMR spectroscopic and GPC measurement. The results are summarized in **Table 11**. GPC analysis of the obtained PCL samples displayed monomodal and relatively narrow molecular weight distributions (PDI = 1.12-1.22). The experimental molecular weights were close to the calculated values. From the results, it was suggested that a single PCL chain was produced per metal center. Similar results have been reported previously for aluminum complexes based on anilido-imine ligand (Yao *et al.,* 2008). All tested complexes showed a high catalytic activity when benzyl alcohol was used as an initiator/chain transfer agent. The resulting PCLs also showed expected molecular weights.

In comparison, the activities of aluminum Salan complexes in the series are lower than that of four-coordinate aluminum complexes such as aluminum complexes bearing a bidentate ligand (Arbaoul *et al*., 2008; Iwasa *et al*., 2008; Yao *et al*., 2008) or a tridentate ligand (Ma and Wang 2011). However, their activities are comparable with that of other five-coordinate aluminum complexes such as aluminum complexes bearing a tetradentate ligand (Endo *et al.*, 1987; Alcazar-Roman *et al*., 2003) or two bidentate ligands (Nomura *et al.*, 2005; Huang *et al*., 2001).

2.4 Copolymerization of *rac*-lactide and *ε*-Caprolactone

The synthesis of *rac*-LA/*ε*-CL copolymerization using aluminum complexes such as $Al(O^iPr)_3$ or $Al(acac)_3$, where acac is acetylacetone, has been widely studied in recent years (Barakat *et al.*, 1994; Tian *et al.*, 1997). When both monomers are polymerized, a block copolymer was obtained. Nevertheless, only few aluminum Salan complexes used as initiators for the living ROP block copolymerization of *rac*-LA/*ε*-CL have been reported (Wang and Ma, 2012).

Copyright by Kasetsart University All rights reserved

Table 11 The ε-CL polymerization data for aluminum Salan complexes[a]

Catalyst	Time (h)	Conversion (%)[b]	M_n(th) (g mol^{-1})[c]	M_n(GPC) (g mol^{-1})[d]	PDI[d]
L^{1A}AlMe	6	98	11190	11000	1.19
L^{2A}AlMe	6	92	10540	10030	1.13
L^{3A}AlMe	6	84	9680	9100	1.12
L^{4A}AlMe	6	92	10530	10420	1.21
L^{1B}AlMe	6	90	10290	9800	1.16
L^{2B}AlMe	6	86	9910	9150	1.16
L^{3B}AlMe	6	81	9280	8760	1.22
L^{4B}AlMe	6	92	10530	10220	1.16
L^{1C}AlMe	6	96	11000	10040	1.17
L^{2C}AlMe	6	93	10720	10900	1.17
L^{3C}AlMe	6	89	10200	10480	1.20

[a]Polymerizations were carried out in toluene at 70 ˚C in the presence of benzyl alcohol, $[CL]_0$=83.3 mM, [Al]=0.83 mM. $[CL]_0$/[Al]=100. [b]Monomer conversion determined by ^{1}H NMR spectroscopy. [c]Calculated by ([M]/[Al]) × 144.14 × (% conv.) + 107.13. [d]Determined by GPC (THF), relative to PS standards, the value of M_n was calculated according to M_n=0.56M_n(GPC).

To gain further insight into the ROP of cyclic ester monomers by aluminum Salan complexes, the copolymerizations of ε-CL and *rac*-LA by all complexes investigated (**Figure 85**). The polymerizations were carried out in toluene at 70 ˚C. The concentration of *rac*-LA and ε-CL was fixed at 0.42 M, which resulted in the overall initial monomer concentration of 0.83 M. The progress of polymerizations was monitored by ^{1}H NMR spectroscopy by taking aliquots from the reaction mixture. The polymerizations were allowed to proceed to high conversion of both monomers (>85%) as illustrated in **Figure 86**.

Copyright by Kasetsart University All rights reserved

The composition of the copolymer was determined by ^{1}H NMR spectroscopy through the ratio of the intensity of methine photon from lactidyl unit and the methylene proton of the caproly unit (**Figure 87**, left). The lactidyl/caproly ratios agreed well with the feed ratio, as expected at high conversion of both monomers. Both M_n and PDI were analyzed by GPC, using polystyrene standards. The raw data and corrected molecular weights are listed in **Table 12**. For all complexes, the corrected M_n values are in good agreement with the calculated theoretical values, and PDIs are relatively narrow compared to the copolymers obtained from $Sn(Oct)_2$ (Storey and Sherman, 2002; Zhang *et al.*, 1994) and $AlO^{i}Pr_3$ (Vanhoorne *et al*., 1992)

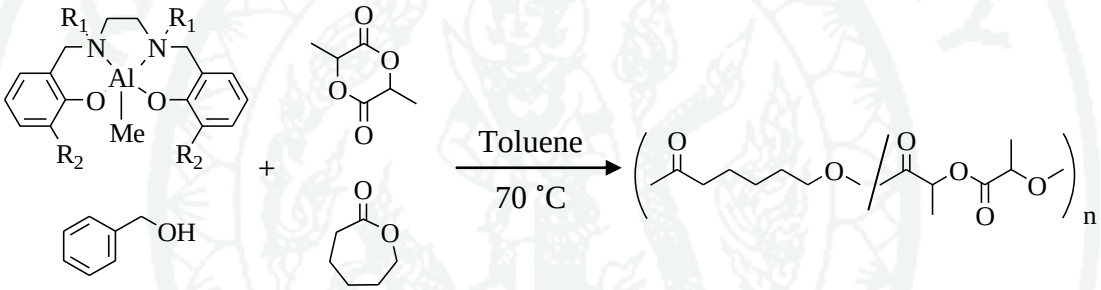

Figure 85 Copolymerization of ε-CL and *rac*-LA initiated by aluminum Salan complexes.

The chain microstructure of the copolymer was determined by ^{13}C NMR spectroscopy. This method is sensitive to monomer sequences. The peaks were assigned according to literature (Vanhoorne *et al.*, 1992; Kasperczyk and Bero, 1991; 1993). The average lengths of lactidyl unit (L_{LL}) and caproyl unit (L_C) were calculated from the equations as previously reported by Kasperczyk and Bero (Kasperczyk and Bero, 1991; 1993). The calculated values are reported in **Table 12**. For example, the ^{13}C NMR spectra of PLA-*co*-PCL using complexes **L^{1B}AlMe-L^{4B}AlMe** were shown in **Figure 87** (right).

Copyright by Kasetsart University All rights reserved

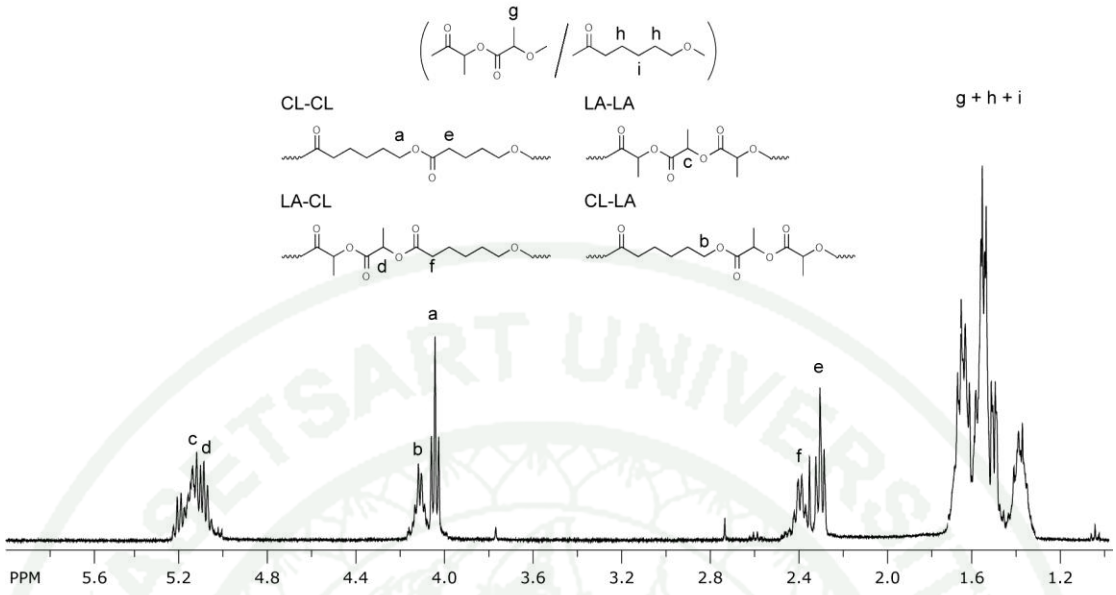

Figure 86 ^{1}H NMR spectrum of PLA-*co*-PCL.

The average lengths of lactidyl are in the range of 1.59-1.93 whereas the average lengths of caproyl are in the range of 6.39-11.17. For the spectra of copolymers obtained from **L^{1A}AlMe**, **L^{2A}AlMe** and **L^{4A}AlMe**, no second mode transesterification were observed. However, in the case of complex **L^{3A}AlMe**, the presence of a signal at δ 170.8 ppm which belongs to CLC triad suggested that the second mode transesterification (T_{II}) was occurred. The second mode transesterification was not observed in the previous copolymerization studies using aluminum Salen complexes **(*R*,*R*)-1**, **(*S*,*S*)-1** (Florczak and Duda, 2008), and **4b** (Nomura *et al.*, 2010). The T_{II} was also observed from the copolymerization using **L^{3A}AlMe** (see **Figure 87**).

Copyright by Kasetsart University All rights reserved

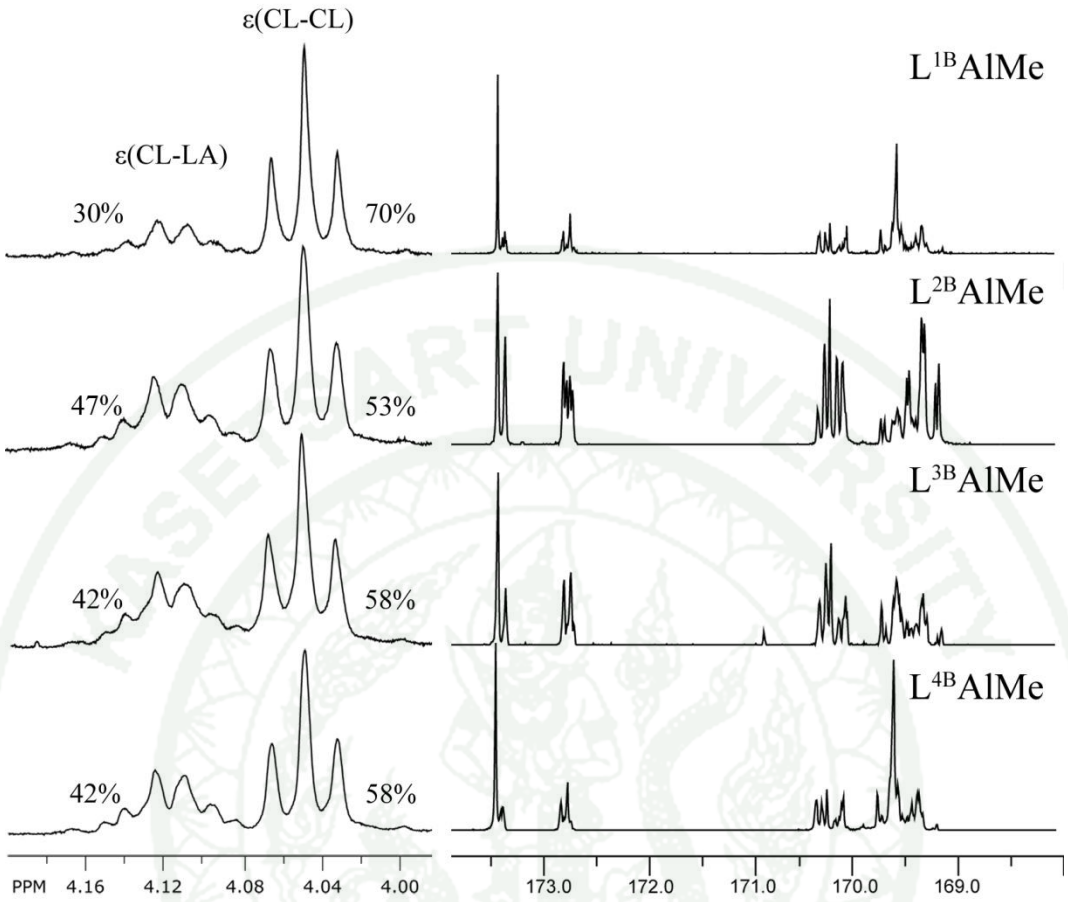

Figure 87 (left) ^{1}H NMR spectrum of ε- and α-methylene protons of PLA-*co*-PCL, (right) ^{13}C NMR spectrum of carbonyl carbons of PLA-*co*-PCL.



(*R*,*R*)-1 **4b**
(*S*,*S*)-1

Figure 88 Aluminum complexes **(*R*,*R*)-1**, **(*S*,*S*)-1** and **4b**.

Copyright by Kasetsart University All rights reserved

The degree of randomness values (*R*) of the copolymer were in the range of 0.09-0.32 suggesting that the block copolymer was formed. The average lengths T_{II} and *R* are reported in **Table 12**. Differential scanning calorimeter (DSC) was used to determine the glass transition temperatures (T_g) of the copolymer. The well phase separated block copolymer from **L^{1A}AlMe**, **L^{1B}AlMe** and **L^{1C}AlMe** exhibits the T_g values closed to the T_g values of isotactic PLA. However the two T_g values expected to observe for the block of PCL and PLA were not observed in this study (See **Appendix Figures 5-6**). The lower T_g values as compared to the unsubstituent system were observed. The lower T_g values are the characteristic of the higher content of CL and heterotactic or atactic PLA block.

Copyright by Kasetsart University All rights reserved

Table 12 Copolymerization of *ε*-CL and *rac*-LA with aluminum Salan complexes[a].

Catalyst	Time (h)	CL/LA[b] (mol%)	L_{CL}[c]	L_{LA}[c]	T_{II}[d] (%)	R[e]	T_g (˚C)	M_n(GPC)[f]	M_n[g]	PDI[f]
L^{1A}AlMe	6	33/66	11.17	1.93	0	0.09	22	17860	13720	1.10
L^{2A}AlMe	12	47/53	7.00	1.80	0	0.26	-9	24040	10350	1.22
L^{3A}AlMe	720	48/52	6.39	1.73	6	0.30	-27	18140	10930	1.11
L^{4A}AlMe	12	39/61	7.84	1.71	0	0.21	-14	19100	10940	1.17
L^{1B}AlMe	12	30/70	9.78	1.77	0	0.15	18	19060	10900	1.20
L^{2B}AlMe	12	47/53	5.78	1.71	0	0.32	-14	19100	10530	1.07
L^{3B}AlMe	720	42/58	7.00	1.80	19	0.25	-27	18420	11460	1.16
L^{4B}AlMe	24	42/58	9.19	1.86	0	0.19	-11	20050	13720	1.22
L^{1C}AlMe	24	40/60	7.14	1.66	2	0.42	6	21240	19630	1.11
L^{2C}AlMe	48	47/53	6.71	1.59	0	0.28	-9	24050	12760	1.07
L^{3C}AlMe	48	42/58	7.38	1.70	0	0.24	-9	22320	10240	1.16

[a]Polymerizations were carried out in toluene at 70 ˚C. Ratio of $[CL]_0/[LA]_0$ was fixed at 1; $[CL]_0=[LA]_0=$ 0.42 M; $[Al]=[PhCh_2OH]=$ 4.2 mM. [b]CL/LA mole ratio in the copolymer was determined by ^{1}H NMR. [c]Averaged sequence lengths of caproly and lactidyl unit in the copolymer were determined by ^{13}C NMR. [d]Yield of the second mode transesterification. [e]Degree of randomness. [f]Molar mass and dispersity determinated by GPC in THF at 40 ˚C relative to polystyrene standards. [g]Molar mass determinated by GPC in THF at 40°C relative to polystyrene standards corrected by the Mark-Houwink correction factor ($M_{n,}(GPC_{corr}) = M_n(GPC_{raw}) \times 0.56 \times \%PCL_{NMR} + M_n(GPC_{raw}) \times 0.58 \times \%PLA_{NMR}$)

Copyright by Kasetsart University. All rights reserved

CONCLUSIONS

The synthesis and characterization of two families of aluminum complexes have been described. All complexes were evaluated as initiators for the ring-opening polymerization of lactide.

The first family is aluminum complexes supported by bis(pyrrolidene) Schiff base ligands. All complexes were obtained in a monomeric form as confirmed by an evidence in the crystal structure of complex **L^{3}AlMe**. Complex **L^{3}AlMe** displays a distorted square pyramidal geometry with τ and χ values of 0.18 and 0.36, respectively. All complexes in the family were tested as initiator for the ring-opening polymerization of *L*-LA and *rac*-LA in toluene at 70 ˚C and found to be efficient initiators. The polymers with controlled molecular weights and narrow molecular weight distributions were produced. The flexibility of backbone significantly affects the ability to control stereochemistry of monomer enchainment. The highest stereoselectivity over the ROP of *rac*-LA was obtained from **L^{3}AlMe** (P_m = 0.80). Other C_3 backbone complexes polymerized *rac*-LA to form isotactic biased polymer with the P_m values in the range of 0.69-0.73. The uses of rigid C_2 complexes resulted in moderate isoselectivity (P_m values in the range of 0.61-0.64). PLA produced by **L^{7}AlMe** with a butylenes backbone is atactic. Studies of the kinetics of the polymerization consistently reveal the-first order in monomer in all cases. The activity of aluminum complexes **L^{1}AlMe**-**L^{7}AlMe** toward lactide polymerization decreases in the order **L^{4}AlMe** > **L^{2}AlMe** > **L^{3}AlMe** > **L^{7}AlMe** > **L^{5}AlMe** > **L^{1}AlMe** > **L^{6}AlMe**. It was also observed that the rate of *rac*-LA polymerization was lower than that of *L*-LA polymerization. This may be attributed to the rearrangement of ligand geometry for mismatching monomer enantiomer during the polymerization process. Complex **L^{3}AlMe** exhibited a well controlled character of polymerization as indicated by the ability to polymerize *rac*-LA at a high loading of monomer to initiator ratio. In addition, a high degree of isoselectivity was observed up to high monomer to initiator ratios. The P_m values of resulting polymers remained almost unchanged in the range of P_m = 0.78-0.80.

Copyright by Kasetsart University All rights reserved

The second family is aluminum complexes supported by Salan ligands. ^{1}H NMR analyses revealed that all complexes in this family exhibit broad resonance which is indicative of fluxional solution state structures. It is also apparent that as the phenoxy substituents become bulkier, the fluxionality of the complexes diminishes. Catalytic studies demonstrated that all complexes are efficient initiators for the ROP of *rac*-LA. The molecular weight distributions of the polymers were narrow. The corrected M_n values were close to the theoretical values indicating the well-controlled behavior of the complexes. The size of the substituent at the *ortho* position of the phenoxy ring was found to have a remarked influence on the polymerization rate. Increasing the bulkiness of the phenoxy substituent leads to significantly slow the polymerization rate. For instance, the fastest polymerization rate was observed for the polymerization using the unsubstituted complex **L^{1A}AlMe**. In contrast, the slow polymerization rates were observed for complexes **L^{3A}AlMe and L^{3B}AlMe** with the *tert*-butyl substituted phenoxy rings. The rate of polymerization follows the phenoxy substituents in the order H > Ph > ^{i}Pr >> ^{t}Bu. The microstructure of the resulting PLA is dependent on the ligand substituted pattern. The unsubstituted aluminum complexes gave rise to isotactic PLAs, whereas the isopropyl and phenyl substituted complexes afforded heterotactic PLAs. Atactic PLAs were produced by the *tert*-butyl substituted complexes. The introduction of bulky substituents on the nitrogen donors was found to slow down the polymerization rate. The polymerization rates of Group A complexes were faster than those of Group B and Group C complexes. In addition, the presence of bulky substituents on the nitrogen donors resulted in poor stereocontrol. In the case of Group C complexes, the lack of stereocontrol was observed in all cases. All complexes also showed good activity in the polymerization of *ε*-CL. The substituents on both phenoxy rings and nitrogen donors showed no significant effect on the polymerization activities of *ε*-CL. In comparison, the polymerization of *ε*-CL required shorter time to reach full conversion as compared to the polymerization of *rac*-LA. The copolymers of *rac*-LA and *ε*-CL using aluminum Salan complexes were successfully prepared. The amount of *ε*-caprolactone in the resulting copolymer is lower than the initial concentration in the feed. This indicated the lower reactivity of ε-CL in the copolymerization comparing to the homopolymerization. The ^{13}C NMR spectra and DSC results reveals the formation of the block copolymers.

Copyright by Kasetsart University All rights reserved

LITERATURE CITED

Addison, A.W., T.N. Rao, J. Reedijk, J. van Rijn and G.C. Verschoor. 1984. Synthesis, structure, and spectroscopic properties of copper(II) compounds containing nitrogen-sulphur donor ligands; the crystal and molecular structure of aqua[1,7-bis(N-methylbenzimidazol-2′-yl)-2,6-dithiaheptane]copper(II) perchlorate. **J. Chem. Soc., Dalton Trans.** 7:1349-1356.

Agatemor, C. and M.P. Shaver 2013. Tacticity-Induced Changes in the micellization and degradation properties of poly(lactic acid)-block-poly(ethylene glycol) copolymers. **Biomacromolecules** 14(3):699-708.

Ajellal, N., M. Bouyahyi, A. Amgoune, C.M. Thomas, A. Bondon, I. Pillin, Y. Grohens, J.-F. Carpentier. 2009. Syndiotactic-enriched poly(3-hydroxy butyrate)s *via* stereoselective ring-opening polymerization of racemic *β*-butyrolactone with discrete yttrium catalysts. **Macromolecules** 42(4):987-993.

Alaaeddine, A., C.M. Thomas, T. Roisnel and J.-F. Carpentier. 2009. Aluminum and yttrium complexes of an unsymmetrical mixed fluorous alkoxy/phenoxy-diimino ligand: Synthesis, structure, and ring-opening polymerization catalysis. **Organometallics** 28(5):1469-1475.

Albertsson, A.-C. and R. Palmgren. 1996. Cationic polymerization of 1,5-dioxepan-2-one with Lewis acids in bulk and solution. **J. Macromol. Sci., Pure Appl. Chem.** 33(6):747-758.

_____, and V. Kumar. 2003. Recent developments in ring opening polymerization of lactones for biomedical applications. **Biomacromolecule** 4(6):1466-1468.

Alcazar-Roman, L.M., B.J. O'Keefe, M.A. Hillmayer and W.B. Tolman. 2003. Electronic influence of ligand substituents on the rate of polymerization of *ε*-caprolactone by single-site aluminium alkoxide catalysts. **Dalton Trans.** 3082-3087.

Alfred, R. and L.W.H. Howard. 1972. Universal calibration in GPC. **J. Polym. Sci., Part A:Polym. Chem.** 10(1):217-235.

Allen, S.D., R.R. Valente, H. Lee, A.E. Cherian, D.L. Bunning, N.A. Clinton, O.S. Fruchey and B.D. Dombek. 2010. Process for *β*-lactone production. **PCT Int. Appl.** WO 2010 118128 A1 20101014.

Altomare, A., M.C. Burla, M. Camalli, G.L. Cascarano, C. Giacovazzo, A. Guagliardi, A.G.G. Moliterni, G. Polidori, R.J. Spagna. 1999. A new tool for crystal structure determination and refinement. **Appl. Cryst.** 32:115-119.

Copyright by Kasetsart University All rights reserved

Amgoune A., T.M. Christophe, S. Ilinca T. Roisnel and T.J. Carpentier. 2006. Highly active, productive, and syndiospecific yttrium initiators for the polymerization of racemic *β*-butyrolactone. **Angew. Chem. Int. Ed. Engl.** 45(17):2782-27844.

_____, C. M. Thomas and J.-F. Carpentier. 2007. Yttrium complexes as catalysts for living and immortal polymerization of lactide to highly heterotactic PLA. **Macro. Rapid Commun.** 28(6):693-697.

_____, _____, T. Roisnel and J.-F. Carpentier. 2005. Ring-opening polymerization of lactide with Group 3 metal complexes supported by dianionic alkoxy-amino-bisphenolate ligands: Combining high activity, productivity, and selectivity. **Chem. -Eur. J.** 12(1):169-179.

_____, L. Lavanant, C.M. Thomas, Y. Chi, R. Welter, S. Dagorne and J.-F. Carpentier. 2005. An aluminum complex supported by a fluorous diamino-dialkoxide ligand for the highly productive ring-opening polymerization of *ε*-caprolactone. **Organometallics** 24(25):6279-6282.

Arnold, P.L., J.-C. Buffet, R. P. Blaudeck, S. Sujecki and C. Wilson. 2009. Ligand recognition processes in the formation of homochiral C_3-Symmetric LnL_3 complexes of a chiral alkoxide. **Chem.-Eur. J.** 15(33):8241-8250.

_____, _____, _____, _____, A. J. Blake, and C. Wilson. 2008. C_3-symmetric lanthanide tris(alkoxide) complexes formed by preferential complexation and their stereoselective polymerization of *rac*-lactide. **Angew. Chem., Int. Ed.** 47(32):6033-6036.

Atwood, D.A., J. Benson, J. A. Jegier, N.F. Lindholm, K.J. Martin, R. J. Pitura and D. Rutherford. 1995. Synthesis and structural characterization of tetradentate (N_2O_2) ligand complexes of zinc. **Main Group Chem.** 1(1):99-113.

_____, and M.J. Harvey. 2001, Group 13 compounds incorporating Salen ligands. **Chem. Rev.** 101(1):37-52.

Azpeitia, H.F.S., S.A. Cortes-Llamas, F.A. Vengoechea-Gómez, E. Rufino-Felipe, N. T. Crespo-Velasco and M.-Á. Muñoz-Hernández. 2011. Synthesis and characterization of aluminum complexes incorporating Schiff base ligands derived from pyrrole-2-carboxaldehyde. **Main Group Chemistry**. 10(2):127-140.

Bacchi, A., M. Carcelli, L. Gabba, S. Ianelli, P. Pelagatti, G. Pelizzi and D. Rogolino. 2003. Syntheses, characterization and X-ray structure of palladium(II) and nickel(II) complexes of tetradentate pyrrole containing ligands. ***Inorg. Chim. Acta.*** 342:229-235.

Copyright by Kasetsart University All rights reserved

Bakewell, C., R.H. Platel, S.K. Cary, S.M. Hubbard, J. M. Roaf, A.C. Levine, A.J.P. White, N.J. Long, M. Haaf, and C.K. Williams. 2012. Bis(8-quinolinolato)aluminum ethyl complexes: Isoselective initiators for *rac*-lactide polymerization. **Organometallics** 31(13):4729-4736.

_____, T.-P.-A. Cao, N. Long, X. F. Le Goff, A. Auffrant and C.K. Williams. 2012. Yttrium phosphasalen initiators for *rac*-lactide polymerization: Excellent rates and high iso-selectivities. **J. Am. Chem. Soc.** 134 (51):20577-20580.

Balasanthiran, V., M.H. Chisholm, C.B. Durra and J.C. Galluccia. 2013. Single-site bismuth alkoxide catalysts for the ring-opening polymerization of lactide. **Dalton Trans.** (42): 11234-11241.

Balsells, J., P.J. Carroll and P.J. Walsh. 2001. Achiral tetrahydrosalen ligands for the synthesis of c_2-symmetric titanium complexes: A structure and diastereoselectivity study. **Inorg. Chem.** 40(22):5568-5574.

Basko, M. 2012. Activated monomer mechanism in the cationic polymerization of *L,L*-lactide. **Pure Appl. Chem.** 84(10):2081-2088.

Baxter, E.W. and A.B. Reitz. 2002. Reductive aminations of carbonyl compounds with borohydride and borane reducing agents. **Org. Reac. (Hoboken, NJ, United States)** 59.

Beck J.M., R.J. Pounder and A.P. Dove. 2010. Synthesis of poly(lactide)s with modified thermal and mechanical properties. **Macromol. Rapid Commun.** 31(22):1923-1937.

Beek, T.A.V., P. Maas, B.M. King , E. Leclercq, A.G.J. Voragen and A. DeGroot. 1990. Bitter sesquiterpene lactones from chicory roots. **J. Agric. Food Chem.** 38(4):1035-1038.

Berube, C.D., S. Gambarotta, G.P.A. Yap and P.G. Cozzi. 2003. Di- and trivalent dinuclear samarium complexes supported by pyrrole-based tetradentate Schiff bases. **Organometallics** 22(3):434-439.

Bhaw-Luximon, A., D. Jhurry and N. Spassky. 2000. Controlled polymerization of *D,L*-lactide using a Schiff's base Al-alkoxide initiator derived from 2-hydroxyacetophenone. **Polym. Bull.** 44(1):31-38.

_____, _____, S. M. Timol and Y. Lochee. 2006. Polymerization of ε-caprolactone and its copolymerization with γ-butyrolactone using metal complexes. **Macromol. Symp**. 231:60-68.

Copyright by Kasetsart University All rights reserved

Bhowon, M.G., H.L.K. Wah, A. Dosieah, M. Ridana, O. Ramalingum, and D. Lacour. 2004. Synthesis, characterization, and catalytic activity of metal schiff base complexes derived from pyrrole-2-carboxaldehyde. ***Synth. React. Inorg. Met. Org. Chem.*** 34(1):1-16.

Biela, T., A. Duda and S. Penczek. 2006. Enhanced melt stability of star-shaped stereocomplexes as compared with linear stereocomplexes. **Macromolecules** 39(11):3710-3713.

Bouyahyi, M., E. Grunova, N. Marquet, E. Kirillov, C.M. Thomas, T. Roisnel and J.-F. Carpentier. 2008. Aluminum complexes of fluorinated dialkoxy-diimino salen-like ligands: Syntheses, structures, and use in ring-opening polymerization of cyclic esters. **Organometallics** 27 (22):5815-5825.

_____, T. Roisnel and J.F. Carpentier. 2012. Aluminum complexes of bidentate fluorinated alkoxy-imino ligands: syntheses, structures, and use in ring-opening polymerization of cyclic esters. **Organometallics** 31(4):1458.

Bovey, F.A. and P.A. Mirau. 1996. NMR of polymer. **Academic Press**, San Diego.

Bredereck, H., G. Simchen, S. Rebsdat, W. Kantlehner, P. Horn, R. Wahl, H. Hoffmann and P. Grieshaber. 1968. Orthoamide, I darstellung und eigenschaften der amidacetale und aminalester. **Chem. Ber.** 101(1):41-50.

_____, _____, and U. Schenck. 1968. Orthoamide, VI. Über die umsetzung von aminalestern mit sekundären aminen zu tris-amino-methanen. **Chem. Ber**. 101(9):3058-3061.

_____, _____, H. Hoffmann, P. Horn and R. Wahl. 1967. Stability of aminal esters and their reactions with aromatic aldehydes. **Angew. Chem., Int. Ed. Engl.** 6(4):356-357.

Buffet, J.C. and J. Okuda. 2011. Initiators for the stereoselective ring-opening polymerization of *meso*-lactide. **Polym. Chem**. 2:2758-2763.

_____, A.N. Martin, M. Kol and J. Okuda. 2011. Controlled stereoselective polymerization of lactide monomers by group 4 metal initiators that contain an (OSSO)-type tetradentate bis(phenolate) ligand. **Polym. Chem.** 2:2378-2384.

Burness, J.H., L.T. Taylor and J.G. Dillard. 1976. The chemical effect of X-radiation on a tetradentate Schiff base ligand. ***J. Elect. Spec. Rel. Phen.*** 8(6):483-486.

Cabaj, J.E., D. Kairys and T.R. Benson. 2007. Development of a commercial process to produce oxandrolone. **Org. Process Res. Dev.** 11(3):378-388.

Copyright by Kasetsart University All rights reserved

Cameron, P.A., D. Jhurry, V.C. Gibson, A.J.P. White, D.J. Williams and S. Williams. 1999. Controlled polymerization of lactides at ambient temperature using [5-Cl-Salen]AlOMe. **Macromol. Rapid. Commun.** 20:616-618.

Chai, Z.Y., C. Zhang and Z.X. Wang. 2008. Synthesis, characterization, and catalysis in ε-caprolactone polymerization of aluminum and zinc complexes supported by *N*,*N*,*N*-chelate ligands. **Organometallics** 27(7):1626-1633.

Chamberlain, B. M., B. A. Jazdzewski, R. Pink, M. A. Hillmyer and W. B. Tolman. 2000. Controlled polymerization of *d*,*l*-lactide and ε-caprolactone by structurally well-defined alkoxo-bridged di- and triyttrium(III) complexes. **Macromolecules** 33(11):3970-3977.

Chamberlain, B.M., M. Cheng, D.R. Moore, T.M. Ovitt, E.B. Lobkovsky and G.W. Coates. 2001. Polymerization of lactide with zinc and magnesium β-diiminate complexes: Stereocontrol and mechanism. **J. Am. Chem. Soc.** 123(14):3229-3238.

Chang, J.C., Y.C. Chen, A. Datta, C.H. Lin, C.S. Hsiao and J.H. Huang. 2011. Synthesis and protonolysis of neutral aluminum dihydride compounds stabilized by tridentate-substituted pyrrolyl ligands: Synthesis, structural characterization and ring-opening polymerization of ε-caprolactone. **J. Organomet. Chem.** 696(23):3673-3680.

Chatterjee, C., M.H. Chisholm. 2011. The influence of the metal (Al, Cr, and Co) and the substituents of the porphyrin in controlling the reactions involved in the copolymerization of propylene oxide and carbon dioxide by porphyrin metal(III). **Inorg. Chem.** 50(10):4481-4492.

Che, C.-M. and S.-C. Chan. 2005. Organic light-emitting devices. ***U.S. Pat. Appl. Publ.*** US 20050244672 A1 20051103.

Chen, C.T., C.A. Huang, B.H. Huang. 2003. Aluminium metal complexes supported by amine bis-phenolate ligands as catalysts for ring-opening polymerization of ε-caprolactone. **Dalton Trans.** 19:3799-3803.

_____, _____, and _____. 2004. Aluminum complexes supported by tridentate aminophenoxide ligand as efficient catalysts for ring-opening polymerization of ε-caprolactone. **Macromolecules** 37(21):7968-7973.

Chen, H.-L., S. Dutta, P.-Y. Huang and C.-C. Lin. 2012. Preparation and characterization of aluminum alkoxides coordinated on salen-type ligands: highly stereoselective ring-opening polymerization of *rac*-lactide. **Organometallics** 31(5):2016-2025.

Copyright by Kasetsart University All rights reserved

Chen, H.-Y., H.-Y. Tang and C.-C. Lin. 2006. Ring-opening polymerization of lactides initiated by zinc alkoxides derived from *N*,*N*,*O*-tridentate ligands. **Macromolecules** 39 (11):3745-3752.

Chen, J.-M., W.-J. Ruan, L. Meng, F. Gao and Z.-A. Feng. 2008. Spectroscopic and theoretical studies on axial coordination of bis(pyrrol-2-ylmethyleneamine) phenyl complexes. **Spectrochim. Acta Mol. Biomol.** 71A(1):191-198.

Chen, T., Z. Qin, Y. Qi, T. Deng, X. Ge, J. Wang and X. Hou. 2011. Degradable polymers from ring-opening polymerization of α-angelica lactone, a five-membered unsaturated lactone. **Polym. Chem.** 2:1190-1194.

Chisholm, H.M. and K. Phomphrai. 2003. Conformational effects in *β*-diiminate ligated magnesium and zinc amides. Solution dynamics and lactide polymerization. **Inorg. Chim. Acta** 350:121-125.

_____. 2010. Concerning the ring-opening polymerization of lactide and cyclic esters by coordination metal catalysts. **Pure. Appl. Chem.** 82(8):1647-1662.

_____, S.S. Iyer, M.E. Matison, D.G. McCollum and M. Pagel. 1997. Concerning the stereochemistry of poly(lactide), PLA. Previous assignments are shown to be incorrect and a new assignment is proposed. **Chem. Commun**. 20:1999-2000

_____, J.C. Huffma and K. Phomphrai. 2001.Monomeric metal alkoxides and trialkyl siloxides:(BDI)Mg(O^{t}Bu)(THF) and (BDI)Zn(OSiPh$_3$)(THF). Comments on single site catalysts for ring-opening polymerization of lactides. **J. Chem. Soc., Dalton. Trans.** 3:222-224.

_____, J.C. Gallucci and K. Phomphrai. 2002. Coordination chemistry and reactivity of monomeric alkoxides and amides of magnesium and zinc supported by the diiminato ligand CH(CMeNC$_6$H$_3$-2,6-^{i}Pr$_2$)$_2$. A comparative study. **Inorg. Chem**. 41(10):2785-2794.

_____, _____, and K. Phomphrai. 2004. Well-defined calcium initiators for lactide polymerization. **Inorg. Chem.** 43(21):6717-6725.

_____, _____, K.T. Quisenberry and Z.P. Zhou. 2008. Complexities in the ring-opening polymerization of lactide by chiral Salen aluminum initiators. **Inorg. Chem.** 47(7):2613-2624.

Chmura, A. J., C. J. Chuck, M. G. Davidson, M. D. Jones, M. D. Lunn, S. D. Bull and M. F. Mahon. 2007. A germanium alkoxide supported by a C$_3$-symmetric ligand for the stereoselective synthesis of highly heterotactic polylactide under solvent-free conditions. **Angew. Chem. Int. Ed.** 46(13):2280-2283.

Copyright by Kasetsart University All rights reserved

Chmura, A. J., M.G. Davidson, C.J. Frankis, M.D. Jones and M.D. Lunn . 2008. Highly active and stereoselective zirconium and hafnium alkoxide initiators for solvent-free ring-opening polymerization of *rac*-lactide. **Chem. Commun**. 11:1293-1295.

Chuang, H.J., Y.C. Su and B.T. Ko. 2012. Synthesis and structural characterization of aluminum complexes supported by *N*,*N*,*O*-tridentate ketiminate ligands: Efficient catalysts for ring-opening polymerization of *l*-lactide. **Inorg**. **Chem. Commun.** 18:38-42.

Clarke, R.E. and J.H. Weber. 1968. Complexes of pyrrole-derivative ligands. II. Copper(II) complexes with tetradentate ligands. **J. Inorg. Nucl. Chem.** 30(7):1837-1845.

Coulembier, O., P. Degée, J.L. Hedrick and P. Dubois. 2006. From controlled ring-opening polymerization to biodegradable aliphatic polyester: Especially poly(*β*-malic acid) derivatives. **Prog. Polym. Sci.** 31(8):723-743.

Cross, E., D. Edward, L.E.N. Allan, A. Decken and M.P. Shaver. 2013. Aluminum Salen and Salan complexes in the ring-opening polymerization of cyclic esters: Controlled immortal and copolymerization of *rac*-*β*-butyrolactone and *rac*-lactide. **J. Polym. Sci., Part A:Polym. Chem.** 51(5):1137-1146.

Csihony, S., T.T. Beaudette, A.C. Sentman, G.W. Nyce, R.M. Waymouth and J.L. Hedrick. 2004. Bredereck's reagent revisited: latent anionic ring-opening polymerization and transesterification reactions. **Adv. Synth. Catal.** 346(9-10):1081-1086.

D'Auria, I., M. Lamberti, M. Mazzeo, S. Milione, G. Roviello and C. Pellecchia. 2012. Coordination chemistry and reactivity of zinc complexes supported by a phosphido pincer ligand. **Chem. Eur. J.** 18(8):2349-2360.

Darensbourg D.J. and O. Karroonnirun. 2010. Ring-opening polymerization of *L*-lactide and *ε*-caprolactone utilizing biocompatible zinc catalysts. Random copolymerization of *L*-lactide and *ε*-caprolactone. **Macromolecules** 43(21):8880-8886.

_____, P. Gangul and D. Billodeaux. 2005. Ring-opening polymerization of trimethylene carbonate using aluminum(III) and tin(IV) Salen chloride catalysts. **Macromolecules** 38(13):5406-5410.

_____, W. Choi , O. Karroonnirun and N. Bhuvanesh. 2008. Ring-opening polymerization of cyclic monomers by complexes derived from biocompatible metals. production of poly(lactide), poly(trimethylene carbonate), and their copolymers. **Macromolecules**. 41 (10):3493-3502.

Copyright by Kasetsart University All rights reserved

Datta, A., N.K. Karan, S. Mitra and V. Gramlich. 2003. Synthesis and structural characterization of a (*N*,*N*'-bis[2-(*S*)-pyrrolidylmethyl]-propane-1,3-diamine) nickel(II) complex. **J. Chem. Cryst.** 33(7):579-583.

Dechy-Cabaret, O., B. Martin-Vaca and D. Bourissou. 2004. Controlled ring-opening polymerization of lactide and glycolide. **Chem. Rev.** 104(12):6147-6176.

Dell'Erba, R., G. Groeninckx, G. Maglio, M. Malinconico and A. Migliozzi. 2001. Immiscible polymer blends of semicrystalline biocompatible components:thermal properties and phase morphology analysis of PLLA/PCL blends. **Polymer** 42(18):7831-7840.

Dezelic, M. and G. Dolibic. 1957. Azomethine derivatives of pyrrole-2-aldehyde. **Bull. soc. chimistes rep. populaire Bosnie et Herzegovine.** 6:11-16.

Dillard, J.G. and L.T. Taylor. 1974. X-ray photoelectron spectroscopic study of Schiff base metal complexes. ***J. Elect. Spec. Rel. Phen.*** 3(6):455-60.

Djebbar-Sid, S., O. Benali-Baitich and J.P. Deloume.. 1997. Synthesis, characterization and electrochemical behavior of some copper(II) complexes with linear and tripodal tetradentate ligands derived from Schiff bases. **Polyhedron** 16(13):2175-2182.

Doi, Y. and A. Steinbuchel. 2002. Biopolymers – Polyester. I. Biological systems and biotechnological production. **Wiley-VCH**, Weinheim.

Douglas, A.F., B.O. Patrick and P. Mehrkhodavandi. 2008. A highly active chiral indium catalyst for living lactide polymerization. **Angew. Chem. Int. Ed.** 47(12):2290-2293.

Dove, A.P., V.C. Gibson, E.L. Marshall, H.S. Rzepa, A.J.P. White and D.J. Williams. 2006. Synthetic, structural, mechanistic, and computational studies on single-site *β*-diketiminate tin(II) initiators for the polymerization of *rac*-lactide. **J. Am. Chem. Soc.** 128(30):9834-3843.

Du, H.Z., A. H. Velders, P.J. Dijkstra, Z. Y. Zhong, X.S. Chen and F. Jan. 2009. Polymerization of lactide using achiral bis(pyrrolidene) Schiff base aluminum complexes. **Macromolecules** 42(4):1058-1066.

_____, X. Pang, H.Y. Yu, X.L. Zhuang, X.S. Chen, D.M. Cui, X.H. Wang and X.B. Jing. 2007. Polymerization of *rac*-lactide using Schiff base aluminum catalysts: structure, activity, and stereoselectivity. **Macromolecules** 40(6):1904-1913.

Copyright by Kasetsart University All rights reserved

Dubis, P., C. Jacobs , R. Jerome , P. Teyssie. 1991, Macromolecular engineering of polylactones and polylactides. 4. Mechanism and kinetics of lactide homopolymerization by aluminum isopropoxide **Macromolecules** 24(9):2266-2270.

Duda A. and A. Kowalski. 2009. Chapter 1. Thermodynamic and kinetics of ring-opening polymerization. pp. 1-51. In P. Dubois, O. Coulembier and J.-M. Raquez, eds. Handbook of ring-opening polymerization. **Wiley-VCH**, Weinheim.

_____. 1996. Polymerization of ε-caprolactone initiated by aluminum isopropoxide carried out in the presence of alcohols and diols. Kinetics and mechanism. **Macromolecules** 29(5):1399-1406.

_____. and S. Penczek. 1994, Kinetics of polymerization involving reversible deactivation due to aggregation of active centers. Analytical vs. numerical solution for the ε-caprolactone/dialkylaluminium alkoxide system. **Macromol. Rapid Commun.** 15(7):559-566.

Emig, N., H. Nguyen, H. Krautscheid, R. Reau, J.B. Cazaux and G. Bertrand. 1998. Neutral and cationic tetracoordinated aluminum complexes featuring tridentate nitrogen donors: Synthesis, structure, and catalytic activity for the ring-opening polymerization of propylene oxide and (*d*,*l*)-lactide. **Organometallics** 17(16):3599-3608.

Endo, M., T. Aida and S. Inoue. 1987. Immortal polymerization of ε-caprolactone initiated by aluminum porphyrin in the presence of alcohol. **Macromolecules**. 20(12):2982-2988.

Franceschi, F.G., E. Solari, C. Floriani, N. Re, H. Birkedal and P. Pattison. 2001. Reduction of dioxygen by a dimanganese unit bonded inside a cavity provided by a pyrrole-based dinucleating ligand. ***Chem.-Eur. J.*** 7(7):1468-1478.

Gamze, Y. and A. Kayan. 2012. Synthesis and characterization of Zr, Ti, Al-phthalate and pyridine-2-carboxylate compounds and their use in ring opening polymerization. **Appl. Catal. A-Gen.** 433:223-228.

Ganjali, M.R., A. Ghesmi, M. Hosseini, M.R. Pourjavid, M. Rezapour, M. Shamsipur and M. Salavati-Niasari. 2005. Novel terbium(III) sensor based on a new bis-pyrrolidene Schiff's base. **Sens. Act. B-Chem.** 105(2):334-339.

_____, J. Ravanshad, M. Hosseini, M. Salavati-Niasari, M. R. Pourjavid and M. R. Baezzat. 2004. Novel Dy(III) sensor based on a new bis-1H-pyrrol-2-ylmethylene Schiff's base. **Electroanalysis.** 16(21):1771-1776.

Copyright by Kasetsart University All rights reserved

Ge, H., Y. Hu, S. Yang, X. Jiang and C. Yang. 2000. Preparation, characterization, and drug release behaviors of drug-loaded *ε*-caprolactone/*L*-lactide copolymer nanoparticles. **J. Appl. Polym. Sci.** 75(7):874-882.

Giacomelli, A., T. Rotunno, L. Senatore and R. Settambolo. 1989. Spectrophoto metric study of the equilibria between nickel(II) Schiff base complexes and ammonium-like cations or sodium tetraphenylborate. **Inorg. Chem.** 28(18):3552-3555.

Gibson, V.C., P. Hormnirun and E.L. Marshall. 2004. Remarkable stereocontrol in the polymerization of *racemic* lactide using aluminum initiators supported by tetradentate aminophenoxide ligands. **Polym. Prepr. (Am. Chem. Soc., Div. Polym. Chem.)** 45(2):474-475.

Glasner, H. and E.Y. Tshuva. 2014. C_1-symmetrical titanium(IV) complexes of Salan ligands with differently substituted aromatic rings: enhanced cytotoxic activity. **Inorg. Chem.** 53(6):3170-3176.

Gong, S. and H. Ma. 2008. *β*-Diketiminate aluminium complexes: Synthesis, characterization and ring-opening polymerization of cyclic esters. **Dalton Trans.** (25):3345-3357.

Grigoras, M., G. Stoica, I. Cianga and C.I. Simionescu. 1997. Synthesis and characterization of some pyrrole-based aldimine monomers. ***Rev. Roum. Chim.*** 42(10):993-998.

Gross, R.A. and B. Kalra. 2002. Biodegradable polymers for the environment. **Science** 297(5582):803-807.

Gupta, A.P. and V. Kumar. 2007. New emerging trends in synthetic biodegradable polymers - polylactide:A critique. **Eur. Polym. J.** 43(10):4053-4074.

Gupta, V.K., R.N. Goyal and R.A. Sharma. 2009. Comparative studies of neodymium(III)-selective PVC membrane sensors. **Anal. Chim. Acta.** 647(1):66-71.

Han, X.-Y., Y.-H. Li, H. Wei and Y. Zhang. 2007. Ligand bridged and bis-ligand coordinated titanium complexes: Synthesis, structure and relevance to phenylacetylene hydroanilination catalysis. **Chinese J. Chem.** 25(9):1334-1339.

Haruo, N., Y.Y. Fan, M. Tomokazu, O. Naoko, S. Yoshihito and E. Takeshi. 2005. Feedstock recycling of flame-resisting poly(lactic acid)/aluminum hydroxide composite to *l,l*-lactide. **Ind. Eng. Chem. Res.** 44(5):1433-14.

Copyright by Kasetsart University All rights reserved

Hedrick, J.L., T. Magbitang, E.F. Connor, T. Glauser, W. Volksen, C.J Hawker, V.Y. Lee and R.D. Miller. 2002. Application of complex macromolecular architectures for advanced microelectronic materials. **Chem. Eur. J.** 8(13): 3308-3319.

Hild. F., L. Brelot and S. Dagorne 2011. Novel *N,O,N*-supported tetracoordinate aluminum complexes for the highly controlled and immortal ROP of trimethylene carbonate (TMC) under mild conditions: Access to narrowly disperse poly-tmc and derived copolymers. **Organometallics** 30(20):5457-5462.

Hinshaw, C.J., G. Peng , R. Singh , J.T. Spence , J.H. Enemark, M. Bruck , J. Kristofzski, S.L. Merbs , R.B. Ortega and P.A. Wexler. 1989. Molybdenum(VI)-dioxo complexes with linear and tripodal tetradentate ligands: models for the molybdenum(VI/V) centers of the molybdenum hydroxylases and related enzymes. 1. Syntheses and structures. **Inorg. Chem.** 28(25):4483-4491.

Hofman, A., R. Szymański, S. Słomkowski and S. Penczek. 1984. Structure of active species in the cationic polymerization of *β*-propiolactone and *ε*-caprolactone. **Die Makromol. Chem.** 185(4):655-667.

Holland, J.P., P.J. Barnard, S.R. Bayly, J.R. Simon and J.C. Green. 2009. Electronic absorption spectroscopy and time-dependent density functional theory calculations on the nickel(II) complex of 1,4-bis(pyrrol-2-ylmethyleneamino) butane. **Inorg. Chim. Acta.** 362(2):402-406.

Hormnirun P., E.L. Marshall, V.C. Gibson, R.I. Pugh and A.J.P. White. 2006. Study of ligand substituent effects on the rate and stereoselectivity of lactide polymerization using aluminum Salen-type initiators. **PNAS**. 103(42):15343-15348.

_____, _____, _____, A.J.P. White and D.J. Williams. 2004. Remarkable stereocontrol in the polymerization of *racemic* lactide using aluminum initiators supported by tetradentate aminophenoxide ligands. **J. Am. Chem. Soc.** 126(9):2688-2689.

Huang, C.-H., F.-C. Wang, B.-T. Ko, T.-L. Yu and C.-C. Lin. 2001. Ring-opening polymerization of *ε*-caprolactone and *l*-lactide using aluminum thiolates as initiator. **Macromolecules** 34(3):356-361.

Ikada, Y. and H. Tsuji. 2000. Biodegradable polyesters for medical and ecological applications. **Macromol. Rapid Commun.** 21(3):117-132.

Immel, T.A., U. Groth and T. Huhn. 2010. Cytotoxic titanium Salan complexes: Surprising interaction of Salan and alkoxy ligands. **Chem. Eur. J.** 16(9):2775-2789, S2775/1-S2775/35.

Copyright by Kasetsart University All rights reserved

Iroh, J.O. 1996, Poly(ε-caprolactone). Polymer data handbook, ed. Mark, J.E., **Oxford University Press**, New York:316-317.

Iwasa, N., J. Liu and K. Nomura. 2008. Notable effect of imino substituent for the efficient ring-opening polymerization of ε-caprolactone initiated by Al complexes containing phenoxy-imine ligand of type, $Me_2Al(L)$ [L:O-2-^{t}Bu-6-(RN=CH)C_6H_3; R:2,6-$^{i}Pr_2C_6H_3$, ^{t}Bu, adamantyl, C_6F_5]. **Catal. Commun.** 9(6):1148-1152.

_____, _____, and _____. 2008. Ring-opening polymerization of various cyclic esters by Al complex catalysts containing a series of phenoxy-imine ligands: Effect of the imino substituents for the catalytic activity. **J. Mol. Catal. A - Chemical.** 292(1-2):67-75.

Jacobs, C., P. Dubois, R. Jerome and P. Teyssie. 1991. Macromolecular engineering of polylactones and polylactides. 5. Synthesis and characterization of diblock copolymers based on poly-ε-caprolactone and poly(*L*,*L* or *D*,*L*)lactide by aluminum alkoxides. **Macromolecules** 24(11):3027-3034.

Jenkins, M.J., K.L. Harrison, M.M.C.G. Silva, M.J. Whitaker, K.M. Shakesheff and S.M. Howdle. 2006. Characterisation of microcellular foams produced from semi-crystalline PCL using supercritical carbon dioxide. **Eur. Polym. J.** 41(11):3145-3151.

Jensen, T.R., L.E. Breyfogle, M.A. Hillmyer and W.B. Tolman. 2004. Stereoelective polymerization of *D*,*L*-lactide using *N*-heterocyclic carbene based compounds. **Chem. Commun**. 21:2504-2505.

Jérôme, C. and P. Lecomte. 2008. Recent advances in the synthesis of aliphatic polyesters by ring-opening polymerization. **Adv. Drug Deliv. Rev.** 60(9-10):1056-1076.

Jhurry, D., A. Bhaw-Luximon and N. Spassky. 2001, Synthesis of polylactides by new aluminium Schiff base complexes. **Macromol. Symp.** 175(1):67-.80

Jianminga, R., X. Anguob, W. Hongweia and Y. Hailina. 2014. Review-recent development of ring-opening polymerization of cyclic esters using aluminum complexes. **Des. Monomers Polym**. 17(4):345-355.

John, R.D., J. Jay, M.K. Daniel, B.H. Sukhendu, R.L. Bradford and H.H. Matthew. 2005. Fundamental solution and single-chain properties of polylactides. **J. Polym. Sci., Part B:Polym. Phys.** 43(21):3100-3111.

Jones, R.A., G. Quintanilla-Lopez, S. A. N. Taheri, M. M. Hania, O. Ozturk and H. Zuilhof. 2000. Pyrrole studies. Part 47. ^{13}C NMR spectroscopic characterization of the products of the reaction of formylpyrroles with aniline and diaminobenzenes. **ARKIVOC [online computer file]** 1(3):382-392.

Copyright by Kasetsart University All rights reserved

Jones, R.A., G. Quintanilla-Lopez, O. Ozturk, S.A.N. Taheri, G.B. Karatepe and R.O. Jones. 2001. Pyrrole studies, Part 48. 1 ^{13}C NMR characterization of imines and related compounds derived from pyrrole-2-carboxaldehydes and pyrrole-2,5-dicarboxyaldehydes. ***J. Chem. Res. Synop.*** 8:309-310.

Kamber, N.E., W. Jeong, R.M. Waymouth, R.C. Pratt, B.G.G. Lohmeijer and J.L. Hedrick. 2007. Organocatalytic ring-opening polymerization. **Chem. Rev.** 107(12):5813-5840.

Kasperczyk, J.E. 1995. Microstructure analysis of poly(lactic acid) obtained by lithium *tert*-butoxide as initiator. **Macromolecules** 28(11):2937-3939.

_____. 1996. Microstructural analysis of poly[(*l*,*l*-lactide)-co-(glycolide)] by ^{1}H and ^{13}C NMR spectroscopy. **Polymer** 37(2):201-203.

_____. 2001. NMR investigation of biodegradable polyesters for medical applications. **Macromol. Symp**. 175(1):19-31.

_____, and M. Bero. 1991. Coordination polymerization of lactides. 2. Microstructure determination of poly[(*L*,*L*-lactide)-co-(ε-caprolactone)] with ^{13}C nuclear magnetic resonance spectroscopy. **Macromol. Chem. Phys.** 192(8):1777-1787.

_____, and _____. 1993. Coordination polymerization of lactides. 4. The role of transesterification in the copolymerization of *L*,*L*-lactide and ε-caprolactone. **Macromol. Chem. Phys.** 194(3):913-925.

_____, and _____. 2000. Stereoselective polymerization of *racemic d*,*l*-lactide in the presence of butyllithium and butylmagnesium. Structural investigations of the polymers. **Polymer** 41(1):391-395.

Kathleen, M.S. and A.H. Marc. 2004. Controlled polymerization of α-methyl-β-pentyl-β-propiolactone by a discrete zinc alkoxide complex. **Tetrahedron** 60(34):7177-7185.

Kim, E., E.W. Shin, I.-K. Yoo and J.S. Chung. 2009. Characteristics of heterogeneous titanium alkoxide catalysts for ring-opening polymerization of lactide to produce polylactide. **J. Mol. Catal. A:Chem.** 298(1-2):36-39.

Knani, D., A.L. Gutman and D.H. Kohn. 1993. Enzymatic polyesterification in organic media. Enzyme-catalyzed synthesis of linear polyesters. I. Condensation polymerization of linear hydroxyesters. II. Ring-opening polymerization of ε-caprolactone. **J. Polym. Sci., Part A:Poly. Chem.** 31(5):1221-1232.

Copyright by Kasetsart University All rights reserved

Ko, B.T. and C.-C. Lin. 2001. Synthesis, characterization, and catalysis of mixed-ligand lithium aggregates, excellent initiators for the ring-opening polymerization of *L*-lactide. **J. Am. Chem. Soc.** 123(33):7973-7977.

Koller J. and R.G. Bergman. 2011. Highly efficient aluminum-catalyzed ring-opening polymerization of cyclic carbonates, lactones, and lactides, including a unique crystallographic snapshot of an intermediate. **Organometallics** 30 (11):3217-3224.

Konno, T., K. Tokuda, J. Sakurai and K.-I. Okamoto. 2000. Five-coordinate geometry of cadmium(ii) with octahedral bidentate-S,S complex-ligand cis(*S*)-$[Co(aet)_2(en)]^+$ (aet = 2-aminoethanethiolate): Synthesis, crystal structures and interconversion of S-bridged Co(III) Cd(II) polynuclear complexes. **Bull. Chem. Soc. Jpn.** 73(12):2767-2773.

Kowalski, A., A. Duda and S. Penczek. 1998. Polymerization of *L*,*L*-lactide initiated by aluminum isopropoxide trimer or tetramer. **Macromolecules** 31(7):2114-2122.

_____, J. Libiszowski , A. Duda and S. Penczek. 2000. Polymerization of *l*,*l*-dilactide initiated by tin(II) butoxide. **Macromolecules** 33 (6):1964-1971.

Kricheldorf, H.R., J.M. Jonté and R. Dunsing. 1986. Polylactones. 7. The mechanism of cationic polymerization of *β*-propiolactone and *ε*-caprolactone. **Die Makromol. Chem.** 187(4):771-785.

_____, and R. Dunsing. 1986. Polylactones. 8. Mechanism of the cationic polymerization of *L*,*L*-dilactide. **Die Makromol. Chem**. 187(7):1611-1625.

_____, R. Dunsing and A. Serra. 1987. Polylactones. 10. Cationic polymerization of *δ*-valerolactone by means of alkylating reagents. **Macromolecules** 20(9):2050-2057.

_____, and I. Kreiser. 1987. Polylactones. 11. Cationic copolymerization of glycolide with *L*,*L*-dilactide. **Die Makromol. Chem.** 188(8):1861-1873.

_____, M. Berl and N. Scharnagl. 1988. Poly(lactones). 9. Polymerization mechanism of metal alkoxide initiated polymerizations of lactide and various lactones. **Macromolecules** 21(2):286-293.

_____, and I.K. Saunders. 1990. Polylactones. 19. Anionic polymerization of *L*-lactide in solution. **Makromol Chem.** 191(5):1057-1066.

_____, and S. Eggerstedt. 1997. Polylactones. 41. Polymerizations of *β-d*,*l*-butyrolactone with dialkyltinoxides as initiators. **Macromolecules** 30(19):5693-5697.

Copyright by Kasetsart University All rights reserved

Kricheldorf, H.R., and D. Langanke. 2002. Polylactones. 54. Ring-opening and ring-expansion polymerizations of ε-caprolactone initiated by germanium alkoxides. **Polyme**r 43(6):1973-1977.

_____, and S. Rost. 2005. Biodegradable multiblock copolyesters prepared from ε-caprolactone, *l*-lactide, and trimethylene carbonate by means of bismuth hexanoate. **Macromolecules** 38 (20):8220-8226.

Lamberti, M., I.D'Auria, M. Mazzeo, S. Milione, V. Bertolasi and D. Pappalardo. 2012. Phenoxy-thioether aluminum complexes as ε-caprolactone and lactide polymerization catalysts. **Organometallics** 31(15):5551-5560.

Le Borgne, A., V. Vincens, M. Jouglard and N. Spassky. 1993, Ring-opening oligomerization reactions using aluminium complexes of schiff's bases as initiators. **Makromol. Chem., Macromol. Symp.** 73(1):37-46.

Li C.Y., C.Y. Tsai, C.H. Lin and B.T. Ko. 2011.Synthesis, structural characterization and reactivity of aluminium complexes supported by benzotriazole phenoxide ligands:air-stable alumoxane as an efficient catalyst for ring-opening polymerization of *L*-lactide. **Dalton Trans.** 40:1880-1887.

Li, W.,Y. Wang, L. Yang, A. Szeghalmi, Y. Ye, J. Ma, M. Luo, J.-M. Hu and W. Kiefer. 2007. Spectroscopic and computational studies on self-assembly complexes of bis(pyrrol-2-ylmethyleneamine) ligands linked by alkyl spacers with Cu(II). ***J. Raman. Spec.*** 38(5):483-495.

Lian B., H. Ma, T. P. Spaniol and J. Okuda. 2009. Neutral and cationic aluminium complexes containing a chiral (OSSO)-type bis(phenolato) ligand:synthesis, structures and polymerization activity. **Dalton Trans**.:9033-9042.

Ling, J., J. Shen and T.E. Hogen-Esch. 2009. A density functional theory study of the mechanisms of scandium-alkoxide initiated coordination-insertion ring-opening polymerization of cyclic esters. **Polymer** 50(15):3575-3581.

Liu, B., H. Li, C.-S. Ha, I. Kim and W. Yan. 2008. *β*-ketoamino complexes: Steric and electronic effect of 3-position substituents of the ligands. **Macromol. Res.** 16(5):441-445.

Liu, J., N. Iwasa and K. Nomura. 2008. Synthesis of Al complexes containing phenoxy-imine ligands and their use as the catalyst precursors for efficient living ring-opening polymerisation of ε-caprolactone. **Dalton Trans.** 30:3978-3988.

Liu, X. and D. Cui. 2008. O_2 activation and hydrolysis of Salan rare-earth metal alkyl complexes. **Dalton. Trans**. (28):3747-3752.

Copyright by Kasetsart University All rights reserved

Liu, X., X. Shang, T. Tang, N. Hu, F. Pei, D. Cui, X. Chen and X. Jing. 2007. Achiral lanthanide alkyl complexes bearing *N*,*O* multidentate ligands. Synthesis and catalysis of highly heteroselective ring-opening polymerization of *rac*-lactide. **Organometallics** 26(10):2747-2757.

Liu, Z., W. Gao, J. Zhang, D. Cui, Q. Wu and Y. Mu. 2010. Bis(imino)aryl NCN Pincer aluminum and zinc complexes: Synthesis, characterization, and catalysis on *L*-lactide polymerization. **Organometallics** 29(22):5783-5790.

Lou, X., C. Detrembleur and R. Jérôme. 2003. Novel aliphatic polyesters based on functional cyclic (di)esters. **Macromol. Rapid. Comm.** 24(2):161-1.

Lupton, J.R. 2004. Microbial degradation products influence colon cancer risk: The butyrate controversy. **J. Nutr.** 134(2):479-482.

Ma, H, G. Melillo, L. Oliva, T.P. Spaniol, U. Englert and J. Okuda 2005. Aluminium alkyl complexes supported by [OSSO] type bisphenolato ligands: Synthesis, characterization and living polymerization of *rac*-lactide. **Dalton Trans.** 4:721-727.

_____, T.P. Spaniol and J. Okuda. 2006. Highly heteroselective ring-opening polymerization of *rac*-lactide initiated by bis(phenolato)scandium complexes. **Angew. Chem. Int. Ed.** 45(46):7818-7821.

Ma, W.-A. and Z.-X. Wang. 2011. Zinc and aluminum complexes supported by quinoline-based *N*,*N*,*N*-chelate ligands: Synthesis, characterization, and catalysis in the ring-opening polymerization of ε-caprolactone and *rac*-lactide. **Organometallics** 30(16): 4364-4373.

_____, and Z.-X.Wang. 2011. Synthesis and characterisation of aluminium(III) and tin(II) complexes bearing quinoline-based *N*,*N*,*O*-tridentate ligands and their catalysis in the ring-opening polymerisation of ε-caprolactone. **Dalton Trans.** 40(8):1778-1786.

Malcolm, H.C., J.C. Gallucci and C. Krempner. 2007. Ring-opening polymerization of *l*-lactide by organotin(IV)alkoxides, $R_2Sn(O^iPr)_2$: Estimation of the activation parameters Original. **Polyhedron** 26(15):4436-4444.

Male, N. A.H., M. Thornton-Pett and M. Bochmann. 1997. Synthesis and structure of zirconium(IV) alkyl complexes with bi-, tri-, tetra- and penta-dentate amido ligands. ***J.Chem. Soc., Dalton Trans.:Inorg. Chem.*** (14):2487-2494.

Malgorzata P., D. Piotr, K. Bozena, K. Janusz and S. Anna. 2011. The polymerization mechanism of lactide initiated with zinc (II) acetylacetonate monohydrate. **Polymer** 52(23):5255-5261.

Copyright by Kasetsart University All rights reserved

Marshall, E.L., V.C. Gibson and H.S. Rzepa. 2005. A computational analysis of the ring-opening polymerization of *rac*-lactide initiated by single-site *β*-diketiminate metal complexes: Defining the mechanistic pathway and the origin of stereocontrol. **J. Am. Chem. Soc.** 127(16):6048-6051.

Matsubara, K., C. Terata, H. Sekine, K. Yamatani, T. Harada, K. Eda, M. Dan, Y. Koga and M. Yasuniwa. 2012. Stereoselective ring-opening polymerization of *D,L*-Lactide, initiated by aluminum isopropoxides bearing tridentate nonchiral schiff-base ligands. **J. Polym. Sci. A Polym. Chem.** 50(5):957-966.

Matsukawa, N. 2000. Preparation and property of olefin polymerization catalysts. **Eur. Pat. Appl.** 72.

Matsuo, Y., H. Tsurugi, T. Yamagata, K. Tani and K. Mashima. 2003. Synthesis and structural characterization of 2,5-bis(*N*-aryliminomethyl)pyrrolyl complexes of aluminum. **Bull. Chem. Soc. Jpn.** 76(10):1965-1968.

Mayilmurugan, R., B.N. Harum, M. Volpe, A.F. Sax, M. Palaniandavar and N.C. Moesch-Zanetti. 2011. Mechanistic insight into the reactivity of oxotransferases by novel asymmetric dioxomolybdenum(VI) model complexes. **Chem. Eur. J.** 17(2):704-713, S704/1-S704/6.

McCleverty, J. A. and C. J. Jones. 1971. Transition-metal Schiff base complexes. III. Nickel complexes derive derived from pyrrole-2-carboxaldehyde and aliphatic and aromatic diamines. ***J. Chem. Soc., A, Inorg., Phys., Theorel.*** (8):1052-1060.

Mecking, S. 2004. Nature or Petrochemistry? - Biologically gegradable materials. **Angrew. Chem., Int. Ed.** 43(9):1078-1085.

Meghdadi, S., M. Amirnasr, K. Mereiter, H. Molaee and A. Hajar. 2011. Synthesis, structure and electrochemistry of Co(III) complexes with an unsymmetrical Schiff base ligand derived from 2-aminobenzylamine and pyrrole-2-carboxaldehyde. **Polyhedron** 30(10):1651-1656.

Meretoja W, A.O. Helminen , J.J. Korventausta , V. Haapa-aho, J.V. Seppälä and T. O. Närhi. 2006. Crosslinked poly(*ε*-caprolactone/*D,L*-lactide)/bioactive glass composite scaffolds for bone tissue engineering. **J. Biomed. Mater. Res. A.** 77(2):261-218.

Milione, S., G. Milano, and L. Cavallo. 2012. Pentacoordinated organoaluminum complexes: A computational insight. 31(24):8498-8504.

Minami, M. and S. Kozaki. 2003. Method for producing aliphatic polyester. **US patent** :2003/0023026 A1.

Copyright by Kasetsart University All rights reserved

Mingotaud, A.-F., F. Dargelas and F. Cansell. 2000. Cationic and anionic ring-opening polymerization in supercritical CO_2. **Macromol. Symp.** 153:77-86.

Mohamadou, A. and P.J. Barbier. 1990. Copper(II) and cobalt(III) complexes with tetradentate diimine pyrrole derivatives. ***Inorg. Chim. Acta*** 169(1):17-18.

Mohammed, I. and J.B. Robert. 2012. Fluorous catalyst recycling utilising highly fluorinated zinc compounds: Ring opening polymerisation of ε-caprolactone. **J. Fluorine Chem.** 139:58-62.

Möller, M., R. Kånge and J.L. Hedrick. 2000. Sn(OTf)2 and $Sc(OTf)_3$: Efficient and versatile catalysts for the controlled polymerization of lactones. **J. Polym. Sci:A. Polym. Chem.** 38(11):2067-2074.

Montaudo, G., M.S. Montaudo, C. Puglisi, F. Samperi and N. Spassky. 1996. Evidence for ester-exchange reactions and cyclic oligomer formation in the ring-opening polymerization of lactide with aluminum complex initiators. **Macromolecules** 29(20):6461-6465.

Mu, J.-S., X.-C. Shi and Y.-S. Li. 2011. Ethylene homopolymerization and copolymerization by vanadium(III) complexes containing tridentate or tetradentate iminopyrrolyl ligands. **J. Polym. Sci., Part A: Polym. Chem.** 49(12):2700-2708.

Mueller-Westerhoff, U. T. and G. F. Swiegers. 1994. Azines and imines of 4-*tert*-butyl-1H-pyrrole-2-carboxaldehyde and 5-*tert*-butyl-1H-pyrrole-2-carboxalde hyde. A useful synthesis of the aldehydes. **Synth. Comm.** 24(10): 1389-1393.

Munoz-Hernandez, M.-A., T.S. Keizer, P. Wei, S. Parkin, and D.A. Atwood. 2001. Reactivity and derivatization of five-coordinate, chelated aluminum. **Inorg. Chem.** 40(26):6782-6787.

Munro, O.Q. and G. L. Camp. 2003. Self-recognition in a flexible bis(pyrrole) Schiff base derivative: Formation of a one-dimensional hydrogen-bonded polymer. **Acta Crystallogr. Sect. C-Cryst. Struct. Commun.** C. 59(12): o672-o675.

_____, K. J. Akerman, and P. Akerman. 2011. Synthesis of bis(pyrrolide-imine) and bis(imidazolato-imine) gold(III) Schiff base complexes for the treatment of cancer. ***PCT Int. Appl.*** :WO 2011158176 A2 20111222.

_____, S.D. Joubert and C.D. Grimmer. 2006. Molecular recognition:preorganization of a bis(pyrrole) Schiff base derivative for tight dimerization by hydrogen bonding. **Chem. Eur. J.** 12(31):7987-7999.

Copyright by Kasetsart University All rights reserved

Na, Y.H., Y. He, X. Shuai, Y. Kikkawa, Y. Doi and Y. Inoue. 2002. Compatibilization effect of poly(ε-caprolactone)-*b*-poly(ethyleneglycol) block copolymers and phase morphology analysis in immiscible poly(lactide)/poly (ε-caprolactone) blends. **Biomacromolecules** 3(6):1179-1186.

Nomura, N., R. Ishii, M. Akakura and K. Aoi. 2002. Stereoselective ring-opening polymerization of racemic lactide using aluminum-achiral ligand complexes: Exploration of a chain-end control mechanism. **J. Am. Chem. Soc.** 124(21):5938-5939.

_____, _____, Y. Yamamoto and T. Kondo. 2007. Stereoselective ring-opening polymerization of a *racemic* lactide by using achiral Salen- and HomoSalen-aluminum complexes. **Chem. Eur. J**. 13(16):4433-4451.

_____, A. Akita, R. Ishii and M. Mizuno. 2010. Random copolymerization of ε-caprolactone with lactide using a HomoSalen-Al complex. **J. Am. Chem. Soc**. 132 (6):1750-1751.

_____, T. Aoyama, R. Ishii and T. Kondo. 2005. Salicylaldimine−aluminum complexes for the facile and efficient ring-opening polymerization of ε-caprolactone. **Macromolecules** 38 (13):5363-5366.

O'Keefe, B.J., M.A. Hillmyer and W. B. J. Tolman. 2001. Polymerization of lactide and related cyclic esters by discrete metal complexes. **Chem. Soc., Dalton Trans.** :2215-2224.

Ong, C.J. and F.P. Price. 1978. Blends of poly(ε-caprolactone) with poly(vinyl chloride). I. Morphology. **J. Polym. Sci., Polym. Symp.** 63(1):45-58.

Ouhadi, T., A. Hamitou, R. Jérôme, P. Tessié. 1976. Soluble bimetallic μ-oxo-alkoxides. 8. Structure and kinetic behavior of the catalytic species in unsubstituted lactone ring-opening polymerization. **Macromolecules** 9(6):927-931.

Ovitt, T.M. and G.W. Coates. 1999. Stereoselective ring-opening polymerization of *meso*-lactide: Synthesis of syndiotactic poly(lactic acid). **J. Am. Chem. Soc.** 121(16):4072-4073.

_____, and _____. 2000. Stereoselective ring-opening polymerization of *rac*-lactide with a single-site, *racemic* aluminum alkoxide catalyst: Synthesis of stereoblock poly(lactic acid). **J. Polym. Sci., Part A.:Polym. Chem.** 38(S1):4686-4692.

_____, and _____. 2002, Stereochemistry of lactide polymerization with chiral catalysts:new opportunities for stereocontrol using polymer exchange mechanisms. **J. Am. Chem. Soc.** 124(7):1316-1326.

Copyright by Kasetsart University All rights reserved

Palard, I., M. Schappacher, B. Belloncle, A. Soum and S.M. Guillaume. 2007, Unprecedented polymerization of trimethylene carbonate initiated by a samarium borohydride complex: Mechanistic insights and copolymerization with ε-caprolactone. **Chem. Eur. J.** 13(5):1511-1521.

Pang, X., X. Chen, H. Du, X. Wang and X. Jing. 2007. Enolic Schiff-base aluminum complexes and their application in lactide polymerization. **J. Organomet. Chem.** 692(25):5605-5613.

Pappalardo, D., L. Annunziata and C. Pellecchia. 2009. Living ring-opening homo- and copolymerization of ε-caprolactone and *l*- and *d,l*-lactides by dimethyl (salicylaldiminato)aluminum compounds. **Macromolecules** 42(16):6056-6062.

_____, M. Bruno, M. Lamberti, M. Mazzeo and C. Pellecchia. 2013. Ring-opening polymerization of ε-caprolactone and lactides promoted by Salan- and Salen-type yttrium amido complexes. J. Mol. Cata. A:Chem. 379:303-308.

Penczek, S. 2000. Cationic ring-opening polymerization (CROP) major mechanistic phenomena. **J. Polym. Sci., Part A.:Polym. Chem.** 38(11):1919-1933.

Peng, F., J. Ling, Z. Shen and W. Zhu. 2005. Correlation between phenol structure and catalytic activity of samarium(III) phenolates in polymerization of ε-caprolactone: Part 2. Tertbutyl's electronic and steric effects. **J. Mol. Catal. A:Chem.** 230(1-2):135-141.

Phomphrai K., P. Chumsaeng, P. Sangtrirutnugul, P. Kongsaeree and M. Pohmakotr. 2010. Reverse orders of reactivities in the polymerization of cyclic esters using N_2O_2 aluminium alkoxide complexes. **Dalton Trans.** 39:1865-1871.

Pietrangelo, A., M.A. Hillmyer and W.B. Tolman. 2009. Stereoselective and controlled polymerization of *D,L*-lactide using indium(III) trichloride. **Chem. Commun.** 19:2736-2737.

Pui, A. and I. Berdan 2002. Formation of Cu(II) coordination compounds with Schiff bases. ***Rev. Chim. (Bucharest).*** 53(1); 9-14.

_____, _____, and G. Stoica. 2000. Coordinative compounds of Co(II) with bis(α-pyrrole-aldehyde) ethylenediamine. ***Rev. Roum. Chim.*** 44(3):195-199.

_____, A. Cecal, G. Drochioiu and M. Pui. 2003. Coordination compounds of 3*d* metal ions (M = Mn, Fe, Co, Ni and Cu) with tetradentate diimine pyrrole Schiff bases. ***Rev. Roum. Chim.*** 48(6):439-443.

Purnama, P., Y. Jung, S. Kim and H. Soo. 2012. Stereocomplexation of poly(*L*-lactide) and random copolymer poly(*D*-lactide-*co*-ε-caprolactone) to enhance melt stability. **Macromolecules** 45(9):4012-4014.

Copyright by Kasetsart University All rights reserved

Radano, C.P., G.L. Baker, M.R. Smith. 2000. Stereoselective polymerization of a *racemic* monomer with a *racemic* catalyst: Direct preparation of the polylactic acid stereocomplex from *racemic* lactide. **J. Am. Chem. Soc.** 122(7):1552-1553.

Ragauskas, A.J., C.K. Williams, B.H. Davison, G. Britovsek, J. Cairney, C.A. Eckert, W.J. Frederick Jr., J.P. Hallett, D.J. Leak, C.L. Liotta, J.R. Mielenz, R. Murphy, R. Templer and T. Tschaplinski. 2006. The path forward for biofuels and biomaterials. **Science** 311(5670):484-489.

Rao, V.K., S.S. Reddy, B.S. Krishna, K.R.M. Naidu, C.N. Raju and S.K. Ghosh. 2010. Synthesis of Schiff's bases in aqueous medium:a green alternative approach with effective mass yield and high reaction rates. **Green Chem. Lett. Rev.** 3(3):217-223.

Raupp, F.M. and O. Spring. 2013. New sesquiterpene lactones from sunflower root exudate as germination stimulants for Orobanche Cumana. **J. Agric. Food Chem.** 61 (44):10481-10487.

Rieth, L.R., D.R. Moore, E.B. Lobkovsky and G.W. Coates. 2002. Single-site β-diiminate zinc catalysts for the ring-opening polymerization of β-butyrolactone and β-valerolactone to poly(3-hydroxyalkanoates). **J. Am. Chem. Soc.** 124(51):15239-15248.

Robertson, Jerry E., J. H. Biel, T. F. Jr. Mitchell, W. K. Hoya, and H. A. Leiser. 1963. Hypotensives. VI. Disubstituted alkylenediamines and related compounds. ***J. Med. Chem.*** 6(6):805-807.

Ropson, N., Ph. Dubois, R. Jerome and Ph. Teyssie. 1995. Macromolecular engineering of polylactones and polylactides. 20. effect of monomer, solvent, and initiator on the ring-opening polymerization as initiated with aluminum alkoxides. **Macromolecules** 28(23):7589-7598.

Saiyasombat, W., R. Molloy, T.M. Nicholson, A.F. Johnson, I.M. Ward and S. Poshyachinda. 1998. Ring strain and polymerizability of cyclic esters. **Polymer** 39(23):5581-5585.

Sakai, F., K. Nishikawa, Y. Inoue and K. Yazawa. 2009. Nucleation enhancement effect in poly(*l*-lactide) (PLLA)/poly(ε-caprolactone) (PCL) blend induced by locally activated chain mobility resulting from limited miscibility. **Macromolecules** 42(21):8335-8342.

Sauer, A., A. Kapelski, C. Fliedel, S. Dagorne, M. Kol and J. Okuda. 2013. Structurally well-defined group 4 metal complexes as initiators for the ring-opening polymerization of lactide monomers. **Dalton. Trans.** 42(25):9007-9023.

Copyright by Kasetsart University All rights reserved

Schwarz, A.D., Z. Chu and P. Mountford. 2010. Sulfonamide-supported aluminum catalysts for the ring-opening polymerization of *rac*-lactide. **Organometallics** 29(5):1246-1260.

Sheldrick, G. M.. 2008. A short history of SHELX. **Acta Cryst., Sect. A: Found. Cryst.** 64(1):112-122.

Shuklov, I.A., H. Jiao, J. Schulze, W. Tietz, K. Kühlein and A. Börner. 2010. Studies on the epimerization of diastereomeric lactides. **Tetrahedron Lett.** 52(9):1027-1030.

Song, S., H. Ma and Y. Yang. 2013. Magnesium complexes supported by Salan-like ligands: Synthesis, characterization and their application in the ring-opening polymerization of *rac*-lactide. **Dalton Trans.** 42(39):14200-14211.

Spassky, N., M. Wisniewski, C. Pluta and A. LeBorgne. 1996. Highly stereoelective polymerization of *rac*-lactide with a chiral schiff's base/aluminium alkoxide initiator. **Macromol. Chem. Phys.** 197(9):2627-2637.

Srivastava, S. and A. Kalam. 2002. Synthesis of phenylthallium(III) dichloride and diphenylthallium(III) chloride complexes with bidentate Schiff base ligands: A photoelectron spectroscopic study. ***J. Indian. Chem. Soc.*** 79(6):502-504.

_____, and D. Singh. 1999a. Diorganotellurium(IV) dihalide complexes with bidentate Schiff base ligands - Part II. ***Asian J. Chem.*** 11(4):1511-1513.

_____, and _____. 1999b. Some new organotellurium(II) molecular adducts with bidentate ligands. **Asian J. Chem.** 11(4):1559-1560.

_____, and R. Mishra 1995. Some mercury(II) complexes with bidentate aromatic Schiff base ligands. ***J. Indian Chem. Soc.*** 72(10):719-20.

Stanford, M.J. and A.P. Dove. 2010. Stereocontrolled ring-opening polymerization of lactide. **Chem. Soc. Rev.** 39(2):486-494.

Stéphanie G.-B., D. Delcroix, B. Martín-Vaca, D. Bourissou, C. Navarro and S. Magnet. 2008. Organo-catalyzed ROP of ε-caprolactone: Methanesulfonic acid competes with trifluoromethanesulfonic acid. **Macromolecules** 41(11):3782-3784.

Stern, C., F. Franceschi, E. Solari, C. Floriani, N. Re and R. Scopelliti. 2000. The use of macrocyclic and polydentate ligands in ruthenium organometallic chemistry. ***J. Organo.Chem.*** 593-594:86-95.

Storey, R.F. and J. W. Sherman. 2002. Kinetics and mechanism of the stannous octoate-catalyzed bulk polymerization of ε-caprolactone. **Macromolecules** 35(5):1504-1512.

Copyright by Kasetsart University All rights reserved

Storr, T., L.E. Scott, M.L. Bowen, D.E. Green, K.H. Thompson, H.J. Schugar and C. Orvig. 2009. Glycosylated tetrahydroSalens as multifunctional molecules for Alzheimer's therapy. **Dalton. Trans.** (16):3034-3043.

Sumrit, P. and P. Hormnirun. 2013. Aluminum initiators supported by asymmetric [ONNO']-Type Salan ligands for the ring-opening polymerization of *rac*-lactide. **Macromol. Chem. Phys.** 214(16):1845-1851.

Supathana, P., S. Praban, A. Niewpung, G. Kotpisan, P. Kongsaeree, S. Saithong, T. Khamnaen, P. Phiriyawirut, S. Charoenchaidet, K. Phomphrai. 2013. Syntheses of bis(pyrrolylaldiminato)aluminum complexes for the polymerization of lactide. **Dalton Trans.** 42(42):15191-15198.

Tabthong, S., T. Nanok, P. Kongsaeree, S. Prabpai and P. Hormnirun. Monomethylaluminum and dimethylaluminum pyrrolylaldiminates for the ring-opening polymerization of rac-lactide: effects of ligand structure and coordination geometry. **Dalton Trans.** 43(3):1348-1359.

Taden, I., H.-C. Kang, W. Massa and J. Okuda. 1997. Aluminum complexes of sterically hindered tetradentate Schiff bases: Synthesis, structure, and reactivity toward ε-caprolactone. Organomet. Chem. 540(1-2):189-192.

Tang Z., X. Chen, X. Pang, Y. Yang, X. Zhang and X. Jing. 2004. Stereoselective polymerization of *rac*-lactide using a monoethylaluminum Schiff base complex. **Biomacromolecules.** 5(3):965-970.

_____, _____, Q. Liang, X. Bian, L. Yang, L. Piao and X. Jing. 2003. Strontium-based initiator system for ring-opening polymerization of cyclic esters. **J. Polym. Sci., Part A.:Polym. Chem.** 41(13):1934-1941.

Tang Z.H., V.C. Gibson. 2007. *rac*-Lactide polymerization using aluminum complexes bearing tetradentate phenoxy-amine ligands. **Eur. Polym. J.** 43(1):150-155.

Thakur, K.A.M., R.T. Kean, E.S. Hall, J.J. Kolstad, T.A. Lindgren, M.A. Doscotch, J.I. Siepmann and E.J. Munson. 1997. High-resolution ^{13}C and ^{1}H solution NMR study of poly(lactide). **Macromolecules** 30(12):2422-2428.

_____, _____, _____, _____, and E. J. Munson. 1998a Stereochemical aspects of lactide stereo-copolymerization investigated by ^{1}H NMR: A case of changing stereospecificity. **Macromolecules** 31(5):1487-1494.

Copyright by Kasetsart University All rights reserved

Thakur, K.A.M., R.T. Kean, E.S. Hall, J.J. Kolstad and E. J. Munson. 1998b, An alternative interpretation of the HETCOR NMR spectra of poly(lactide). **Chem. Commun.** 17:1913-1914.

Thomas, C.M. 2010. Stereocontrolled ring-opening polymerization of cyclic esters:synthesis of new polyester microstructures. **Chem. Soc. Rev.** 39:165-173.

Trost, B.M. and M. Preckel. 1973. New synthetic reactions. New approach to geminal alkylation. **J. Am. Chem. Soc.** 95 (23):7862-7864.

Tshuva, E.Y., N. Gendeziuk and M. Kol. 2001. Single-step synthesis of Salans and substituted Salans by Mannich condensation. **Tetrahedron Lett.** 42(36):6405-6407.

Uhrich, K.E., S.M. Cannizzaro, R.S. Langer and K.M. Shakesheff. 1999. Polymeric system for controlled drug release. **Chem. Rev.** 99(11):3181-3198.

Uyama, H. and S. Kobayashi. 1993. 1993. Enzymatic ring-opening polymerization of lactones catalyzed by lipase. **Chem. Lett.** 22(7):1149-1150.

Van den Ancker, T.R., G.W.V. Cave and C. L. Raston. 2006. Benign approaches to the synthesis of bis-imine Schiff bases. ***Green Chemistry*** 8(1):50-53.

Van S., C. Gerard, G. Van Koten, H. Passenier, O. Steinebach and K. Vrieze. 1984. Syntheses and characterization of neutral complexes of zinc(II) with mono- and dianionic pyrrole-2-imine ligands $[(\text{pyrrole-2-CH:N})_n\text{R}]_n$- (n = 1, 2). ***Inorg. Chim. Acta*** 9(2):79-87.

Vanhoorne, P., P. Dubois, R. Jerome and P. Teyssie. 1992. Macromolecular engineering of polylactones and polylactides. 7. Structural analysis of copolyesters of *ε*-caprolactone and *L*- or *D*,*L*-lactide initiated by triisopropoxyaluminum. **Macromolecules** 25(1):37-44.

Vesna, S., S. Pensec and N. Nicolas. 2000. Synthesis and characterization of some block copolymers of lactides with cyclic monomers using yttrium alkoxide as initiator. **Macromol. Symp.** 153 :109-121.

Vieira, I. dos S., E. L. Whitelaw, M.D. Jones, Matthew D. and S. Herres-Pawlis. 2013. Synergistic empirical and theoretical study on the stereoselective mechanism for the aluminum salalen complex mediated polymerization of *rac*-lactide. **Chem. Eur. J.** 19(15):4712-4716.

Wang, Y., H. Fu, A. Peng, Y. Zhao, J. Ma, Y. Ma and J. Yao. 2007. Distinct nanostructures from isomeric molecules of bis(iminopyrrole) benzenes: Effects of molecular structures on nanostructural morphologies. **Chem. Comm. (Cambridge, United Kingdom)** (16):1623-1625.

Copyright by Kasetsart University All rights reserved

Wang, Y.C., S.Y. Shen, Q.P. Wu, D.P. Chen, J. Wang, G. Steinhoff and N. Ma. 2006. Block copolymerization of ε-caprolactone and 2-methoxyethyl ethylene phosphate initiated by aluminum isopropoxide: Synthesis, characterization, and kinetics. **Macromolecules** 39(24):8992-8998.

Wasserman, H.H. and J.L. Ives. 1978. Reaction of singlet oxygen with enamino lactones. Conversion of lactones to α-keto lactones. **J. Org. Chem.** 43 (16):3238-3240.

Watanabe, R., T. Shimada, N. Koyama, T. Ishida and T. Kogane. 2011, Attempted synthesis of axial-equatorial pyrazine-bridged copper(II) complexes toward homometallic ferromagnetic compounds. **Polyhedron** 30:3165-3170.

Wawer, I. and J. Osek. 1985. ^{1}H and ^{13}C nuclear magnetic resonance identification of the products of the reaction of *N*,*N*-dialkylformamide dimethyl acetals with secondary amines. **J. Chem. Soc., Perkin Trans.** 10:1669-1671.

Weber, J.H. 1967. Complexes of pyrrole-derivative ligands. I. Planar nickel(II) complexes with tetradentate ligands. ***Inorg. Chem.*** 6(2):258-262.

Whitehorne, T.J.J. and F. Schaper. 2012. NacnacBnCuO^{i}Pr: A strained geometry resulting in very high lactide polymerization activity. **Chem. Commun.** 48(83):10334-10336.

Whitelaw, E.L., G. Loraine, M.F. Mahon and M.D. Jones. 2011. Salalen aluminium complexes and their exploitation for the ring opening polymerisation of *rac*-lactide. **Dalton Trans.** 40:11469-11473 .

Whiteoak, C.J., G.J.P. Britovsek, V.C. Gibson and A.J.P. White. 2009. Electronic effects in oxo transfer reactions catalysed by Salan molybdenum(VI) *cis*-dioxo complexes. **Dalton Trans.** (13):2337-2344.

_____, R. T. Martin de Rosales, A. J. P. White and G. J. P. Britovsek. 2010. Iron(II) complexes with tetradentate bis(aminophenolate) ligands: Synthesis and characterization, solution behavior, and reactivity with O_2. **Inorg. Chem.** 49(23):11106-11117.

Wilesa, D.M. and G. Scott. 2006. Polyolefins with controlled environmental degradability. **Polym. Degrad. Stabil.** 91(7):1581-1592.

Williams, C.K., L.E. Breyfogle, S.K. Choi, W. Nam, V.G. Young Jr., M.A. Hillmyer and W.B. Tolman. 2003. A highly active zinc catalyst for the controlled polymerization of lactide. **J. Am. Chem. Soc.** 125(37):11350-11359

_____. 2007. Synthesis of functionalized biodegradable polyesters. **Chem. Soc. Rev.** 36(10):1573-1580.

Copyright by Kasetsart University All rights reserved

Wisniewski, M., A. Le Borgne and N. Spassky 1997, Synthesis and properties of (*D*)- and (*L*)-lactide stereocopolymers using the system achiral Schiff's base/ aluminium methoxide as initiator. **Macromol. Chem. Phys.** 198(4):1227-1238.

Wong, Y.-L., Y. Yan, E.S.H. Chan, Q. Yang, T.C.W. Mak and D.K.S. Ng. 1998. *cis*-Dioxo-tungsten(VI) and -molybdenum(VI) complexes with N_2O_2 tetradentate ligands: Synthesis, structure, electrochemistry and oxo-transfer properties. **J. Chem. Soc., Dalton Trans.:Inorg. Chem.** (18):3057-3064.

Wu, B. and R.W. Lenz. 1998. Stereoregular polymerization of [*R*,*S*]-3-butyrolactone catalyzed by alumoxane−monomer adducts. **Macromolecules** 31(11):3473-3477.

Wu, J., T.-L. Yu, C.-T. Chen and C.-C. Lin. 2006. Recent developments in main group metal complexes catalyzed/initiated polymerization of lactides and related cyclic esters. **Coord. Chem. Rev.** 250(5-6):575-728.

_____, X.B. Pan, N. Tang and C.C. Lin. 2007. Synthesis, characterization of aluminum complexes and the application in ring-opening polymerization of *l*-lactide. **Eur. Polym. J.** 43(12):5040-5046.

Xiang, H.-F., S.-C. Chan, K.K.-Y. Wu, C.-M. Che, P.T. Lai. 2005. High-efficiency red electrophosphorescence based on neutral bis(pyrrole)-diimine platinum(II) complex. ***Chem. Commun.*** (11):1408-1410.

Xie, W., D. Chen, X. Fan, J. Li, P.G. Wang, H. N. Cheng and R.G. Nickol. 1999. Lithium chloride as catalyst for the ring-opening polymerization of lactide in the presence of hydroxyl-containing compounds. J**. Polym. Sci. A Polym. Chem.** 34(17):3486-3491.

Yalcin, G. and A. Kayan. 2012. Synthesis and characterization of Zr, Ti, Al-phthalate and pyridine-2-carboxylate compounds and their use in ring opening polymerization. **Appl. Catal. A.** 2012(433):223-228.

Yang, D., W. Huang, J.H. Yu, J.S. Jiang, L.Y. Zhang and M.R. Xie. 2010. A novel shape memory polynorbornene functionalized with poly(*ε*-caprolactone) side chain and cyano group through ring-opening metathesis polymerization. **Polymer** 51(22):5100-5106.

Yang, L., Q. Chen, Y. Li, S. Xiong, G. Li and J.S. Genpei. 2004. Self-assembly of bis(pyrrol-2-ylmethyleneamine) ligands with Cu(II) controlled by bridging [-$(CH2)_n$-] spacers and weak intermolecular C-H···Cu hydrogen bonding. ***Eur. J. Inorg. Chem.*** (7):1478-1487.

Copyright by Kasetsart University All rights reserved

Yang, L., Q. Chen, G.-Q. Yang and J.S. Ma. 2003. Self-assembly of bis(pyrrol-2-yl-methyleneamine)s bridged by flexible linear carbon chains. ***Tetrahedron*** 59(50):10037-10041.

_____, X. Shan, Q. Chen and J.S. Ma. 2004. Self-assembly of 1,4-bis(pyrrol-2-ylmethyleneamino)butane mediated by Ni(II) and weak intermolecular interactions. **J. Chem. Res.** (9):636-637.

Yang, N., L. Xin, W. Gao, J. Zhang, X. Luo, X. Liu and Y. Mu. 2012. Al and Zn complexes bearing *N*,*N*,*N*-tridentate quinolinyl anilido-imine ligands: Synthesis, characterization and catalysis in *L*-lactide polymerization. **Dalton Trans.** 41(37):11454-11463.

Yang, Y., B. Liu, K. Lv, W. Gao, D. Cui, X. Chen and X. Jing. 2007. Pyrrolide-supported lanthanide alkyl complexes. influence of ligands on molecular structure and catalytic activity toward isoprene polymerization. **Organometallics** 26(18):4575-4584.

Yao, W., Y. Mu, A. Gao, Q. Su, Y. Liu and Y. Zhang. 2008. Efficient ring-opening polymerization of ε-caprolactone using anilido-imine-aluminum complexes in the presence of benzyl alcohol. **Polymer** 49(10):2486-2491.

Yong, Y.-C. and J.-J. Zhong. 2010. *N*-Acylated homoserine lactone production and involvement in the biodegradation of aromatics by an environmental isolate of Pseudomonas aeruginosa. **Process Biochem.** 45(12):1944-1948.

Yu R.C., C.H. Hung, J.H. Huang, H.Y. Lee and J.T. Chen. Inorg. Chem. 2002. Four- and five-coordinate aluminum ketiminate complexes: synthesis, characterization, and ring-opening polymerization. **Inorg. Chem.** 41(24):6450-6455.

Yuan, Q.-H. and L.-J. Wan. 2006. Structural comparison of self-organized adlayers of ligands and their metal-coordinated complexes on a Au(III) surface:an STM study. **Chem. Eur. J.** 12(10):2808-2814.

Zamani, H.A., Z. Rafati and S. Meghdadi. 2011. Construction of $Tb^{3+}PVC^{-}$ membrane electrode based on *N*,*N*'-bis(pyrrolylmethylene)-2-amino benzylamine. **E-J. Chem.** 8(Suppl. 1):S203-S210.

Zell, M.T., and B.E. Padden, A.J. Paterick, K.A.M. Thakur, R.T. Kean, M.A. Hillmyer and E.J. Munson. 2002. Unambiguous determination of the ^{13}C and ^{1}H NMR stereosequence assignments of polylactide using high-resolution solution NMR spectroscopy. **Macromolecules** 35 (20):7700-7707.

Copyright by Kasetsart University All rights reserved

Zhang, C. and Z.-X. Wang. 2008. Aluminum and zinc complexes supported by functionalized phenolate ligands:Synthesis, characterization and catalysis in the ring-opening polymerization of *ε*-caprolactone and *rac*-lactide. **J. Organomet.** Chem. 693(19):3151-3158.

Zhang, G., G. Yang and J.S. Ma. 2004. A novel luminescent metallomacrocycle assembled by silver nitrate and 1,3-bis(pyrrol-2-ylmethyleneamino)propane. **Inorg. Chem. Comm.** 7(8):994-997.

_____, _____, _____, and _____. 2005. Novel Network Polymers Formed by Self-Assembly of Silver Nitrate and Pyrrol-2-yl-methyleneamine Ligands with Flexible Spacers. **Cryst. Growth Des.** 5(2):661-666.

Zhang, X., D. A. MacDonald, Mattheus F. A. Goosen and Kim B. McAuley. 1994. Mechanism of lactide polymerization in the presence of stannous octoate: The effect of hydroxy and carboxylic acid substances. **J. Polym. Sci. A: Polym. Chem.** 32(15):2965-2970.

_____, B. Xu, Y.-H. Li and W. Li. 2008. Bis[*N*,*N*'-bis[(1H-pyrrol-2-yl)methylene] cyclohexane-1,2-diamine]titanium(IV) tetrahydrofuran solvate. **Acta Crystallogr. Sect. E.-Struct Rep. Online.** 64(2):m437, m437/1-m437/13.

Zhao W., Y. Wang, X. Liu, X. Chen, D. Cui and E.Y.-X. Chen. 2012. Protic compound mediated living cross-chain-transfer polymerization of rac-lactide:synthesis of isotactic (crystalline)-heterotactic (amorphous) stereomultiblock polylactide. **Chem. Commun.** 48(51):6375-6377.

Zhong, Z., P. J. Dijkstra and J. Feijen. 2002. [(Salen)Al]-Mediated, controlled and stereoselective ring-opening polymerization of lactide in solution and without solvent: Synthesis of highly isotactic polylactide stereocopolymers from *racemic d,l*-lactide. **Angew. Chem., Int. Ed.** 41(23):4510-4513.

_____, _____, and _____. 2003. Controlled and stereoselective polymerization of lactide: kinetics, selectivity, and microstructures. **J. Am. Chem. Soc.** 125 (37):11291-11298.

Copyright by Kasetsart University All rights reserved

APPENDIX

Copyright by Kasetsart University All rights reserved

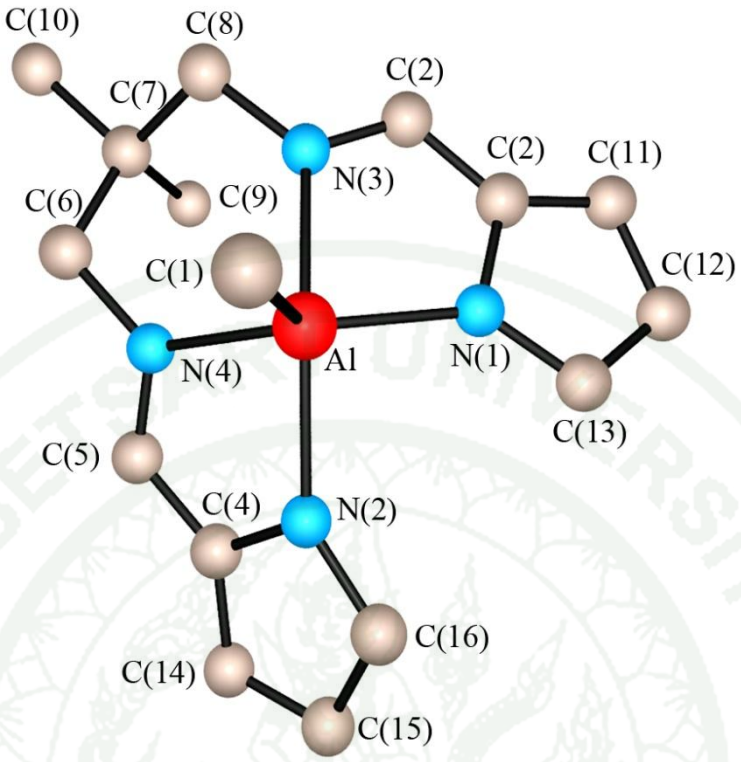

Appendix Figure 1 The molecular structure of complex **L^{3}AlMe.**

Appendix Table 1 Bond lengths (Å) for complex **L^{3}AlMe**

Bond	(Å)	Bond	(Å)	Bond	(Å)
Al–N(1)	1.959(1)	N(3)–C(3)	1.291(2)	C(7)–C(8)	1.533(2)
Al–N(2)	1.976(1)	N(3)–C(8)	1.457(2)	C(7)–C(9)	1.531(2)
Al–N(3)	2.054(1)	N(4)–C(5)	1.289(2)	C(7)–C(10)	1.522(2)
Al–N(4)	2.033(1)	N(4)–C(6)	1.472(2)	C(11)–C(12)	1.397(3)
Al–C(1)	1.967(2)	C(2)–C(3)	1.422(2)	C(12)–C(13)	1.398(3)
N(1)–C(2)	1.376(2)	C(2)–C(11)	1.390(2)	C(14)–C(15)	1.399(3)
N(1)–C(13)	1.363(2)	C(4)–C(5)	1.418(2)	C(15)–C(16)	1.388(3)
N(2)–C(4)	1.382(2)	C(4)–C(14)	1.395(2)		
N(2)–C(16)	1.352(2)	C(6)–C(7)	1.535(2)		

Copyright by Kasetsart University All rights reserved

Appendix Table 2 Bond angles for complex **L^3AlMe**

Angles	(°)	Angles	(°)	Angles	(°)
N(1)-Al-N(2)	92.86(6)	Al-N(3) -C(8)	126.9(1)	C(3)-N(3)-C(8)	119.1(1)
N(1)-Al-N(3)	79.92(6)	Al-N(4)-C(5)	113.7(1)	C(3)-C(2)-C(11)	133.8(2)
N(1)-Al-N(4)	137.59(6)	Al-N(4)-C(6)	126.7(1)	C(4)-N(2)-C(16)	105.8(1)
N(2)-Al-N(3)	148.16(6)	N(1)-C(2)-C(3)	114.9(1)	C(4)-C(14)-C(15)	105.8(2)
N(2)-Al-N(4)	80.43(5)	N(1)-C(2)-C(11)	111.2(2)	C(5)-N(4)-C(6)	119.5(1)
N(3)-Al-N(4)	84.28(5)	N(1)-C(13)-C(12)	110.5(2)	C(5)-C(4)-C(14)	134.9(2)
C(1)-Al-N(1)	115.41(7)	N(2)-C(4)-C(5)	114.5(1)	C(6)-C(7)-C(8)	109.7(1)
C(1)-Al-N(2)	108.95(7)	N(2)-C(4)-C(14)	110.5(1)	C(6)-C(7)-C(9)	110.3(1)
C(1)-Al-N(3)	102.07(7)	N(2)-C(16)-C(15)	111.1(1)	C(6)-C(7)-C(10)	107.9(1)
C(1)-Al-N(4)	106.27(7)	N(3)-C(3)-C(2)	116.5(1)	C(8) -C(7) -C(9)	111.1(1)
Al-N(1)-C(2)	114.7(1)	N(3)-C(8)-C(7)	112.3(1)	C(8)-C(7)-C(10)	108.0(1)
Al-N(1)-C(13)	139.7.(1)	N(4)-C(5)-C(4)	117.5(1)	C(11)-C(12)-C(13)	106.9(2)
Al-N(2) -C(4)	113.5(1)	N(4)-C(6)-C(7)	113.0(1)	C(14)-C(15)-C(16)	106.8(2)
Al-N(2)-C(16)	140.6(1)	C(2)-N(1)-C(13)	105.6(1)		
Al-N(3)-C(3)	114.0(1)	C(2)-C(11)-C(12)	105.8(2)		

Copyright by Kasetsart University All rights reserved

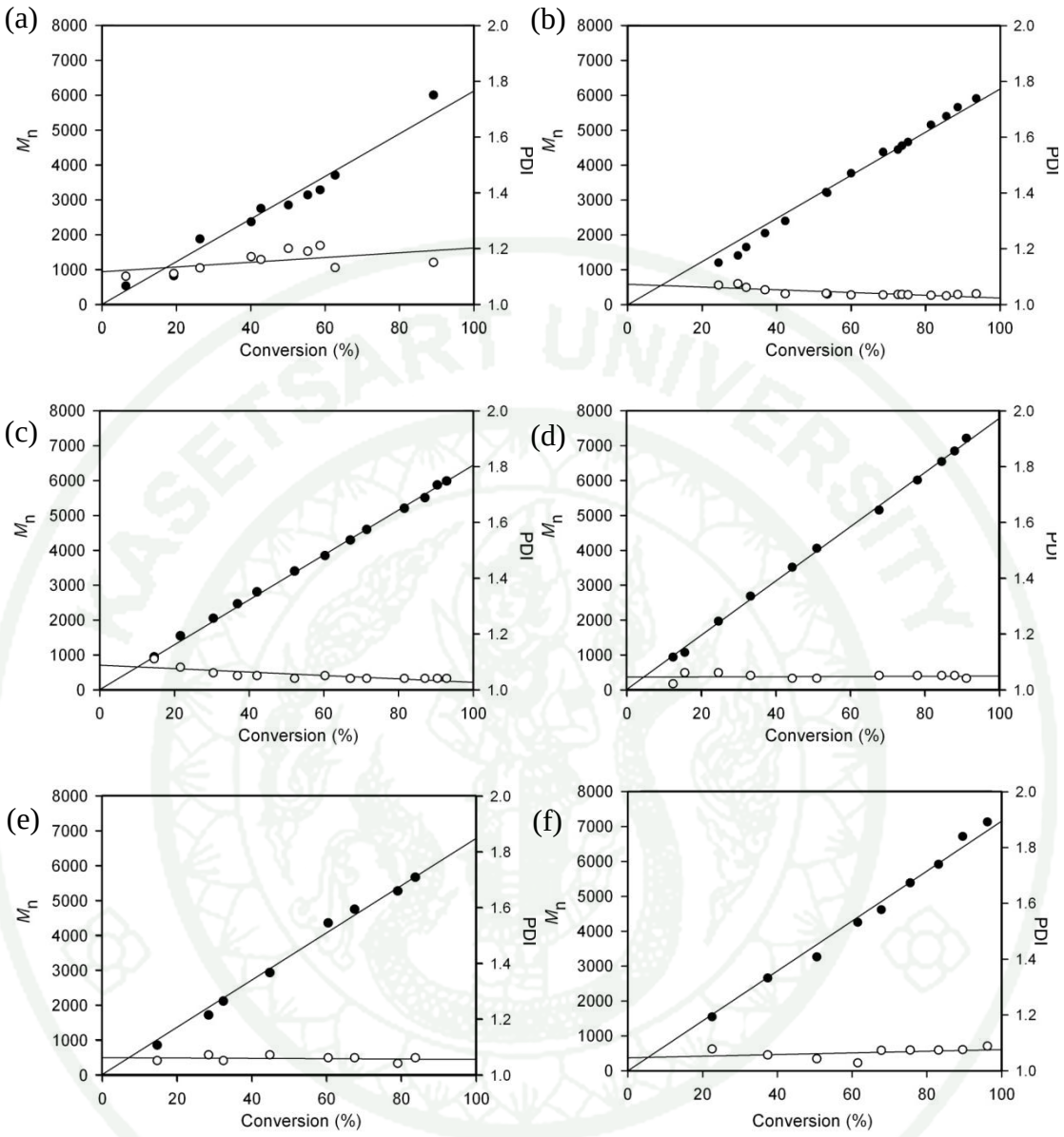

Appendix Figure 2 Plot of M_n as a function of monomer conversion for *rac*-LA polymerization using (a) **L^{1}AlMe**/PhCH$_2$OH, (b) **L^{2}AlMe**/PhCH$_2$OH, (c) **L^{4}AlMe** /PhCH$_2$OH, (d) **L^{5}AlMe**/PhCH$_2$OH, (e) **L^{6}AlMe**/PhCH$_2$OH, , (f) **L^{7}AlMe**/PhCH$_2$OH ([LA]$_0$/[Al] = 50, [Al]/[PhCH$_2$OH] = 1, [LA]$_0$ = 0.42 M, [Al] = 8.33 mM)**.**

Copyright by Kasetsart University All rights reserved

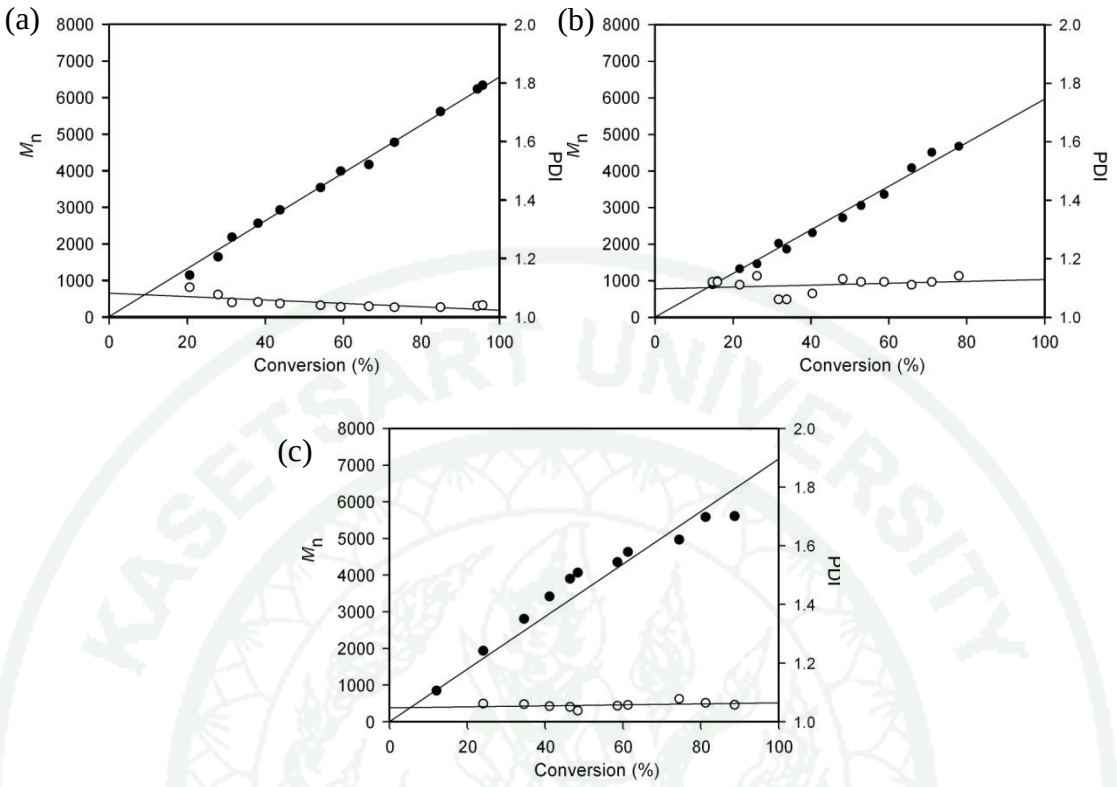

Appendix Figure 3 Plot of M_n as a function of monomer conversion for *rac*-LA polymerization using (a) **L^{2A}AlMe**/$PhCH_2OH$, (b) **L^{3A}AlMe**/ $PhCH_2OH$, (c) **L^{4A}AlMe** /$PhCH_2OH$ ($[LA]_0/[Al]$ = 50, $[Al]/[PhCH_2OH]$ = 1, $[LA]_0$ = 0.42 M, [Al] = 8.33 mM)**.**

Copyright by Kasetsart University All rights reserved

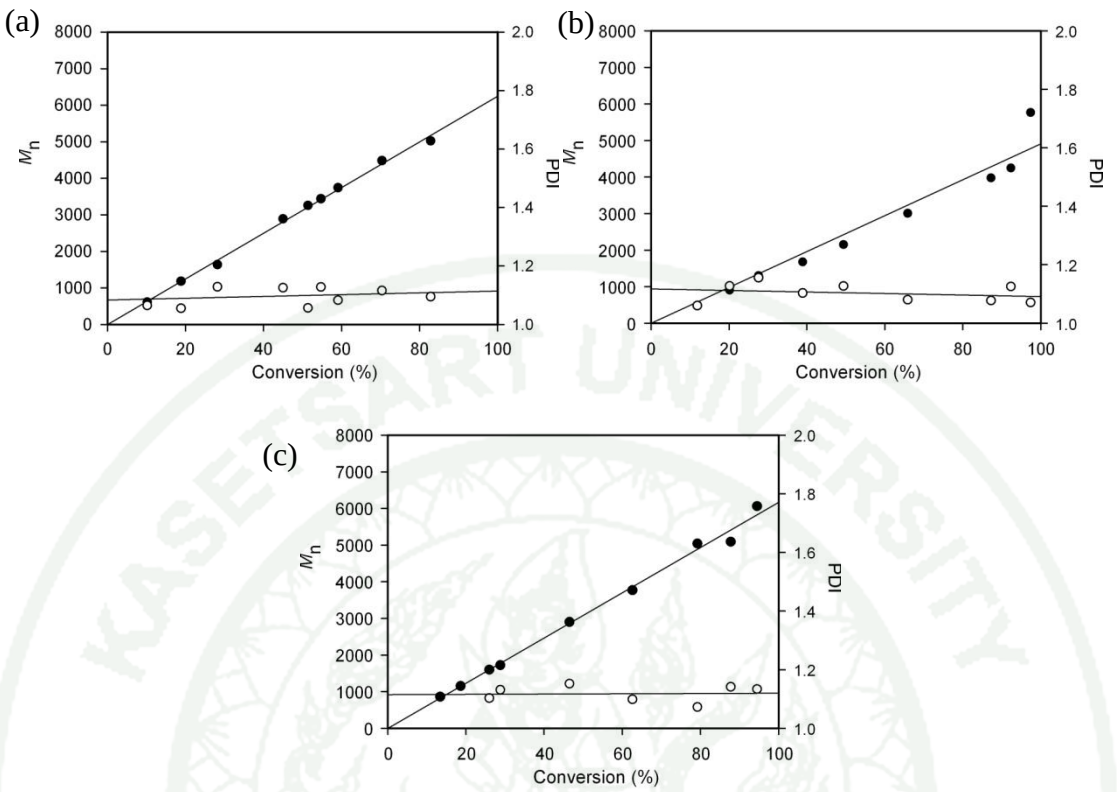

Appendix Figure 4 Plot of M_n as a function of monomer conversion for *rac*-LA polymerization using (a) **L^{1C}AlMe**/$PhCH_2OH$, (b) **L^{2C}AlMe**/ $PhCH_2OH$, (c) **L^{3C}AlMe** /$PhCH_2OH$ ($[LA]_0/[Al]$ = 50, $[Al]/[PhCH_2OH]$ = 1, $[LA]_0$ = 0.42 M, [Al] = 8.33 mM)**.**

Copyright by Kasetsart University All rights reserved

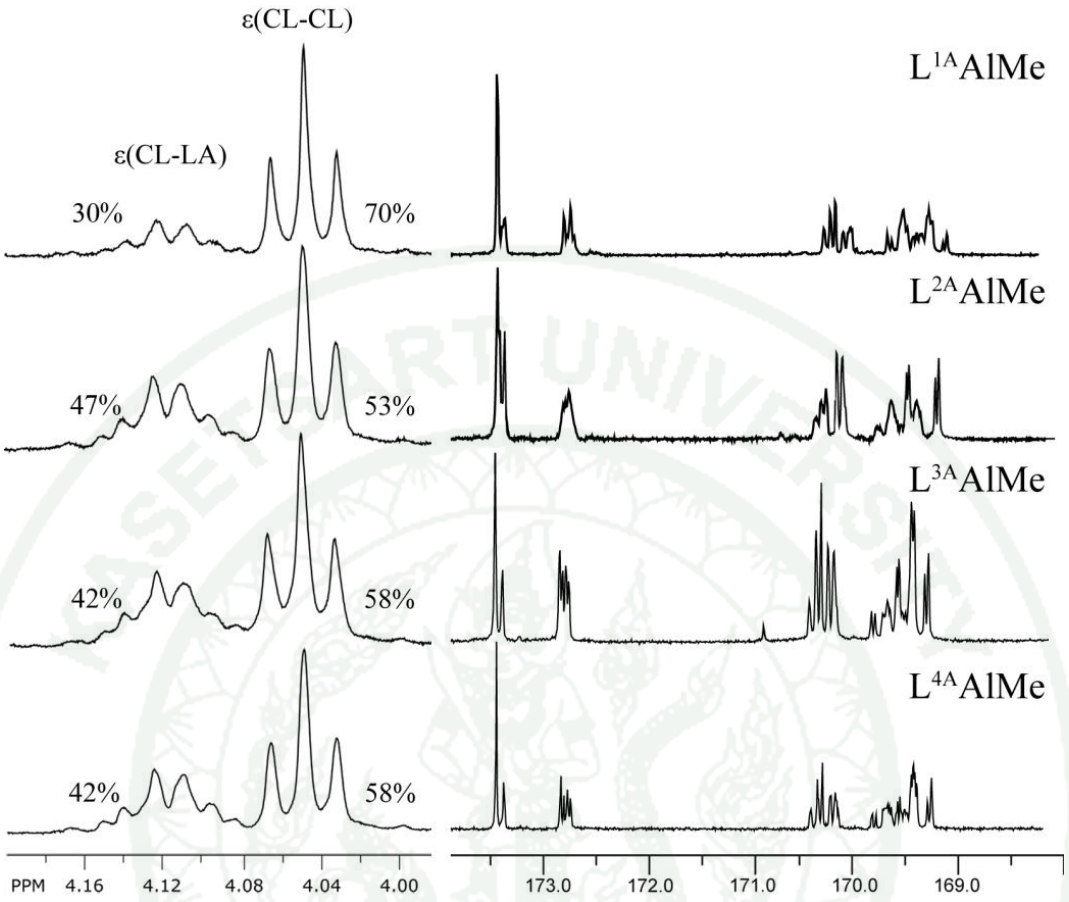

Appendix Figure 5 (left) ^{1}H NMR spectrum of ε- and α-methylene protons of PLA-*co*-PCL, (right) ^{13}C NMR spectrum of carbonyl carbons of PLA-*co*-PCL using Group A complexes.

Copyright by Kasetsart University All rights reserved

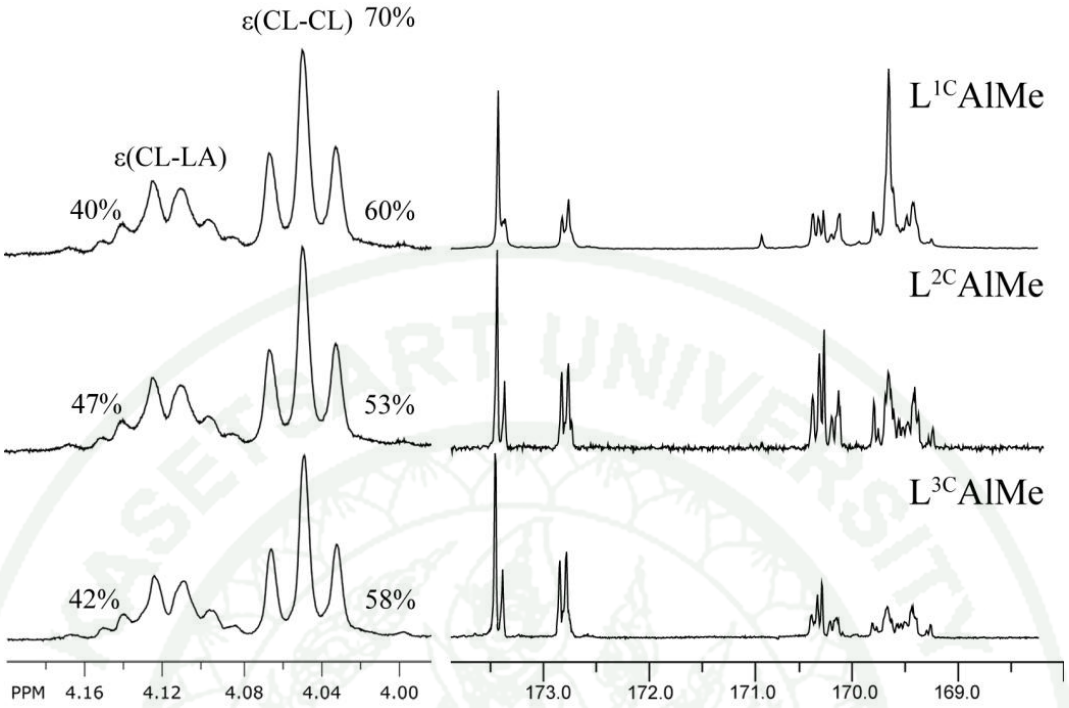

Appendix Figure 6 (left) ^{1}H NMR spectrum of ε- and α-methylene protons of PLA-*co*-PCL, (right) ^{13}C NMR spectrum of carbonyl carbons of PLA-*co*-PCL using Group A complexes.

Copyright by Kasetsart University All rights reserved

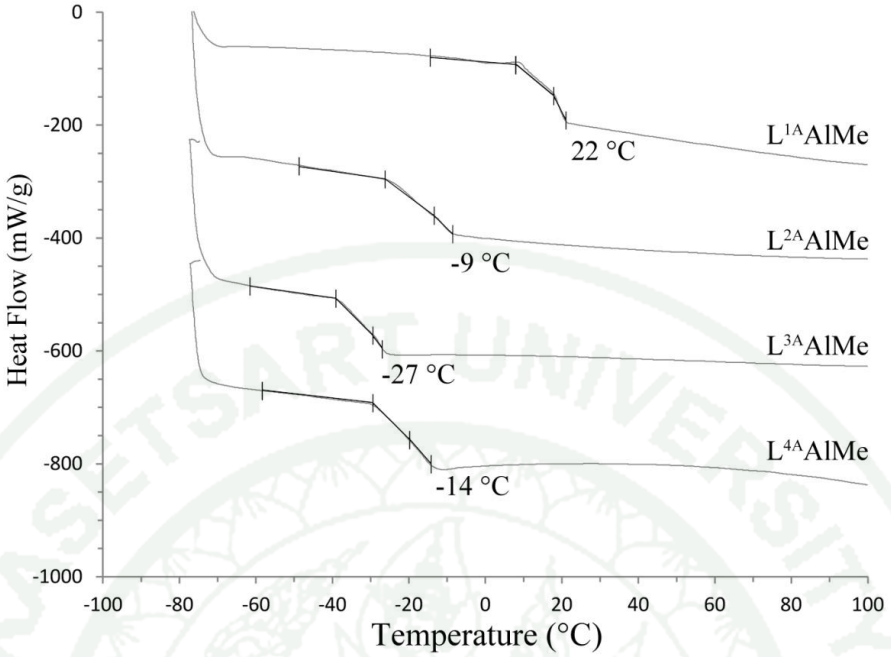

Appendix Figure 7 DSC thermograms of PLA-*co*-PCL using Group A complexes.

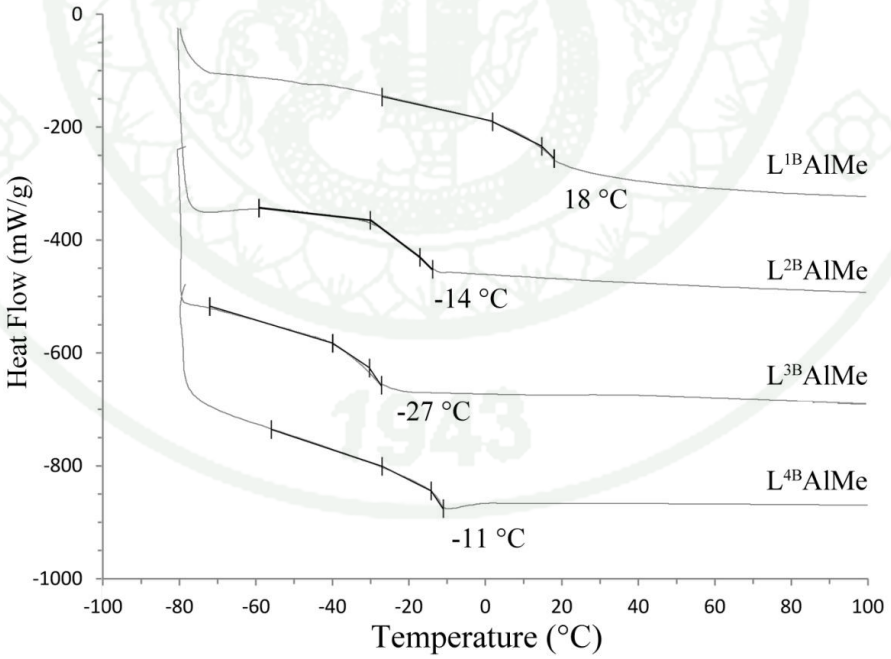

Appendix Figure 8 DSC thermograms of PLA-*co*-PCL using Group B complexes.

Copyright by Kasetsart University All rights reserved

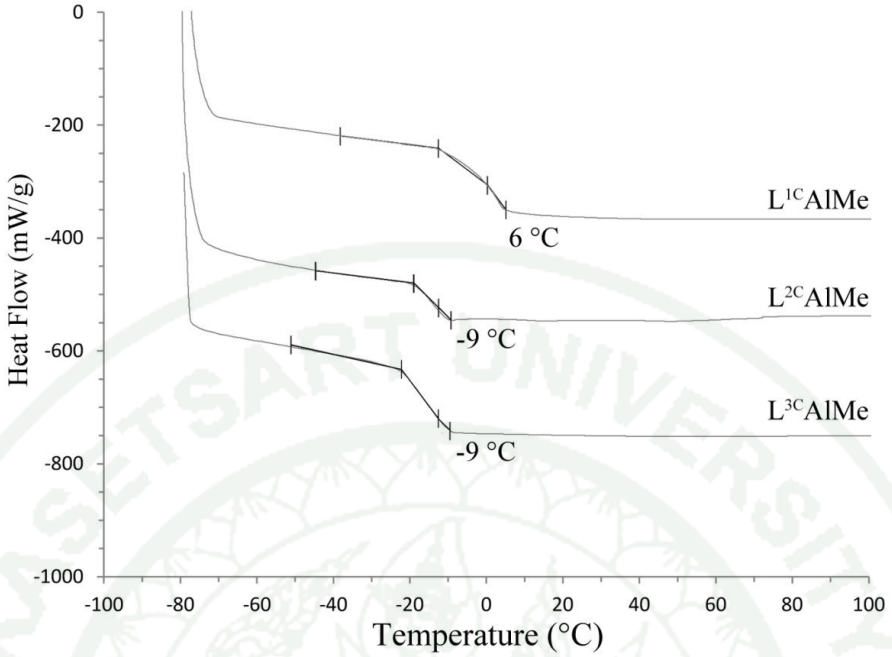

Appendix Figure 9 DSC thermograms of PLA-*co*-PCL using Group C complexes.

Copyright by Kasetsart University All rights reserved

CURRICULUM VITAE

NAME : Mr. Sittichoke Tabthong

BIRTH DATE : February 3, 1985

BIRTH PLACE : Lopburi, Thailand

EDUCATION

YEAR	INSTITUTE	DEGREE/DIPLOMA
2007	Chiangmai Univ.	B.Sc.(Chemsitry)
2009	Kasetsart Univ.	M.S.(Chemistry)

SCHOLARSHIPS

B.Sc. (2004-2007)	Science Achievement Scholarship of Thailand (SAST).
M.Sc. (2007–2008)	The National Center of Excellence for Petroleum, Petrochemicals and Advanced Materials (NCE-PPAM).
M.Sc. (2008–2009)	The Thailand Graduated Institute of Science and Technology (TGIST).
Ph.D. (2009-2011)	The National Center of Excellence for Petroleum, Petrochemicals and Advanced Materials (NCE-PPAM). Faculty of Science Kasetsart University Postgraduate Studentship: ScKUPGS.
Ph.D. (2013-2014)	Financial support from the graduate school Kasetsart University for the publication in an approved international journal.

Copyright by Kasetsart University All rights reserved